UNIVERSITY OF SOUTHAMPTON

FACULTY OF NATURAL AND ENVIRONMENTAL SCIENCE

Chemistry

Volume 1 of 1

THE QUANTITATION OF THERAPEUTIC OLIGONUCLEOTIDES AND THEIR IMPURITIES ANALYSED USING HYPHENATED LIQUID CHROMATOGRAPHY AND MASS SPECTROMETRY

by

Stephanie Louise Powley

Thesis for the degree of Doctor of Philosophy

May 2018

UNIVERSITY OF SOUTHAMPTON

ABSTRACT

FACULTY OF NATURAL AND ENVIRONMENTAL SCIENCE

Chemistry

Thesis for the degree of Doctor of Philosophy

THE QUANTITATION OF THERAPEUTIC OLIGONUCLEOTIDES AND THEIR IMPURITIES ANALYSED USING HYPHENATED LIQUID CHROMATOGRAPHY AND MASS SPECTROMETRY

Stephanie Louise Powley

As demand for therapeutic oligonucleotide drugs to treat a wider range of conditions increases, there is a requirement for a robust method for the quantitation of the impurities within a drug product. The development of a method that can be employed across all laboratories, regardless of the Liquid chromatography – Mass spectrometry instrumentation used, is highly desirable to ensure consistency of testing and to confirm inter-batch variation.

Factors influencing the reliability of quantitation have been investigated, including mobile phase additives, mass analyser type and in-source collision-induced dissociation voltage. Strategies for quantitating the data collected have also been considered and compared. The effect of the oligonucleotide sequence on the level of in-source fragmentation has been observed and discussed.

Recommendations are made for the most appropriate mobile phase reagents, mass analyser type and method of quantitation to be used to allow the development of an analytical method for use across laboratories to accurately and precisely quantitate therapeutic oligonucleotides and their impurities.

Table of Contents

List of Tables

List of Figures

DECLARATION OF AUTHORSHIP

I, Stephanie Louise Powley

declare that this thesis and the work presented in it are my own and has been generated by me as the result of my own original research.

The quantitation of therapeutic oligonucleotides and their impurities analysed using hyphenated liquid chromatography and mass spectrometry

I confirm that:

1. This work was done wholly or mainly while in candidature for a research degree at this University;
2. Where any part of this thesis has previously been submitted for a degree or any other qualification at this University or any other institution, this has been clearly stated;
3. Where I have consulted the published work of others, this is always clearly attributed;
4. Where I have quoted from the work of others, the source is always given. With the exception of such quotations, this thesis is entirely my own work;
5. I have acknowledged all main sources of help;
6. Where the thesis is based on work done by myself jointly with others, I have made clear exactly what was done by others and what I have contributed myself;
7. None of this work has been published before submission

Signed: .....

Date: .....

Acknowledgements

The research undertaken and reported in this thesis and, indeed, the thesis itself could not have been completed without the support and guidance of my supervisor, Professor G. John Langley. I will be forever grateful for the discussion we had during my PhD candidature and for his skill in getting me to think about my work in ways I never thought possible.

My thanks for the funding of this project go to the ESPRC and to AstraZeneca. Within AstraZeneca, I would like to acknowledge the invaluable advice, training and discussion I received from Andy Ray, Nadim Akhtar and Tony Bristow and the support while I was at the Macclesfield site from James Webster. I would also like to thank Dave Benstead for synthesising samples for me to analyse.

To Julie Herniman, thank you for always being there when instruments didn't do what I expected – I have learnt so many troubleshooting skills from you.

Thank you to the BMSS for the opportunity to present a poster at the annual conference, which gave me exposure to the wider mass spectrometry community.

For making my time in the Langley group enjoyable my thanks go to Krina, Waraporn, Stathis and Ammar for making a newbie feel welcome, to Ed, Dovile and Andreas for keeping me entertained, to Maria for her baking skills and to Ana for being my tea-buddy and putting up with my moaning!

Finally, and by no means least important, I'd like to thank my parents and Marc for their unwavering belief in my ability to do this and for Marc's proof-reading skills, even when he didn't have a clue what he was reading about!

Thank you all, this wouldn't have happened without you and I am truly grateful.

Definitions and Abbreviations

ACM	AstraZeneca chromatographic method
ACN	Acetonitrile
APCI	Atmospheric pressure chemical ionisation
CID	Collision induced dissociation
CoV	Coefficient of variance
CRM	Charge residue model
DC	Direct current
DNA	Deoxyribonucleic acid
EDTA	Ethylenediaminetetraacetic acid
ESI	Electrospray ionisation
FDA	Food and Drug Administration
FLN	Full-length n, target oligonucleotide
FWHM	Full width at half maximum
GC	Gas chromatography
HFIP	1,1,1,3,3,3-hexafluoro-2-isopropanol
HPLC	High performance liquid chromatography
ICH	International Conference on Harmonisation of Technical Requirements for Registration of Pharmaceuticals for Human Use
IEM	Ion evaporation model
IMS	Ion mobility spectrometry
IP-HPLC	Ion-pair high performance liquid chromatography
LOD	Limit of detection
LOQ	Limit of quantitation

MeOH	Methanol
mRNA	Messenger ribonucleic acid
MS	Mass spectrometry
MS/MS	Tandem mass spectrometry
Q – ToF	Quadrupole time of flight
QqQ	Triple quadrupole
RF	Radio frequency
RICC	Reconstructed ion current chromatogram
RNA	Ribonucleic acid
RP	Reversed-phase
S/N	Signal to noise ratio
SCM	Southampton chromatographic method
SD	Standard deviation
SIM	Selected ion monitoring
TBuA	Tributylamine
TBuAA	Tributylammonium acetate
TEA	Triethylamine
TEAA	Triethylammonium acetate
TICC	Total ion current chromatogram
TLF	Time-lag focussing
TWIMS	Traveling-wave ion mobility spectrometry
UHPLC	Ultra high performance liquid chromatography

Chapter 1: Introduction

1.1 Oligonucleotides

Oligonucleotides are relatively short chains of nucleic acids (oligo, from the Greek *oligos*, meaning few). They are made up of the nitrogen-containing bases cytosine, guanine, adenine and thymine (DNA) or uracil (RNA) (Figure 1.1) which undergo Watson-Crick base pairing of cytosine and guanine, and adenine and thymine (or uracil in the case of RNA) and contain a backbone consisting of sugar residues and phosphate groups (Figure 1.2). Typically up to 25 bases in length, therapeutic oligonucleotides are usually described as *n*-mer where *n* denotes the number of bases present. Oligonucleotides can act as probes for a particular gene or section of DNA[1], or can have therapeutic applications that are the subject of this project.

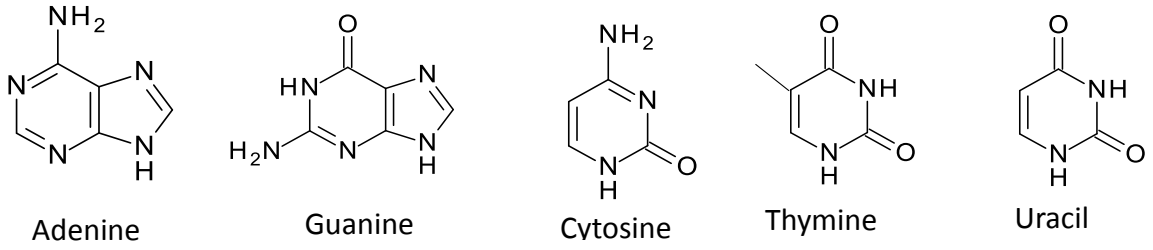

Figure 1.1 - Structures of bases found in DNA and RNA

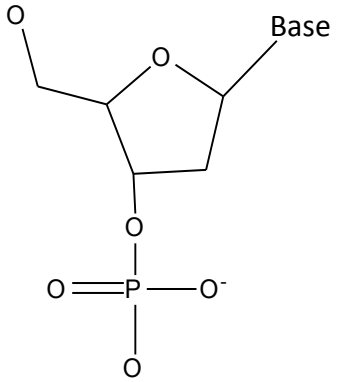

Figure 1.2 - Oligonucleotide backbone unit

Therapeutic oligonucleotides can be broadly grouped into two categories: single-stranded and double-stranded, or duplexed, oligonucleotides[2-3]. Single-stranded

oligonucleotides can be antisense molecules, that is the oligonucleotide is complementary to the “sense” portion of DNA or RNA being targeted [4], or aptamers, used as probes to bind drugs to DNA and RNA targets[5]. Antisense DNA oligonucleotides can act as a substrate for the enzyme ribonuclease H when targeting mRNA; the enzyme then destroys the RNA, preventing translation of the mRNA[6]. Alternatively, the oligonucleotide can bind strongly to the RNA target and prevent translation by a mechanism known as the steric block[4].

Double-stranded oligonucleotides are used in RNA interference (RNAi) mechanisms and can be grouped into short interfering RNA (siRNA) and microRNA (miRNA) [7]. The focus of this project is single-stranded antisense oligonucleotides under 25 nucleotides in length and the analysis and quantitation of their impurities across multiple instrument platforms.

1.1.1 Oligonucleotide synthesis

The synthesis of oligonucleotides falls into three main sections: synthesis of the starting materials; solid phase synthesis to build the desired sequence; and the purification of the oligonucleotide. The starting materials for the majority of therapeutic oligonucleotides are phosphoramidites (Figure 1.3) with dimethoxytrityl (DMT) protecting groups, utilising the phosphoramidite method of solid phase synthesis as described by Beaucage and Caruthers in 1981[8].

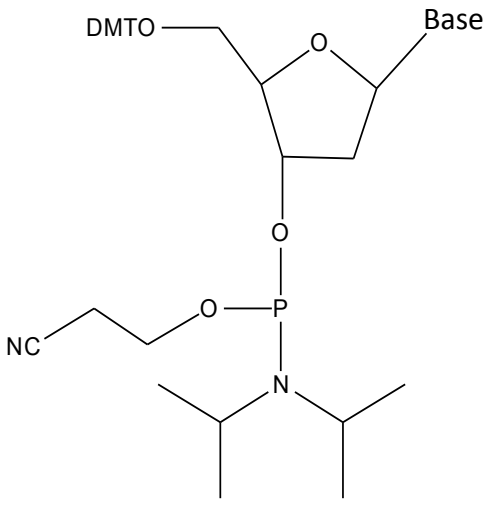

Figure 1.3 - A generic DMT protected phosphoramidite

The four steps of building an oligonucleotide sequence on a solid phase support are illustrated in Figure 1.4. For each base required in the sequence, the coupling step takes place to join the base to the solid support (for the start of the sequence) or to the previous base. Oxidation then occurs using iodine in the presence of water, tetrahydrofuran (THF) and pyridine[9]. For phosphorothioate modified oligonucleotides (see Figure 1.5), this step is replaced by a sulfurisation step where a sulfur containing molecule, such as 3H-1,2-benzodithiole-3-one 1,1-dioxide[10], is used to create the phosphorothioate backbone. The capping step is undertaken to block sequences that have not reacted correctly during the cycle from being added to in the next cycle, in an attempt to reduce the number of full-length and n-1 impurities in the product. The DMT groups are removed from the nucleotides in the detritylation step using di- or trichloroacetic acid in dichloromethane[9] to allow the next base in the sequence to be coupled.

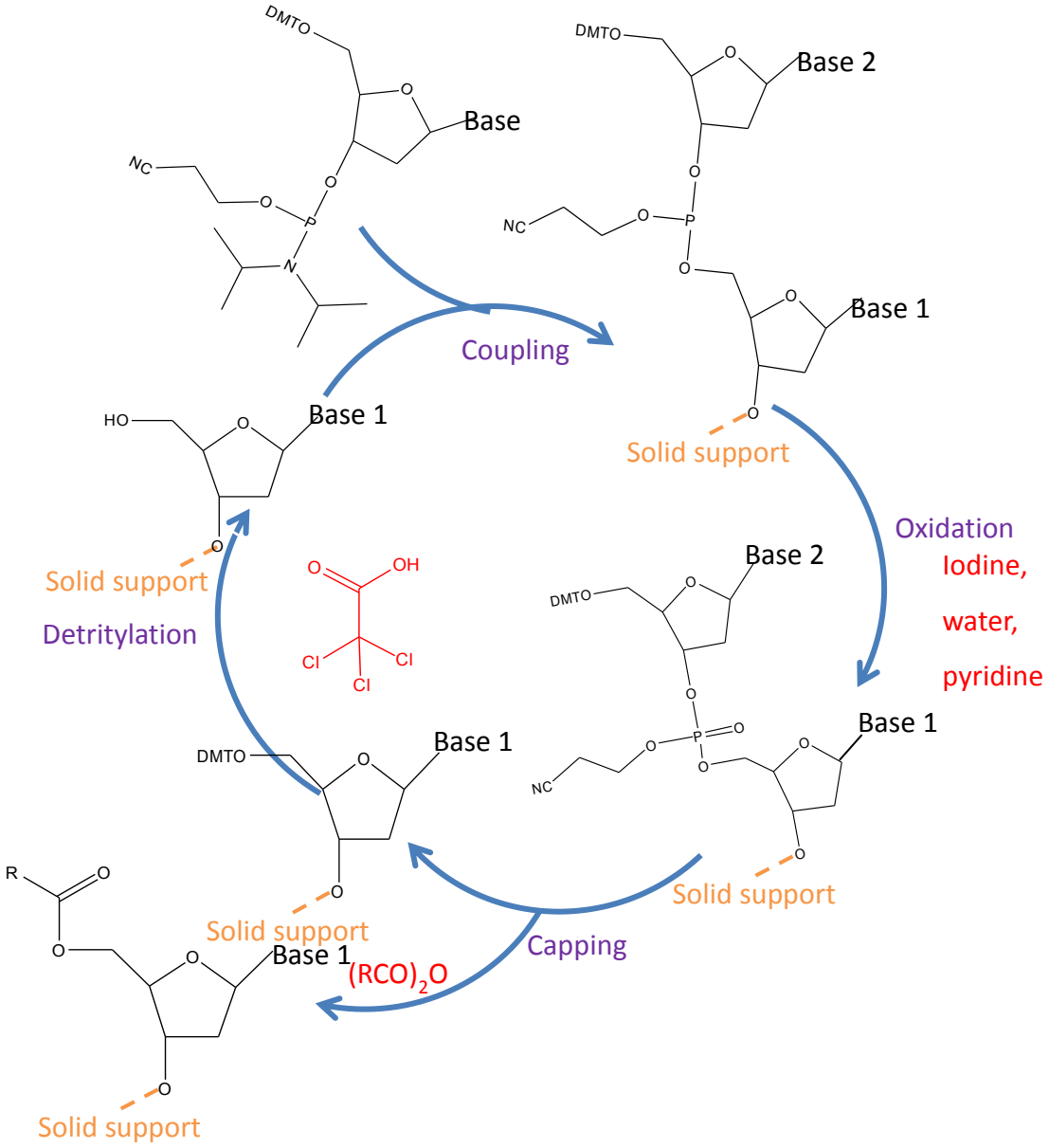

Figure 1.4 - Oligonucleotide solid phase synthesis cycle showing the stages of synthesis (purple text) in an example of a second base being added to a pre-existing base

When the sequence has been completed, it must be removed from the solid phase support and have the DMT group removed from the final nucleotide using ammonia to cleave the oligonucleotide from the support and detritylate the base. The resulting oligonucleotide product is then purified, commonly using chromatography to separate out sequences of the wrong length. In some cases,

the purification takes place after cleavage, with the final detritylation step occurring last[9].

1.1.2 Therapeutic oligonucleotide modifications

Therapeutic oligonucleotides are typically modified from naturally-ocurring DNA to increase stability in the body. A common modification of natural DNA is the replacement of a non-bridging oxygen in the phosphodiester linkage with a sulfur atom forming a phosphorothioate (Figure 1.5), reducing the likelihood of the oligonucleotide being digested by nuclease enzymes and encouraging binding to serum proteins allowing more efficient transfer into tissues[2, 11].

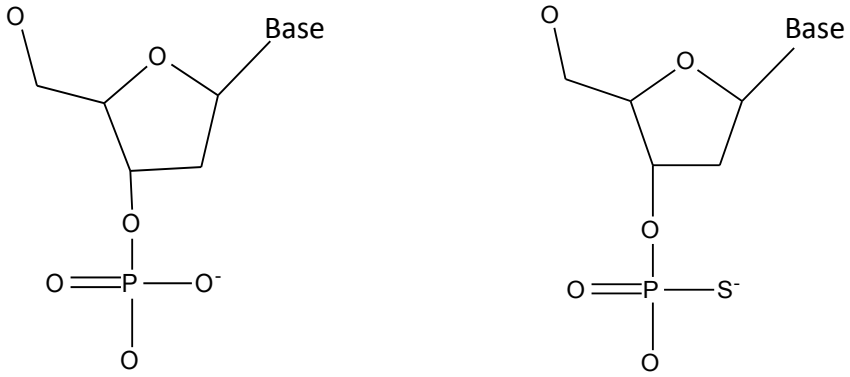

Figure 1.5 - Oligonucleotide modification: (a) phosphodiester; (b) phosphorothioate

Modification of other parts of the natural molecule, such as the sugar or heterocyclic base portions, is also possible, referred to as a second-generation modification[12]. These modifications also enhance stability of oligonucleotides and improve their binding affinity to the RNA target.

Modifications involving constraint of nucleotides are becoming more common[13]. Two examples of these constraint modifications are 2´,4´-constrained 2´*O*-methoxyethyl (cMOE) and 2´,4´-constrained ethyl (cEt) as shown in Figure 1.6.

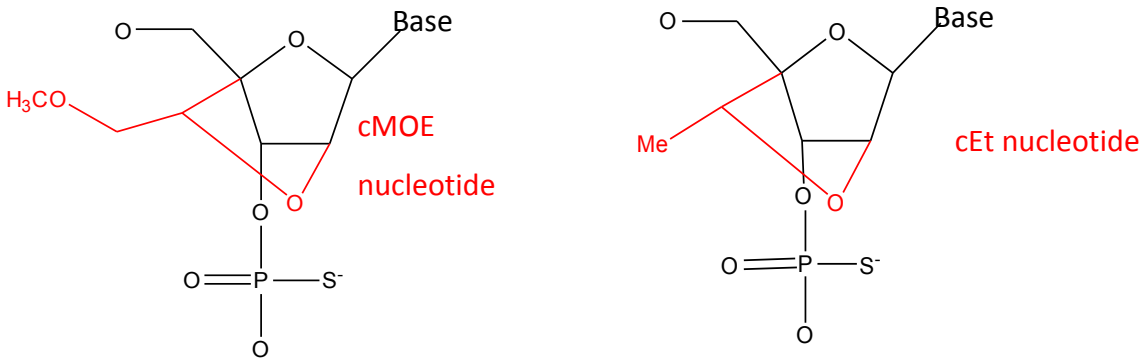

(a) (b)

Figure 1.6 - Constrained oligonucleotide modifications: a) cMOE; b) cEt

The addition of cMOE nucleotides to therapeutic oligonucleotides increases their resistance to enzymatic degradation and cMOE and cEt nucleotides can improve the levels of hybridisation with the target RNA sense strand as a result of an alteration in the sugar ring conformation causing an N-type sugar pucker to ensure that the oligonucleotide has the correct stereochemistry to allow the bases to pair with the RNA target [14].

Four antisense oligonucleotides have received FDA approval to date. Fomiversen (Vitravene) was licenced in 1998 for treatment of the eye condition cytomegalovirus retinitis. Mipomersen (Kynamro), used to treat homozygous familial hypercholesterolemia, was approved in 2013. In late 2016, Nusinersen (Spinraza) and Eteplirsen (Exondys 51) were approved for use in patients with spinal muscular atrophy and Duchenne muscular dystrophy, respectively.

1.1.3 Oligonucleotide impurities

Impurities in therapeutic oligonucleotide drugs are of interest to pharmaceutical manufacturers because the level of purity must be communicated to regulatory bodies when making licence applications for clinical studies or launching to market. The levels of impurity accepted will be based on toxicological studies, batch analysis and the limitations of the manufacturing process and analytical capabilities[15].

Understanding the purity of the sample is crucial to ensure that the desired therapeutic effect is achieved. The International Conference on Harmonisation of Technical Requirements for Registration of Pharmaceuticals for Human Use (ICH) publishes guidelines on the requirements for applying for registration of new drugs. Two of these are of particular interest for drug impurities and, although oligonucleotides are outside of their direct scope, many of the principles can be applied to therapeutic oligonucleotides[15-17]. In the USA, manufacturers must comply with Food and Drug Administration (FDA) codes, which require the submission of information on the purity of drug products before clinical trials can commence or a product can be launched[18].

The complexity of identification of all impurities present in an oligonucleotide sample means that reporting of total deletion (i.e. n-1) or addition (n+1) sequences is deemed adequate as long as these classes of impurity along with other types, as discussed below, are resolved from the target oligonucleotide[15].

The number of steps involved in the synthesis of oligonucleotides introduces many opportunities for impurities to occur[19] along with impurities present in starting materials. Some of the most common impurities found in oligonucleotide samples are sequence deletions and additions, where one or more base is lost from or added to the intended oligonucleotide during the coupling steps of synthesis. Other impurities are residual protecting groups from the cleavage such as isobutyryl or benzoyl containing oligonucleotides and impurities introduced in the capping step of phosphoramidite synthesis. The use of capping solutions can create an impurity of a N^2-acetyl-2,6-diaminopurine residue in place of a guanine residue, indicated by a peak at 41 *m/z* units greater than the oligonucleotide of interest[20]

Impurities introduced during processing or by degradation of the product after synthesis include depurinations where an adenine or guanine base is lost from the oligonucleotide[21], also known as abasic impurities, and dehydrations of these depurinations. Phosphodiester impurities, in the case of phosphorothioate oligonucleotides, occur when one or more non-bridging oxygens remain on the backbone either as a result of a failure in the phosphorothioation process[15], or P-O exchange in the sample[22].

Impurities caused by sequence deletions or additions and depurinations are closely related to the oligonucleotide of interest and, therefore, can be difficult to separate[23-24]. Impurities of the same size as the target oligonucleotide, such as a sequence error, are even more difficult to resolve from the target compound. Residual protecting groups can be separated by mass, having an increased mass over the target oligonucleotide; for example, a residual benzoyl group leads to a peak at 104 *m/z* units higher than the target species[25]. Phosphodiesters can typically be separated chromatographically from the pure oligonucleotide as they have a different retention time[22], this separation would be confirmed by high resolution mass spectrometry.

The large number of steps involved in the synthesis of therapeutic oligonucleotides mean that high levels of purity are much harder to achieve than for small drug molecules. At the 2017 *Aspects of Quality Throughout the Development of Oligonucleotides* symposium, leading oligonucleotide researcher Dr Susan Srivatsa suggested that the most important focus for purity testing of therapeutic oligonucleotides is the safety of the product rather than the absolute purity. This would require an understanding of the medicinal activity and toxicity of each class of impurity. A phosphodiester impurity, for example, will be as safe as a fully phosphorothioated oligonucleotide but slightly less active and sequence deletions from within the sequence will not be therapeutically active but would be unlikely to be less safe than the intended drug, whereas a terminal sequence deletion will still be active but may have a different action from that intended[26].

1.2 Liquid Chromatography

High Performance Liquid Chromatography (HPLC) is a method of chromatographically separating different compounds based on their level of interaction with the liquid mobile phase and the stationary phase of the column. This technique is suitable for a wide range of compounds including those of high molecular weight, not having the requirements of thermal stability and volatility for gas chromatography[27]; HPLC instruments can separate polar and non-polar analytes and can be used for ionic samples.

Separation of compounds is effected by the differences in their interaction with the mobile and stationary phases depending on their chemical properties and on the type of interactions between the compound and the stationary phase. Chemical properties affecting separation include polarity and ionisation potential. The stronger the interaction between the analyte and the stationary phase the longer the compound will be retained on the column. The affinity of a compound for the stationary phase under a given set of chromatographic parameters is described by the distribution constant[28] Kx:

$$\mathrm{Kx} = \left(\frac{Concentration\ in\ stationary\ phase}{Concentration\ in\ mobile\ phase}\right) \qquad \text{Equation 1.1}$$

A compound with a higher K value will be retained on the column for longer than one with a lower value of K and will, therefore, have a longer retention time. A Kx value of greater than one indicates the compound is retained on the column and interacts with the stationary phase; values below one mean the analyte is not retained and is not undergoing chromatographic separation.

The resolution (R) of chromatographic peaks is a measure of how well separated two analytes are using a given chromatographic column, mobile phase and conditions. There are two methods of calculating resolution. The first method uses the retention time of each peak and the peak width as shown in Equation 1.2, where t_{R2} and t_{R1} are the retention times of the second and first peaks being studied, respectively and w_{b1} and w_{b2} are the peak widths of each peak[29] as illustrated in Figure 1.7.

$$R = \frac{(t_{R2} - t_{R1})}{(w_{b1} + w_{b2})/2} \qquad \text{Equation 1.2}$$

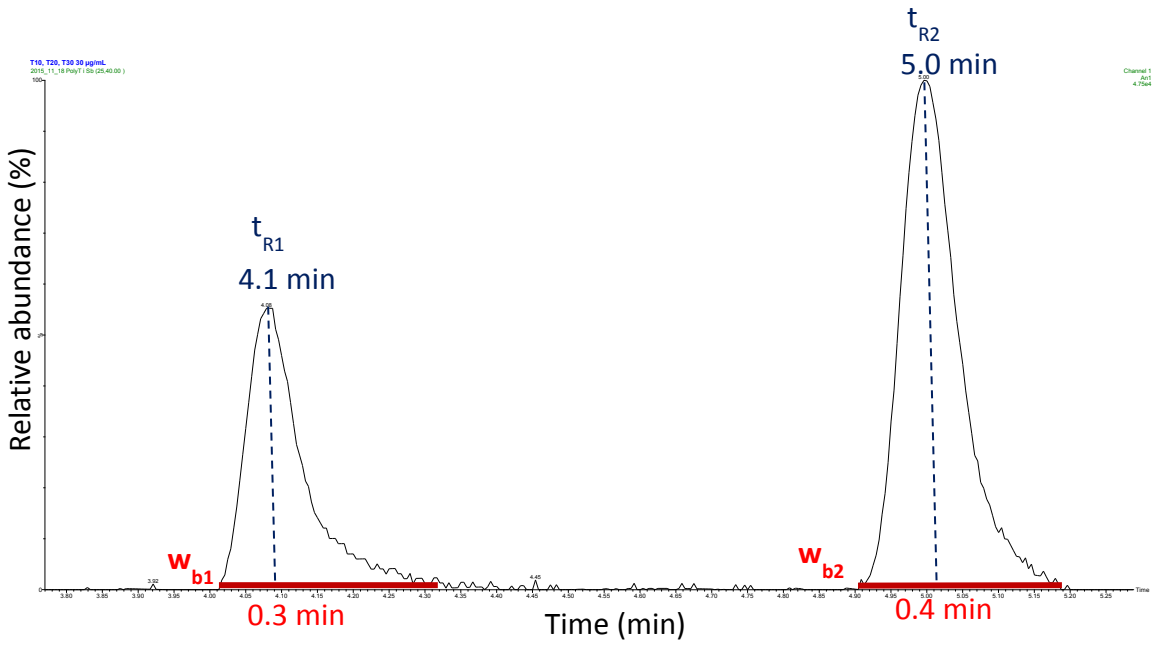

Figure 1.7 - Illustration of t_R (blue dashed line) and w_b (solid red line) from Equation 1.2

The second method for calculating resolution uses the retention time of each peak and the peak width at half height as shown in Equation 1.3, where t_{R2} and t_{R1} are the retention times of the second and first peaks being studied, respectively and $b_{0.5(1)}$ and $b_{0.5(2)}$ are the peak widths at half height for each peak as illustrated in Figure 1.8. A factor of 1.177 is applied to the calculation to take into account the use of the peak width at half height.

$$R = \frac{1.177(t_{R2} - t_{R1})}{b_{0.5(1)} + b_{0.5(2)}} \qquad \text{Equation 1.3}$$

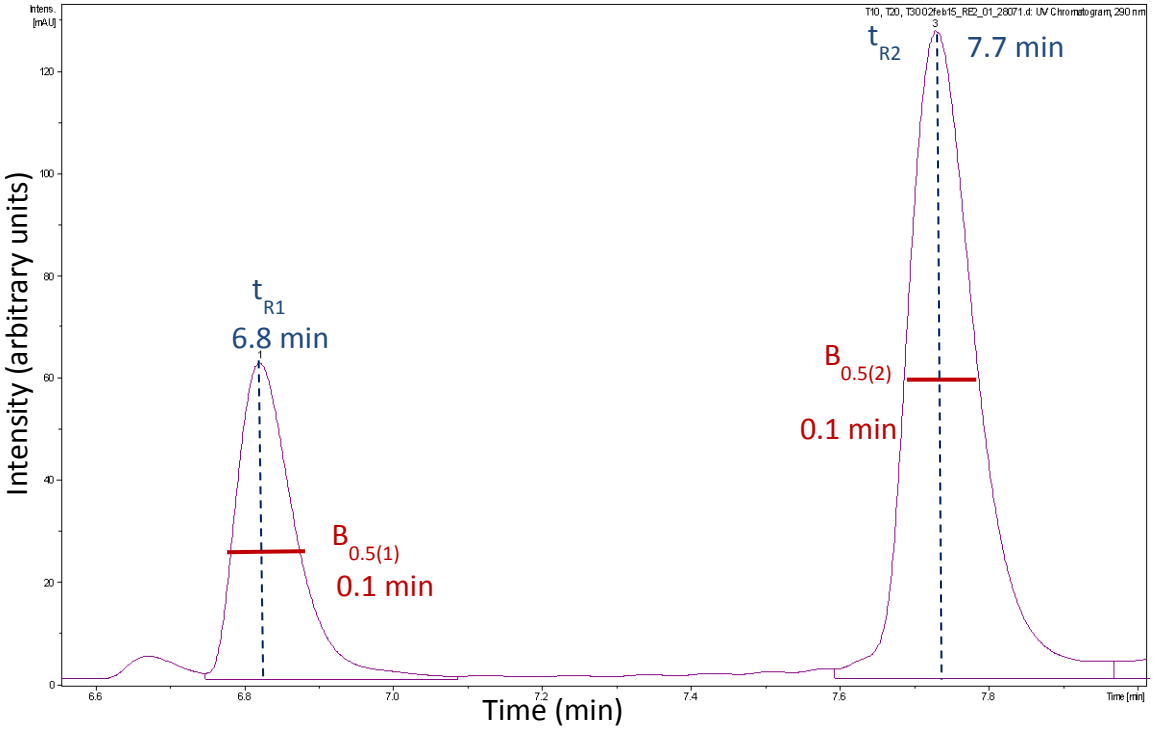

Figure 1.8 - Illustration of t_R (blue dashed line) and $b_{0.5}$ (solid red line) from Equation 1.3

The use of Equation 1.3 reduces the complexity of calculating resolution for peaks which are not baseline resolved or exhibit a degree of tailing or fronting by utilising the peak width at half height.

The factors affecting resolution are efficiency, capacity factor or retention and selectivity[29].

1.2.1 Efficiency (N)

For efficient separation to take place, chromatographic peaks should be as sharp as possible. The broadness of a peak is analogous to the Height Equivalent to Theoretical Plate (HETP) measurement of resolving power of the column as described by the Van Deemter equation[30] (Equation 1.4)

$$\mathrm{HETP} = \mathrm{A} + \left(\frac{\mathrm{B}}{\mu}\right) + (\mathrm{C}\mu) \qquad \text{Equation 1.4}$$

where A refers to the eddy diffusion of the column; B refers to the molecular diffusion occurring within the column; C refers to the mass transfer of analyte molecules in the column; and μ refers to the linear velocity of the system. A theoretical plate is the distance required for an analyte to complete one equilibration between the stationary phase and mobile phase.

The A term of the Van Deemter equation, eddy diffusion, is related to the packing of the stationary phase in the analytical column; the greater the number of paths available to an analyte molecule during its transit through the column, the larger the eddy diffusion and the broader the chromatographic peak. In a column with large particles, the difference in time taken for an analyte to travel from one end of the column to the other can be large, creating a high level of eddy diffusion and broad peaks. Small particle size reduces the time an analyte molecule can spend within a particle, lowering the eddy diffusion (see Figure 1.9). As shown in Figure 1.12, eddy diffusion is largely unaffected by the linear velocity of the mobile phase; this is a result of the rate of transfer of molecules in and out of particle pores being significantly faster than typical linear velocities employed in HPLC.

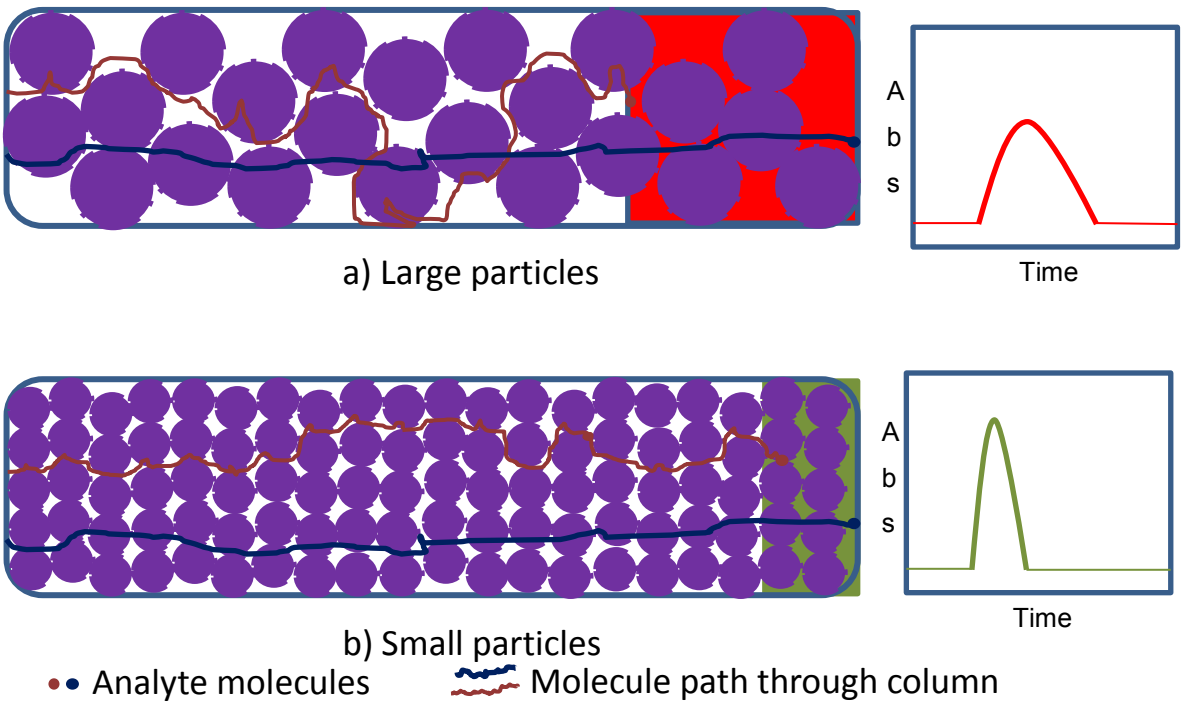

Figure 1.9 – Effect of particle size on eddy diffusion and chromatographic peak width; the two molecule paths shown for each particle size indicate the potential difference in time taken for different molecules of the same analyte to travel through the column depending on the level of eddy diffusion encountered

Longitudinal diffusion, the B term of the Van Deemter equation, is a measure of how much the analyte molecules within a band of sample disperse during analysis. Analyte molecules will tend to disperse from the centre of the band to the edges as a result of concentration gradients within the system, with the greatest dispersion in the direction of flow. The longer the sample spends travelling through the HPLC system, the broader the analyte band becomes and, therefore, the B term is strongly affected by the mobile phase flow rate with higher flow rates leading to lower diffusion and broadening. Correct installation of the column and tubing to reduce internal volumes of the system also helps to reduce longitudinal diffusion and is especially important in HPLC-MS systems where lower flow rates are required for MS compatibility.

The third, C, term of the Van Deemter equation is mass transfer; as analyte molecules travel through the chromatographic column, they may enter the pores of the stationary phase to different depths (see Figure 1.10). Stagnant mobile phase collects in the pores and molecules can only be released from this by diffusion. This means that analyte molecules which travel deeper into the pores will take longer to reach the detector than those only entering the pore to a shallow depth or those not entering the pore at all (see Figure 1.11). The difference in time taken to arrive at the detector creates the width of the peak, such that a higher C term indicates a broader chromatographic peak.

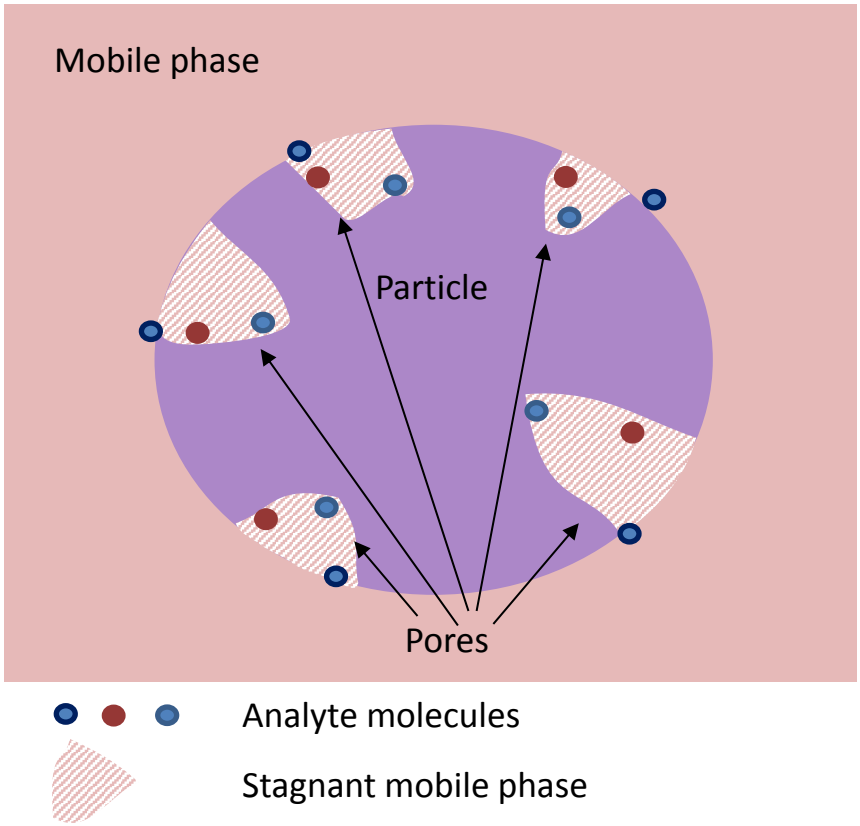

Figure 1.10 – Potential depth of entry into particle pores of analyte molecules

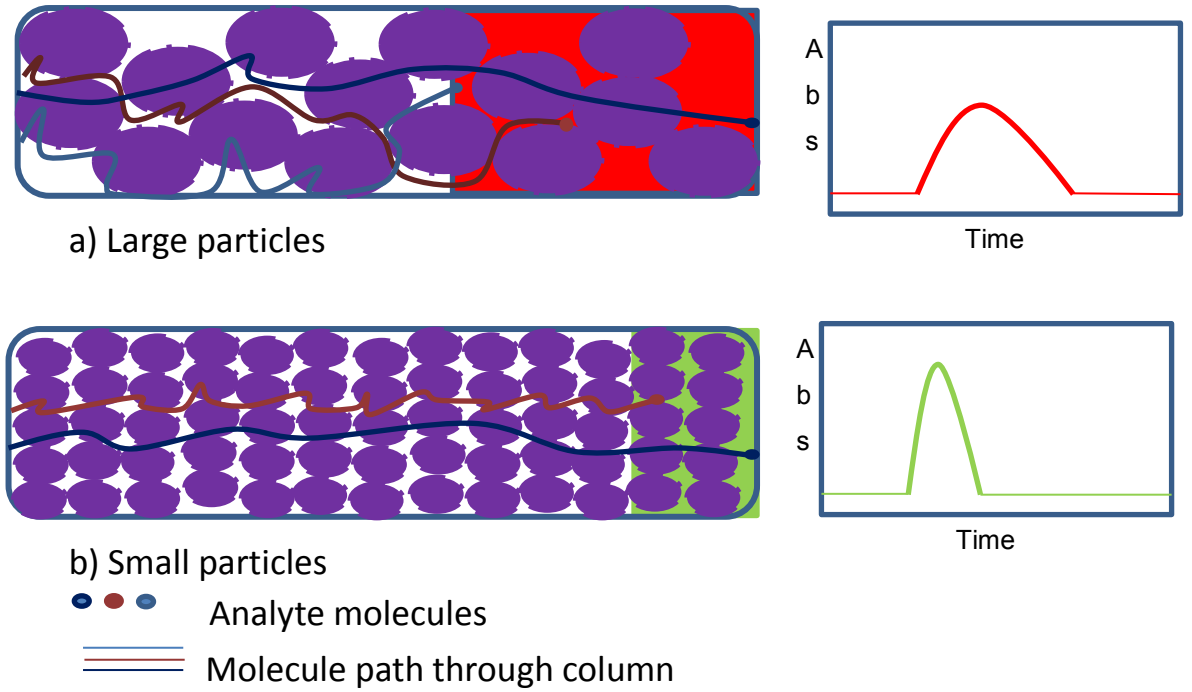

Figure 1.11 - Effect of particle size on mass transfer and chromatographic peak width

The effect of mass transfer can be reduced by several mechanisms. Firstly, the use of smaller particle sizes reduces the mass transfer effect as the smaller the particle, the shallower the pores and, therefore, the difference in time to reach the

detector between molecules is reduced. A reduction in linear velocity also has an effect, as at slower flow rates the molecules not entering the pores or only entering to a shallow depth do not travel as far along the column in the time it takes the more deeply entering molecules to diffuse out of the pores. In the case of reversed-phase chromatography, increasing the temperature of the column increases the rate of analyte molecule diffusion out of the pores and reduces band broadening.

The higher the HETP value derived from the Van Deemter equation, the broader the chromatographic peak produced because a higher HETP value equates to a lower number of theoretical plates as the efficiency of the column (measured in theoretical plates) is inversely proportional to the height of the plates.

$$\mathrm{H} = \frac{L}{N} \qquad \text{Equation 1.5}$$

Where H is the height of the theoretical plates, L is the length of the column and N is the number of theoretical plates. A high value of N means that the analyte has more chances to equilibrate between the stationary and mobile phases and chromatographic separation is improved.

To produce high quality peaks with good resolution, the linear velocity – as determined by HPLC flow rate - is optimised to the lowest possible HETP value with given values of A, B & C as depicted in a Van Deemter plot (Figure 1.12).

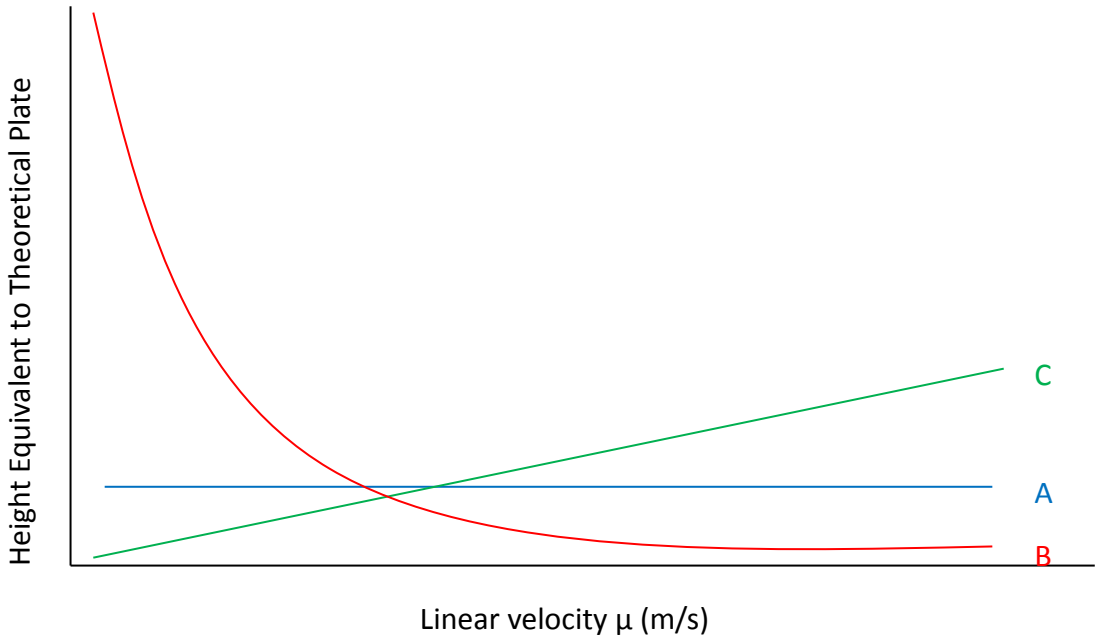

Figure 1.12 – Plot of the terms of the Van Deemter equation relative to linear velocity.

A Van Deemter plot can be created for any analyte, based on Figure 1.12, taking into account all three terms of the Van Deemter equation; this chart can be used to predict the flow rate that will provide the best efficiency for that analyte. Figure 1.13 shows a theoretical Van Deemter plot for a hypothetical analyte.

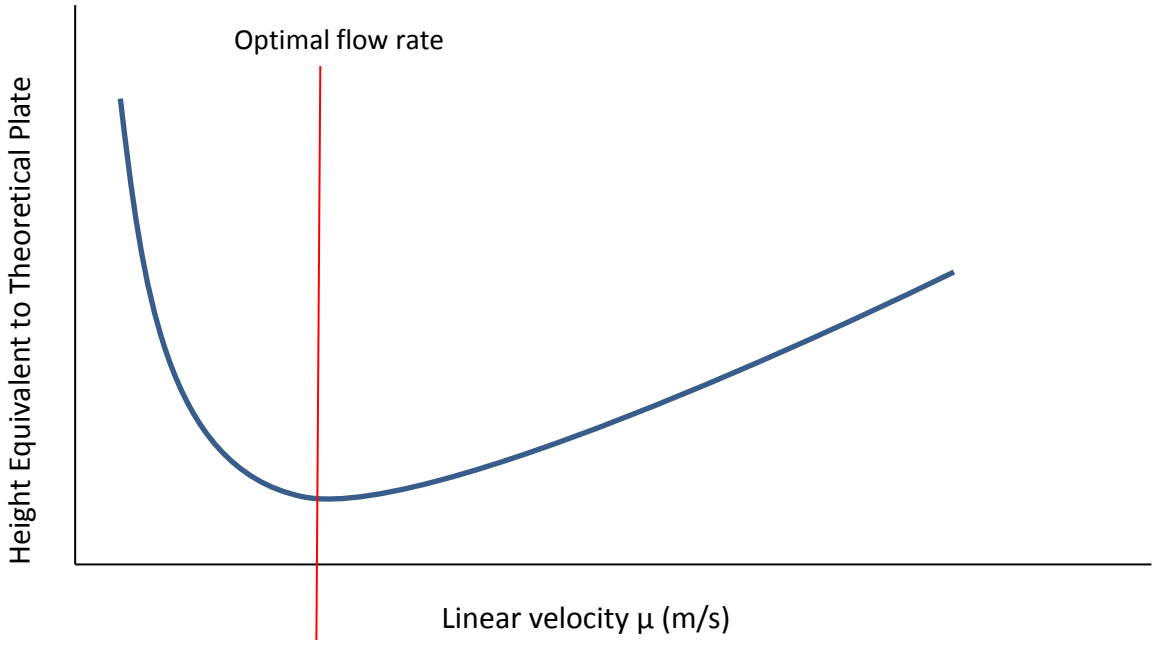

Figure 1.13 – Theoretical Van Deemter plot for a hypothetical analyte showing the efficiency of the column at changing linear velocities and indicating the optimal point on the curve.

The size of the stationary phase particles in the HPLC column are of importance for the efficiency of the chromatographic separation and the analysis time; smaller particles reduce the eddy diffusion and effects of mass transfer within the column, leading to sharper peaks and allowing the use of faster mobile phase flow rates. In a standard HPLC system, however, there is a limit to the minimum particle size and maximum flow rates that can be used without increasing the back pressure of the system to unsustainable levels. Some newer HPLC systems can support the back pressure generated by the use of sub-2 μm particles and ultra-high performance liquid chromatography (UHPLC) instruments are designed to operate at much higher back pressures than HPLC systems (up to 1000 bar vs. up to 400 bar), allowing the fast analysis of samples with the use of small particles and fast flow rates of over 1 mL/minute.

1.2.2 Capacity factor or retention (k)

The capacity factor of a column is a measure of how well retained a given analyte is by the stationary phase of the column under given chromatographic conditions[29]. The retention of an analyte is calculated as shown in Equation 1.6

$$\mathrm{k} = \frac{t_R - t_0}{t_0} \qquad \text{Equation 1.6}$$

where t_R is the retention time of the analyte of interest and t_0 is the retention time of a non-retained compound (see Figure 1.14). The non-retained compound can be the mobile phase solvent or an added analyte, such as uracil for reversed-phase chromatography systems which is known to not interact with the stationary phase.

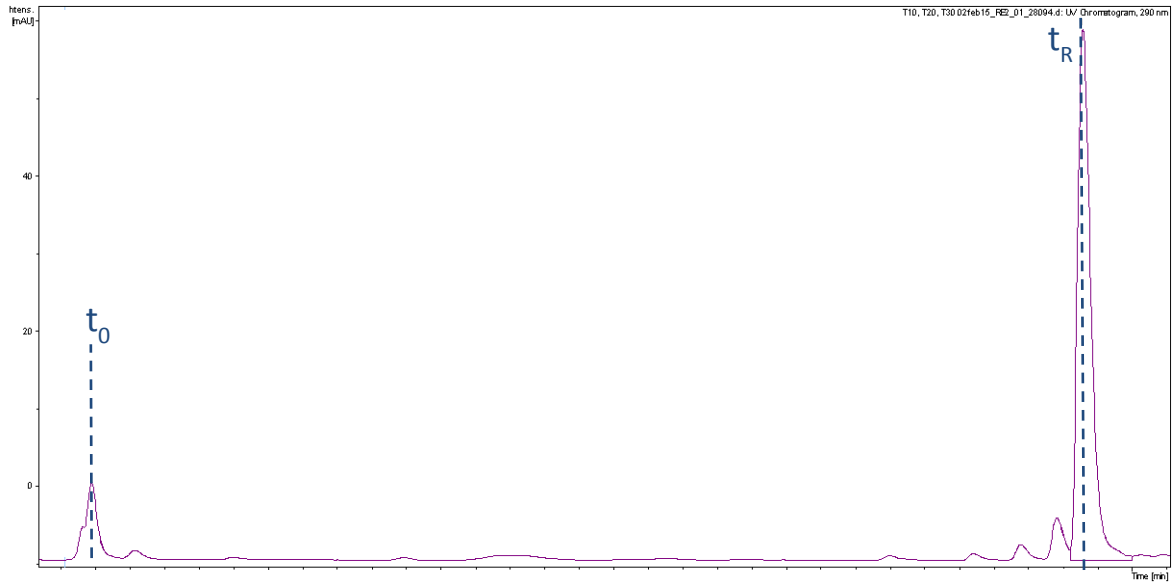

Figure 1.14 – Illustration of t_0 and t_R as used in Equation 1.6

Retention of an analyte on the column for reversed-phase systems is most effectively adjusted between analyses by an alteration of the polarity of the organic component of the mobile phase – increasing the polarity increases retention from one analytical experiment to the next and *vice versa*.

A low value of k indicates poor retention and may negatively impact resolution as the analytes of interest may be inadequately retained and co-elute with the mobile phase solvent. If multiple analytes of interest have low k values, they may be insufficiently separated from each other as the time spent on the column is not long enough to allow differentiation. A very high value of k would lead to long analysis times, which are undesirable for routine and high throughput analysis.

1.2.3 Selectivity (α)

The selectivity of a chromatographic column refers to its ability to differentiate between two different analytes in a sample; the retention of each peak (k) is used to calculate the selectivity of the system, shown in Equation 1.7

$$\alpha = \frac{k_2}{k_1} \qquad \text{Equation 1.7}$$

where k_1 is the retention or capacity factor of the first peak of interest and k_2 is the capacity factor of the second peak. Selectivity can be altered by changing chromatographic parameters such as mobile phase pH, stationary phase, mobile

phase constituents and, in the case of reversed-phase chromatography, temperature of the column[27].

The effect of each of these three factors on resolution for isocratic chromatographic separations is indicated in Equation 1.8.

$$\mathrm{R} = {}^{1}/_{4}\sqrt{N} * \frac{\alpha - 1}{\alpha} * \frac{k}{1 + k} \qquad \text{Equation 1.8}$$

Separation mechanisms utilised in HPLC include normal-phase, reversed-phase, ion-pairing and ion exchange; the latter three are of particular interest in the analysis of oligonucleotides.

1.2.4 Reversed-phase HPLC

Reversed-phase HPLC (RP-HPLC) is so named because it is the opposite of the antecedent normal-phase chromatography; in RP-HPLC, the mobile phase is more polar than the stationary phase[29]. Probably the most commonly used stationary phase is RP-HPLC is C18 (an alkyl chain of 18 carbons in length), but C8, cyano, phenyl and amino based stationary phases are also suitable for reversed-phase separations. Mobile phases used for RP-HPLC are generally a mixture of water and an organic solvent such as methanol or acetonitrile. The composition of the mobile phase can be altered to increase or decrease its polarity to encourage the analytes to partition onto the stationary phase or elute into the mobile phase and thus into the detector respectively. In the case of gradient mobile phase elution in RP-HPLC, the composition of the mobile phase begins at a high percentage of aqueous component, repelling non-polar, hydrophobic, analytes onto the stationary phase. As the analysis progresses, the percentage of the organic mobile phase component is increased; this has the effect of attracting analytes from the stationary phase back into the mobile phase depending on their polarity and hydrophobicity, with more non-polar or hydrophobic compounds requiring a higher percentage of organic constituent for elution.

1.2.4.1 RP-HPLC column chemistries

RP-HPLC columns typically consist of a silica support bead onto which stationary phases are bonded. Silica beads used in the manufacture of chromatographic

columns are highly porous, creating a large surface area over which the separation of analytes can occur. Particles using a combination or hybrid of silica and organosiloxanes are also available, such as the Waters BEH particle[31], promising improved chemical stability and reduced silanol active sites over silica particles. To create the stationary phase, chlorosilanes of the stationary phase type of choice (*e.g.* C18 or C8) are reacted with the surface silanol groups of the support bead to create silyl ether linkages, thereby bonding the stationary phase to the support bead (see Figure 1.15). Chlorosilanes can contain one, two or three chlorine atoms and can form one, two or three silyl ether linkages, respectively; the multiple linkages formed by di- and tri-chlorosilanes create a more stable stationary phase, with a wider operating pH range, as the increased number of linkages reduces the likelihood of the stationary phase being removed from the silanol group of the support bead by hydrolysis at low pH[32].

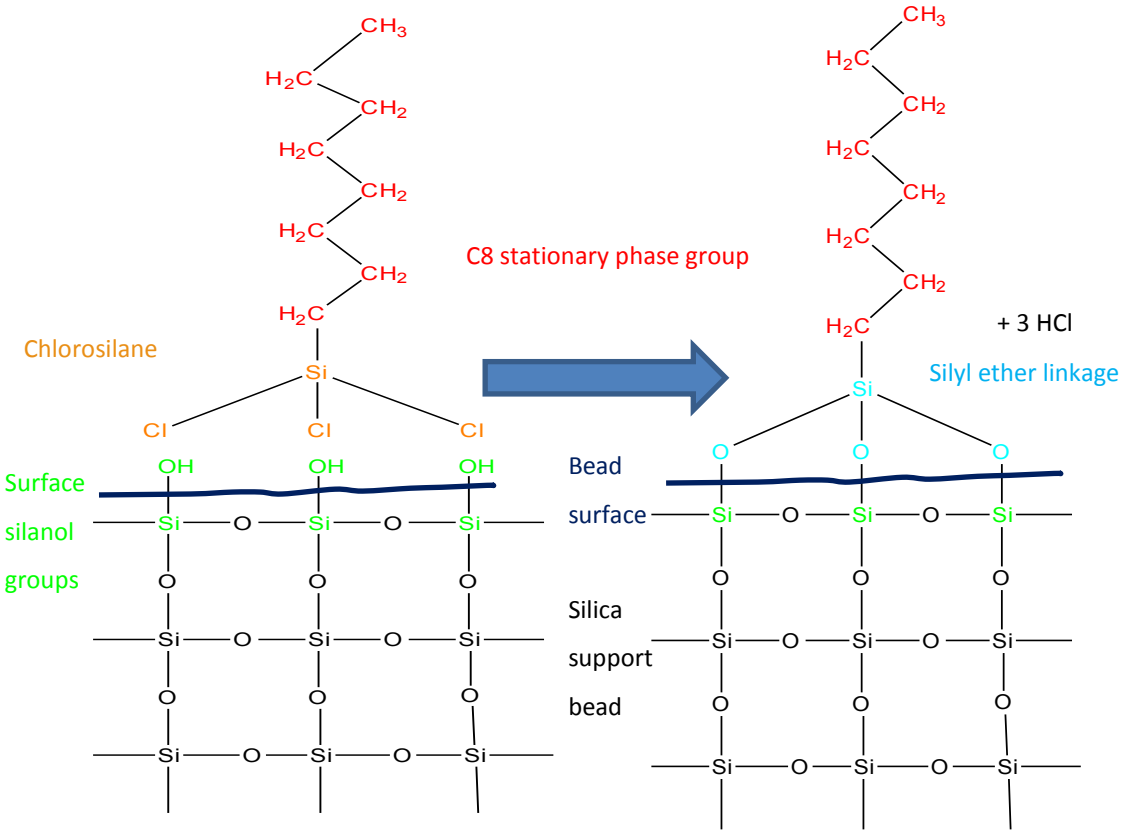

Figure 1.15 - Addition of the stationary phase to a silica support bead for RP-HPLC columns, using C8 as an example stationary phase

During the process of adding the stationary phase, not all surface silanol groups will react; this creates the possibility of analyte molecules interacting with

remaining silanol groups and being retained for a different length of time than those molecules interacting with the stationary phase. To reduce the number of silanol groups available for interaction, chromatographic columns are often end-capped with a less reactive group such as trimethylsilyl.

The stationary phase of RP-HPLC columns is less polar than the mobile phase, encouraging retention of non-polar compounds; the polarity of the stationary phase can be selected to improve separation of analytes with polar functional groups. Of the commonly used RP-HPLC stationary phases, C18 is the least polar, giving the greatest retention for non-polar analytes, with polarity increasing through shorter alkyl groups (*e.g.* C8 and C4) to the more polar cyano, phenyl and amino stationary phases. Decreasing the length of alkyl chain typically reduces the retention time of analyte molecules but has little effect on the selectivity or elution order of analytes when comparing C18 and C8 columns; much shorter alkyl chains and other stationary phases affect the retention time, selectivity and elution order of analytes.

1.2.5 Ion-pairing HPLC

Ion-pair chromatography (IP-HPLC) uses added reagents to allow separation of amphoteric analytes where the use of pH control to suppress the ionisation is unsuitable[27]; this technique is often combined with RP-HPLC columns to give a method of separation known as ion-pair reversed-phase chromatography (IP-RP-HPLC). IP-RP-HPLC is particularly useful for the chromatographic separation of weakly basic or acidic compounds and ionic compounds that would require a working pH outside of the tolerance of RP-HPLC columns to ensure full ion suppression and, therefore, retention.

Ion-pair reagents allow analytes to be retained on the stationary phase by two mechanisms. The analyte and the charged functional group of the ion-pair reagent can form a neutral complex in the mobile phase with the hydrophobic portion of the ion-pair reagents then interacting with the stationary phase as in standard RP-HPLC. Conversely, the ion-pair reagent can interact hydrophobically with the stationary phase and ion exchange will then occur between the analyte and the functional group of the reagent, creating retention. There has been some debate about which of the two mechanisms is dominant and this may depend on the HPLC conditions and the reagent used[33-34]. It has been suggested that the former

mechanism dominates in low concentrations of ion-pair reagent with the latter becoming dominant as the ion-pair reagent concentration increases.

Common ion-pair reagents for the separation of acidic analytes include triethylamine (TEA) and triethylammonium acetate (TEAA), while ion-pair reagents for basic analytes tend to be acids, such as trifluoroacetic acid[35-36] and hexanesulfonic acid. If the HPLC separation is to be coupled to a mass spectrometer, the choice of ion-pair reagents and buffers is critical as will be discussed later.

1.2.6 Ion exchange HPLC

Ion exchange chromatography uses a charged stationary phase to create interactions with analytes holding the opposite charge[27]; this mechanism has successfully been used to separate oligonucleotides. Long oligonucleotides have a greater number of negative charges than shorter ones, making anion-exchange chromatography particularly suitable for separating sequence deletions and additions from the target analyte[37].

Ion exchange HPLC has been used for the detection of oligonucleotides by UV, with mixed-mode reversed-phase and anion exchange columns having the potential to chromatographically separate oligonucleotides from their impurities at least as well as IP-RP-HPLC[38]. The non-volatile salts and buffers that are typically used in ion exchange chromatography make this technique unsuitable for coupling to mass spectrometers using electrospray ionisation (ESI-MS)[39].

1.3 Mass Spectrometry

At its most basic, a mass spectrometer (MS) is an analytical instrument that can produce gas phase ions of the analyte of interest, separate those ions by their mass to charge ratio (*m/z*) and detect and record the number of ions of each *m/z* unit produced. The separation of ions, and in some cases the ionisation of the sample, occurs under vacuum to prevent air from masking the signals created by the analytes of interest, creating fragmentation of the ion of interest or affecting the energy or flight time of the ions (Figure 1.16). There are several methods of creating ions for analysis, depending on the type of analyte and the chromatographic method (if any) used to introduce the sample to the MS, these

include: electron ionisation; atmospheric pressure ionisation, including electrospray ionisation (ESI) and atmospheric pressure chemical ionisation (APCI); matrix- assisted laser desorption/ionisation (MALDI); and inductively coupled plasma (ICP). For analysis of oligonucleotides, the most commonly used ionisation techniques are ESI and MALDI.

Following ionisation, there are various types of mass analyser used to separate the ions. Commonly utilised analysers are quadrupoles, octopoles, time-of-flight (TOF) and ion trap systems. Quadrupole and TOF mass analysers will be considered in more detail here as they have been widely used for the analysis of therapeutic oligonucleotides and are used in this research.

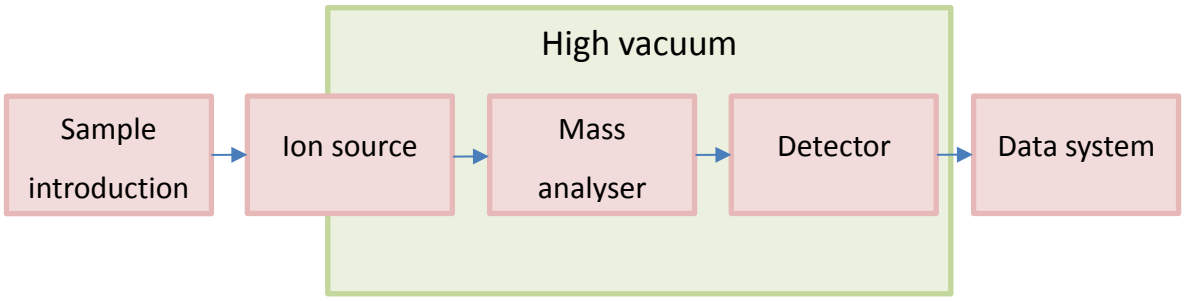

Figure 1.16 - Schematic representation of a generic mass spectrometer – the ion source may be under vacuum or at atmospheric pressure depending on the instrumentation used

1.3.1 Electrospray Ionisation

Electrospray ionisation (ESI) is an atmospheric pressure ionisation technique, meaning that the formation of ions occurs before the sample enters the section of the instrument under vacuum. In ESI, a potential difference is applied between the capillary tip bringing sample from the HPLC system and the sampling cone where the ions are transferred into the mass analyser; the charge applied to each part will depend on which mode has been selected. In positive ion ESI, the capillary tip has a positive potential with respect to the sampling cone and cationic analyte ions are repelled from the tip and attracted to the sample cone. In negative ion ESI the potentials are reversed to favour anionic sample ions.

The charge on the capillary tip causes the formation of charged droplets that are repelled by the capillary tip. As the liquid emerges from the capillary tip it undergoes coulombic repulsion in response to the number of ions with the same

charge in close proximity, changing the shape of the meniscus to the straight sided "Taylor cone" (Figure 1.17) which leads to the expulsion of a stream of droplets[40]. As the droplets pass through the desolvation zone between the capillary and the sampling cone, solvent is lost and the groups of ions within a droplet split into individual gas phase ions; there are two theories to explain how this process occurs (Figure 1.18 and Figure 1.19). The charged residue model (CRM) published by Dole *et al*. in 1968 proposes that the droplets continue to become smaller as a result of coulombic repulsion until, as the solvent evaporates from a single molecule of an analyte, any charge carried by the solvent is transferred to the analyte molecule[41]. The ion evaporation model (IEM) proposed by Iribarne & Thompson in 1976 suggests that individual ions evaporate out of droplets with a radius smaller than 10nm[42]. Recent investigations have suggested that the IEM is the best fit for small molecules, whereas for large molecules such as oligonucleotides the CRM provides a better explanation of the formation of ions[43-44]. An interesting observation made by Hogan *et al*. is that in the presence of buffers such as TEA, TEAA or ammonium acetate a mixture of the two models occurs; it is suggested that buffers require less energy than large analyte molecules to undergo evaporation, so the initial process follows the IEM and then once the buffer has been lost, the CRM continues as expected[45].

ESI is a "soft" ionisation technique, meaning that very little fragmentation occurs in the ion source. The ions generated by ESI can be protonated or deprotonated analyte molecules with the notation $[M + H]^+$ or $[M – H]^-$ formed by positive and negative ion ESI respectively; other ions may be formed with the addition of other cations such as sodium, potassium or ammonium, leading to adducts such as $[M + Na]^+$, the generic notation here would be $[M + X]^+$. Large molecules, such as oligonucleotides can hold multiple charges, i.e. $[M - nX]^{n-}$, where X = H, Na, K, etc.

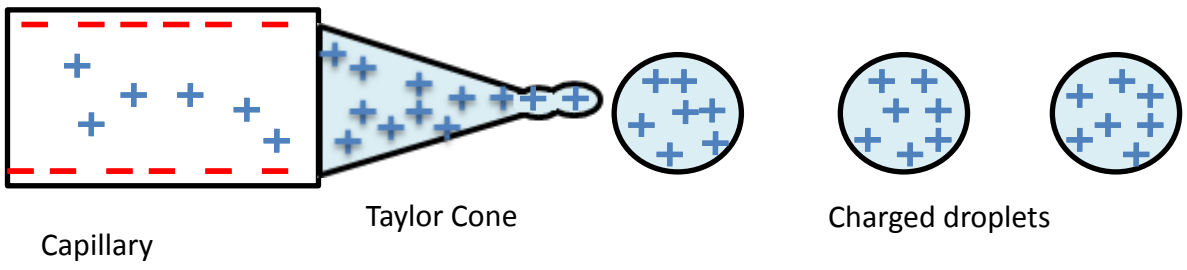

Figure 1.17 - Depiction of the Taylor Cone formation

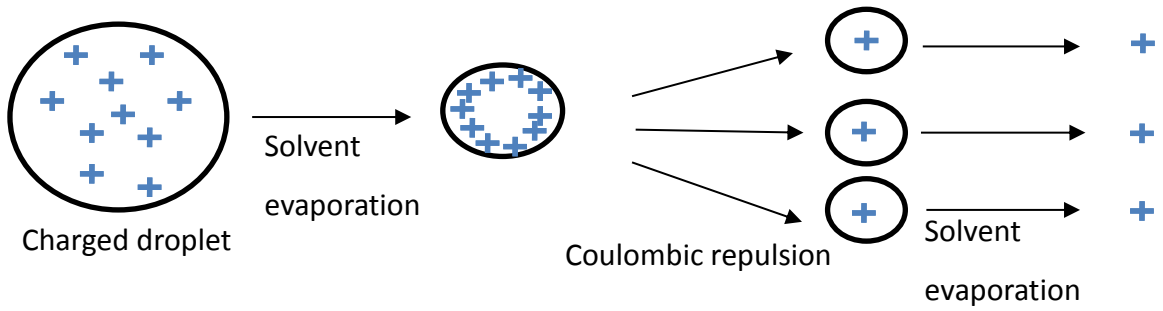

Figure 1.18 - Depiction of the charge residue model

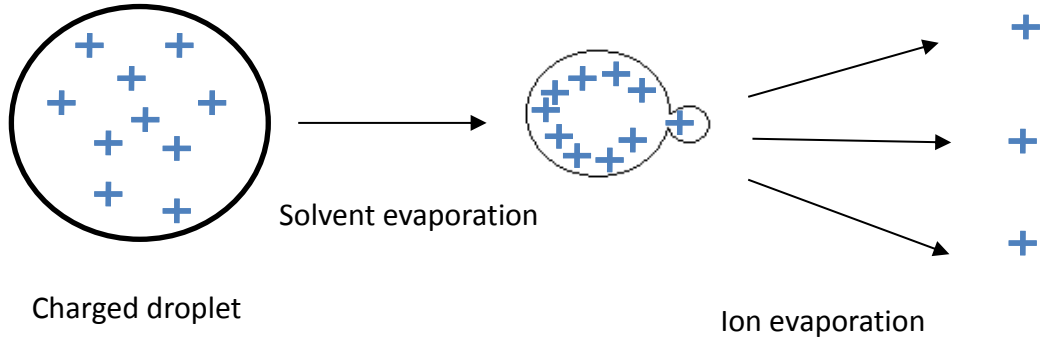

Figure 1.19 - Depiction of the ion evaporation model

For efficient ion transmission from an ESI source, the positioning of the capillary relative to the sampling orifice allowing ions into the mass analyser must be optimised for the analyte of interest. Modern ESI sources typically have an orthogonal position for the sampling orifice or cone relative to the capillary to reduce the number of charged droplets, neutral molecules and solvent ions reaching the mass analyser in relation to the number of analyte ions. Figure 1.20 illustrates the Waters Z-Spray orthogonal source design.

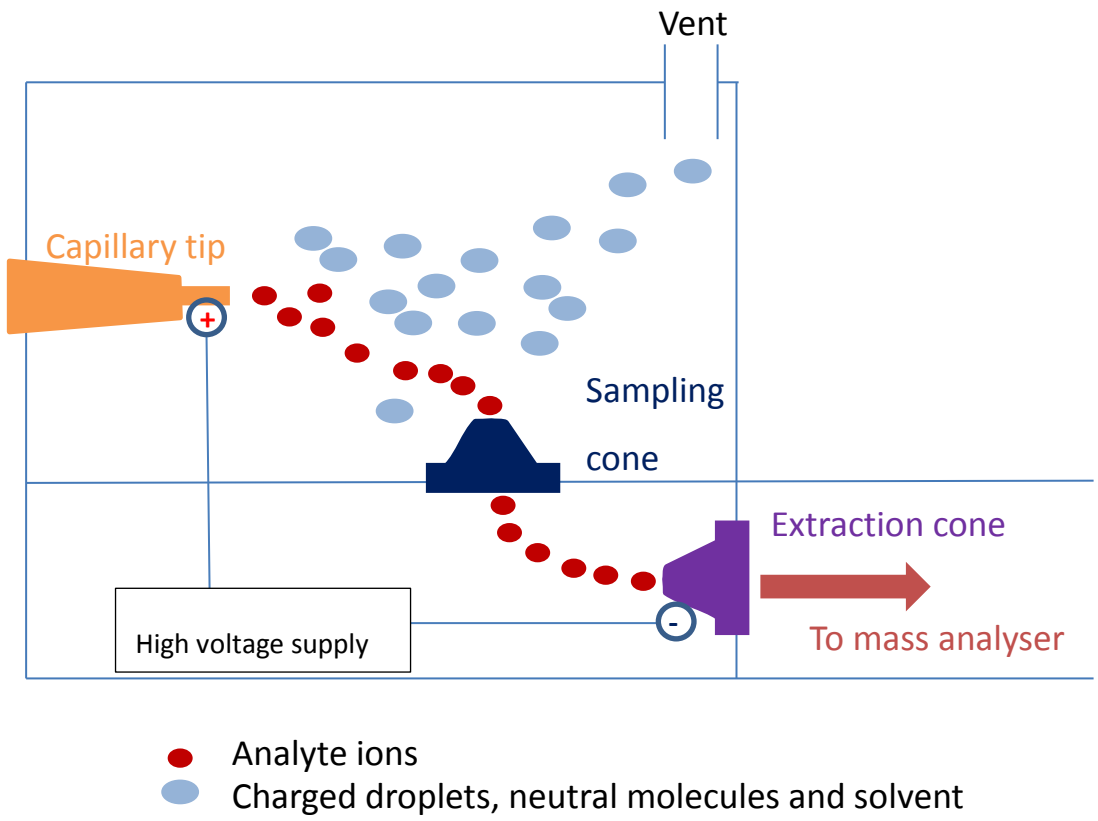

Figure 1.20 – Depiction of a Waters Z-Spray orthogonal ESI source operating in positive ionisation ESI

1.3.2 Matrix-Assisted Laser Desorption/Ionisation

Matrix-assisted laser desorption/ionisation (MALDI) also forms protonated or deprotonated molecules and adducts with the same notation as those used in ESI. An advantage of MALDI over ESI for the analysis of large molecules is the production of intact $[M + H]^+$ or $[M – H]^-$ ions rather than the multiply-charged ions generated by ESI; this simplifies the mass spectrum but is only suitable for mass detectors capable of detecting large ions. MALDI ions are generated from a solid sample. The sample is mixed with a matrix of small organic molecules that absorb in the UV wavelengths, applied to a plate and allowed to crystalise. Common MALDI matrices for oligonucleotide analysis are 3-hydroxypicolinic acid, often combined with picolinic acid, and dihydroxybenzoic acid[46].

Irradiation of the sample on the plate with a laser causes excitation of the matrix molecules propelling them and associated analyte molecules into a desolvation zone (Figure 1.21); this process is known as desorption and leads to the ionisation of the analyte molecules[47]. The mechanisms of ion formation in MALDI are not

fully understood but Zenobi and Knochenmuss suggested in 1998 that the main mechanism for oligonucleotides is gas-phase proton transfer[48]. Gas-phase proton transfer in positive ionisation MALDI involves the transfer of a proton from an excited matrix molecule and a ground-state analyte molecule[49]. In negative ionisation MALDI, hydrogen transfer is believed to occur between the analyte molecule and the radical matrix anion produced by irradiation with the laser, giving a deprotonated analyte molecule $[M - H]^-$ [50].

MALDI is suitable for large biomolecules and is less sensitive to detrimental effects of contaminants such as salt than ESI, making it a suitable ionisation technique for oligonucleotides and other similar molecules. In the case of oligonucleotides, sequences containing more than 60 nucleotides are difficult to effectively ionise by MALDI[21]. For the analysis of oligonucleotides impurities, MALDI is less suitable than ESI as it cannot be directly coupled to an HPLC system and, therefore, introduces an extra sample preparation step; an online HPLC separation of the oligonucleotides and impurities in the sample before the MS analysis is more efficient.

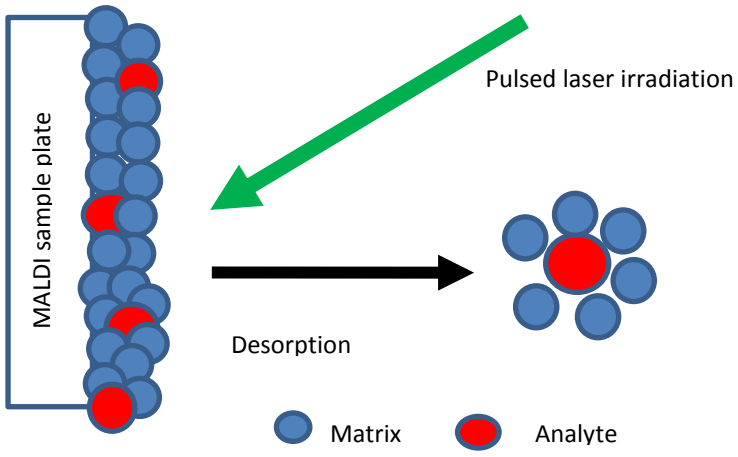

Figure 1.21 - Depiction of MALDI ionisation

1.3.3 Quadrupole Mass Analysers

Quadrupole mass analysers separate by *m/z* in a sequential manner, allowing only ions of one *m/z* unit through to the detector at any one time. Quadrupoles are made up of four rods to which are applied a fixed DC voltage and alternating radio frequency (RF) voltages. Quadrupole analysers have an upper mass limit of

around 2000 – 5000 *m/z* units; although oligonucleotides are larger than this, the multiple charging of ESI[19] means that their *m/z* are within the operating range of the analysers.

1.3.3.1 Quadrupole design and operation

The quadrupole mass analyser consists of four rods, ideally hyperbolic in cross-section[51] but, in practice, usually circular for ease and precision of manufacture, to which a DC voltage for mass resolution and alternating RF voltages are applied. The alternating RF voltages cause the selected ions to be attracted to and repelled by each pair of rods in quick succession on a stable trajectory; ions not currently selected for have a collisional trajectory and, therefore, do not reach the detector as they collide with the rods (Figure 1.22). The potential of each rod is denoted by +(U + Vcos(ωt)) or –(U + Vcos(ωt)) where U is the positive or negative applied DC voltage, V is the applied RF potential and ω is the angular frequency of the RF waveform[51].

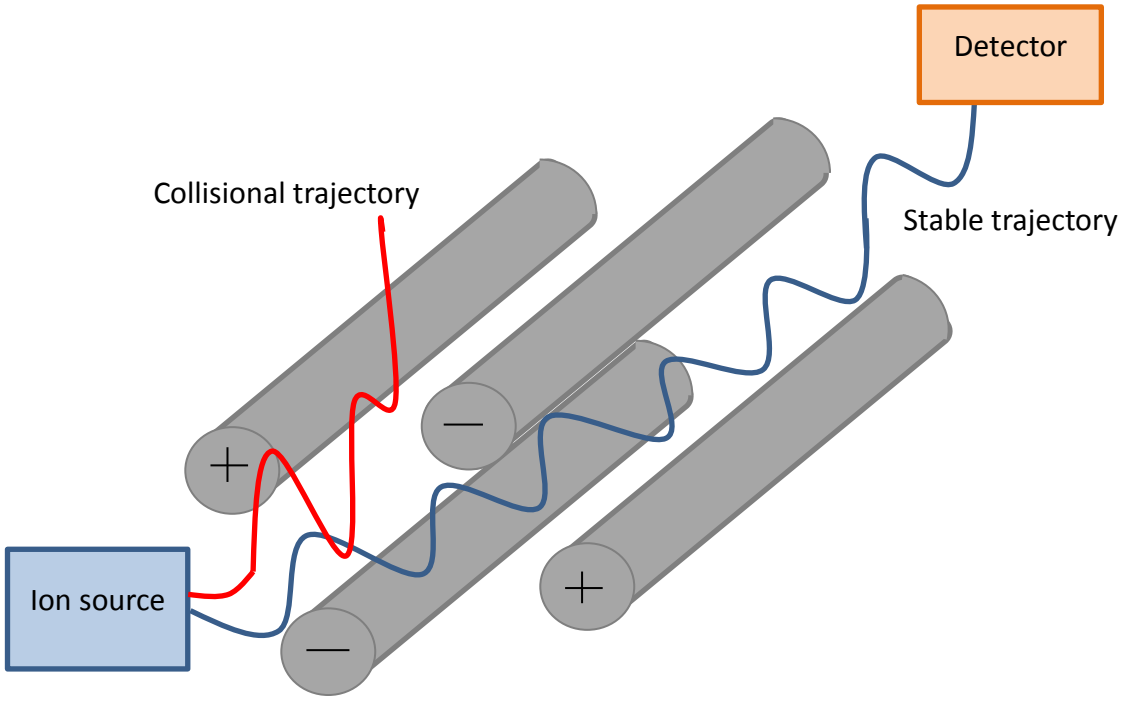

Figure 1.22 - Depiction of quadrupole ion selection

1.3.3.2 Quadrupole ion motion

The axes of motion of ions in a quadrupole are x (horizontal), y (vertical) and z (through the quadrupole); as long as the position of an ion on the x and y axes is

within the distance between the rods, r_0, then the ion can pass through the quadrupole. There are two parameters which are important for determining the stable trajectories of ions within a quadrupole mass analyser, known as *a* and *q*. These unitless parameters are calculated using the derivations of the Mathieu equation, Equations 1.9 and 1.10

$$a = \frac{8zU}{mr_0^2\omega^2} \qquad \text{Equation 1.9}$$

$$q = \frac{4zV}{mr_0^2\omega^2} \qquad \text{Equation 1.10}$$

Where z is the charge of the ion, m is the mass of the ion, U is the positive or negative applied DC voltage, V is the applied RF potential, ω is the angular frequency of the RF waveform and r_0 is the distance between the rods, as mentioned above.

Figure 1.23 shows the stable regions of the x and y axes for a quadrupole given equations 1.9 and 1.10. Region A is known as the first stability region and is the region most commonly employed because it uses the most easily achieved voltages; Figure 1.24 shows an enlargement of this region.

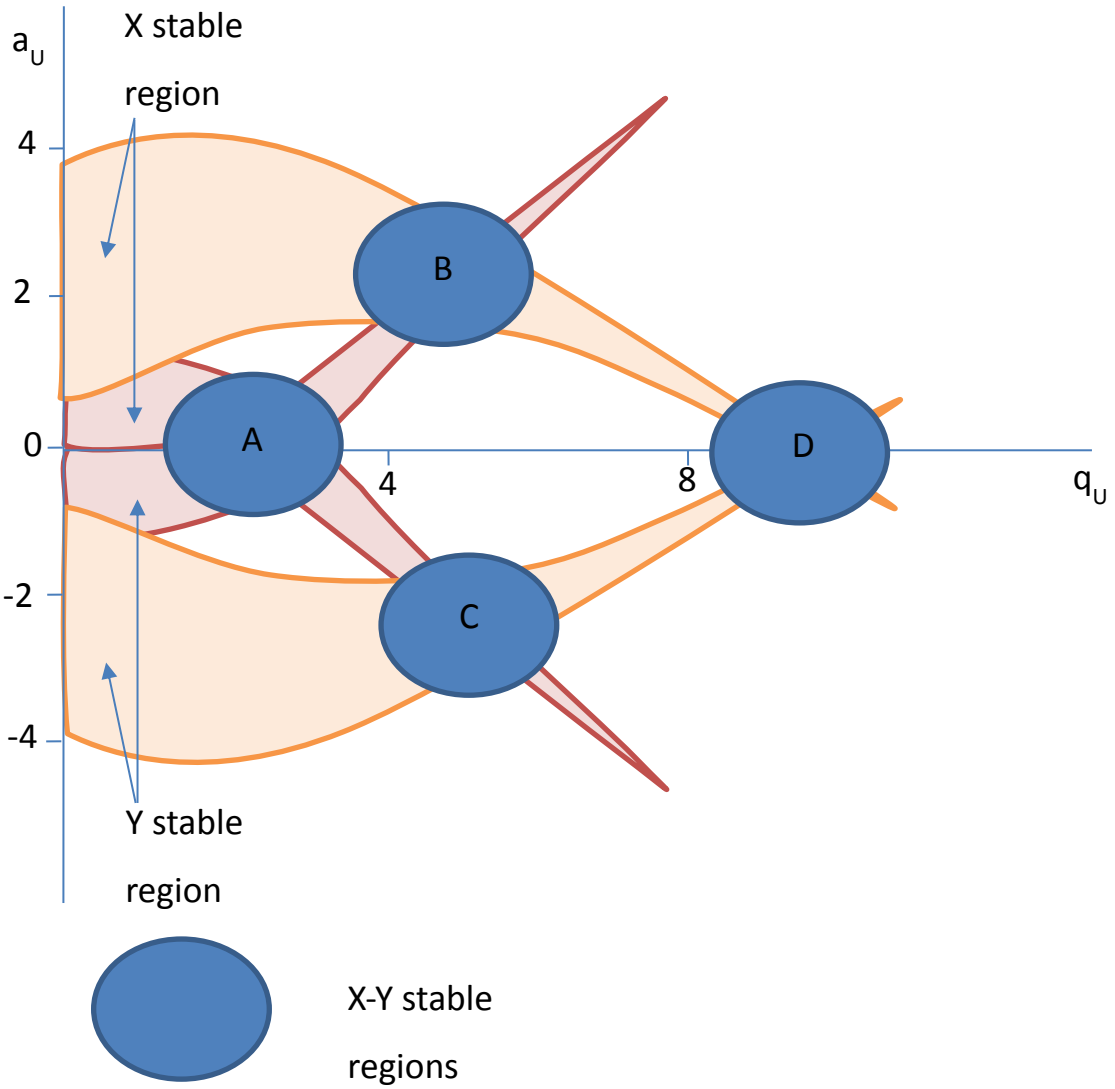

Figure 1.23 - Mathieu diagram showing stable regions of operation of a quadrupole mass analyser

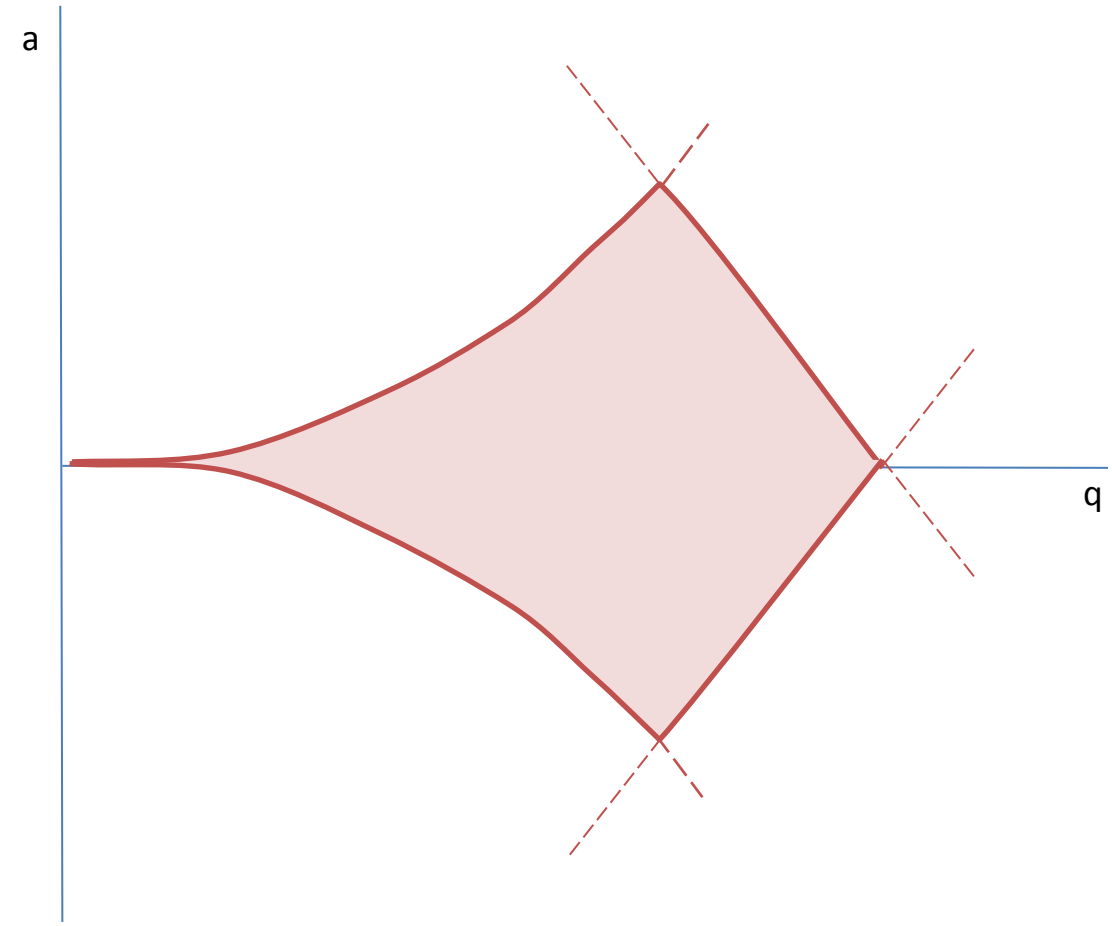

Figure 1.24 - Stability region A from Figure 1.19

1.3.3.3 Quadrupole sensitivity and resolution

Resolution in mass spectrometry refers to the ability of the mass analyser to distinguish between ions with different *m/z* values. Quadrupoles are typically capable of differentiating between, for example, ions of *m/z* 100 and 101 but not between *m/z* 100.1 and *m/z* 100.2.

Sensitivity is a measure of how many ions of a given *m/z* are required to be detected before they are registered as a peak. The lower the sensitivity, the more ions are required before their presence is registered.

The two main parameters in a quadrupole mass analyser that affect the resolution and sensitivity of the system are the offset and the gain as illustrated in Figure 1.25 and Figure 1.26. An increase in resolution is accompanied by a reduction in sensitivity (and *vice versa*) so for each ion of interest, a compromise must be made to adjust the offset and gain to achieve an acceptable resolution and sensitivity.

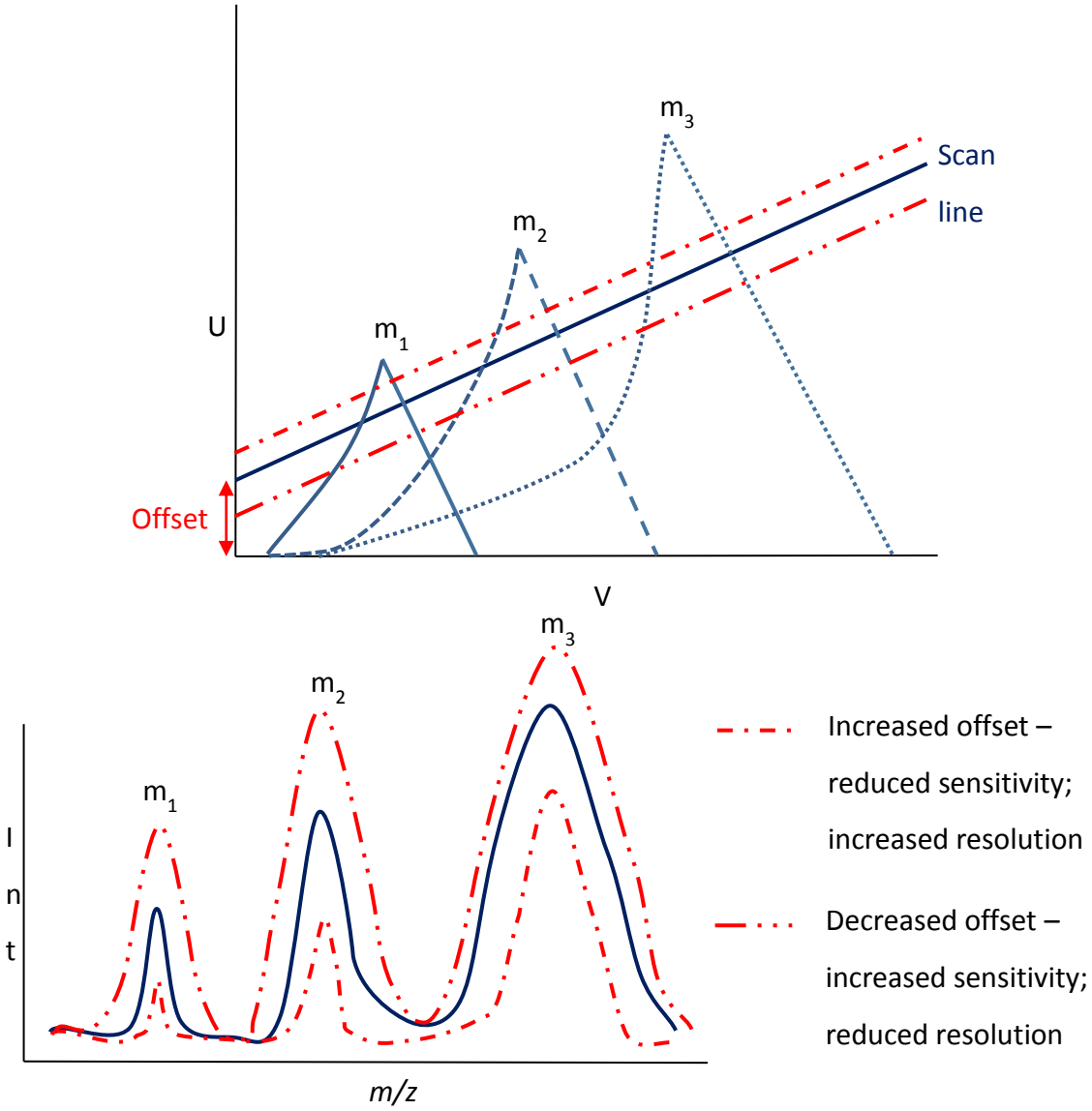

Figure 1.25 - The effect of changing quadrupole offset on the sensitivity and resolution of the mass analyser for ions with *m/z* $m_1<m_2<m_3$

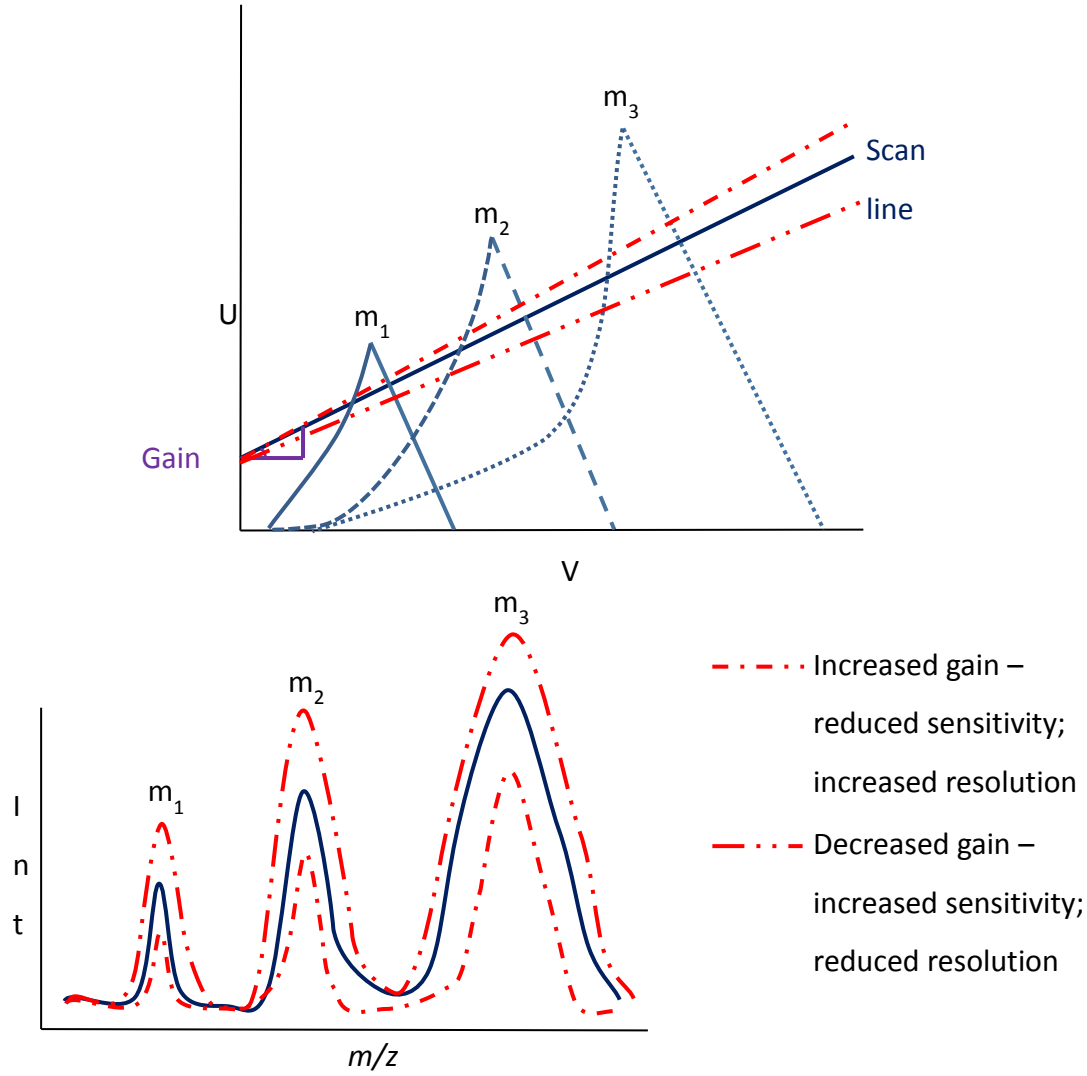

Figure 1.26 - The effect of quadrupole gain on the sensitivity and resolution of the mass analyser for ions with *m/z* $m_1<m_2<m_3$

1.3.4 Time-of-Flight Mass Analysers

Time-of-flight mass analysers (TOF) measure by the length of time taken for ions to reach the detector end of a flight tube; ions with a higher *m/z* will take longer to reach the detector and are, therefore, distinguished from ions with lower *m/z* values (Figure 1.27).

Unlike quadrupoles, TOFs theoretically have no upper mass limit but, in practice, the difference in flight time between two ions of different high masses is smaller than the difference between a high mass ion and a low mass ion, making high mass resolution less accurate.

1.3.4.1 TOF mass resolution

The problem of accuracy of detection of high *m/z* ions is reduced in modern TOF analysers by the use of reflectrons, electrodes or lenses which create an electrostatic charge and improve the mass resolution of TOFs in two ways. Firstly, the addition of the reflectron acts as an ion mirror to increase the effective path length (Figure 1.28), extending the time ions spend in the flight tube, increasing the differences in flight time between high mass ions. The use of reflectrons also improves resolution by correcting for differences in kinetic energy of ions of the same *m/z*; ions with greater initial kinetic energy will have a greater velocity than those with less energy and will travel deeper into the reflectron and spend longer in the flight tube overall than ions with less energy – this difference in time spent in the flight tube allows ions with different kinetic energies but the same *m/z* to reach the detector closer together, sharpening the peak[52].

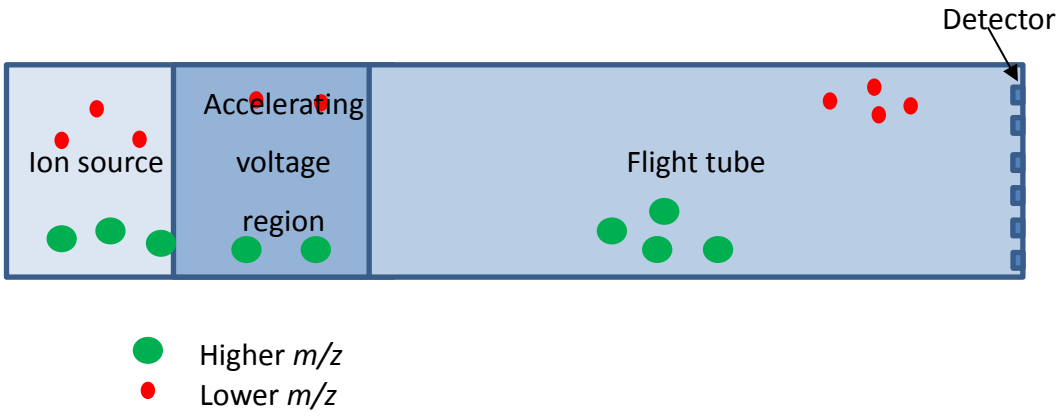

Figure 1.27 - Depiction of a linear time-of-flight mass analyser

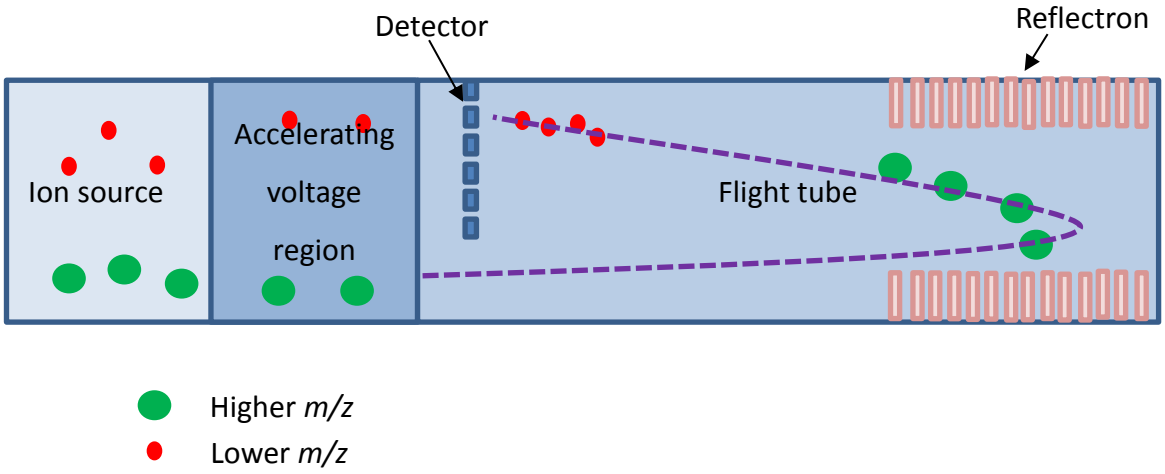

Figure 1.28 - Depiction of a reflectron time-of-flight mass analyser

Another method of improving mass resolution of TOF analysers in a manner similar to the second function of reflectrons is to use time-lag focussing (TLF); use of TLF introduces a delay of several hundred nanoseconds between the ions being formed by the ion source (typically, for this technique, MALDI) and the acceleration of the ions in the analyser. The delay allows ions of the same *m/z* unit to be detected simultaneously, with ions that have a lower initial energy receiving more energy from the repeller in the analyser than those ions which are more energetic to begin with – this allows all ions of the same *m/z* to travel at the same speed once in the flight tube, creating sharper peaks and enhancing mass resolution[53].

1.3.4.2 Adaptations for ionisation sources

TOF analysers need packets of ions to be able to monitor times of flight; this meant that initially they were better suited to use with pulsed ion sources such as MALDI. Orthogonal introduction systems such as the use of pusher electrodes (see Figure 1.29) that introduce a pulse of ions into the analyser mean that TOFs can now be used with continuous ion production sources such as ESI[54].

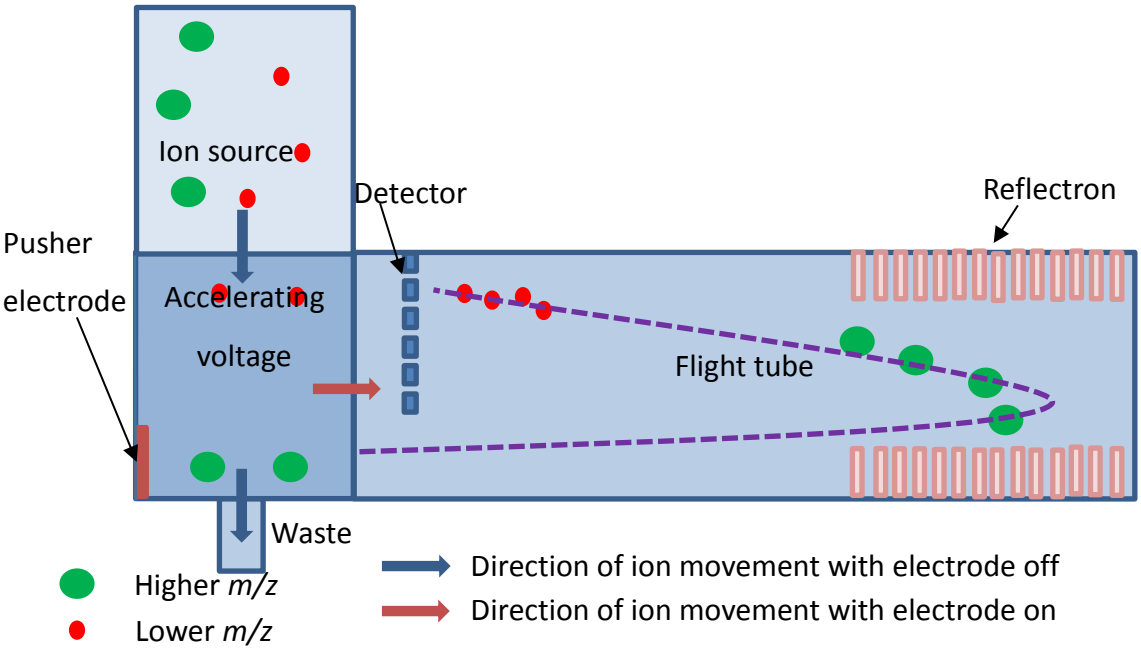

Figure 1.29 – Depiction of an orthogonal ion introduction TOF analyser, using a pusher electrode to send packets of ions into the flight tube

1.3.5 Quadrupole Time-of-flight (Q-TOF) analysers

Some instruments, such as the Waters Synapt, use a hybrid quadrupole-TOF analyser. When TOF analysis only is required, the quadrupole is operated in RF-only mode[52]. This allows all ions through the quadrupole, which is used as an ion guide. Separation of the ions by *m/z* occurs in the TOF portion of the analyser.

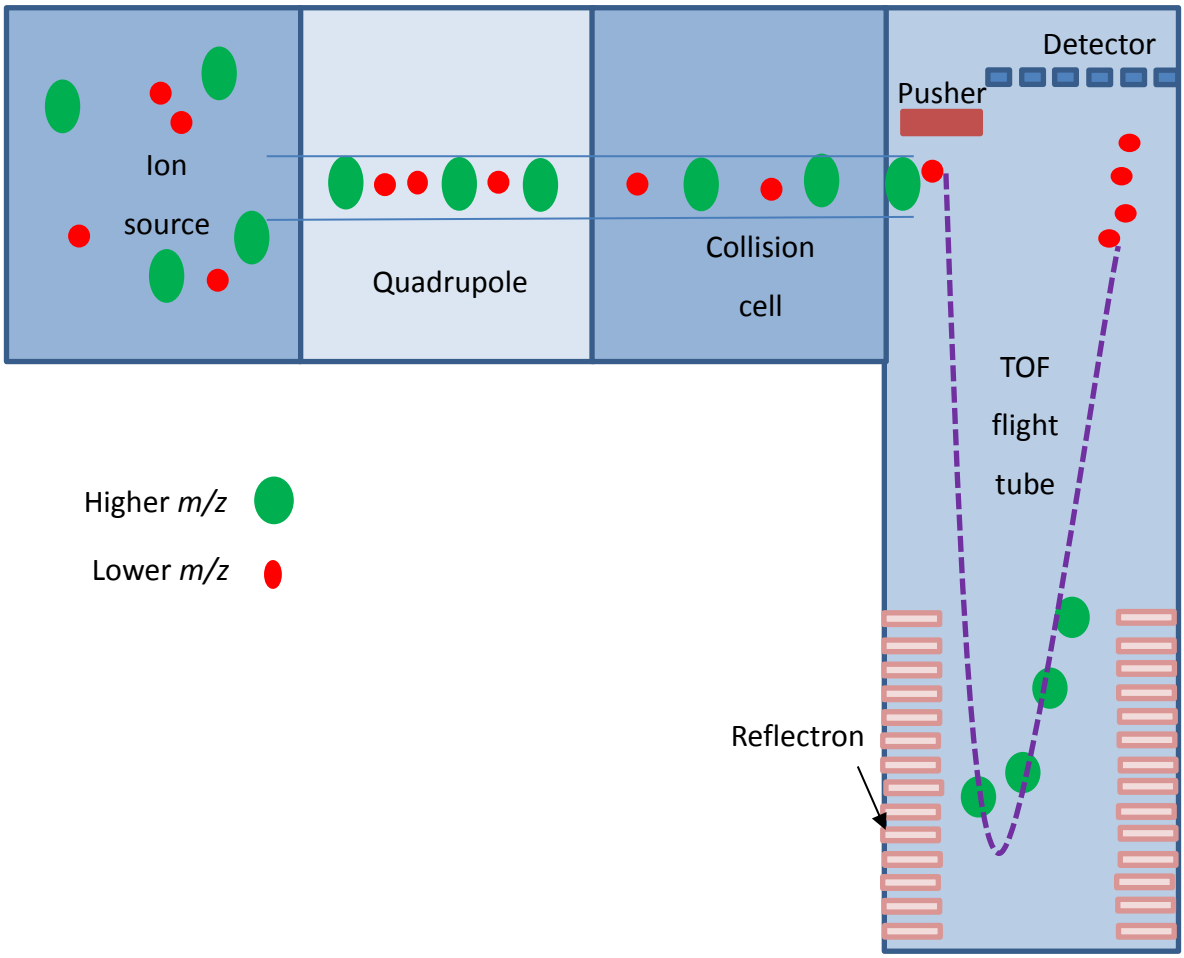

Figure 1.30 - Schematic depiction of a Q-TOF mass analyser

If tandem MS analysis is required (see 1.3.7) a DC voltage can be applied to the quadrupole to select an ion or ions of interest and the collision cell will be active to create fragmentation before the product ions are separated and detected in the TOF flight tube.

1.3.6 Vacuum systems

To ensure that ions reach the detector efficiently, high levels of vacuum are required. If ions pass through a mass spectrometer without sufficient vacuum, collisions can occur between the analyte ions and molecules of air and water preventing them from being detected and reducing sensitivity of the instrument. Operating the mass spectrometer under a vacuum also helps to prevent corrosion of the metal surfaces inside the system by removing air and water vapour [55].

For all mass analysers, a “roughing” pump is required to create a vacuum of around 10^{-3} mbar, before a high-vacuum pump, such as a turbomolecular pump, is employed to obtain the required pressure, as shown in Table 1.1. The roughing

pump can be a rotary pump or a scroll pump. Rotary pumps contain mineral oil and use vanes attached to a drive shaft which push air through a compression chamber to achieve a vacuum as shown in Figure 1.31. Scroll pumps use multiple Archimedes spirals, one orbiting as the other remains static, to create pockets where air can be compressed to generate a vacuum as shown in Figure 1.32. Scroll pumps do not use oil and are much quieter and cooler in operation, making them a popular alternative to rotary pumps in modern instruments. The typical maximum vacuum achieved by a scroll pump is 10^{-2} mbar, so multiple pumps may be employed to create a sufficiently low pressure before the high-vacuum pump takes over.

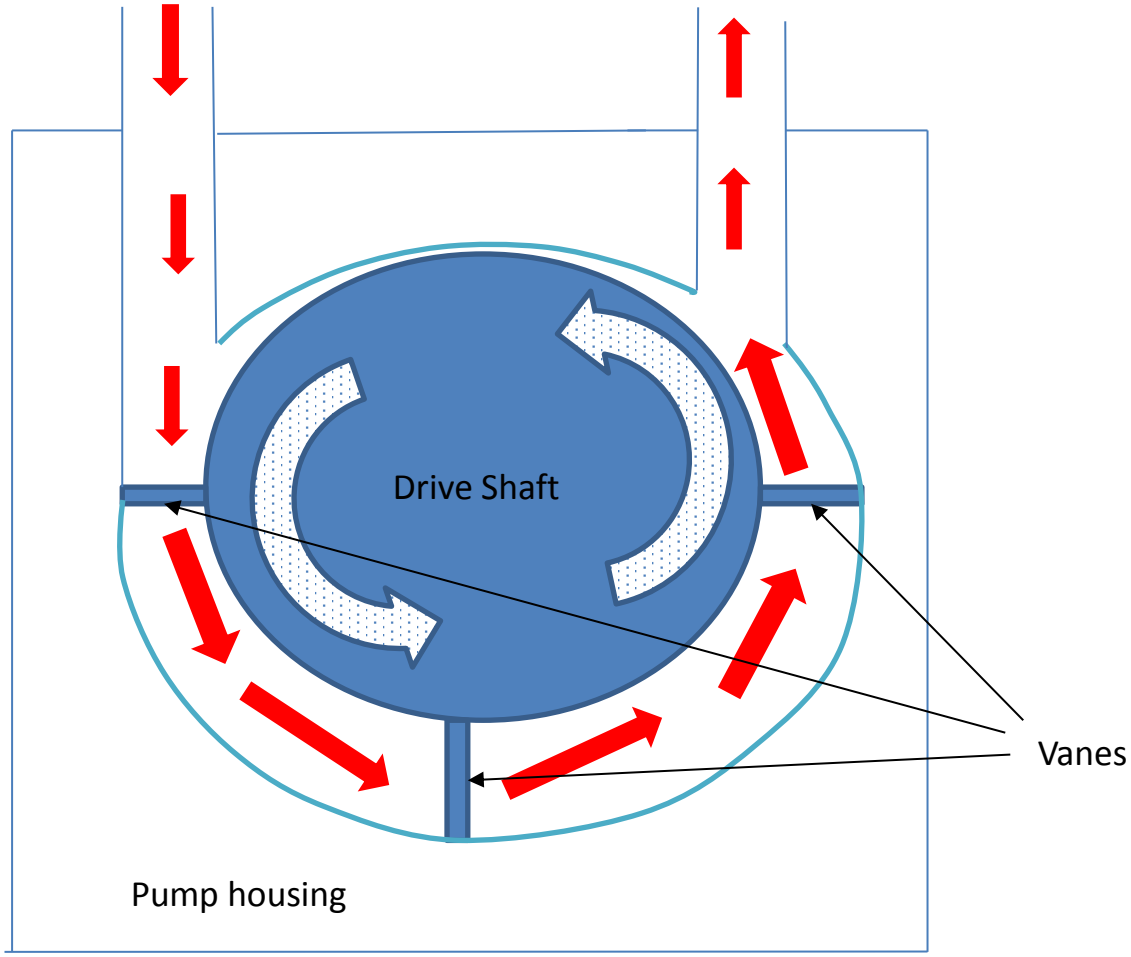

Figure 1.31 - Schematic representation of a rotary vacuum pump

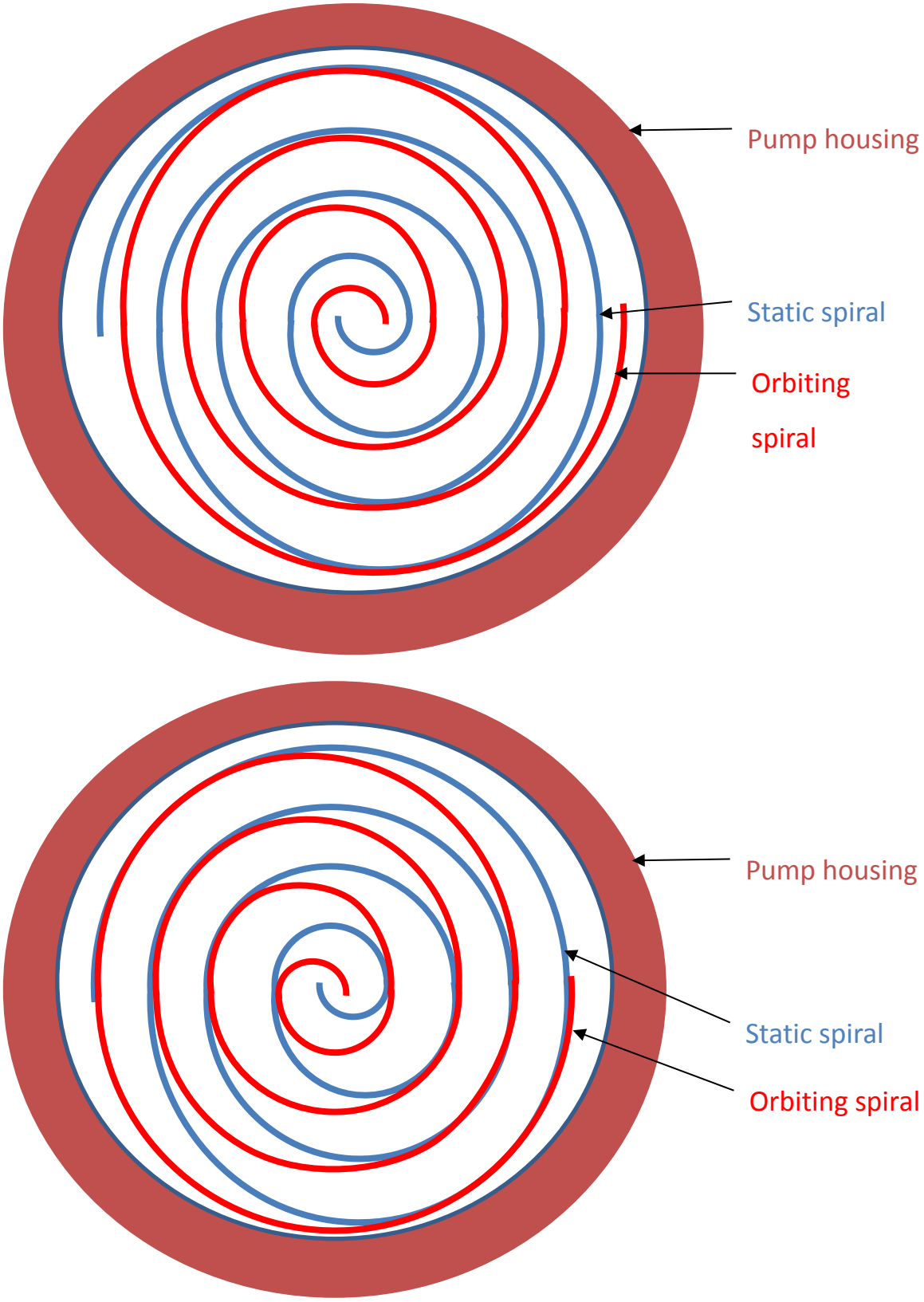

Figure 1.32 - Schematic representation of a scroll pump showing two positions of the orbiting spiral

The turbomolecular pump consists of several turbine-like rotating blades, which are angled and spaced so as to compress remaining gas molecules after the low-

vacuum is generated by the roughing pump. The bearings around the motor turning the blades can be made of steel and lubricated with oil, ceramic lubricated with grease or magnetic beads that do not require lubrication. Magnetic bearings are preferable as they are quieter and there is no risk of hydrocarbon contamination from lubricants [55]. Turbomolecular pumps are capable of achieving a vacuum pressure as low as 10^{-10} mbar and multiple pumps are often used to ensure stability of very high vacuums. Figure 1.33 shows a representation of a turbomolecular pump.

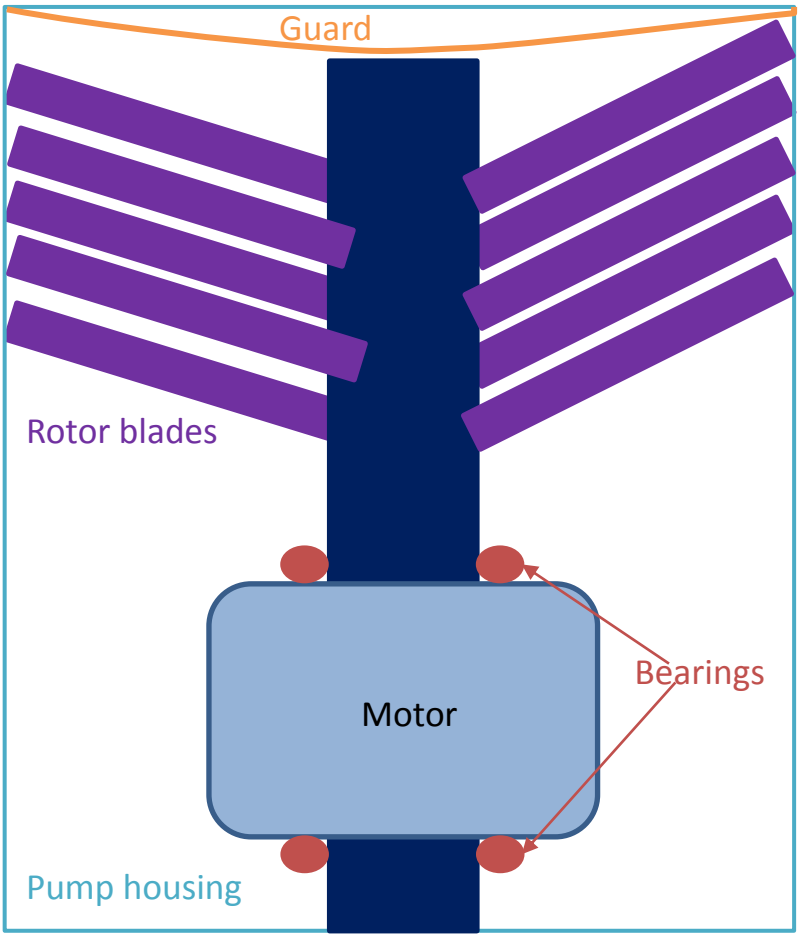

Figure 1.33 - Schematic representation of a turbomolecular vacuum pump

Table 1.1 – Vacuum pressures and mean free path lengths for different mass analysers

Analyser	Vacuum pressure (mbar)	Mean free path length (m)
Ion trap	$<10^{-4}$	0.5
Quadrupole	$<10^{-4}$	0.5
TOF	$<10^{-8}$	5000
Magnetic sector	$<10^{-8}$	5000
Fourier transform ion cyclotron resonance	$<10^{-10}$	500000

1.3.7 Tandem MS

Tandem MS is a term which comprises several types of analyser including triple quadrupole, Q-TOF and ion trap configurations. The two different types of tandem MS that can be performed, depending on the analyser type are tandem MS in space and tandem MS in time. Tandem MS in space can be undertaken using triple quadrupoles and hybrid mass spectrometers *e.g.* Q-TOFs and involves the selection of one or more precursor ions in the first quadrupole, which are then fragmented in a collision cell before being analysed in the final analyser. Tandem MS in time, using an analyser such as an ion trap, retains the chosen ion and then fragments it in the same space. When tandem MS in space is used, it is possible to detect fragments of fragments which are not produced by tandem MS in time. This is because when using tandem MS in space, the precursor ion and its fragments are all present in the collision cell. When tandem MS in time is used, voltages are applied that only allow a selected m/z or m/z range to be retained in the ion trap, preventing fragments from being fragmented further. The use of tandem MS allows greater confidence in the identification of a compound by fragmenting the molecular species into fragments; if a unique transition can be determined then this becomes diagnostic for a particular analyte. Investigating the fragmentation of an analyte can help determine its structure and, for oligonucleotides, tandem MS in space can be used to confirm the order of bases within the molecule, known as sequencing, thus aiding identification of the target molecule from any substituted impurities[56-57].

1.4 Ion mobility

Ion mobility spectrometry (IMS) is a method of separating ions by placing them into an electric field at atmospheric pressure; ions accelerate in the electric field and the ratio of the velocity of the ion in the field to the magnitude of the electric field is known as the ion mobility[58]. In a low electric field, the velocity of the ion is proportional to the magnitude of the field and the ion mobility constant (K) is given by Equation 1.11 where q is the charge on the ion, N is the number density of the buffer gas (usually nitrogen), k is Boltzmann's constant, T is the absolute temperature, m is the mass of the buffer gas, M is the mass of the ion and Ω is the collision cross-section of the ion[59].

$$K = \left(\frac{3q}{16N}\right)\left(\frac{2\Pi}{kT}\right)^{\frac{1}{2}}\left(\frac{m+M}{mM}\right)^{\frac{1}{2}}\left(\frac{1}{\Omega}\right) \qquad \text{Equation 1.11}$$

The collision cross-section of an ion is determined by its ionic size, shape and polarizability[58]. Equation 1.11 can be used to calculate the collision cross-section of ions when using traditional "drift-time" IMS. A more modern development in IMS, which has been used in the analysis of oligonucleotides is "traveling-wave" IMS (TWIMS) where a high electrical field is swept through the cell; this sweep forms pulses of ions as the "wave" of electric field passes[59]. Typically, the larger the collision cross-section of an ion, the slower its transit through the mobility cell; the number of charges on an ion can, however, alter this situation. A larger, doubly charged ion could travel faster than a smaller ion with only a single charge[60].

All IMS instruments consist of a sample introduction area, an ionisation region, a separation (or drift) region and a detection region with a mechanism for recording the data (Figure 1.34). Drift-time IMS instruments utilise a neutral drift gas, such as nitrogen, helium or argon; this gas may flow in the opposite direction to the ions and the carrier gas and remove non-ionised molecules. An ion gate is used to allow packets of ions into the drift region allowing separation to occur and the velocity of the ions to be detected (Figure 1.35). In the case of TWIMS instruments, the counter-current flow of drift gas does not occur, although the separation region is still filled with neutral drift gas, and a series of ring electrodes have alternating voltage pulses applied to them (with each electrode having the opposite voltage to its neighbours) (Figure 1.36)[61].

Ions for separation by IMS can be generated by ESI and MALDI ion sources, meaning that it is suitable for the analysis of oligonucleotides. It is possible to couple IMS systems to a variety of MS analysers (IMS-MS), including TOF and quadrupole analysers. The Waters Synapt instrument[62] combines a quadrupole mass analyser with a TWIMS mobility cell and a TOF analyser allowing the use of the quadrupole as a mass filter and giving the opportunity for the mobility cell to act as collision cell for the analysis of fragment ions[59].

Figure 1.34 - Schematic depiction of a generic ion mobility spectrometer

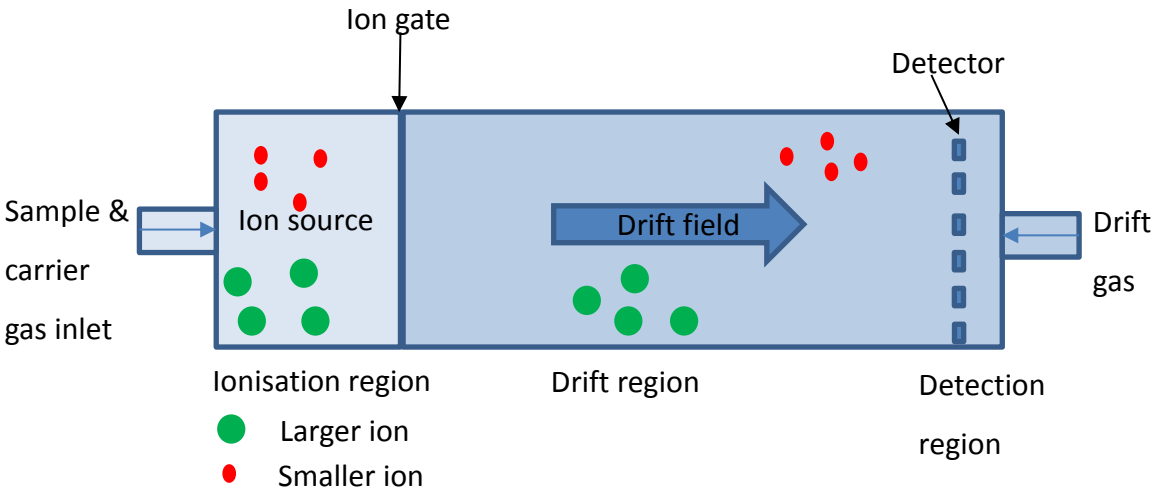

Figure 1.35 - Depiction of a drift-time ion mobility spectrometer

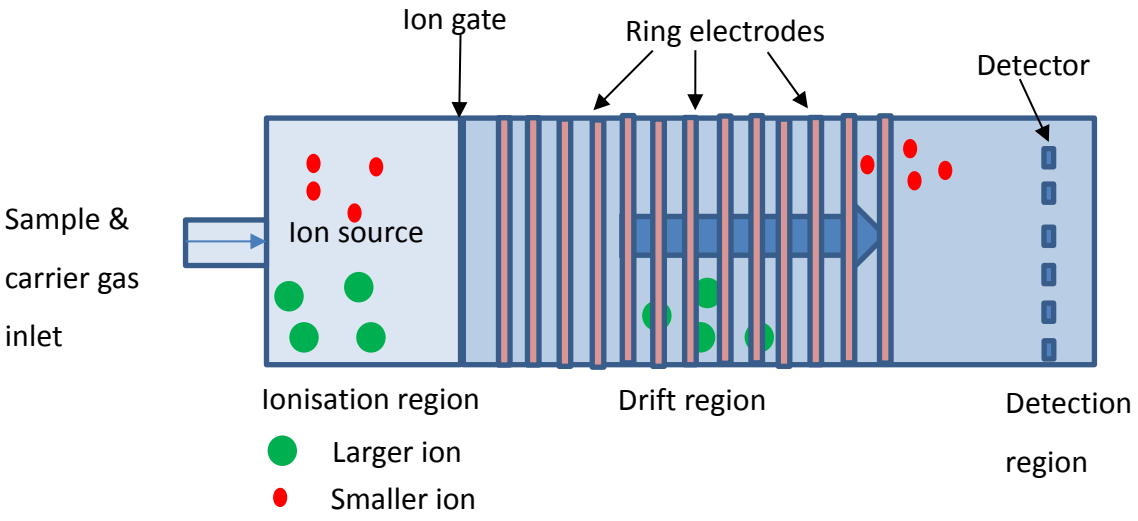

Figure 1.36 - Depiction of a traveling-wave ion mobility spectrometer

1.5 Analysis of oligonucleotides and their impurities

The use of HPLC techniques for the purification and analysis of oligonucleotides was pioneered in the 1970s, with an early paper on the subject being published in 1978[63]. By the 1990s, the use of hyphenated HPLC and mass spectrometry systems had begun utilising both on-line and off-line HPLC separations, including those described by Glover *et al.* in 1995 [64]

The use of RP-HPLC has been shown to be unable to adequately separate oligonucleotides from each other and their impurities. In the case of double-stranded DNA oligonucleotides, this has been attributed to inability of the hydrophilic backbone of DNA to interact with the stationary phase of the column leading to poor retention of analytes with insufficient time for separation to occur[65]. The highly polar nature of nucleic acids may also play a role in reducing retention[66]. The conditions required for high quality chromatographic separation of oligonucleotides and good MS sensitivity are also not highly compatible; the low pH and high aqueous content of mobile phases suited to good separation lead to inefficient ionisation, particularly in ESI techniques[67]. Ion exchange chromatography has traditionally been considered unsuitable for hyphenated HPLC-MS, as discussed by Rudge *et al.* in their 2011 paper as the salts required for effective chromatographic resolution suppress ionisation to the extent that ESI ionisation is impossible [66]. Recent research has been published regarding the use of a two-dimensional LC system, where the sample is separated by an ion exchange column and desalted using a reversed-phase column before ESI analysis, for the analysis of oligonucleotides [68]. A two-dimensional approach may allow for more effective separation of impurities from target oligonucleotides, but is currently a slower and more expensive process than RP-IP-HPLC. In the case of other bio-pharmaceuticals, such as proteins, advances have been made in the direct hyphenation of ion exchange chromatography and ESI mass spectrometry. Volatile buffers, such as ammonium acetate [69-70] and ammonium formate [69] have been used for positive ionisation ESI with sensitive instruments without excessive ionisation suppression. Suitable volatile buffers for negative ionisation ESI may be found to allow ion exchange separation of oligonucleotides prior to ESI analysis but, currently, IP-RP-HPLC is the most suitable technique.

Understanding of the limitations of RP-HPLC led researchers to investigate the use of ion-pair chromatography to achieve better separation. A commonly used ion pair reagent in the 1990s was TEA, which had the effect of suppressing the formation of sodium and potassium adducts and, therefore, increasing negative ion ESI sensitivity along with improving chromatographic retention as observed by Grieg and Griffey in 1995 [71]. Use of ion-pair reagents improves the analysis of oligonucleotides by HPLC-MS, but increasing the concentrations of reagents such as TEA has a detrimental effect on ESI ionisation efficiency and the methods developed using this technique in the 1990s were a compromise between good chromatographic resolution and acceptable ESI sensitivity[19]. In 1997, Apffel *et al.* from Hewlett-Packard, published the results of research they had carried out into using 1,1,1,3,3,3-hexafluoro-2-isopropanol (HFIP) along with TEA in the mobile phase[72-73]. The authors propose that this combination provides more efficient ionisation as a result of the highly volatile nature of HFIP, which allows it to be quickly lost during desolvation, raising the pH of the droplets to encourage the dissociation of the TEA-oligonucleotide ion pair [72]. After the introduction of this combination of ion-pair reagents, developments in the analysis of oligonucleotides progressed down various avenues including column types, the use of new technologies and the optimisation of reagent concentrations.

In 2013 and 2014, Biba *et al.* published two papers on the use of core shell columns for the analysis of oligonucleotides; these columns seem to provide high quality chromatographic separation of oligonucleotides from impurities and the more recent paper indicates that some columns are able to overcome the rapid deterioration in chromatography seen in the 2013 study when using a column temperature greater than 60°C and neutral pHs[23-24]. High column temperatures are required to denature double-stranded oligonucleotides to enable separation of the analyte and its impurities which may differ only slightly in mass, charge or size [74]. Some manufacturers, such as Waters are developing columns specifically for the analysis of oligonucleotides. These columns are designed to be compatible with IP-RP-HPLC reagents and claim to encourage improved mass transfer of oligonucleotides in the stationary phase to yield better separation [75].

The development of UHPLC technologies has meant that the use of smaller particle size columns has become possible as a result of the higher back pressures tolerated by UHPLC systems compared to conventional HPLCs. The

use of close to or sub-2 µm columns with a column temperature above ambient and slow flow rates of less than 1 mL/min seems to give the most efficient separation of oligonucleotides and their impurities with shorter run times, creating a faster throughput of samples [74]. The advances made with the advent of UHPLC mean that chromatographic resolution is better than that obtained with HPLC systems and the use of this technology represents a significant step forward in the analysis of oligonucleotides by allowing for faster analysis.

Optimisation of the ion-pair reagents, their concentrations and the solvents used has been the subject of recent research. In 2013, Chen and Bartlett published a paper investigating these variables; they found that the use of a mobile phase made up of 25 mM HFIP and 15 mM di-isopropylethylamine (DIEA) in an ethanol/water solution gave the best sensitivity and allowed a limit of quantitation (LOQ) of 2.5 ng/mL to be achieved [76], around a two-fold improvement on the previous lowest reported LOQ of 4 ng/mL obtained using 2.85 mM TEA and 100 mM HFIP with methanol as the organic portion of the mobile phase [77]. Researchers from Oxford University published a study in 2014 comparing the performance of a range of ion-pair reagents combined with HFIP. In their paper, they observe that the improvements in retention of oligonucleotides and the ionisation efficiency of the sample does not correspond in a simple way with increasing ion-pair reagent concentration and that a high concentration of HFIP can reduce ionisation efficiency. Optimal concentrations of each ion-pair reagent and HFIP were determined, with the final conclusion that the best chromatographic and MS performance was generated using a combination of 15 mM hexylamine and 50 mM HFIP[78].

As the separation of oligonucleotides from their impurities and the identification and possible quantitation of impurities requires unambiguous confirmation of the nature of the molecules, tandem MS techniques are being developed to allow this to be carried out routinely. Ivleva *et al.* from Waters issued an application note in 2008 on the use of UPLC/MS/MS (UPLC is the Waters trade name for their UHPLC system) to determine the structure of oligonucleotides. This application note involves the use of the Waters OST reversed-phase column and a TOF mass analyser and allowed the characterisation of a 21-mer RNAi oligonucleotide [56]. Other methods of determining the structure of the analyte in question involve the

fragmentation of the ions using collision-induced dissociation [57] or the off-line fragmentation by digestion with analysis of the digestion products [3].

Several studies have recently used IMS-MS for the structural elucidation of oligonucleotides and other biological molecules. In 2009, Williams *et al.*[79] used the Waters Synapt to analyse adducts of a hexamer oligonucleotide with an organometallic anti-cancer compound, utilising the traveling-wave IMS and TOF MS/MS to determine the collision cross-section and elucidate the binding sites on the oligonucleotide. Fisher *et al.*[60] have also used CID and MS/MS combined with IMS to sequence a range of 20-mer siRNA oligonucleotides in a manner which the researchers believe is at less risk of errors in assignment and provides the opportunity for increased throughput and automation of the sequencing of analytes. A team from Baylor University in Texas have been using IMS-MS to investigate the potential rearrangement of oligonucleotide fragment ions during CID and the impact on sequencing[80]. The studies here were not directly researching oligonucleotide impurities but a better understanding of the structure of the target analytes and impurities and more effective sequencing will have a beneficial impact on this analysis.

1.6 Quantitation of oligonucleotide impurities

In Section 1.1.3, the classes of impurities were discussed; for these impurities to be quantitated and reported for a given oligonucleotide, a limit below which an impurity can be disregarded must be set. For the method developed by a third party and used by AstraZeneca[81], this limit is set to 0.2 % of the reconstructed (or extracted) ion current chromatogram (RICC or EICC) peak area of the target oligonucleotide, based on the performance of the method during validation.

Oligonucleotides form multiply-charged ions, meaning that there are multiple ions that could be chosen to use for quantitation (Figure 1.37). The presence of multiple charge envelopes means that the intensity of any one ion chosen for selected ion monitoring or recording (SIM or SIR) is reduced when compared to the situation in singly-charged small molecule analysis[82]. Currently, there are no regulatory guidelines or requirements on how impurities should be quantitated and there is a risk that different laboratories using different approaches could yield inconsistent reported levels of impurities for the same product batch. This project

will investigate a range of methods of quantitation of the same samples with the intent of recommending best practice.

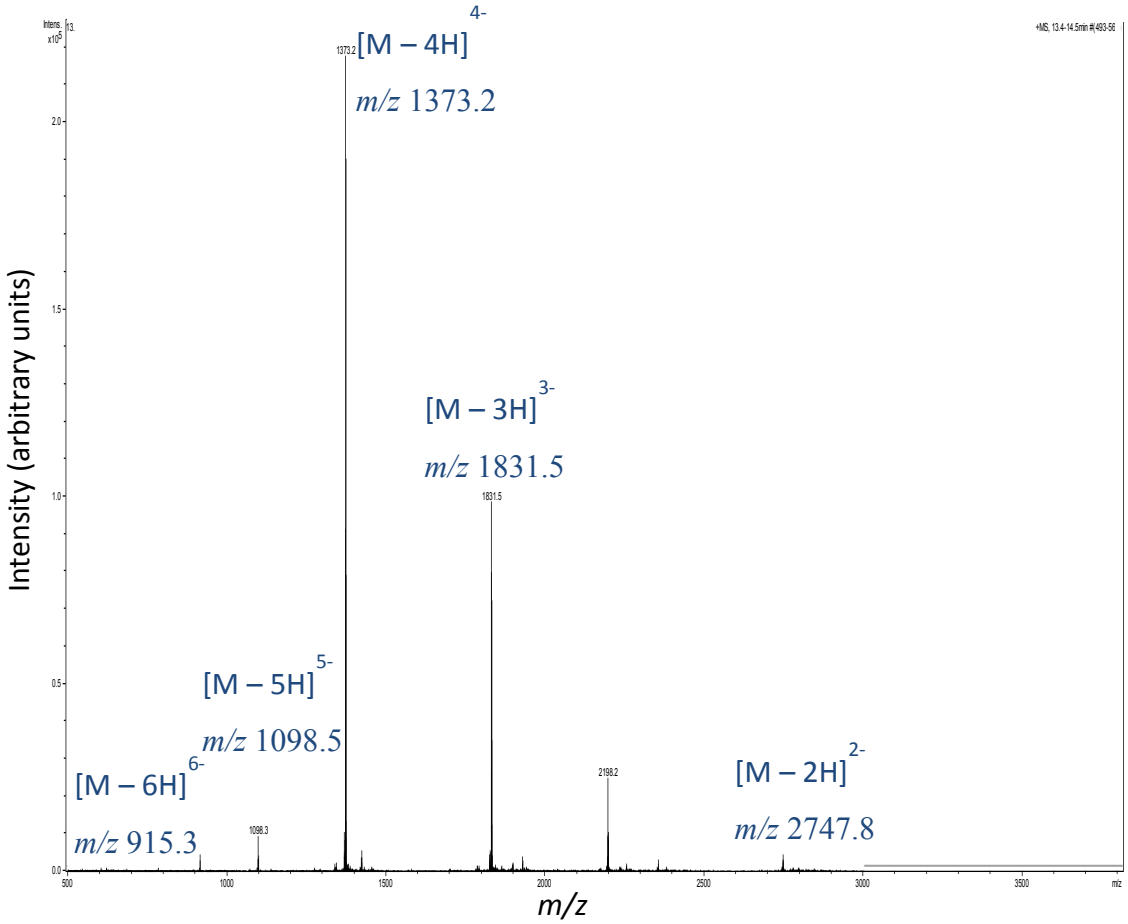

Figure 1.37 - Negative ionisation ESI mass spectrum of SP_Oligo_01 analysed using Agilent 6130 quadrupole instrument showing multiple charge states

1.7 Aims of the project

Current methods of quantifying impurities in therapeutic oligonucleotides are validated for individual manufacturers' instrumentation. The development of a generic method able to be used in laboratories world-wide regardless of the manufacturer or mass spectrometer type used will allow improved robustness of analysis, the ability to compare easily between laboratories and improved precision of inter-batch variation analysis. This project aims to determine critical parameters and factors which must be understood in order for a generic method to be developed.

Chapter 2: Experimental

For the majority of experiments undertaken during this project, two chromatographic methods and four LC-MS instruments were used. This chapter will summarise the chromatographic methods and the standard, optimised MS parameters used for sample analysis. Where different parameters have been used, these will be set out in the appropriate chapter.

2.1 Chromatographic methods

2.1.1 Southampton chromatographic method

All samples analysed using the Southampton chromatographic method (SCM), unless otherwise stated, use the mobile phase composition shown in Table 2.1, for all types of instrument used. As discussed in the introduction, the mobile phase additives used in this method are triethylammonium acetate (TEAA) and 1,1,1,3,3,3-hexafluoro-2-isopropanol (HFIP). The HPLC parameters set for samples analysed using the SCM and the mobile phase gradient used, unless otherwise stated, are shown in Table 2.1

Table 2.1 - Southampton chromatographic method parameters

Parameter	Details
Mobile Phase A composition	Water + 100 mM HFIP & 10mM TEAA
Mobile Phase B composition	Acetonitrile + 20 mM TEAA
Mobile phase flow rate Waters Synapt G2-Si/Acquity & Waters ZQ/Agilent 1100	0.25 mL/min
Mobile phase flow rate Bruker MicrOTOF/Dionex Ultimate 3000	0.1 mL/min
Column temperature	40 °C
% Mobile phase B at 0 min	5
% Mobile phase B at 14 min	40
% Mobile phase B at 15 min	5
Injection volume	4 µL

2.1.2 AstraZeneca chromatographic method

All samples analysed using the AstraZeneca chromatographic method[81] (ACM), unless otherwise stated, use the reagents shown in Table 2.2 to prepare the mobile phase composition as shown in Table 2.3, for all types of instrument used. The mobile phase additives used in this method are: tributylammonium acetate (TBuAA); tributylamine (TBuA); and ethylenediaminetetraacetic acid (EDTA). The HPLC parameters set for samples analysed using the ACM and the mobile phase gradient used, unless otherwise stated, are shown in Table 2.3.

Table 2.2 - AstraZeneca chromatographic method reagents

Reagent solution	Preparation	Total Volume (mL)
100 mM TBuAA Stock	24 mL TBuA 6 mL glacial acetic acid ACN	1000
100 mM EDTA stock	7.3 g EDTA 12 mL TBuA water	250

Table 2.3 - AstraZeneca chromatographic method parameters

Parameter	Details
Mobile Phase A composition	Water + 10% acetonitrile, 5 mM TBuAA & 1 µM EDTA
Mobile Phase B composition	80% Acetonitrile + 5 mM TBuAA, 1 µM EDTA & water
Mobile phase flow rate	0.25 mL/min
Column temperature	50 °C
% Mobile phase B at 0 min	45
% Mobile phase B at 22 min	80
% Mobile phase B at 25 min	80
% Mobile phase B at 26 min	45
% Mobile phase B at 30 min	45
Injection volume – Waters & Bruker	4 µL
Injection volume - Agilent	10 – 30 µL

2.2 MS parameters

2.2.1 Waters ZQ MS

The Waters ZQ MS is a single quadrupole instrument and all data were acquired using negative ionisation ESI. The source parameters optimised for this instrument were: capillary voltage; in-source fragmentation (cone) voltage; desolvation/drying temperature; desolvation/drying gas flow rate and cone gas flow rate. The values investigated for each parameter are shown in Table 2.4 and the statistical software MiniTab was used to find the optimal value for each parameter based on the RICC peak area for an oligonucleotide sample. The optimised values for each parameter were used for all samples analysed, unless otherwise stated.

Table 2.4 - MS source parameter values investigated for the optimisation of the Waters ZQ MS

Parameter	**Setting**			**Optimised value**
Capillary voltage	2.7 kV	3.0 kV	3.3 kV	**3.0 kV**
Cone voltage	20 V	50 V	80 V	**20 V**
Desolvation temperature	200 °C	250 °C	300 °C	**300 °C**
Desolvation gas flow rate	200 L/h	300 L/h	400 L/h	**400 L/h**
Cone gas flow rate	20 L/h	35 L/h	50 L/h	**50 L/h**

2.2.2 Waters Synapt G2-Si MS

The Waters Synapt G2-Si MS is a Q-TOF IMS-MS instrument and all data were acquired using negative ionisation ESI. The instrument was used in MS mode; MS/MS and IMS modes were not used. The source parameters optimised for this instrument were: capillary voltage; in-source fragmentation (cone) voltage; desolvation/drying temperature; desolvation/drying gas flow rate and cone gas flow rate. The values investigated for each parameter are shown in Table 2.5 and MiniTab was used to find the optimal value for each parameter based on the RICC peak area for an oligonucleotide sample. The optimised values for each parameter were used for all samples analysed, unless otherwise stated.

Table 2.5 - MS source parameter values investigated for the optimisation of the Waters Synapt G2-Si MS

Parameter	Setting			Optimised value
Capillary voltage	2.7 kV	3.0 kV	3.3 kV	**3.0 kV**
Cone voltage	20 V	50 V	80 V	**20 V**
Desolvation temperature	200 °C	250 °C	300 °C	**300 °C**
Desolvation gas flow rate	200 L/h	300 L/h	400 L/h	**400 L/h**
Cone gas flow rate	20 L/h	35 L/h	50 L/h	**50 L/h**

2.2.3 Bruker MicrOTOF

The Bruker MicrOTOF MS is a time-of-flight instrument and data were acquired using negative ionisation ESI. The source parameters used are set out in Table 2.6

Table 2.6 - MS source parameters used for samples analysed using the Bruker MicrOTOF MS

Parameter	Setting
Capillary voltage	4.0 kV
Drying (desolvation) gas flow	360 L/h
Drying (desolvation) gas temperature	230 °C

2.2.4 Agilent 6130

The Agilent 6130 MS is a single quadrupole instrument and all data were acquired using negative ionisation ESI. The AstraZeneca MS method sets out two conditions with different drying gas temperatures and flow rates. Table 2.7 shows the parameters used for analysis using this instrument.

Table 2.7 - MS source parameters used for sample analysis using the Agilent 6130 MS

Parameter	Value
Capillary voltage	4.0 kV
Fragmentor (Cone) voltage	100 V
Drying gas (Desolvation) temperature – standard condition	275 °C
Drying gas (Desolvation) temperature – harsh condition	350 °C
Drying (Desolvation) gas flow rate – standard condition	720 L/h
Drying (Desolvation) gas flow rate – harsh condition	780 L/h

2.3 Samples and sample preparation

In the course of this research, two 16-mer drug products were analysed along with four 13-mer and one 12-mer sequences specifically synthesised for this project. Samples were provided by AstraZeneca as an aqueous solution or in phosphate buffers. The drug products were supplied with a concentration in mg/mL and dilutions into water were made from the original samples to known concentrations. The dilution of the 12- and 13-mer samples will be discussed in Chapter 6:.

2.3.1 Sample sequences

The sequences of the 13-mer and 12-mer samples are shown in Table 2.8. SP_Oligo_01 and SP_Oligo_02 are proprietary drug products, 16 bases in length with a phosphorothioate backbone modification and secondary modifications.

Table 2.8 - Sequences of samples analysed

Sample	Sequence	Number of bases
SP_Oligo_04	G-G-G-A-A-A-C-C-C-T-T-T-T	13
SP_Oligo_05	G-G-A-A-A-C-C-C-T-T-T-T	12
SP_Oligo_06	A-A-A-G-G-C-C-C-G-T-T-T-T	13
SP_Oligo_07	C-A-A-A-G-C-C-C-G-T-T-T-T	13
SP_Oligo_08	C-C-C-A-A-A-G-G-G-T-T-T-T	13

Chapter 3: Instrument sensitivity

In order to develop a robust method for the quantitation of impurities in therapeutic oligonucleotide samples, it is essential that the sensitivity of the instrumentation being used is determined. For quantitation purposes, sensitivity is described by the limit of detection and the limit of quantitation of a given sample using a selected method and instrument.

The limit of detection (LOD) for a sample is defined as the concentration that produces a peak with an area or height of three times the background noise in the chromatogram (3:1 signal to noise ratio). The LOD is the lowest concentration that can be reliably detected for a given sample using a specified method; the lower limit of quantitation (LLOQ) for a sample is defined as the concentration that produces a peak with a 10:1 signal to noise ratio and is the lowest concentration that can be used for quantitation purposes.

The LOD and LLOQ for the two 16-mer drug product samples were investigated for analysis using the Southampton chromatographic method with the Dionex Ultimate 3000/Bruker MicrOTOF and the Southampton and AZ chromatographic methods with the Agilent 1100/Waters ZQ and Waters Acquity/Synapt G2-Si instruments.

3.1 Bruker MicrOTOF sensitivity

Three replicates of concentrations 1.0, 0.1 and 0.01 mg/mL of each 16-mer sample were analysed on three successive days and samples of 0.2 mg/mL and 0.02 mg/mL were analysed over two days. The preparation of the samples analysed is shown in Table 3.1.

Table 3.1 - Sample preparation for Bruker MicrOTOF sensitivity investigation

Sample	Concentration (mg/mL)	Volume used (µL)	Final volume (mL)	Final concentration (mg/mL)	Solvent
SP_Oligo_01 undiluted	167.0	60.0	10.0	1.00	Water
SP_Oligo_01 1.0 mg/mL	1.0	100.0	1.0	0.10	Water
SP_Oligo_01 1.0 mg/mL	1.0	10.0	1.0	0.01	Water
SP_Oligo_01 1.0 mg/mL	1.0	200.0	1.0	0.20	Water
SP_Oligo_01 1.0 mg/mL	1.0	20.0	1.0	0.02	Water
SP_Oligo_02 undiluted	50.0	200.0	10.0	1.00	Water
SP_Oligo_02 1.0 mg/mL	1.0	100.0	1.0	0.10	Water
SP_Oligo_02 1.0 mg/mL	1.0	10.0	1.0	0.01	Water
SP_Oligo_02 1.0 mg/mL	1.0	200.0	1.0	0.20	Water
SP_Oligo_02 1.0 mg/mL	1.0	20.0	1.0	0.02	Water

Figure 3.1 shows the RICC of the *m/z* range *m/z* 1727 – 1947 for SP_Oligo_01 at concentrations of 1, 0.1 and 0.01 mg/mL with the peak area and the signal to noise ratio (S/N) of the peak recorded. These values were recorded for all replicates analysed and the mean signal to noise ratio calculated for each concentration for both 16-mer samples.

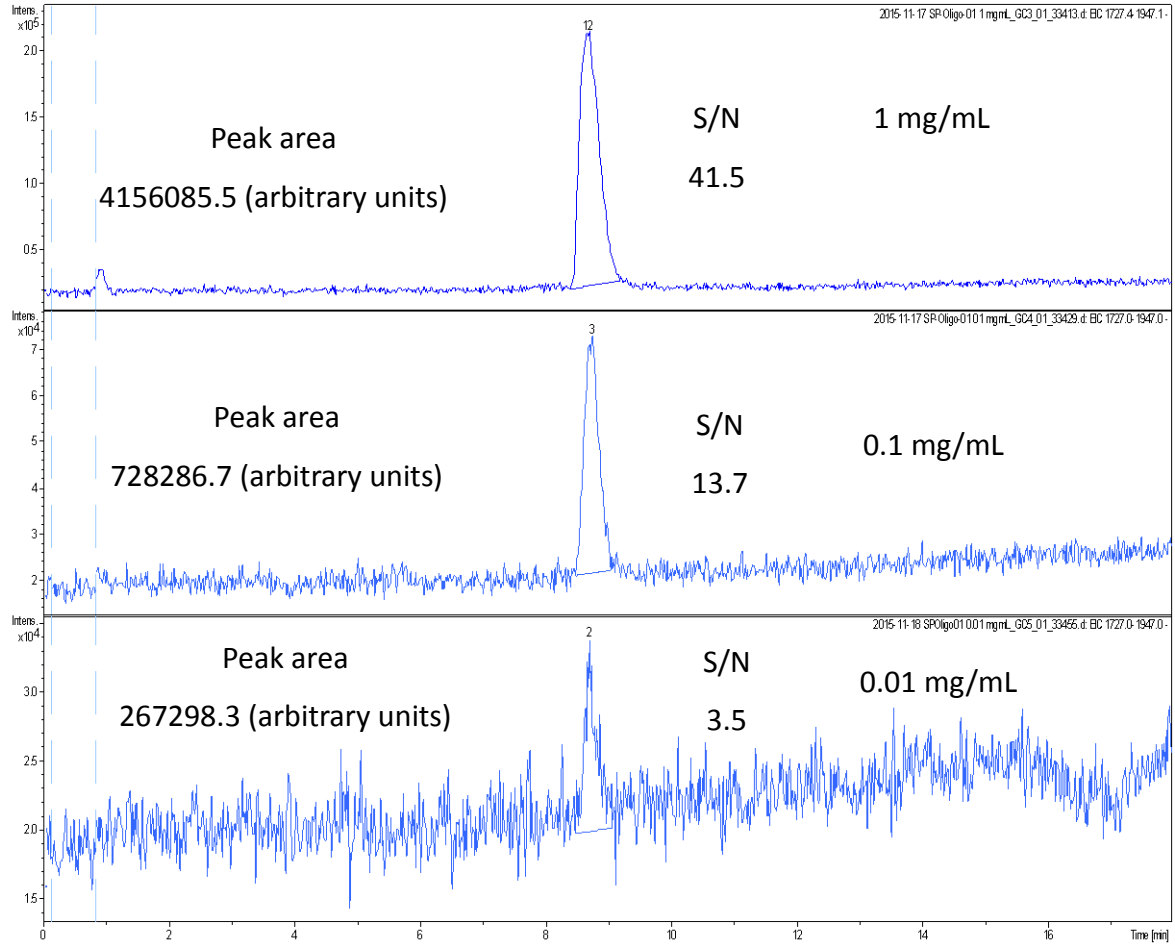

Figure 3.1 - RICC of SP_Oligo_01 at 1, 0.1 and 0.01 mg/mL (*m/z* 1727 – 1947)

The mean signal to noise ratio for each sample at each concentration is shown in Table 3.2.

Table 3.2 - Mean signal to noise ratios for sample concentrations 1.0, 0.2, 0.1, 0.02 & 0.01 mg/mL analysed using Dionex Ultimate 3000/Bruker MicrOTOF

Concentration (mg/mL)	**Signal to noise ratio**	
	SP_Oligo_01	**SP_Oligo_02**
1.0	45 ± 1	51 ± 2
0.2	22 ± 1	23 ± 2
0.1	14 ± 1	15 ± 1
0.02	6.3 ± 0.2	6.7 ± 0.2
0.01	3.6 ± 0.1	3.9 ± 0.1

The signal to noise ratios for the 0.2 and 0.02 mg/mL concentrations are approximately double those for the 0.1 and 0.01 mg/mL samples, indicating that for both 16-mer oligonucleotides, the LOD for analysis using the Southampton chromatographic method and the Dionex Ultimate 3000/Bruker MicrOTOF is 0.01 mg/mL (approximately 1.8 μM) and the LLOQ is 0.1 mg/mL (approximately 18 μM).

3.2 Waters ZQ sensitivity

The concentrations analysed for each sample using the Agilent 1100 and Waters ZQ and how they were prepared are shown in Table 3.3. A minimum of three replicates were analysed for each concentration of each sample.

Table 3.3 - Sample preparation for Waters ZQ sensitivity investigation

Sample	Concentration (mg/mL)	Volume used (μL)	Final volume (mL)	Final concentration (mg/mL)	Solvent
SP_Oligo_01 undiluted	167.0	60.0	10.0	1.00	Water
SP_Oligo_01 1.0 mg/mL	1.0	500.0	1.0	0.50	Water
SP_Oligo_01 1.0 mg/mL	1.0	250.0	1.0	0.25	Water
SP_Oligo_01 1.0 mg/mL	1.0	100.0	1.0	0.10	Water
SP_Oligo_01 1.0 mg/mL	1.0	50.0	1.0	0.05	Water
SP_Oligo_02 undiluted	50.0	200.0	10.0	1.00	Water
SP_Oligo_02 1.0 mg/mL	1.0	500.0	1.0	0.50	Water

Sample	Concentration (mg/mL)	Volume used (µL)	Final volume (mL)	Final concentration (mg/mL)	Solvent
SP_Oligo_02 1.0 mg/mL	1.0	250.0	1.0	0.25	Water
SP_Oligo_02 1.0 mg/mL	1.0	100.0	1.0	0.10	Water
SP_Oligo_02 1.0 mg/mL	1.0	50.0	1.0	0.05	Water

For each injection, an RICC was generated using all of the *m/z* ranges, encompassing the ^{12}C, ^{13}C and adduct peaks of the target oligonucleotide, related to the charge states for each sample as shown in Table 3.4.

Table 3.4 - Charge states and *m/z* ranges used for RICC generation in Waters ZQ sensitivity investigation

Charge state	*m/z* range	
	SP_Oligo_01	SP_Oligo_02
-9	606.02 - 625.47	588.00 - 617.69
-8	681.48 - 702.50	660.44 - 697.26
-7	779.52 - 801.31	754.27 - 801.76
-6	900.91 - 938.25	888.45 - 915.77
-5	1090.75 - 1138.21	1055.91 - 1105.77
-4	1361.52 - 1409.75	1331.41 - 1389.60

Figure 3.2 shows an example of the RICCs for SP_Oligo_01 at concentrations of 1.0, 0.5, 0.25 and 0.1 mg/mL with the peak area and S/N of the peak shown. Signal to noise ratios were recorded for all replicates analysed for each sample.

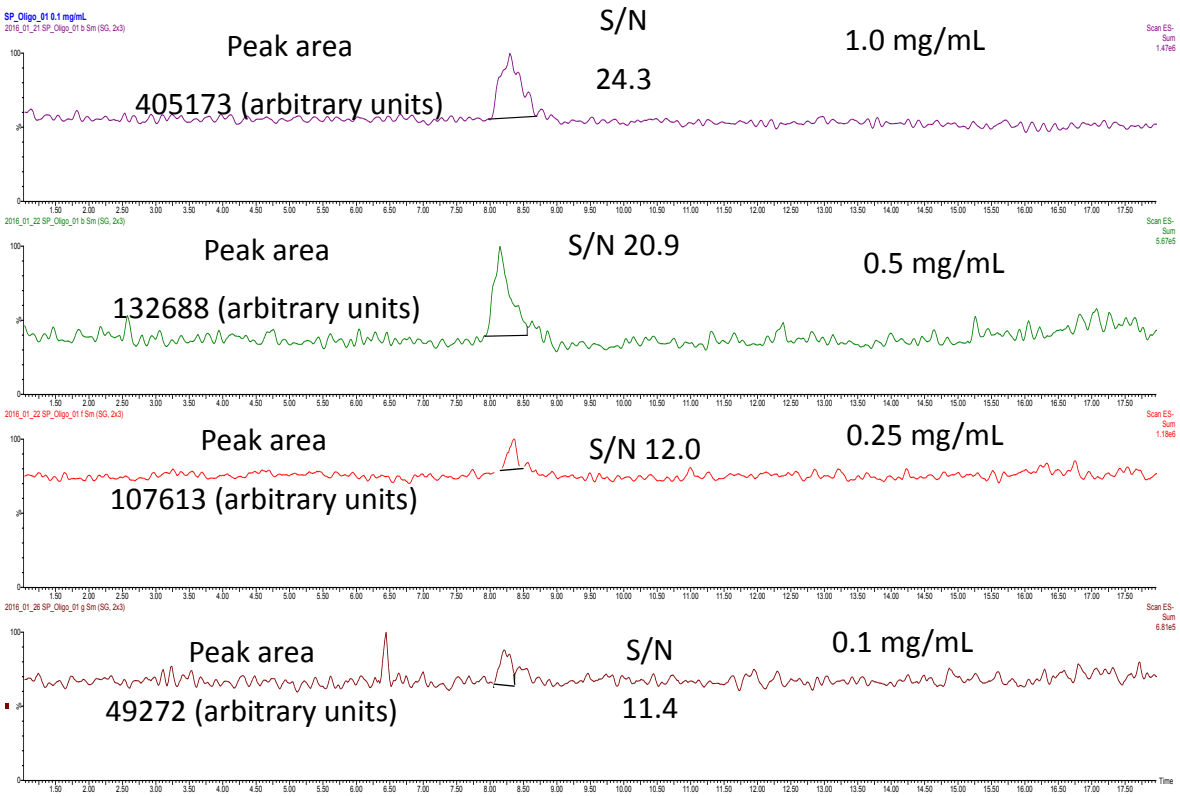

Figure 3.2 - RICC of SP_Oligo_01 at 1.0, 0.5, 0.25 and 0.1 mg/mL (*m/z*: 606.016 - 625.47; 681.484 - 702.5; 779.516 - 801.31; 900.906 - 938.25; 1090.75 - 1138.21; 1361.516 - 1409.75) analysed using Agilent 1100/Waters ZQ and the Southampton chromatographic method

The mean signal to noise ratio for each sample at each concentration is shown in Table 3.5. These values are means of samples analysed using the Southampton and AZ chromatographic methods; the low ± figures indicate that the two chromatographic methods are consistent in their signal to noise ratios.

Table 3.5 - Mean signal to noise ratios for sample concentrations 1.0, 0.5, 0.25, 0.1 & 0.05 mg/mL analysed using Agilent 1100/Waters ZQ

Concentration (mg/mL)	Signal to noise ratio	
	SP_Oligo_01	SP_Oligo_02
1.0	30 ± 2	23 ± 3
0.5	17 ± 2	19 ± 2
0.25	13 ± 1	9 ± 1
0.1	9 ± 0.8	7 ± 0.5
0.05	5 ± 0.2	4 ± 0.4

The data presented in Table 3.5 show that the LOD for the samples analysed is 0.05 mg/mL (50 µg/mL, approximately 9 µM) and the LLOQ is 0.25 mg/mL (approximately 45 µM) when using the Waters ZQ instrument using either chromatographic method investigated.

3.3 Waters Synapt sensitivity

The concentrations analysed for each sample using the Waters Acquity and Waters Synapt G2-Si and how they were prepared are shown in Table 3.6. A minimum of three replicates were analysed for each concentration of each sample.

Table 3.6 – Sample preparation for Waters Synapt sensitivity investigation

Sample	Concentration (mg/mL)	Volume used (µL)	Final volume (mL)	Final concentration (µg/mL)	Solvent
SP_Oligo_01 undiluted	167.0	60	10.0	1000	Water
SP_Oligo_01 1.0 mg/mL	1.0	200	1.0	200	Water
SP_Oligo_01 1.0 mg/mL	1.0	100	1.0	100	Water
SP_Oligo_01 1.0 mg/mL	1.0	20	1.0	20	Water
SP_Oligo_01 1.0 mg/mL	1.0	10	1.0	10	Water
SP_Oligo_01 1.0 mg/mL	1.0	2	1.0	2	Water
SP_Oligo_01 10 µg/mL	0.01	100	1.0	1	Water
SP_Oligo_02 undiluted	50.0	200	10.0	1000	Water
SP_Oligo_02 1.0 mg/mL	1.0	200	1.0	200	Water
SP_Oligo_02 1.0 mg/mL	1.0	100	1.0	100	Water
SP_Oligo_02 1.0 mg/mL	1.0	20	1.0	20	Water
SP_Oligo_02 1.0 mg/mL	1.0	10	1.0	10	Water
SP_Oligo_02 1.0 mg/mL	1.0	2	1.0	2	Water
SP_Oligo_02 10 µg/mL	0.01	100	1.0	1	Water

For each injection, an RICC was generated using all of the *m/z* ranges, encompassing the ^{12}C, ^{13}C and adduct peaks of the target oligonucleotide, related to the charge states for each sample as shown in Table 3.7.

Table 3.7 - Charge states and *m/z* ranges used for RICC generation in Waters Synapt sensitivity investigation

Charge State	***m/z* range**	
	SP_Oligo_01	**SP_Oligo_02**
-4	1365.73 - 1439.66	1314.80 - 1377.63
-3	1775.06 - 1912.60	1750.84 - 1859.64

Figure 3.3 shows an example of the RICCs for SP_Oligo_01 at concentrations of 200, 20 and 2 µg/mL with the peak area and signal to noise ratio of each peak recorded.

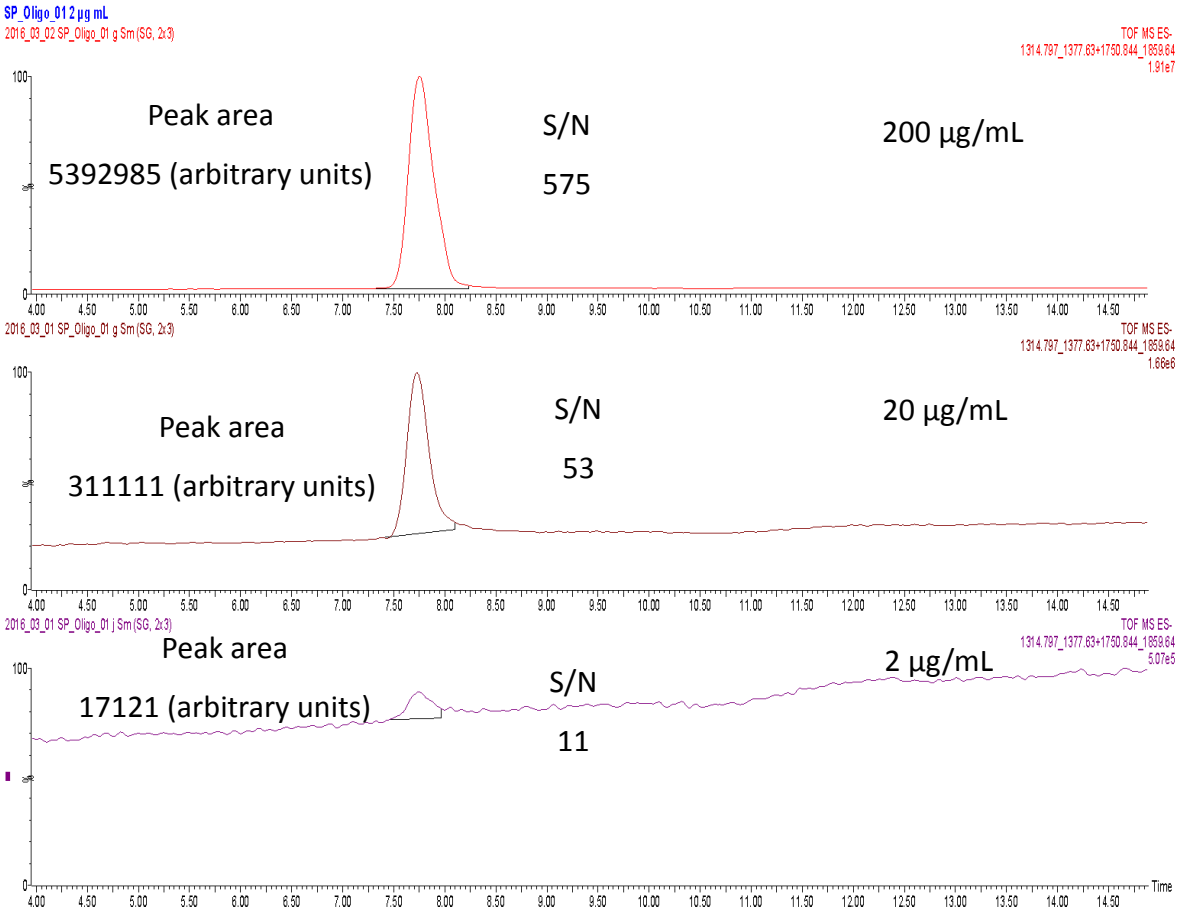

Figure 3.3 - RICC of SP_Oligo_01 at 200, 20 and 2 µg/mL (m/z 1314.797 - 1377.63 + 1750.844 - 1859.64) analysed using Waters Acquity/Waters Synapt and the Southampton chromatographic method, showing 4 - 15 minutes

The signal to noise ratio was recorded for each replicate analysed and the mean value for each sample at each concentration is shown in Table 3.8.

Table 3.8 - Mean signal to noise ratios for sample concentrations 200, 100, 20, 10, 2 and 1 µg/mL analysed using Waters Acquity/Waters Synapt

Concentration (µg/mL)	Signal to noise ratio	
	SP_Oligo_01	SP_Oligo_02
200	558 ± 25	467 ± 58
100	283 ± 12	358 ± 43
20	60 ± 3	47 ± 6
10	25 ± 1	22 ± 3
2	11 ± 0.6	10 ± 1
1	4.2 ± 0.1	3.6 ± 0.4

The data presented in Table 3.8 show that the LOD for the two 16-mer samples analysed using the Waters Acquity UHPLC/Waters Synapt is 1 µg/mL (approximately 0.18 µM) and the LLOQ is around 2 µg/mL (approximately 0.36 µM or 360 nM). The replicates used to calculate the mean signal to noise ratios were analysed using both the Southampton and AZ chromatographic methods. The low ± values indicate that the LOD and LLOQ quoted are valid for both methods.

3.4 Linearity

When the RICC peak areas for the replicates analysed at each concentration are plotted on a chart, the linear regression can be calculated. The highest concentration analysed that gives a linear regression R^2 value greater than 0.99 can be said to be the upper limit of quantification (ULOQ) for a given analyte and method of analysis.

3.4.1 Bruker MicrOTOF linearity

Figure 3.4 and Figure 3.5 show the full concentration range analysed using the Bruker MicrOTOF for SP_Oligo_01 and SP_Oligo_02. The linear regression R^2 value is below 0.99, indicating that 1000 µg/mL is above the ULOQ for these

samples when analysed using the Southampton chromatographic method and the Bruker MicrOTOF.

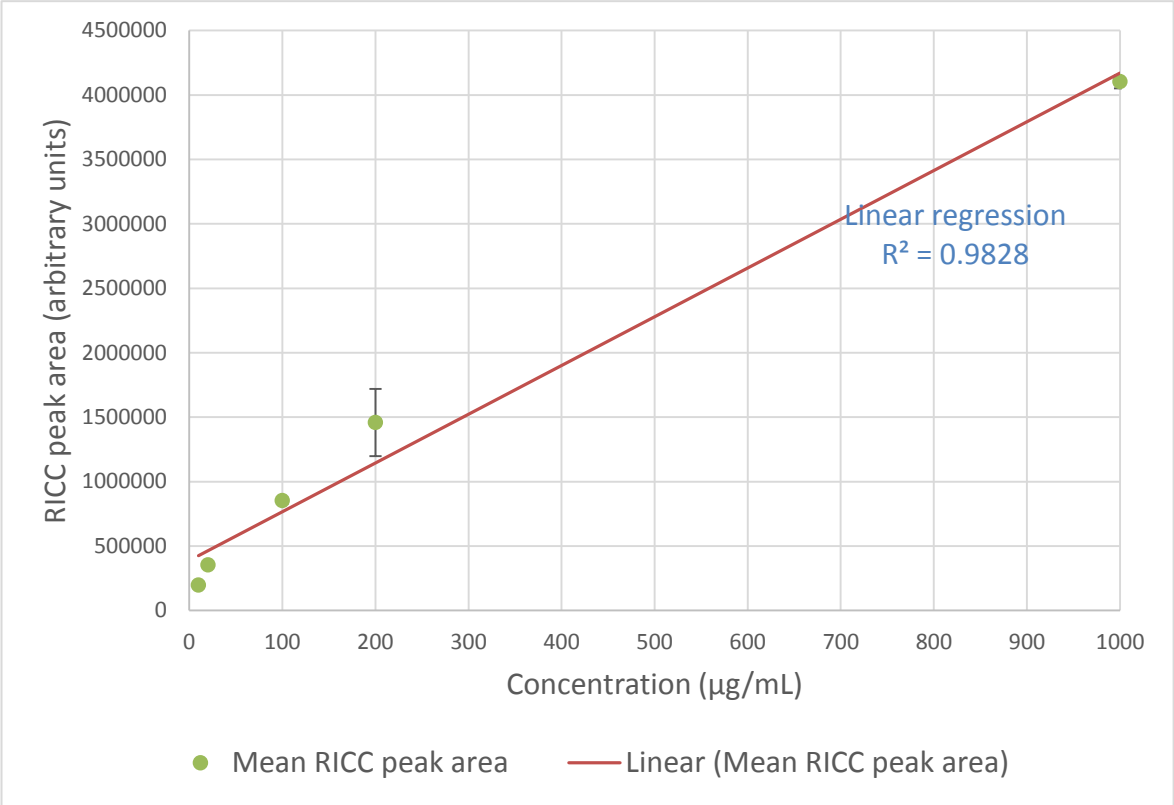

Figure 3.4 – Linearity of SP_Oligo_01 for 10 – 1000 µg/mL analysed using Bruker MicrOTOF

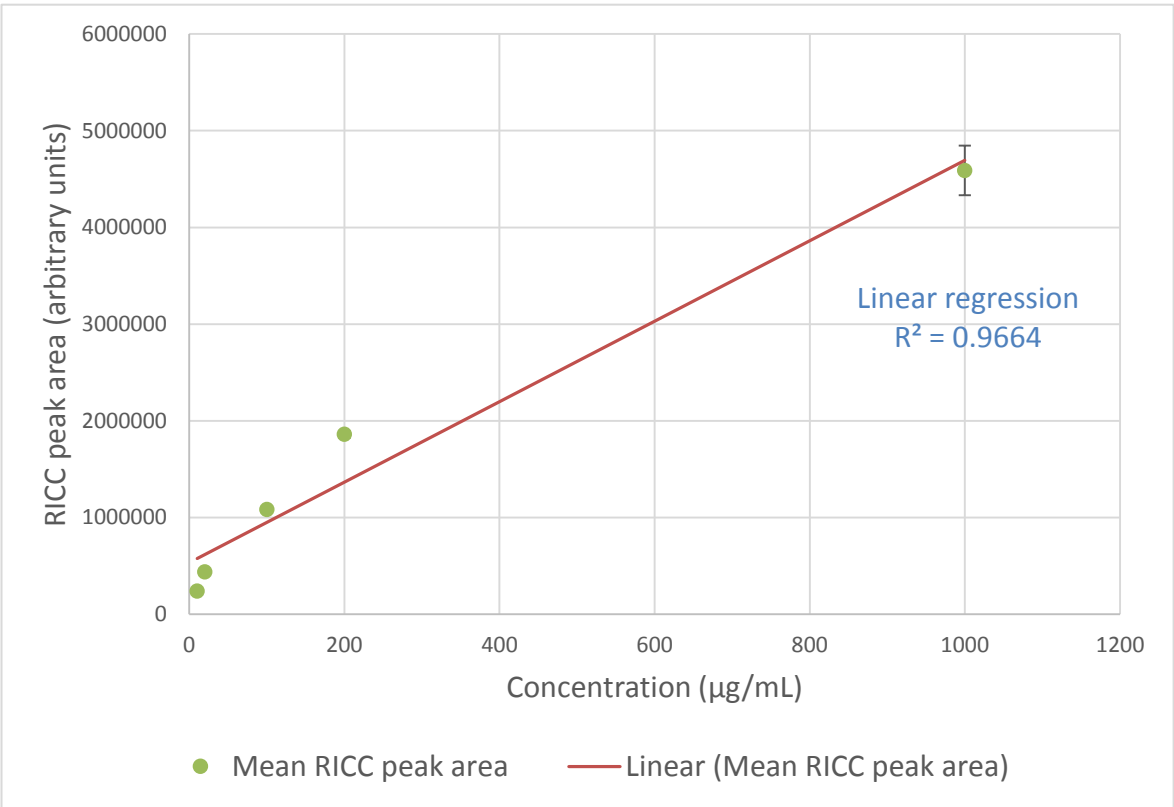

Figure 3.5 - Linearity of SP_Oligo_02 for 10 – 1000 µg/mL analysed using Bruker MicrOTOF

When the concentration range is reduced to 10 – 200 µg/mL, the linear regressions for both samples give an R^2 greater than 0.99 (Figure 3.6 and Figure 3.7). The ULOQ for the concentrations of these samples analysed using the Southampton chromatographic method and the Bruker MicrOTOF MS is 200 µg/mL.

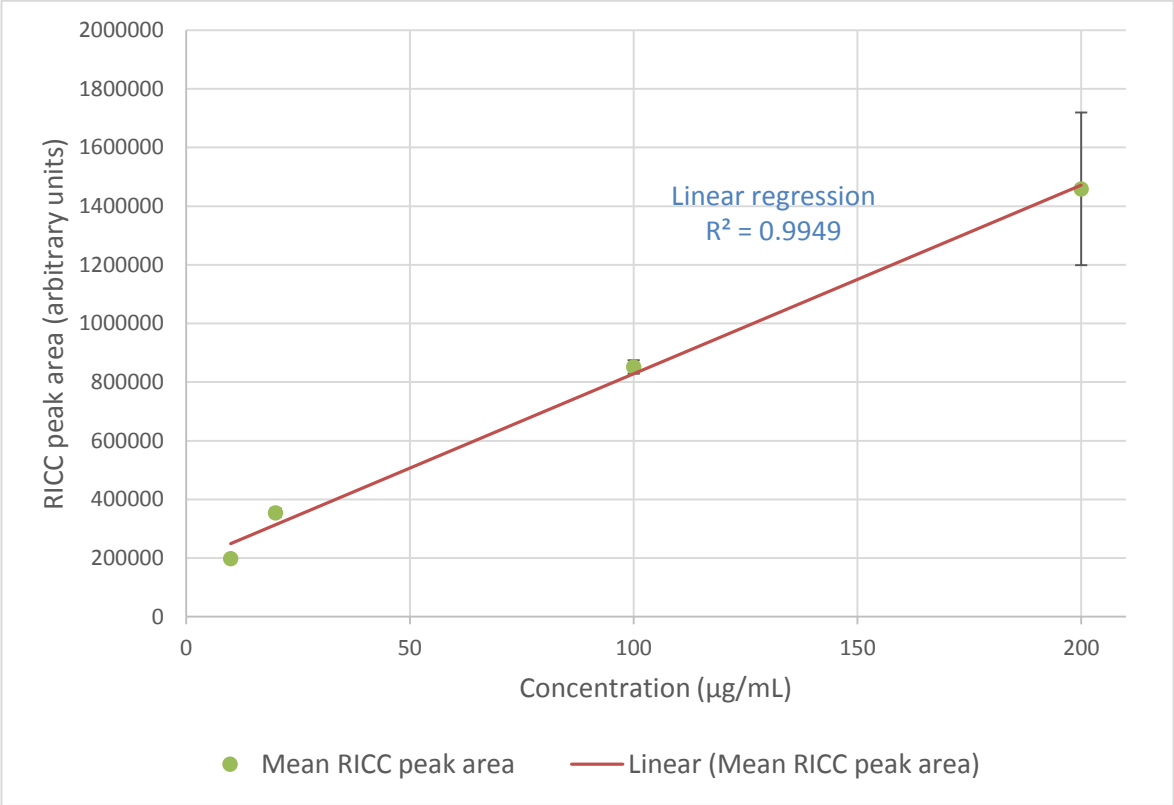

Figure 3.6 - Linearity of SP_Oligo_01 for 10 – 200 µg/mL analysed using Bruker MicrOTOF

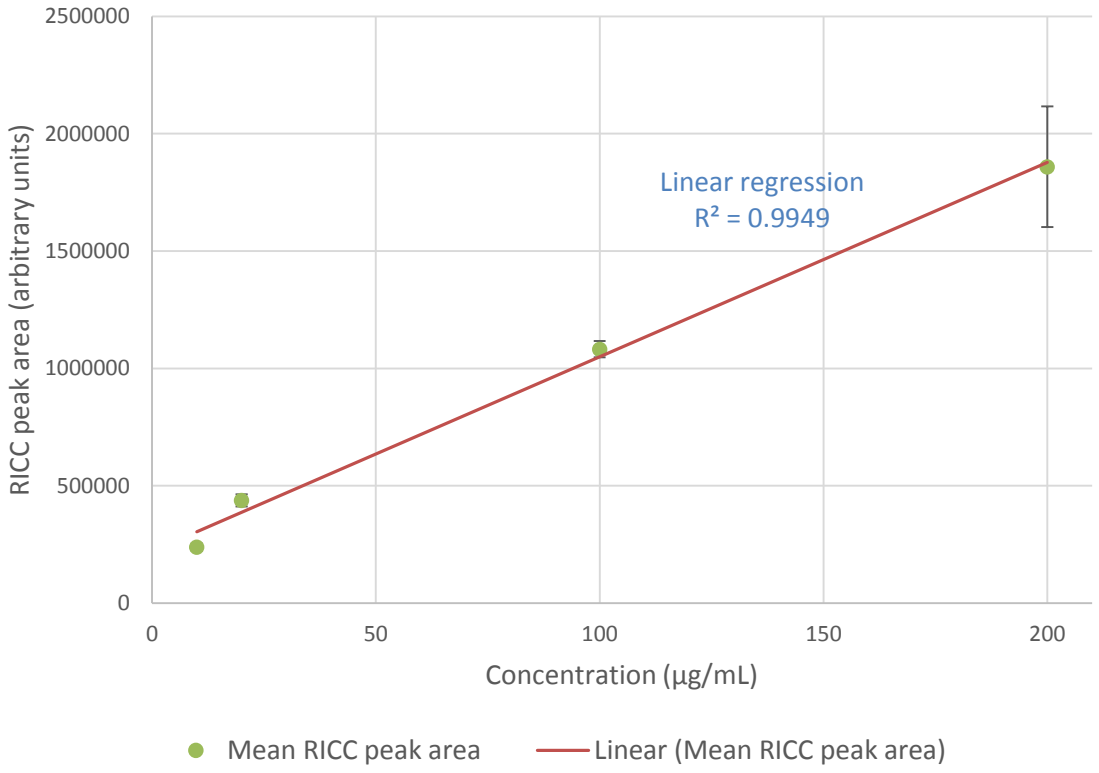

Figure 3.7 - Linearity of SP_Oligo_02 for 10 – 200 µg/mL analysed using Bruker MicrOTOF

3.4.2 Waters ZQ linearity

The linear regressions for SP_Oligo_01 and SP_Oligo_02 analysed using the Waters ZQ MS are shown in Figure 3.8 and Figure 3.9. The R^2 values for the full range of concentrations analysed are lower than 0.99, indicating that the linear range does not extend to all of these concentrations.

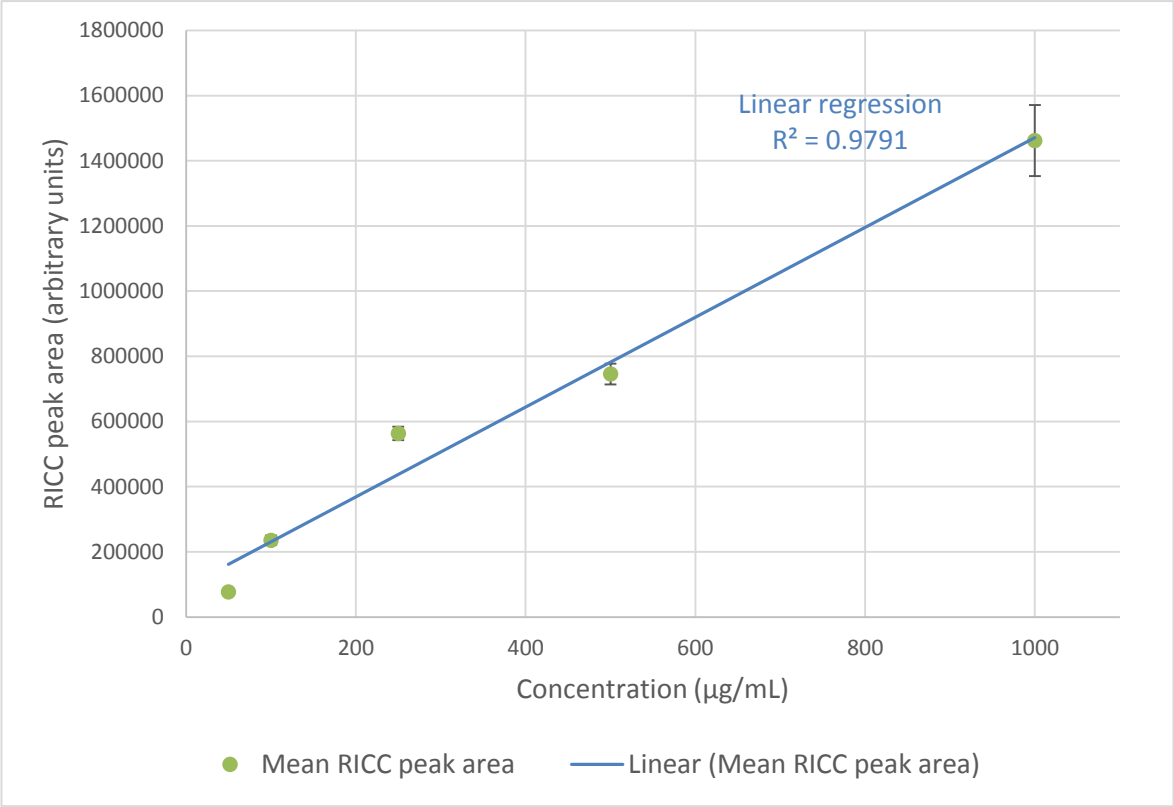

Figure 3.8 - Linearity of SP_Oligo_01 for 50 – 1000 µg/mL analysed using Waters ZQ

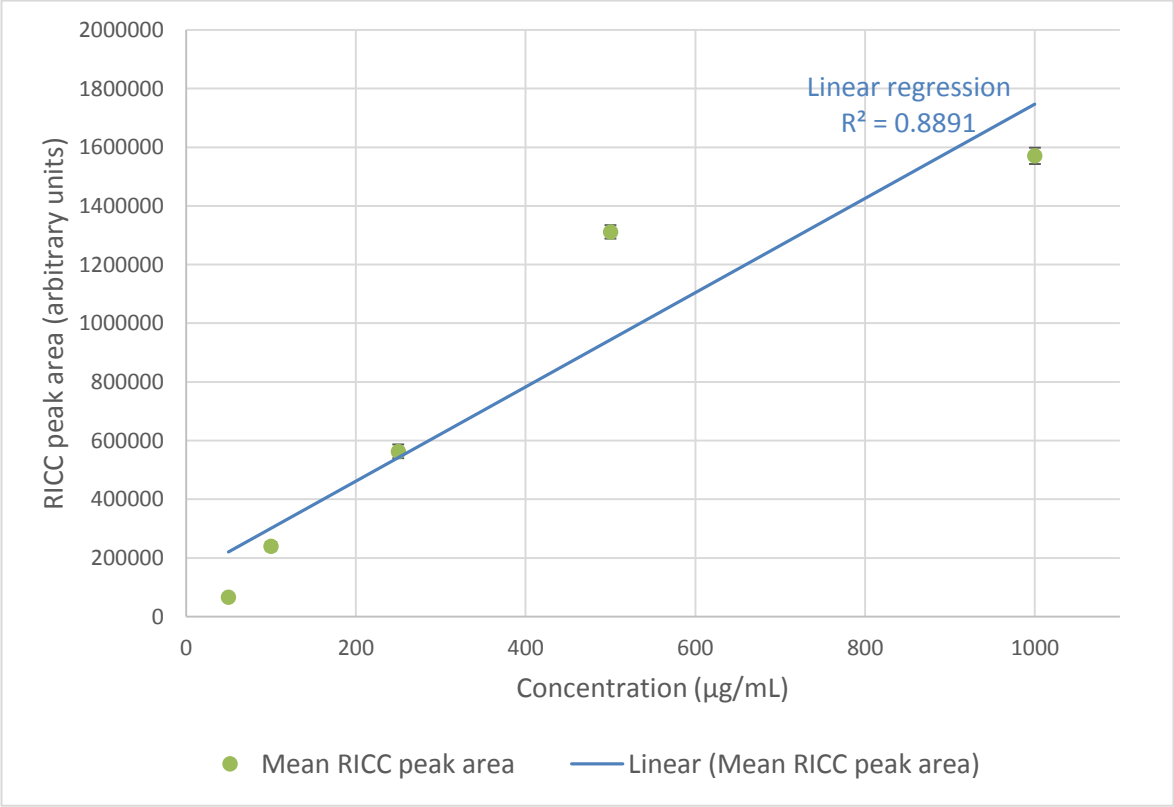

Figure 3.9 - Linearity of SP_Oligo_02 for 50 – 1000 µg/mL analysed using Waters ZQ

When the concentration ranges are reduced to 50 – 250 µg/mL for SP_Oligo_01 (Figure 3.10) and 50 – 500 µg/mL for SP_Oligo_02 (Figure 3.11), the R^2 values are greater than 0.99, showing a linear correlation.

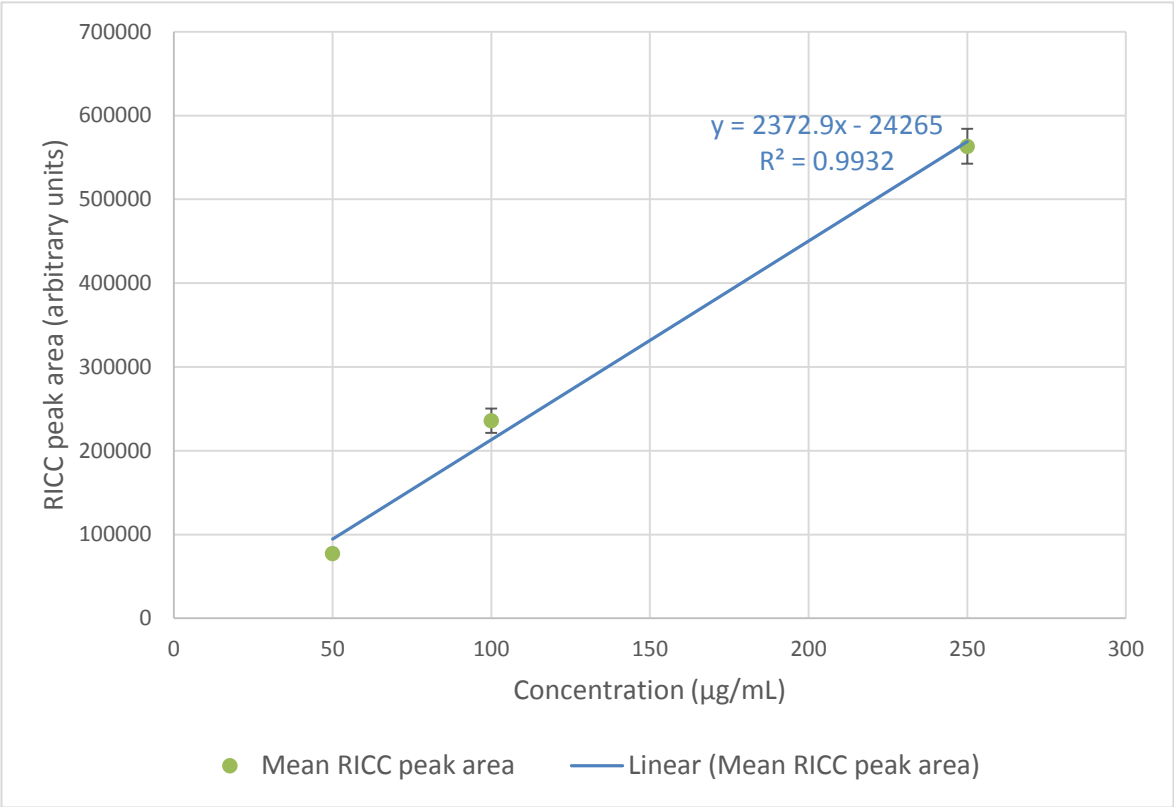

Figure 3.10 - Linearity of SP_Oligo_01 for 50 – 250 µg/mL analysed using Waters ZQ

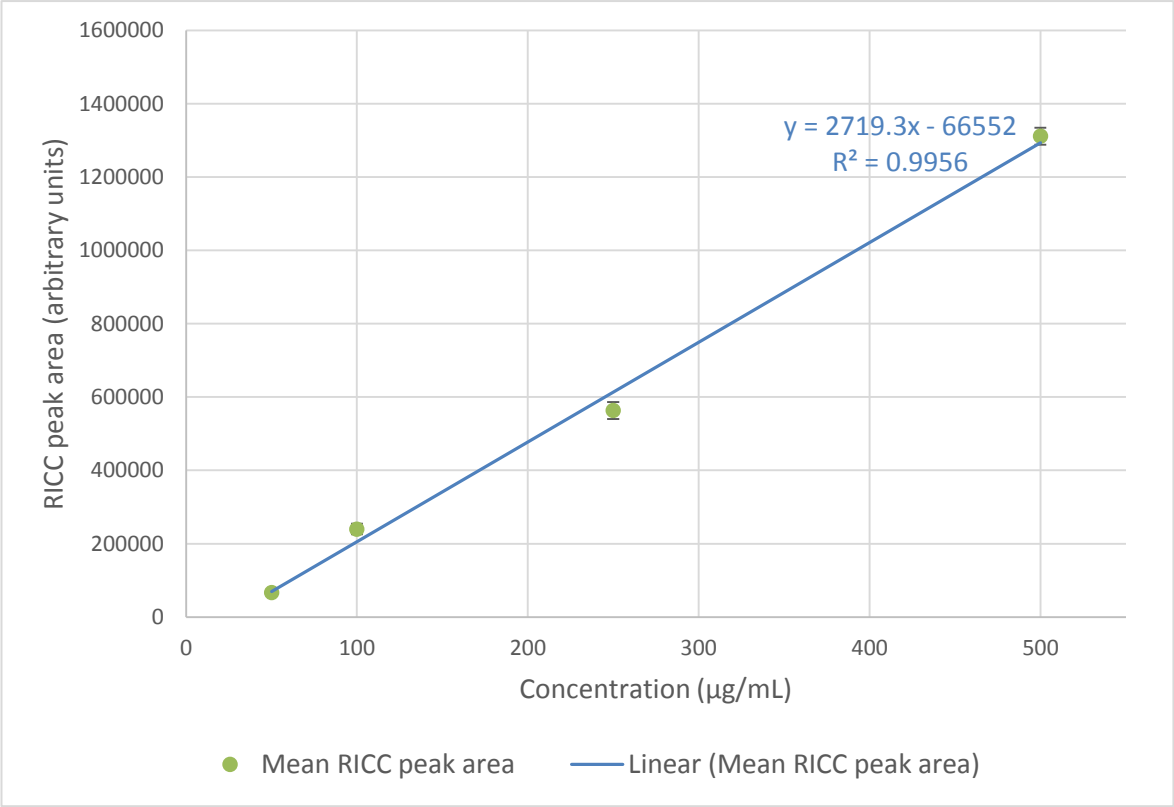

Figure 3.11 - Linearity of SP_Oligo_02 for 50 – 500 µg/mL analysed using Waters ZQ

For sample SP_Oligo_01 analysed using the Southampton and AZ chromatographic methods and the Waters ZQ MS, the ULOQ is 250 µg/mL and for SP_Oligo_02 it is 500 µg/mL.

3.4.3 Waters Synapt linearity

The linear regressions for SP_Oligo_01 and SP_Oligo_02 analysed using the Waters Synapt are shown in Figure 3.12 and Figure 3.13. For each sample, the R2 for the range 1 – 200 µg/mL is greater than 0.99, therefore the ULOQ for these samples analysed using the Southampton and AZ chromatographic methods and the Waters Synapt MS is 200 µg/mL.

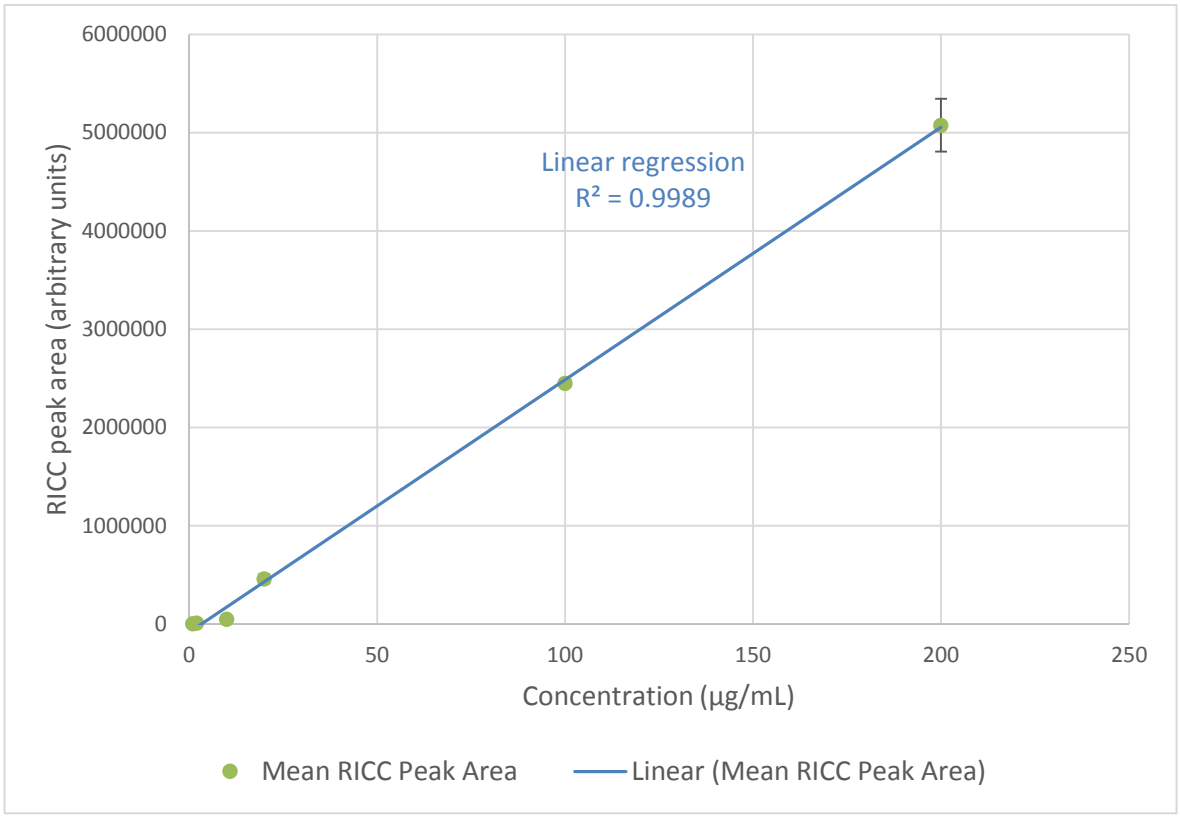

Figure 3.12 - Linearity of SP_Oligo_01 for 1 – 200 µg/mL analysed using Waters Synapt

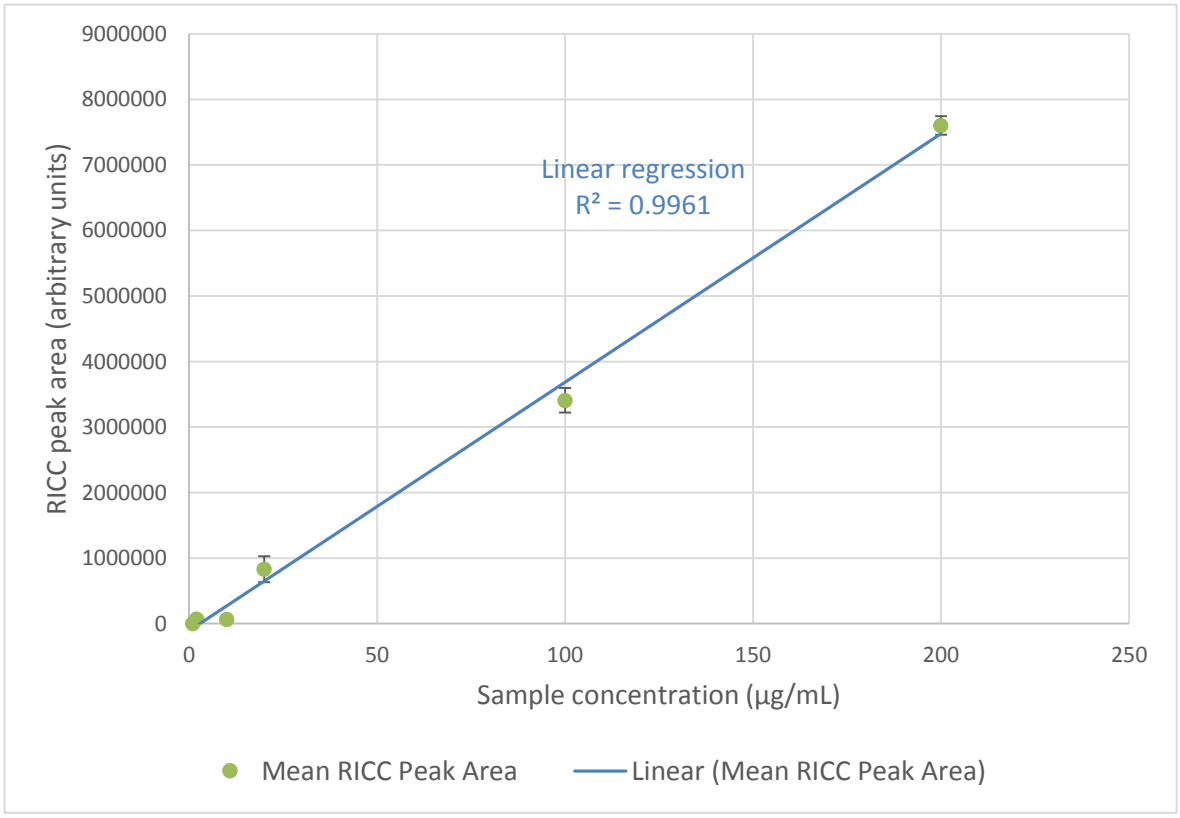

Figure 3.13 - Linearity of SP_Oligo_02 for 1 – 200 µg/mL analysed using Waters Synapt

3.5 Sensitivity conclusions

The results of these sensitivity investigations suggest that legacy instruments, such as the Waters ZQ single quadrupole MS are inherently not sufficiently sensitive to analyse the concentrations of oligonucleotides required for impurity analysis. In order to accurately and precisely quantify impurities at a level of 0.2 % of the target oligonucleotide (full-length n or FLN), low LLOQs are required to prevent overloading of the main oligonucleotide in the instrument. Table 3.9 summarises the LOD and LLOQ values calculated for each instrument.

Table 3.9 - Summary of LOD and LLOQ values for all instruments investigated

Instrument (MS)	LOD		LLOQ	
	µg/mL	µM	µg/mL	µM
Bruker MicrOTOF	10	1.8	100	18
Waters ZQ	50	9	250	45
Waters Synapt	1	0.18	2	0.36

The linear range for samples SP_Oligo_01 and SP_Oligo_02 varies according to the instrument used. More modern, sensitive instruments have a wider linear range, meaning that analytes with greater differences in concentration are able to be quantified when analysed using the Waters Synapt compared to the Waters ZQ.

The LLOQ for the oligonucleotide samples analysed using the Waters Synapt is around 50-times lower than that observed using the Bruker MicrOTOF and around 125-times lower than that achieved using the Waters ZQ. The increased sensitivity and the wider linear range observed when using the Waters Synapt support the inference that more modern instruments are the most appropriate for the analysis and quantitation of very low-level impurities in therapeutic oligonucleotides.

Chapter 4: Oligonucleotide charge envelopes

When phosphorothioate oligonucleotides are ionised using negative ionisation ESI, deprotonation most commonly occurs at the thiol group of the backbone[25]. The presence of multiple thiol groups allows for analyte ions to have between one and n – 1 (where n is the number of bases in the sequence) negative charges. The number of charge states present in the mass spectrum and the ions within each is referred to as a charge envelope.

The distribution of ions across the possible charge states affects the sensitivity of the analysis and the complexity of the spectrum generated. When the ions are distributed across fewer charge states, the sensitivity will be increased over a spectrum with more charge states present and the spectrum with fewer charge states will also be less complex[83] and, therefore, make the presence and level of impurities easier to identify and interpret.

The charge envelope of an oligonucleotide sample can be manipulated by changing various factors including mobile phase additives and buffers[84], mobile phase solvents and the pH of the solution [83] and is also affected by the type of mass analyser used[85]. It is essential to understand the differences in charge state distribution between instruments and methods and the effects of each variable to ensure consistent quantitation of oligonucleotide impurities.

The effect of mobile phase additives and solvents and their pH on the mass spectra of therapeutic oligonucleotides has been studied by several groups of researchers over the last 20 years, from Cheng *et al.*[83], Muddiman *et al.*[84] and Apffel *et al.*[73] in the 1990s, through to Erb & Oberacher[86] in 2014 and Basiri *et al.*[87] in 2017 with many others in between. The mass analyser aspect has been significantly less researched, with the main papers on the subject being published by Premstaller and Huber[85, 88] in 2001.

4.1 Mobile phase additives

Previously published research by Cheng *et al*.[83] and Muddiman *et al.* [84] has shown that addition of reagents such ammonium acetate and piperidine can alter the charge state distribution of oligonucleotide samples. In the research presented in

this thesis, different reagents are used for each chromatographic method, although both methods utilise acetates as buffers and ion-pair reagents.

Figure 4.1 shows the differences in charge envelope between the negative ionisation ESI mass spectra of SP_Oligo_01 analysed using the Waters Synapt mass spectrometer and the Southampton and AZ chromatographic methods (SCM and ACM, respectively).

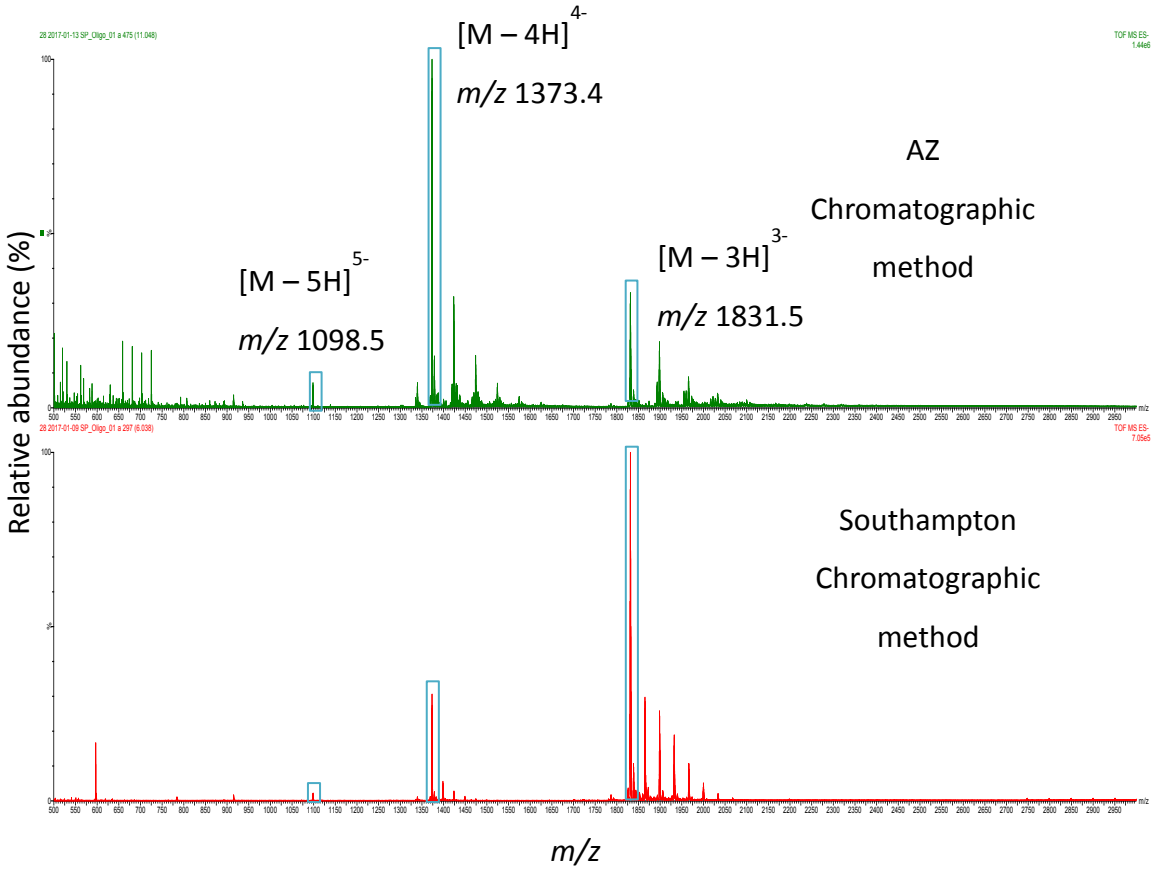

Figure 4.1 - Negative ionisation ESI mass spectra of SP_Oligo_01 analysed using the Waters Synapt and the AZ and Southampton chromatographic methods

The presence of tributylammonium acetate and EDTA in the AZ chromatographic method compared to the triethylammonium acetate and HFIP in the Southampton chromatographic method produces a charge state distribution with a greater proportion of ions having four negative charges than three and a greater relative proportion of ions in the -5 charge state.

The distribution of ions across a greater number of charge states means that the sensitivity of any one ion is reduced, this produces the risk of impurities being too low in abundance to accurately and precisely quantitate. If impurities do not

display the same charge state distribution as the target oligonucleotide, then quantitation relative to the target ion may yield different vales depending on which ion is selected causing differences in reported impurity levels between methods.

Cech and Enke[89] suggested that oligonucleotide samples analysed using HFIP as an additive display lower charge states than those analysed using 2,2,2-trifluoroethanol (TFE) as a result of the lower gas-phase proton affinity of HFIP. Basiri *et al.*[90] theorise that the lower pKa of HFIP compared to TFE (9.3 and 12.4, respectively[91]) leads to increased protonation of oligonucleotides, resulting in lower charge states. It seems likely that this is also the case when comparing EDTA and HFIP as the highest pKa value of EDTA is 10.3[92].

4.2 Organic content of the mobile phase

A potential approach for improving the consistency of oligonucleotide impurity quantitation is to use an internal standard. This is a compound added in known concentrations to every sample and to calibration standards so that the ratio of the peak area or ion intensity of the sample can be compared to that of the internal standard compound to give a concentration and differences between replicates related to sample preparation or injection volume are accounted for. In the case of therapeutic oligonucleotides, an oligonucleotide sequence that elutes away from the sample sequence is required to ensure peak areas are not compromised by lack of chromatographic resolution resulting from ion suppression or enhancement.

To ensure that eluting at a different point in the gradient does not alter the ionisation efficiency and charge envelope of an oligonucleotide, the effect of changing the mobile phase gradient to alter the percentage organic content at which an oligonucleotide elutes was investigated. The RICC peak areas for different charge states and the distribution of ions across the charge envelope were monitored for changes. The behaviour of the charge envelope was studied for the Southampton and AZ chromatographic methods using the Waters Synapt mass spectrometer and Waters Acquity UHPLC.

4.2.1 Southampton chromatographic method

In order to investigate the effect of mobile phase organic content on charge state distribution, five methods based on the Southampton chromatographic method, using its ion-pair reagents and buffers, were created that caused elution of the SP_Oligo_01 peak at different percentages of organic mobile phase composition; the gradients used in these methods are shown in Table 4.1.

Table 4.1- Mobile phase gradients for Southampton chromatographic method-based test methods. Initial composition is 5% organic for all methods

Method	Time (min)	% Organic	Method	Time (min)	% Organic
Southampton	14	40	Test Method 3	5	40
	15	5		14	40
	18	5		15	5
Test Method 1	13	40		18	5
	14	40	Test Method 4	17	40
	15	5		18	5
	18	5	Test Method 5	12	25
Test Method 2	10	40		13	25
	14	40		15	40
	15	5		16	5
	18	5		18	5

Figure 4.2 shows the variation in retention time (RT) of the UV SP_Oligo_01 peak at 260 nm for each method analysed. The percentage organic composition of the mobile phase at the retention time of the sample was calculated using the RT and the gradient of the method as shown in Table 4.1.

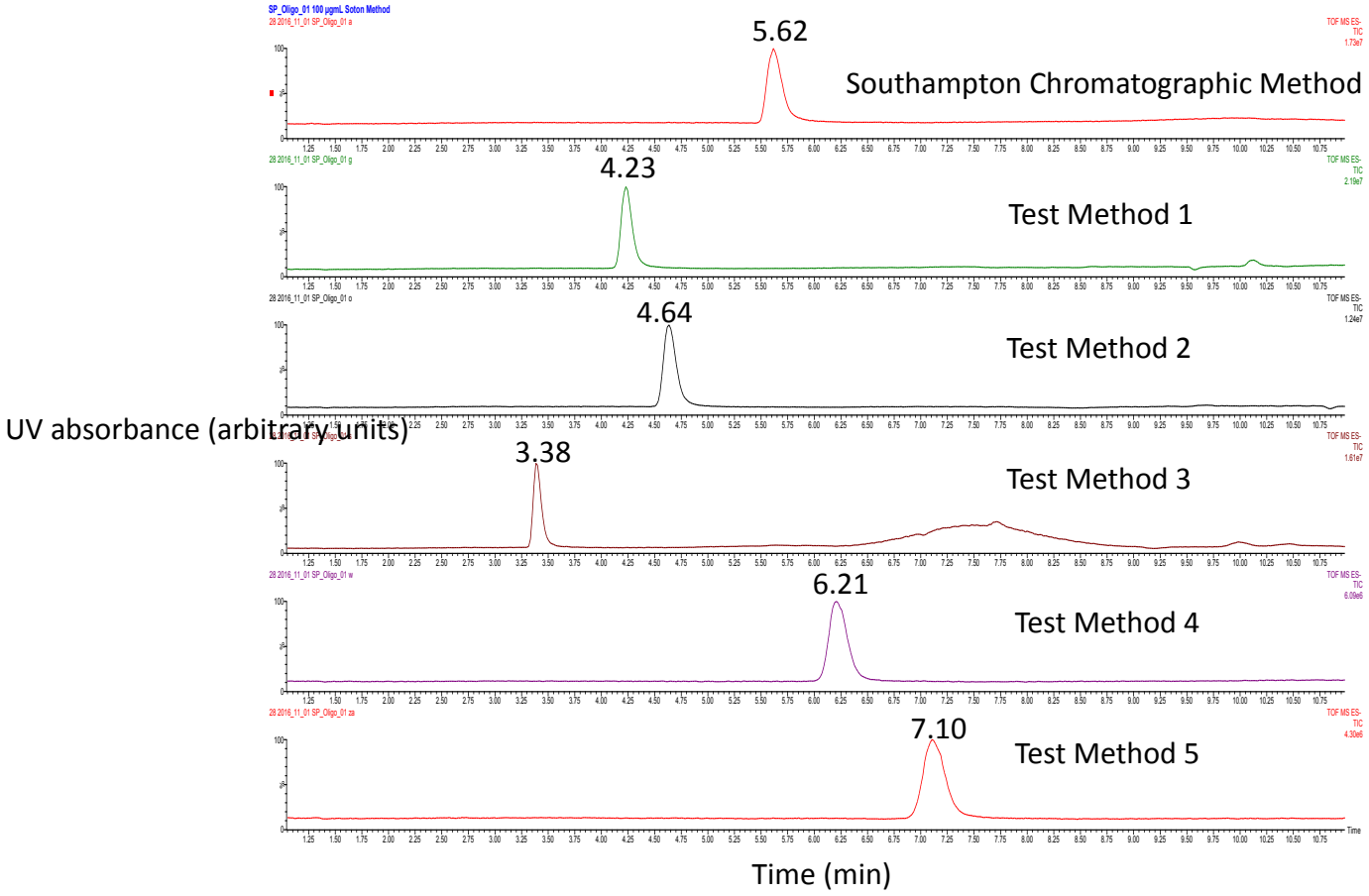

Figure 4.2 - 260 nm UV chromatograms showing retention times of SP_Oligo_01 for each Southampton chromatographic method-based test method (see Table 4.1 for gradients)

Table 4.2 shows the mean of the RICC peak areas of ten replicates for the -3 (*m/z* 1831.5) and -4 (*m/z* 1373.7) charge states of SP_Oligo_01 along with the mean ratio of the charge states across all ten replicates analysed for each method arranged by the percentage of organic mobile phase composition at which the sample elutes. The results from the table are presented graphically in Figure 4.3 and Figure 4.4. Figure 4.4 shows that there is only a small difference in the distribution of ions between the -3 and -4 charge states across the different methods, with the ratio of these two charge states remaining consistent at 0.23 – 0.27 for the ratio of -4/-3.

The RICC peak areas vary across the test methods, as can be seen in Figure 4.3. The methods with the lowest two percentages of organic content show the lowest RICC peak areas for the -3 and -4 charge state ions, corresponding with the results published by Bleicher and Bayer in 1994[93]. The variation in the replicates

mean that peak areas for the highest percentage of organic content (Test method 3) overlap with the peak areas for the method with a 10% lower organic content (Test method 4). The data related to peak areas and the ratio of charge states were analysed in MiniTab using a One-Way ANOVA test. The results of these tests are shown in Figure 4.5 and Figure 4.6 and indicate that peak areas vary according to method, but there is no obvious pattern between the organic content and the peak area and the mean of the ratio of the charge states is not significantly different across the test methods.

Table 4.2 – Mean RICC peak areas and charge state ratios for each test method. n = 10

Method	**% Organic**	**Mean RICC peak area -3 charge state (arbitrary units)**	**Mean RICC peak area -4 charge state (arbitrary units)**	**Mean ratio -4 charge state/-3 charge state**	**Coefficient of Variance (CoV) (%)**		
					-3	**-4**	**Ratio**
Test Method 5	17	198701 ± 21219	52663 ± 5684	0.26 ± 0.002	34	34	2
Test Method 4	18	293175 ± 24936	63813 ± 6608	0.27 ± 0.002	33	33	2
Southampton Chromatographic method	19	451017 ± 33126	121761 ± 7406	0.27 ± 0.006	23	19	7
Test Method 2	21	334634 ± 32472	84275 ± 6682	0.26 ± 0.005	31	25	6
Test Method 1	23	415576 ± 35639	102175 ± 7219	0.25 ± 0.005	27	22	6
Test Method 3	28	300772 ± 62769	69907 ± 5650	0.23 ± 0.003	28	26	5

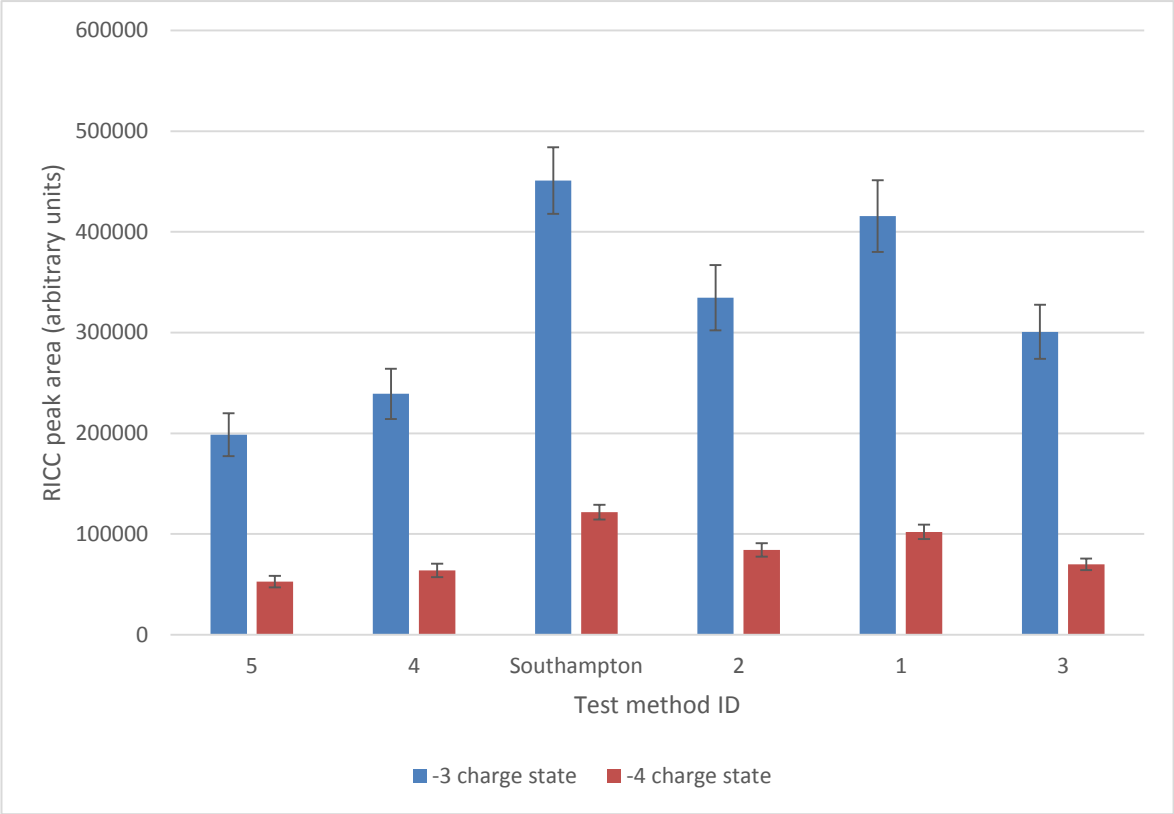

Figure 4.3 – RICC peak areas for the -3 and -4 charge states of SP_Oligo_01 analysed using the Waters Synapt and the Southampton chromatographic method-based test methods. n = 10

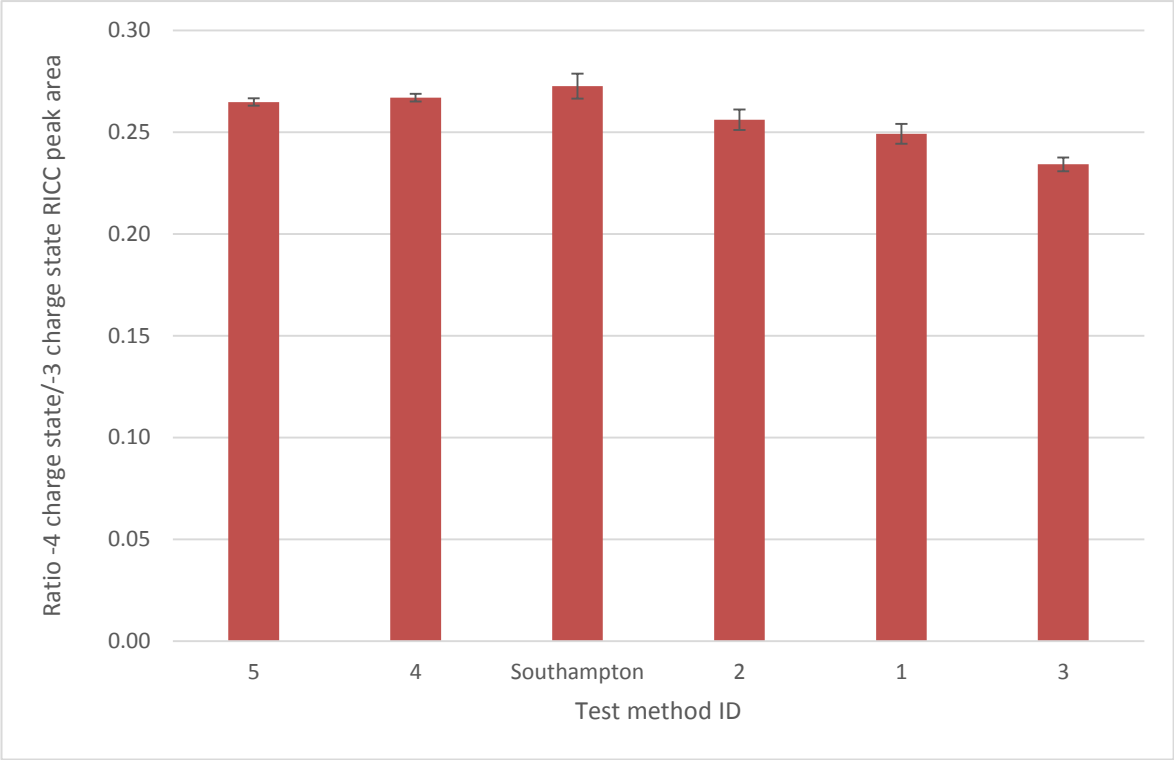

Figure 4.4 – Ratio of RICC peak areas for the -3 and -4 charge states of SP_Oligo_01 analysed using the Waters Synapt and the Southampton chromatographic method-based test methods. n = 10

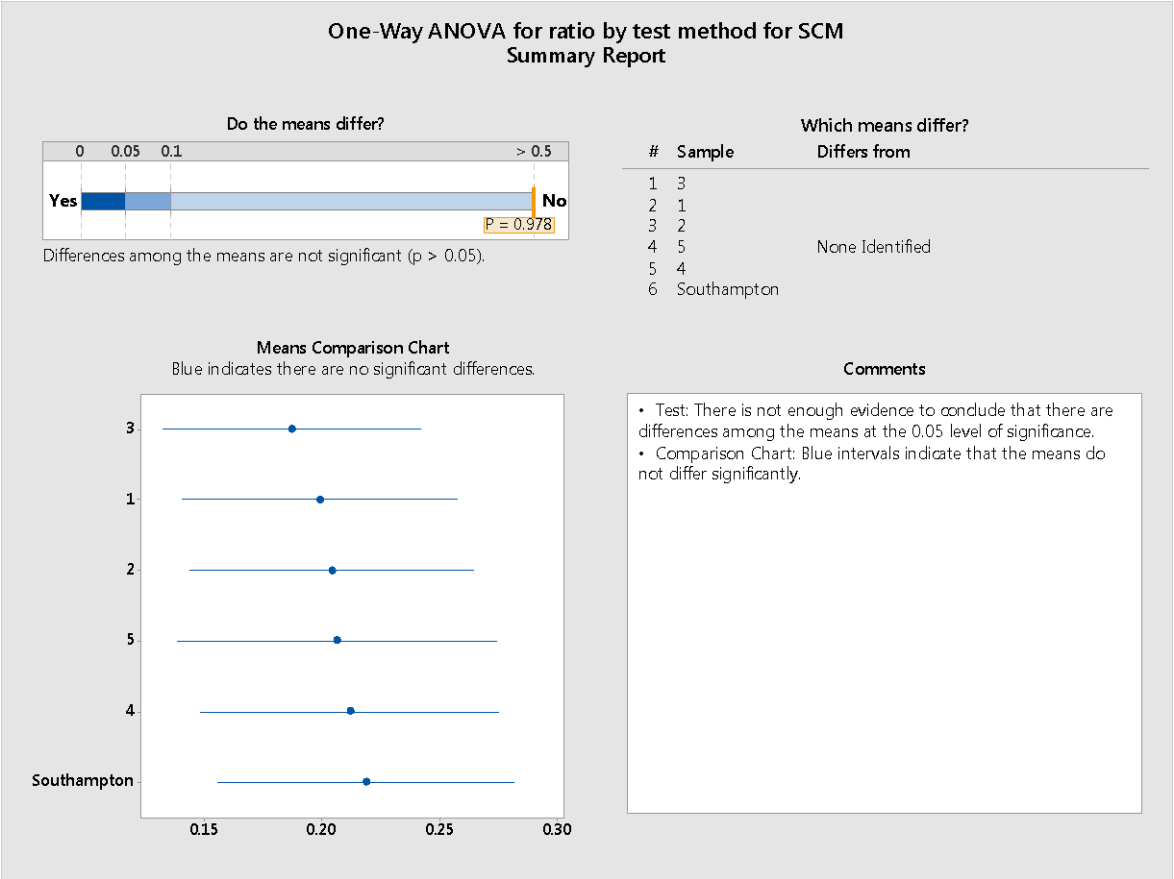

Figure 4.5 – One-Way ANOVA test summary results for differences in means of the ratio of -4/-3 charge states of SP_Oligo_01 analysed using the Waters Synapt and Southampton chromatographic method-based test methods. n = 10

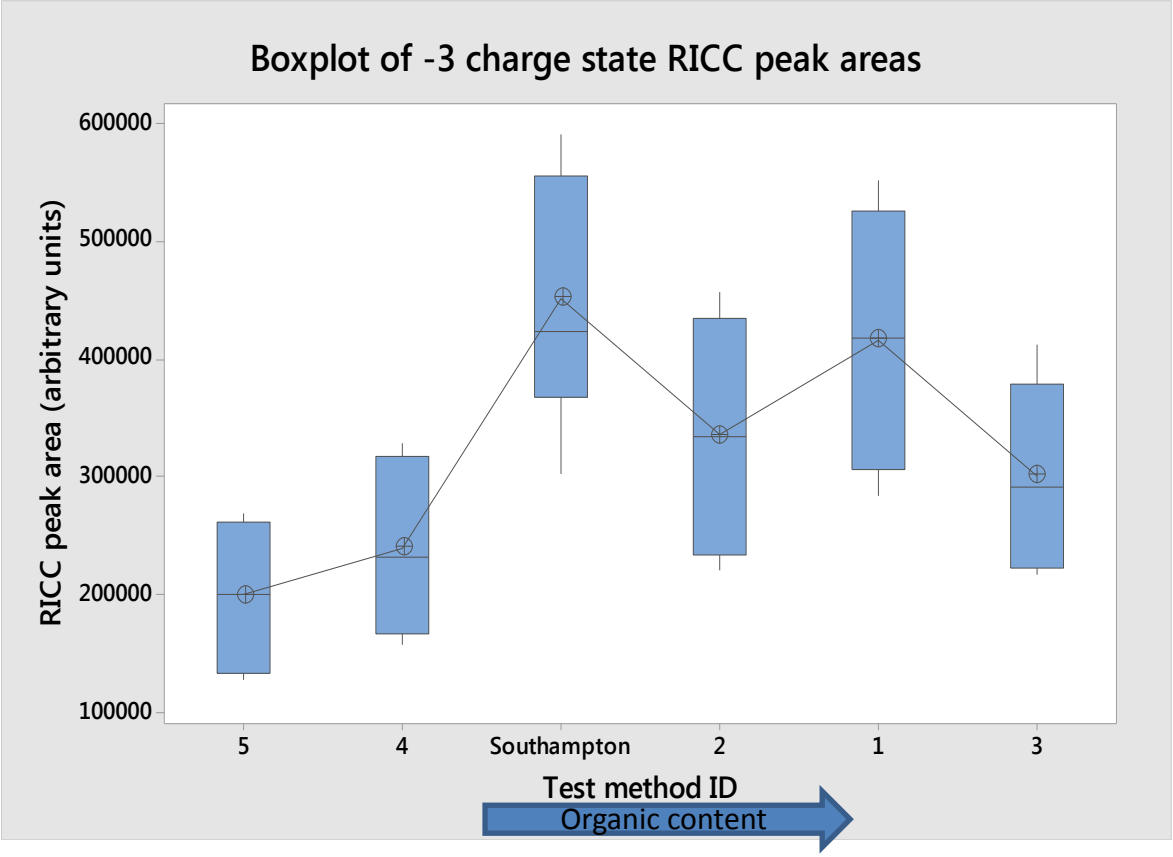

Figure 4.6 - Boxplot of RICC peak areas for the -3 charge state of SP_Oligo_01 by test method, analysed using the Waters Synapt and Southampton chromatographic method based methods. n = 10

4.2.2 AZ chromatographic method

Five methods based on the AZ chromatographic method, using its ion-pair reagents and buffers, were created that caused elution of the SP_Oligo_01 peak at different percentages of organic mobile phase composition; the gradients used in these methods are shown in Table 4.3.

Table 4.3 - Mobile phase gradients for AZ chromatographic method-based test methods. Initial composition is 45% organic for all methods

Method	Time (min)	% Organic	Method	Time (min)	% Organic
AZ Chromatographic method	22	80	Test Method 3	5	80
	25	80		25	80
	26	45		26	45
Test Method 1	22	60	Test Method 4	22	50
	25	80		25	80
	26	45		26	45
Test Method 2	10	80	Test Method 5	12	60
	25	80		13	60
	26	45		25	80
				26	45

Figure 4.7 shows the variation in retention time (RT) of the UV SP_Oligo_01 peak at 260 nm for each method analysed. The percentage organic composition of the mobile phase at the retention time of the sample was calculated using the RT and the gradient of the method as shown in Table 4.3.

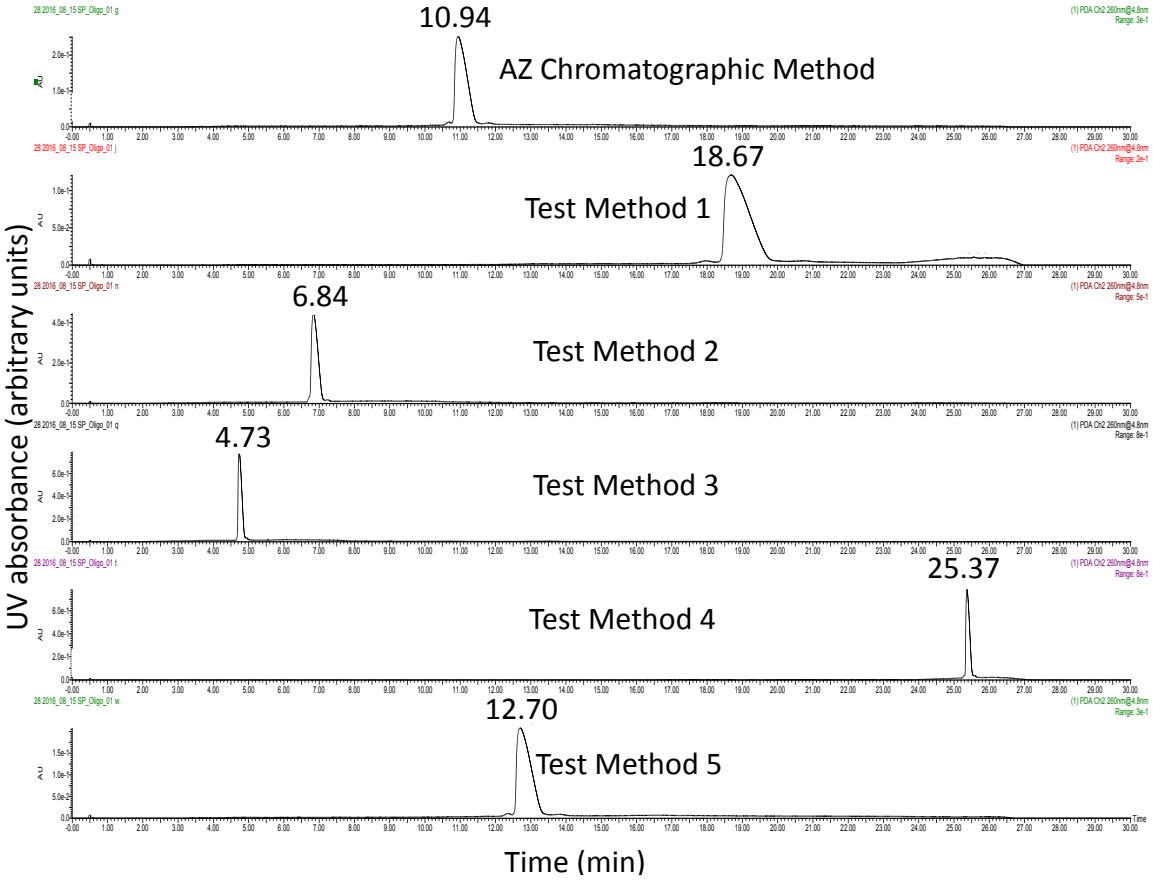

Figure 4.7 - 260 nm UV chromatograms showing retention times of SP_Oligo_01 for each AZ chromatographic method-based test method

Table 4.4 shows the mean RICC peak area for the -3 and -4 charge states of SP_Oligo_01, along with the mean ratio of the charge states across six replicates analysed for each test method and nine replicates analysed for the AZ chromatographic method. Table 4.4 is sorted by the percentage of organic mobile phase composition at which the sample elutes. The results presented in the table are shown graphically in Figure 4.8 and Figure 4.9, where it becomes evident that there is no difference in the charge state distribution across the different methods, with the ratio of the charge states remaining consistent between 0.42 and 0.52 for the ratio -4/-3 charge states (Figure 4.9). The RICC peak areas vary across the test methods, as shown in Figure 4.8, but there is no correlation between the RICC peak area and the organic content of the mobile phase at the point of elution, with the largest peak areas observed at the lowest percentage of organic content (Test method 1) and the smallest in the middle of the range (Test method

4) for the -3 charge state and the highest organic percentage (Test method 3) for the -4 charge state.

Table 4.4 – Mean RICC peak areas and charge state ratios for each test method. n = 10

Method	**% Organic**	**Mean RICC peak area -3 charge state (arbitrary units)**	**Mean RICC peak area -4 charge state (arbitrary units)**	**Mean ratio -4 charge state/-3 charge state**
Test Method 1	58	1404944 ± 183030	743532 ± 230967	0.46 ± 0.10
Test Method 5	60	918349 ± 62746	427262 ± 143667	0.42 ± 0.13
Test Method 4	63	668463 ± 54637	374775 ± 94102	0.52 ± 0.10
AZ Chromatographic method	64	1389336 ± 140338	727858 ± 140442	0.49 ± 0.05
Test Method 2	70	1040465 ± 146431	512956 ± 130212	0.45 ± 0.06
Test Method 3	79	739761 ± 79732	350701 ± 86739	0.44 ± 0.08

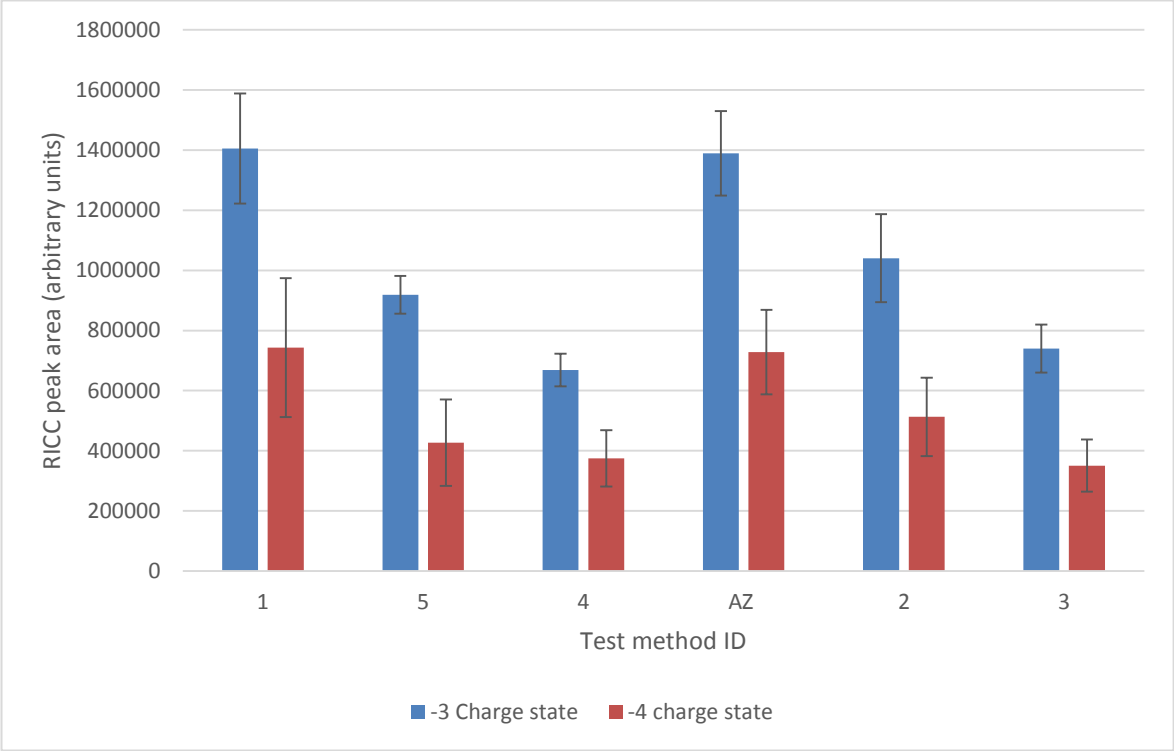

Figure 4.8 - RICC peak areas for the -3 and -4 charge states of SP_Oligo_01 analysed using the Waters Synapt and the AZ chromatographic method-based test methods. n = 10

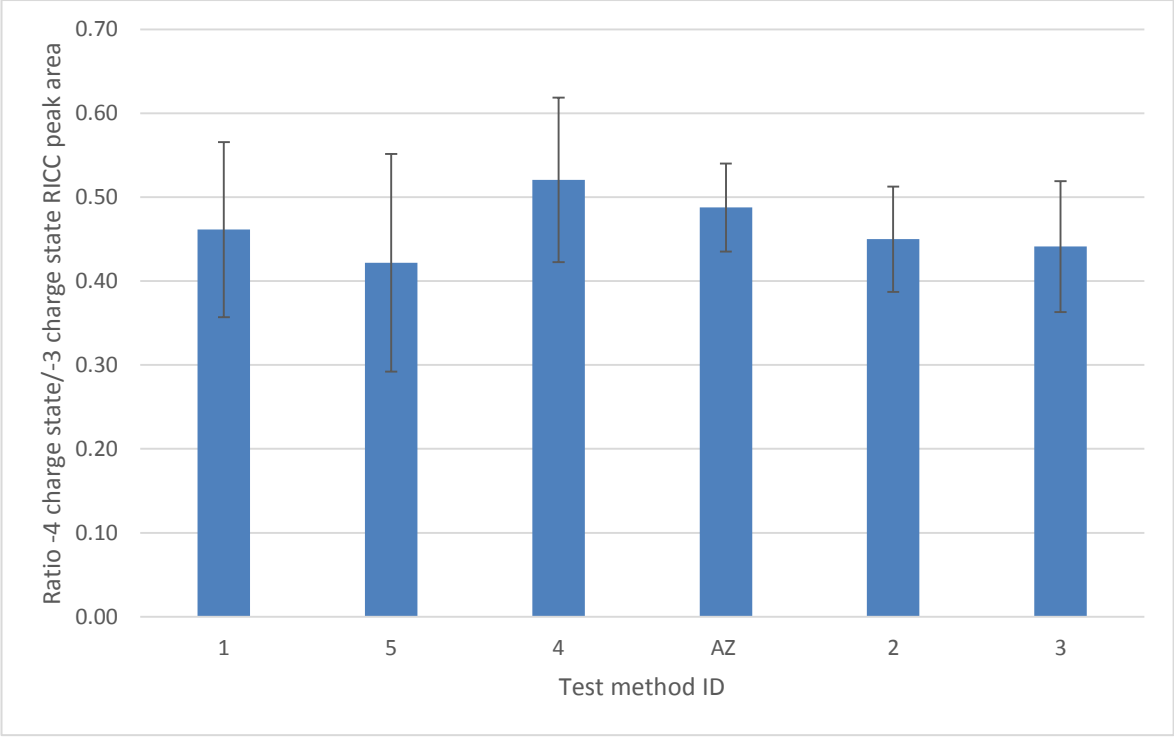

Figure 4.9 – Ratio of RICC peak areas for the -3 and -4 charge states of SP_Oligo_01 analysed using the Waters Synapt and the AZ chromatographic method-based test methods. n = 10

The range of organic content percentages investigated for each chromatographic method had no impact on the charge state distribution between the -3 and -4 charge states for the sample SP_Oligo_01 analysed using the Waters Synapt mass spectrometer. There is no obvious relationship between the RICC peak area and the percentage of organic content at which the oligonucleotide elutes, regardless of the mobile phase additives used, although differences in peak area have been observed between the methods analysed. These findings lead to the conclusion that, with appropriate validation of the chosen internal standard sequence and its behaviour, it is valid to consider the use of an internal standard to improve the confidence in quantitation of oligonucleotide impurities.

4.3 Mobile phase solution pH

The ion-pair reagents and buffers used in the Southampton and AZ chromatographic methods give the organic and aqueous mobile phases different pHs. Table 4.5 shows the pH of the individual mobile phases and the pH of the mixture of mobile phases at the relevant combination for the initial and final compositions of the gradients.

Table 4.5 - Mobile phase pH

Solution	pH
AZ chromatographic method mobile phase A (aqueous)	5.7
AZ chromatographic method mobile phase B (organic)	7.6
AZ chromatographic method initial composition (45% organic)	6.8
AZ chromatographic method final composition (80% organic)	7.1
Southampton chromatographic method mobile phase A (aqueous)	6.3
Southampton chromatographic method mobile phase B (organic)	9.5
Southampton chromatographic method initial composition (5% organic)	6.4
Southampton chromatographic method final composition (40% organic)	7.1

To investigate the influence of the pH of the mobile phase on the charge state distribution of oligonucleotides, the Southampton chromatographic method aqueous and organic mobile phases were adjusted to pH 4 using acetic acid and to pH 9.5 using triethylamine to give a consistent pH across the whole analytical gradient.

Figure 4.10 shows the negative ionisation ESI mass spectra of SP_Oligo_01 using the Southampton chromatographic method and at the two pHs investigated. Analysis at pH 9.5 distributes more ions into the -3 charge state than the -4 charge state, compared to the Southampton chromatographic method with a pH of around 7. The more acidic solutions, at pH 4, show a significant decrease in both charge states usually seen in negative ionisation ESI mass spectra using the Waters Synapt.

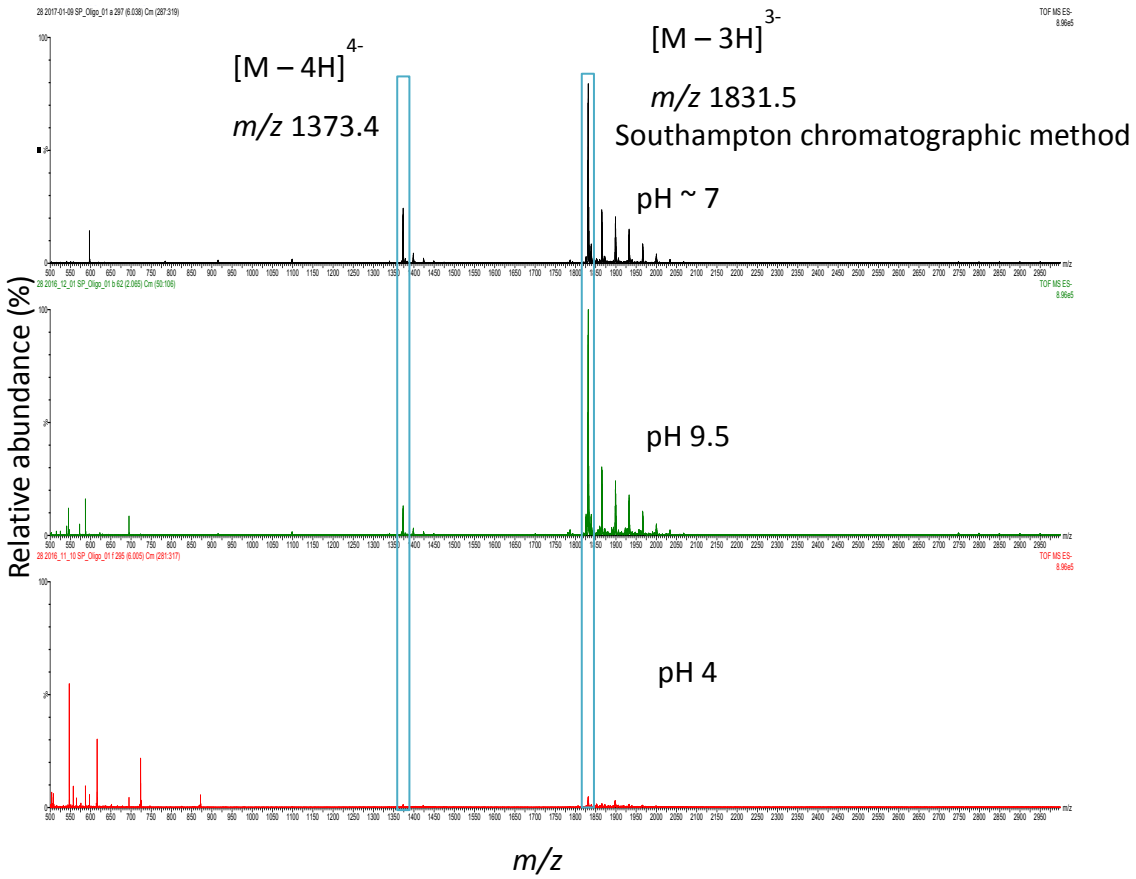

Figure 4.10 - Negative ionisation ESI mass spectra of SP_Oligo_01 analysed using the Waters Synapt and Southampton chromatographic method mobile phases at the pH shown. Ions shown are normalised to the abundance of the $[M - 3H]^{3-}$ ion analysed at pH 9.5

Table 4.6 shows the mean RICC peak areas for the -3 and -4 charge state ions and the ratio of -4 to -3 peak areas for ten replicates analysed at each pH. These data confirm that samples analysed with a mobile phase pH of 4 have a peak area an order of magnitude lower than those analysed using the Southampton chromatographic method or using a mobile phase pH of 9.5, as would be expected from research previously published by other authors on the pH of oligonucleotides[87].

Table 4.6 - Mean RICC peak areas and charge state ratios for each pH tested. n = 10

pH	Mean RICC peak area -3 charge state (arbitrary units)	Mean RICC peak area -4 charge state (arbitrary units)	Mean ratio -4 charge state/ -3 charge state
4	53928 ± 4670	14479 ± 1370	0.27 ± 0.01
7	451017 ± 33126	121761 ± 7406	0.27 ± 0.01
9.5	224207 ± 16527	34680 ± 3942	0.15 ± 0.01

4.4 Mass analyser type

Oligonucleotide samples were analysed using Waters ZQ and Agilent 6130 quadrupole mass analysers and Waters Synapt Q-TOF and Bruker MicrOTOF time of flight mass analysers in the course of this research. Figure 4.11 to Figure 4.16 show the negative ionisation ESI mass spectra of SP_Oligo_01 for each mass analyser used and, for the Waters Synapt and Waters ZQ, for the Southampton and AZ chromatographic methods.

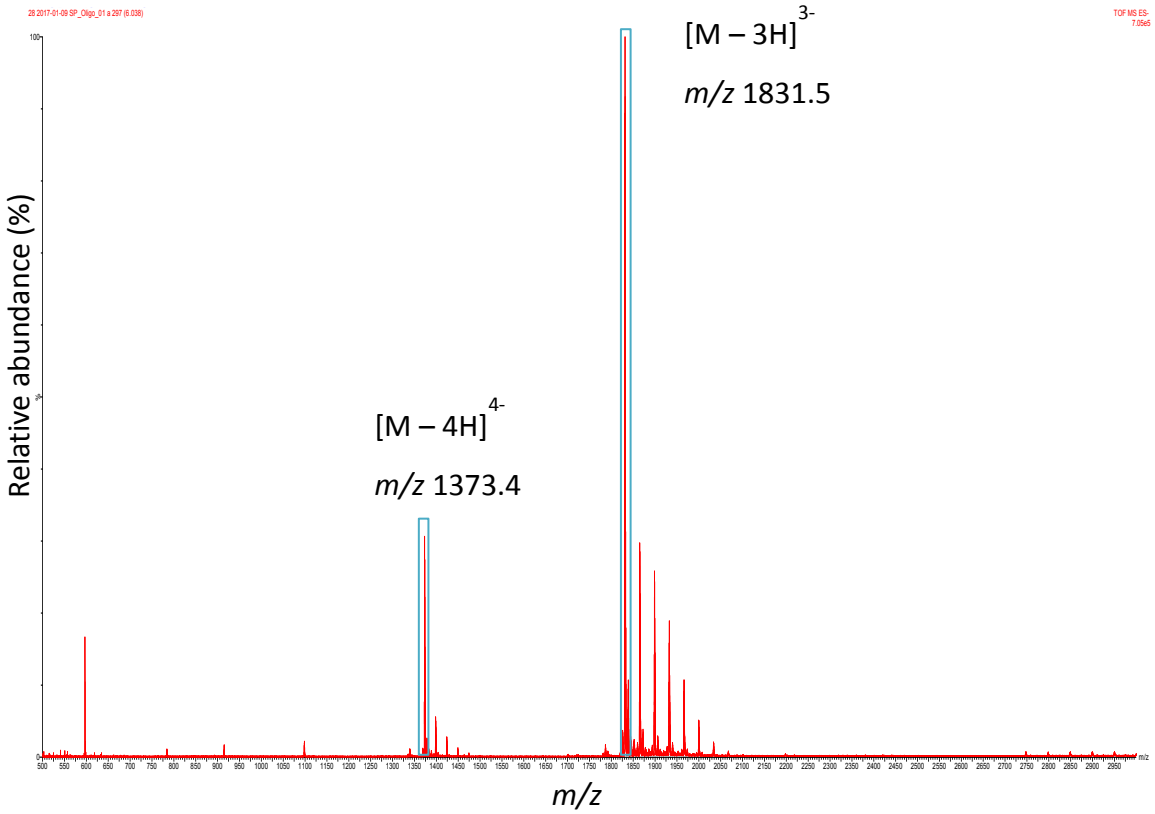

Figure 4.11 - Negative ionisation ESI mass spectrum of SP_Oligo_01 analysed using the Waters Synapt and Southampton chromatographic method

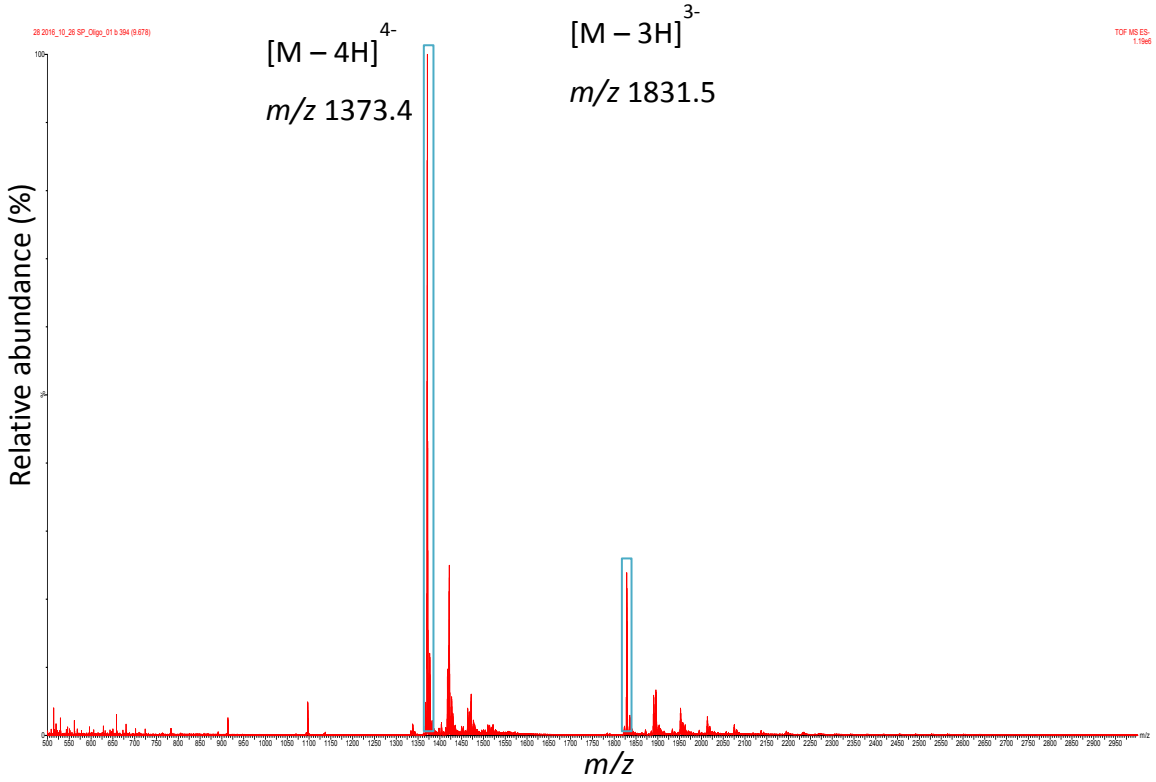

Figure 4.12 - Negative ionisation ESI mass spectrum of SP_Oligo_01 analysed using the Waters Synapt and AZ chromatographic method

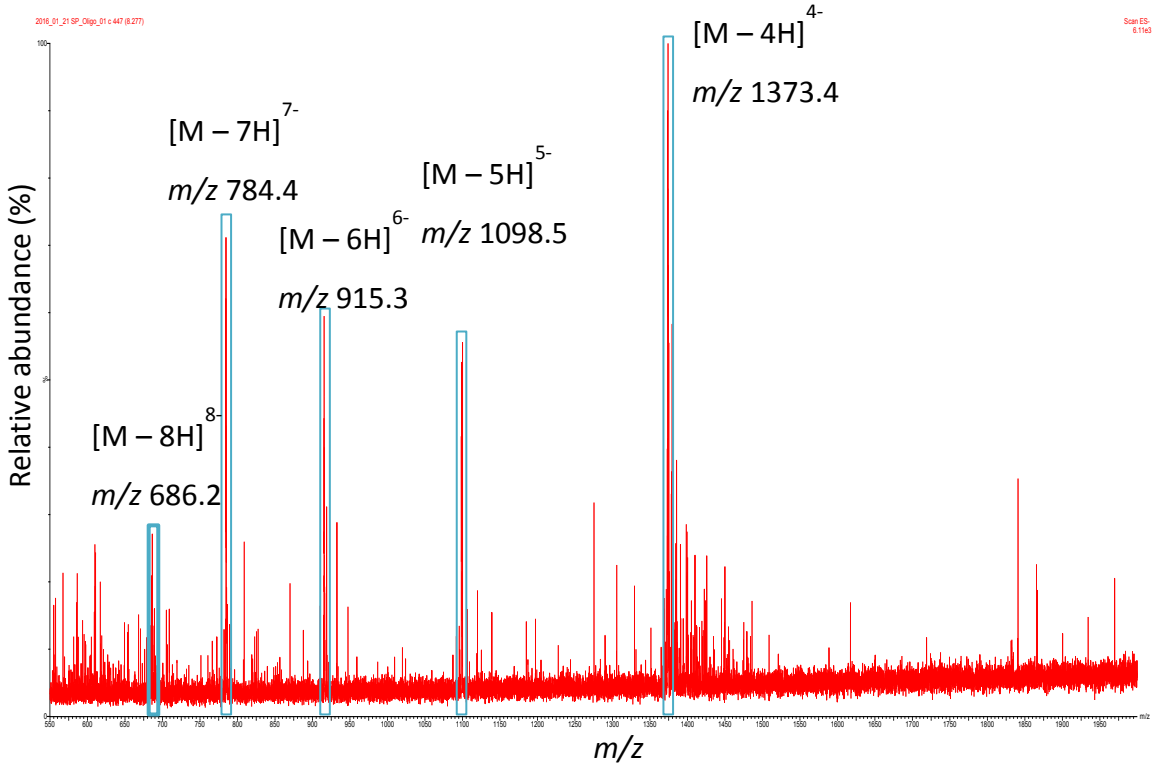

Figure 4.13 - Negative ionisation ESI mass spectrum of SP_Oligo_01 analysed using the Waters ZQ and Southampton chromatographic method

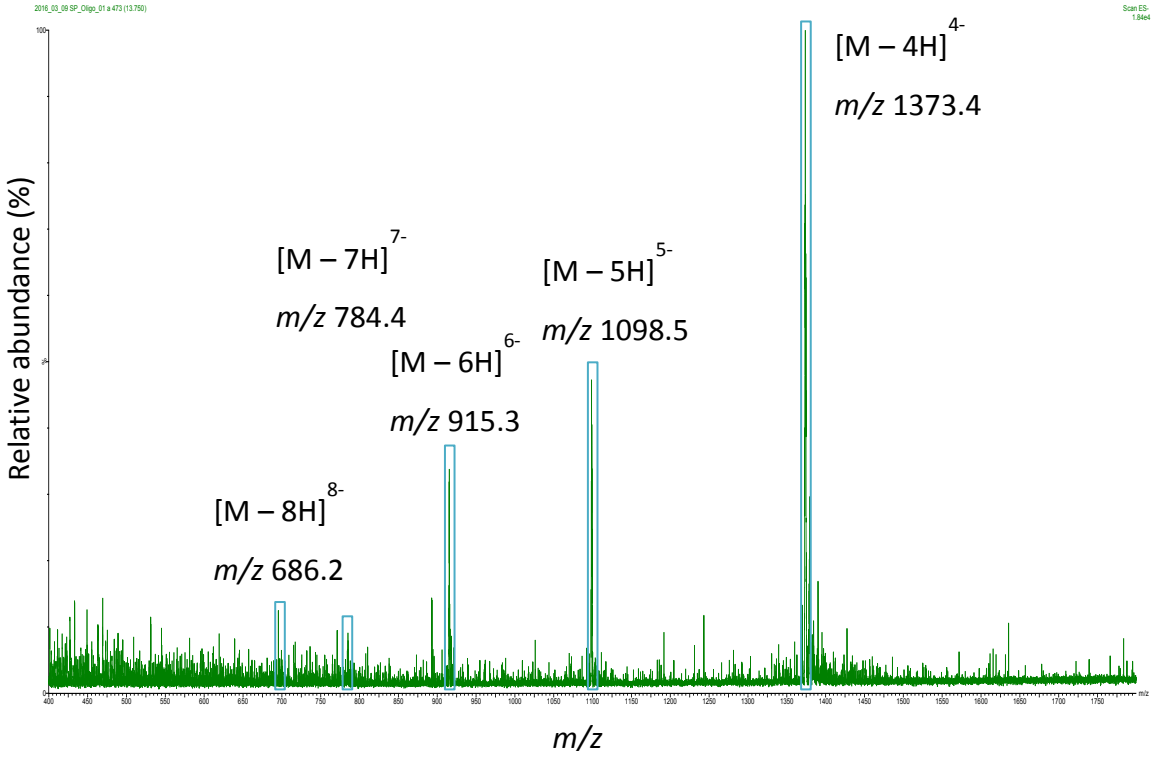

Figure 4.14 - Negative ionisation ESI mass spectrum of SP_Oligo_01 analysed using the Waters ZQ and AZ chromatographic method

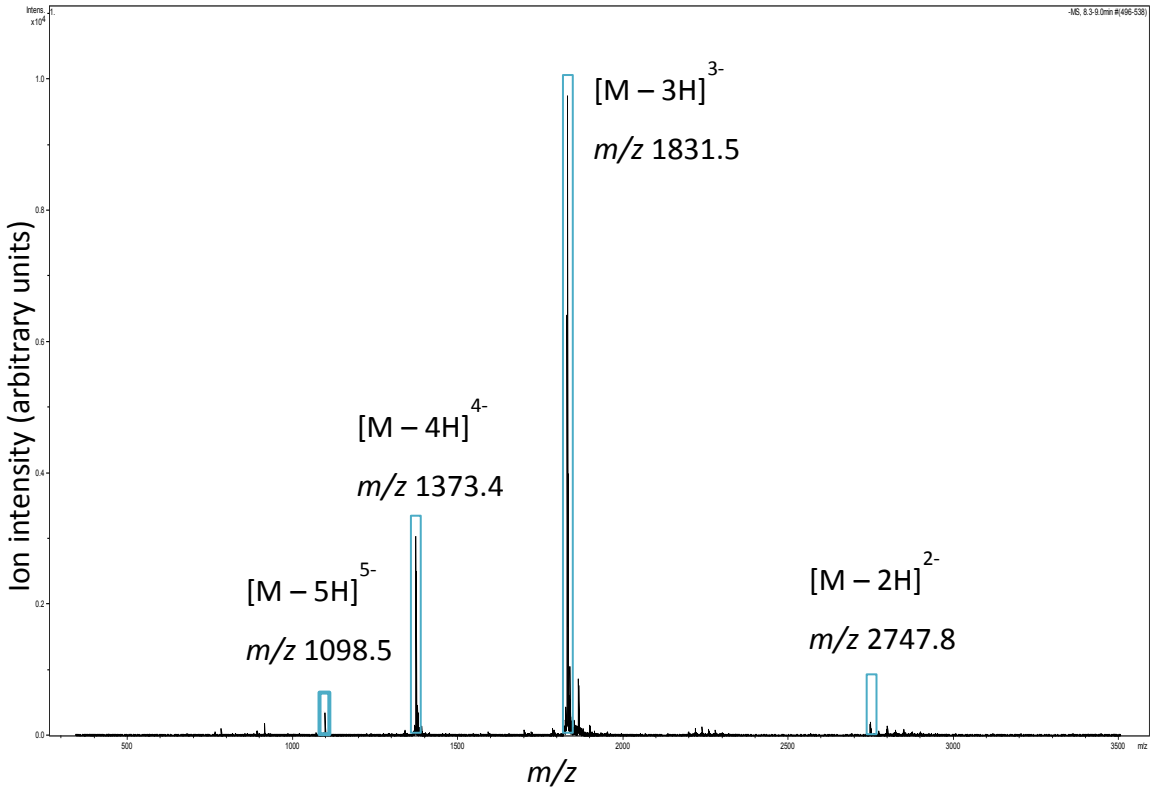

Figure 4.15 - Negative ionisation ESI mass spectrum of SP_Oligo_01 analysed using the Bruker MicrOTOF and Southampton chromatographic method

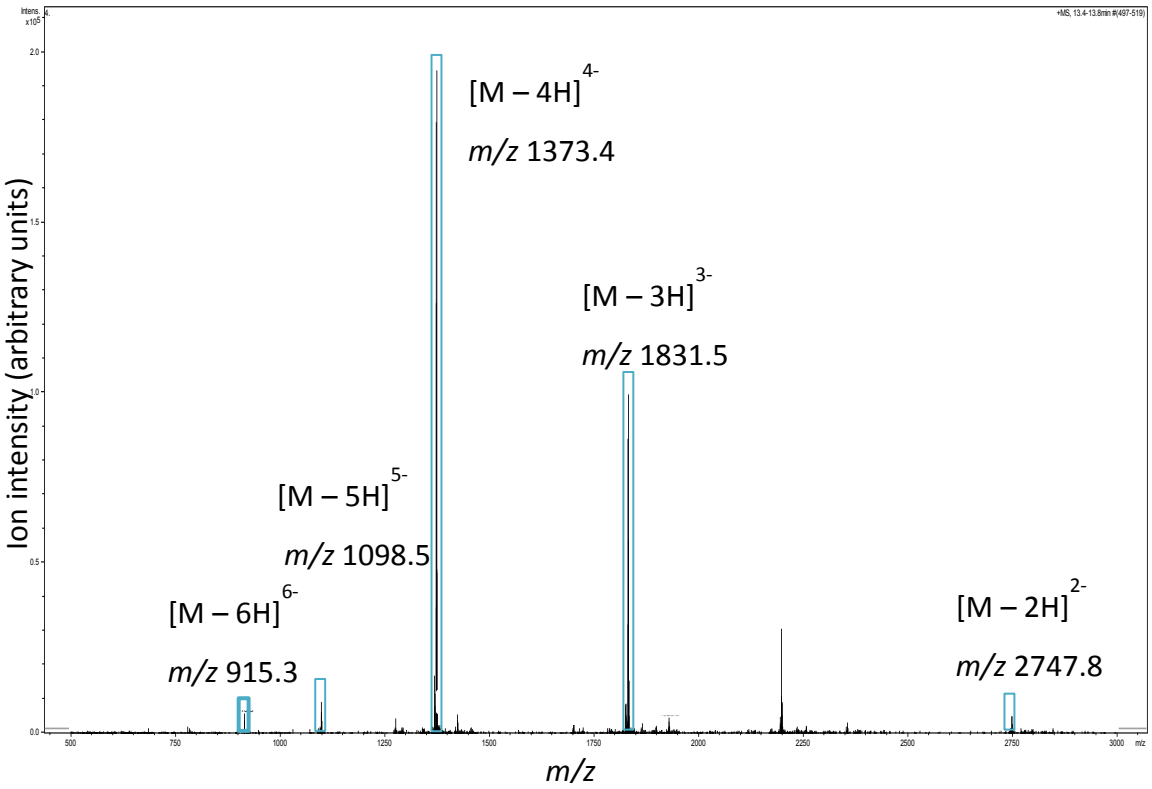

Figure 4.16 - Negative ionisation ESI mass spectrum of SP_Oligo_01 analysed using the Agilent 6130 and AZ chromatographic method

The figures presented above indicate that each instrument and, where investigated, each method has a different charge state distribution. It is also apparent that samples analysed using time of flight mass analysers have a narrower charge state distribution than those analysed using quadrupole mass analysers regardless of chromatographic method or instrument manufacturer.

The percentage contribution of the RICC peak area of the most abundant ion for each charge state observed was calculated relative to the RICC peak areas of the sum of the peak areas for all charge states observed. Table 4.7 shows the mean percentage of the RICC peak area for each charge state in relation to the sum of all RICC peak areas.

Table 4.7 - Mean percentage contribution of charge states by instrument and method (ND = not detected)

Instrument	Chromatographic Method	Mean % of total RICC peak area						
		-2 charge state	-3 charge state	-4 charge state	-5 charge state	-6 charge state	-7 charge state	-8 charge state
Waters Synapt	Southampton (n = 10)	2.5 ± 0.03	90.7 ± 0.1	6.8 ± 0.1	0.02 ± 0.003	ND	ND	ND
	AZ (n = 10)	0.3 ± 0.01	37.4 ± 0.2	56.8 ± 0.2	3.3 ± 0.04	1.7 ± 0.01	0.5 ± 0.005	ND
Waters ZQ	Southampton (n = 10)	ND	ND	48.9 ± 2.0	15.8 ± 1.1	8.6 ± 0.6	20.6 ± 1.5	6.1 ± 0.4
	AZ (n = 10)	ND	ND	66.2 ± 0.9	25.4 ± 0.7	6.0 ± 0.4	2.0 ± 0.1	0.5 ± 0.1
Bruker MicrOTOF	Southampton (n = 10)	1.1 ± 0.04	68.5 ± 0.2	26.2 ± 0.2	1.8 ± 0.1	2.3 ± 0.05	ND	ND
Agilent 6130	AZ (n = 4)	1.2 ± 0.1	35.0 ± 1.7	60.1 ± 1.6	2.5 ± 0.1	1.2 ± 0.03	ND	ND

For the replicates analysed using the Waters Synapt and the Southampton chromatographic method, most of the ions are in the -3 charge state (90.7 %) with small numbers of ions, relatively, distributed between the -2, -4 and -5 charge states. The concentration of ions into a single charge state means that there is greater sensitivity and, therefore, confidence in quantitation based on this ion and that interpretation of the mass spectrum generated is comparatively more straightforward than for a replicate where the ions are more widely distributed.

When the Waters Synapt is used to analyse SP_Oligo_01 in conjunction with the AZ chromatographic method, the dominant ion is the -4 charge state but, unlike the Southampton chromatographic method, this only accounts for 56.8% of the total peak area. The -3 charge state accounts for approximately two-thirds of the peak area of the -4 charge state and the remaining four charge states observed total 5.8% of the total peak area. For replicates analysed using the same mass

spectrometer and the Southampton chromatographic method, charge states other than -3 and -4 only account for 2.52% of the total peak area. The increased spread of distribution of ions means that the sensitivity of the most dominant charge state will be reduced for samples analysed using the AZ chromatographic method compared to the Southampton chromatographic method. The mass spectrum generated when using the TBuAA and EDTA additives in AZ chromatographic method is also more complex and harder to interpret than when using the TEAA and HFIP additives of the Southampton chromatographic method.

Replicates analysed using the Waters ZQ mass spectrometer, using both the Southampton and AZ chromatographic methods have the -4 charge state as the dominant ion at 48.9% and 66.2% respectively. The higher charge states for all replicates analysed using the Waters ZQ make up a larger contribution of the total RICC peak area than those observed for replicates analysed using the Waters Synapt. There is a less marked difference between the two chromatographic methods for replicates analysed using the Waters ZQ, with the AZ chromatographic method producing a less complex spectrum in this case. The low sensitivity of the Waters ZQ, as discussed in Chapter 3: combined with the distribution of ions means that the sensitivity of any selected ion is low and quantitation of the levels of impurities will be challenging.

The charge distribution produced by analysis using the Bruker MicrOTOF with the Southampton chromatographic method resembles that generated using the Waters Synapt and the Southampton chromatographic method. In the case of replicates analysed using the Bruker MicrOTOF, the -3 charge state ion is dominant but only accounts for 68.5% of the total RICC peak ion. Charge states other than -3 and -4 contribute 5.2% to the total peak area, meaning that the mass spectrum is more complex than that produced using the Waters Synapt but less than that generated using the Waters ZQ. The presence of a quadrupole mass filter before the TOF mass analyser in the Waters Synapt may account for the differences observed between the two instruments using the same chromatographic method.

In common with all replicates analysed using the AZ chromatographic method, those analysed using the Agilent 6130 mass spectrometer show the -4 charge state as the dominant ion at 60.1% of the total RICC peak area. For these replicates, the -3 charge state accounts over half as much of the total as the -4

charge state and the overall distribution is similar to that of replicates analysed using the Waters Synapt and the AZ chromatographic method. These data, when compared to the Waters Synapt and Waters ZQ data, show that the chromatographic method plays a key role in the distribution of charge states and that newer quadrupole mass analysers, such as the Agilent 6130, will produce more sensitive and less complex mass spectra than legacy instruments such as the Waters ZQ.

Figure 4.17 shows the charge state distribution as indicated by the contribution of the individual ions to the sum of the RICC peak areas. Figure 4.18 shows the distribution of ions across the charge states in samples of SP_Oligo_01 analysed using time of flight mass analysers and Figure 4.19 shows the charge state distribution in samples analysed using quadrupole mass analysers.

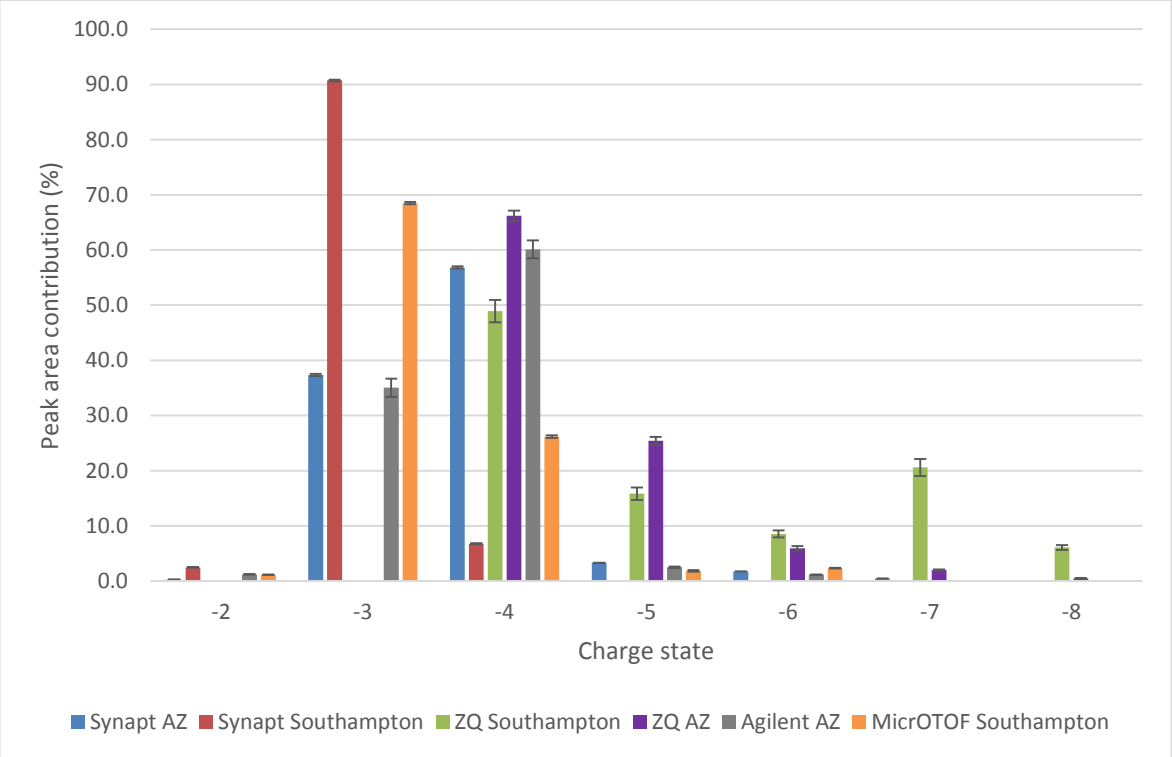

Figure 4.17 - RICC peak area contribution of each charge state of SP_Oligo_01 by instrument and method (see Table 4.7 for number of replicates)

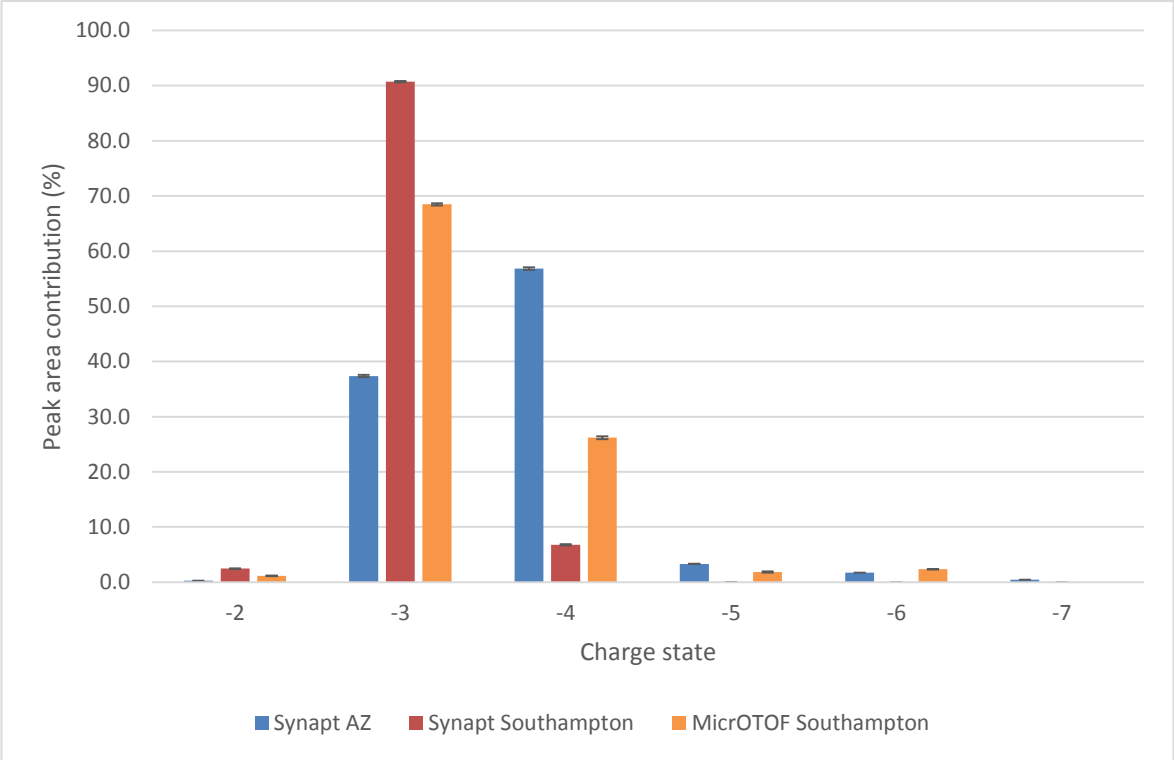

Figure 4.18 - Charge state distribution for SP_Oligo_01 analysed using Waters Synapt and Bruker MicrOTOF time of flight mass analysers (see Table 4.7 for number of replicates)

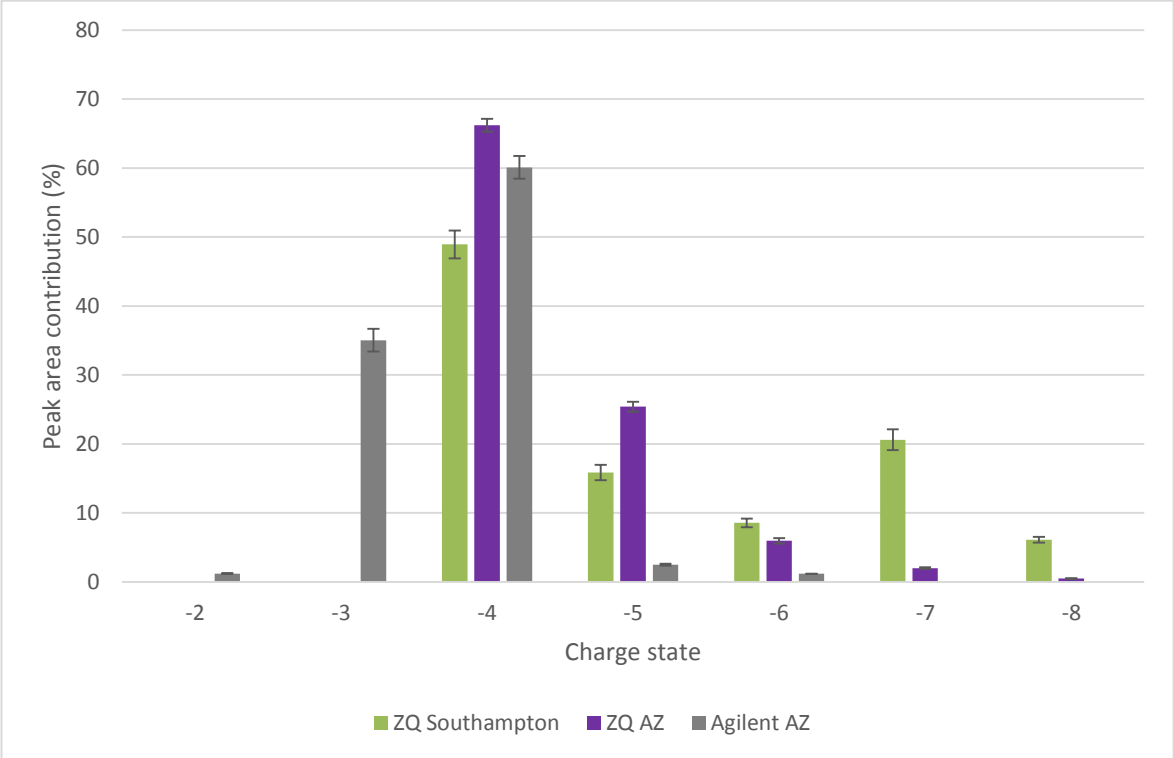

Figure 4.19 - Charge state distribution for SP_Oligo_01 analysed using Waters ZQ and Agilent 6130 quadrupole mass analysers (see Table 4.7 for number of replicates)

The figures above demonstrate that, for samples analysed using time of flight mass analysers, the ions are predominantly distributed across the -3 and -4 charge states, with the -2, -5, -6 and -7 charge states having relatively negligible contributions. For replicates of SP_Oligo_01 analysed using quadrupole mass analysers, the ions are distributed across more charge states and, in the case of the Waters ZQ, higher charge states dominate compared to TOF-analysed replicates.

The pattern of distribution observed in these data with fewer, lower charge states observed is analogous to the results presented by Premstaller *et al.*[88] in their comparison of quadrupole and quadrupole – ion trap instruments for the analysis of oligonucleotides, which they suggest could be a result of the pulsed introduction of ions into the mass analyser. Ions are introduced into a TOF or QTOF in pulses in the same way as for an ion trap instrument, so the data presented in this chapter support this theory.

The manufacturer of the mass spectrometer does not affect the pattern observed in terms of the number of charge states ions are distributed across but the more modern Agilent 6130 shows a less evenly distributed pattern than the older Waters ZQ instrument.

4.5 Charge envelope conclusions

The results presented in this chapter show that the ion-pair reagents and buffers added to the mobile phase for chromatographic separation influence the charge state distribution of oligonucleotide mass spectra. The data suggest that the pKa and gas-phase proton affinity of the additives are important factors in the resulting distribution. Differences in charge envelopes between chromatographic methods using the same instrumentation affect the reproducibility of quantitative data between laboratories as the sensitivity of the ion chosen changes in response to changes in the charge distribution.

Previous research[93] has indicated that increasing the organic content of the mobile phase can alter charge state distribution. The data presented here suggest that, within the ranges investigated, there is no significant difference in the distribution of ions when the organic content of the mobile phase at the point of elution is varied. The consistency of charge state ratios and RICC peak areas across the

range of organic content elution points implies that the use of an internal standard to improve quantitation precision, eluting away from the target oligonucleotide, is feasible provided the ionisation and behaviour of the standard is fully validated.

At low pH, the oligonucleotide sample analysed was not efficiently ionised but the distribution of ions between the -3 and -4 charge state was consistent with that seen at pH 7. When the pH is increased to 9.5, the distribution of ions is pushed towards lower charge states; the RICC peak area also increased when pH 9.5 was used, agreeing with the results of Bleicher and Bayer[93].

When oligonucleotide samples are analysed using time of flight mass analysers, the ions generated are distributed over fewer charge states than when the same samples are analysed using quadrupole mass analysers. The suggestion that ion trap instruments display a narrower charge envelope than quadrupole mass analysers because of the introduction of ions in pulses in ion traps and the limitation of tuning ion trap analysers compared to quadrupoles[88] is supported by the TOF and QTOF data presented here. Ions are introduced as pulses in TOF and QTOF instruments and optimisation of source parameters must cover the whole *m/z* range rather than a single *m/z* or a smaller range as can be the case for quadrupole instruments. The narrowest charge distribution is produced by the QTOF Waters Synapt. The presence of a quadrupole mass filter before the TOF mass analyser may mean that, if ion transmission at the ends of the *m/z* range is reduced in ion trap and TOF instruments as Premstaller *et al.* theorise[88], the mass filter reduces this still further, concentrating ions in a few charge states.

When a single charge state ion is chosen for the quantitation of oligonucleotide impurities, the sensitivity of this ion and the distribution of ions into this charge state are critical. For any given chromatographic method and mass spectrometer, it is most sensible to select the dominant charge state present in the mass spectrum to ensure the best sensitivity possible. If the most dominant charge state varies between methods, there is a risk that the distribution of ions in the impurities under investigation is not identical to the target oligonucleotide, leading to differences in reported impurity levels. The relative differences in sensitivity between the methods and instruments can also cause differences in impurity levels reported as more variation will be seen in ions with low sensitivity and the confidence in the quantitation will be reduced or peak areas may be below the limit of detection, purely because the ions are so widely distributed.

A narrower charge state distribution leads to increased sensitivity for the ions generated, making quantitation of oligonucleotides and their impurities more straightforward and increasing the likelihood of accurate and precise results. Ideally, for high-quality quantitation, time of flight mass analysers would be used but these data also show that newer quadrupole mass analysers such as the Agilent 6130 provide a narrower charge envelope than legacy instruments such as the Waters ZQ.

The higher mass resolution achievable when using a TOF or QTOF mass analyser compared with a quadrupole mass analyser is an advantage for the quantitation of oligonucleotides and their impurities as it allows for more accurate selection of the ions of interest and makes it possible to differentiate between the ^{12}C and ^{13}C ions, which is not easily accomplished using a low-resolution quadrupole instrument.

For robust quantitation of oligonucleotide impurities, the charge envelope generated by the mass analyser and mobile phase additives used in a given method must be understood. To ensure the greatest sensitivity and least complexity of mass spectra, the use of HFIP as a mobile phase additive and a time of flight mass analyser is recommended.

Chapter 5: Fragmentation of oligonucleotides

Fragmentation of oligonucleotides in the mass spectrometer can create ions that are identical to ions formed from the synthetic impurities. The loss of a nucleoside base known as abasic or, specifically for the loss of guanine and adenine, depurination impurities, can occur in the synthesis of the therapeutic oligonucleotide and these losses can also occur in the ion source region of the mass spectrometer. As the origin of these ions cannot be readily determined in a mass spectrum, it is essential to reduce the in-source fragmentation of oligonucleotides to ensure that accurate quantitation of these impurities is achieved[21].

For the purposes of the research presented in this chapter, depurination impurities have been investigated. The phosphodiester impurity, where one backbone group is not converted to a phosphorothioate, is considered for SP_Oligo_01 and SP_Oligo_02 as a control impurity. This impurity is not created in the mass spectrometer, ensuring that any differences observed in the levels of depurination are related to the experiment undertaken rather than to any variation in the sample between days or methods. The impurities considered in these experiments and the ID numbers assigned to them throughout this chapter are presented in Table 5.1.

Table 5.1 - Impurities investigated

Impurity	Impurity type	Impurity source	Impurity ID number
Phosphodiester	Modification	Synthesis	1
Loss of guanine	Abasic	Synthesis/Mass Spectrometer fragmentation	2
Loss of adenine & loss of guanine + H_2O			3
Loss of adenine + H_2O			4

The source design, the in-source fragmentation voltage and the column temperature were investigated to determine their impact on depurination. During the analysis of samples SP_Oligo_01 and SP_Oligo_02, differences in the levels of fragmentation were noted which were theorised to be related to the

oligonucleotide sequence. Four oligonucleotides with the same ratio of bases, but different sequences, were synthesised by AstraZeneca specifically for this study and analysed to investigate the relationship between sequence and degree of fragmentation.

Differences in levels of in-source fragmentation caused by the ion source design have been noted previously by Bristow *et al.*[94], and the effect of in-source fragmentation voltages on the intensity of response in bio-molecules in general has been much studied, including in oligonucleotides specifically in a paper by Guo *et al*[95]. The behaviour of different oligonucleotide sequences has been investigated by Suzuki *et al.*[96] and Nyakas *et al*.[97], amongst others. Column temperature effects have been researched from a chromatographic focus (*e.g.* Biba *et al.*[24]) but there is little, if any, evidence of published literature on any effect on fragmentation of oligonucleotides.

5.1 Quantitation of impurities

The method of impurity quantitation currently used by AstraZeneca selects the most prominent ion of the most dominant charge state of the target oligonucleotide (the full-length, fully thioated oligonucleotide, for calculation purposes called “full-length n” or FLN) peak. The peak area for the RICC of this ion is then recorded and used, along with the peak areas of impurity ions, to calculate the percentage of the total sample of each ion. As discussed in Section 4.1, the dominant charge state differs depending on the chromatographic method used. The -4 charge state is dominant for the AZ chromatographic method (ACM), while for the Southampton chromatographic method (SCM) the -3 charge state dominates (see Figure 5.1). In keeping with the AstraZeneca method of ion selection, -3 charge state ions are recorded for replicates analysed using the SCM with -4 charge state ions recorded for replicates analysed using the ACM.

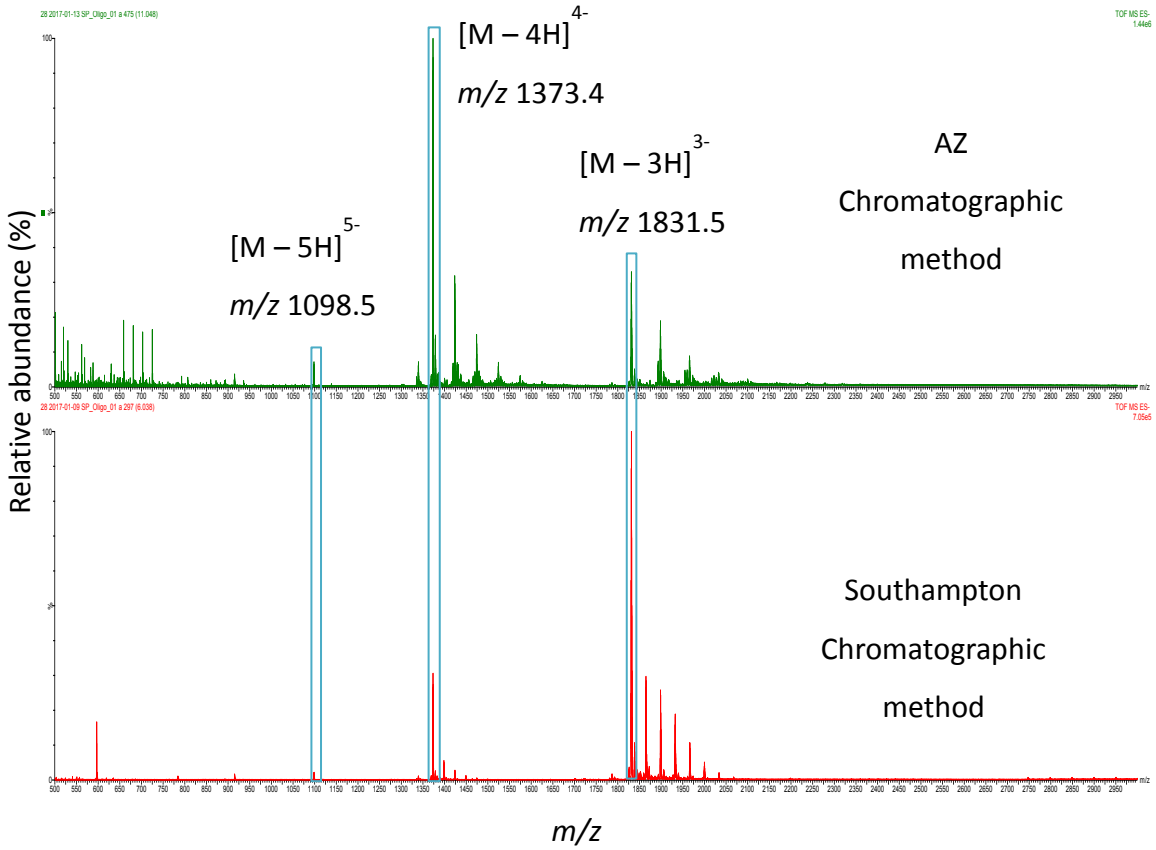

Figure 5.1 - Negative ionisation ESI mass spectra of SP_Oligo_01 analysed using the Waters Synapt and the ACM and SCM showing the dominant charge states

To simplify the quantitation of impurities for this chapter, the RICC peak area of the dominant ion of the dominant charge state (as determined by the FLN peak) for each impurity is calculated as a percentage of the RICC peak area of the FLN ion. Figure 5.2 shows an example of the ions used and their respective percentages.

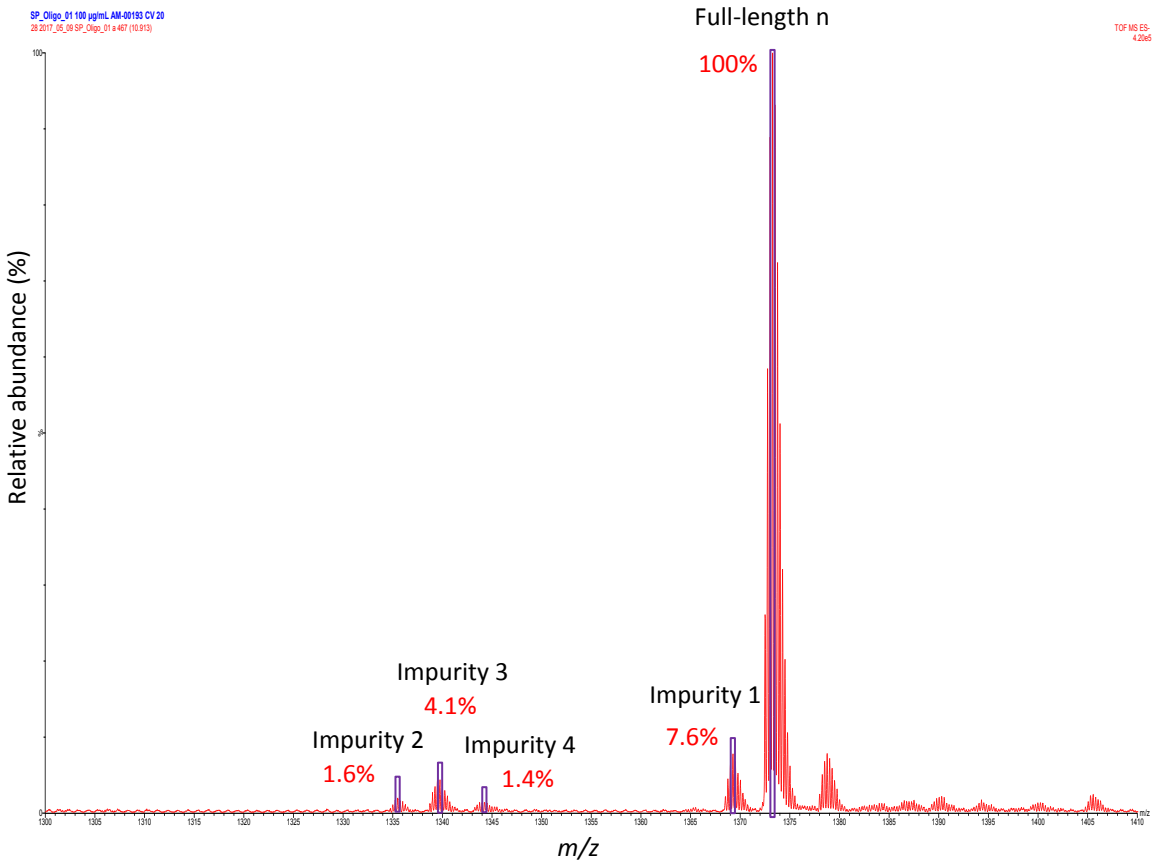

Figure 5.2 - Negative ionisation ESI mass spectrum of SP_Oligo_01 showing the impurities investigated and ions selected. Analysed using the ACM and the Waters Synapt (see Table 5.2 for *m/z* of ions)

Equation 5.1 shows how the level of impurity as a percentage of the FLN peak is calculated, with Equation 5.2 showing an example based on the RICCs of the FLN and impurity 1 from the mass spectrum shown in Figure 5.2.

$$\%\ of\ FLN\ = \left(\frac{RICC\ peak\ area\ of\ impurity}{RICC\ peak\ area\ of\ FLN}\right) * 100 \qquad \text{Equation 5.1}$$

$$\left(\frac{12176\ (arbitrary\ units)}{160252\ (arbitrary\ units)}\right) * 100 = 7.6\% \qquad \text{Equation 5.2}$$

There are no specifications provided by regulators such as the FDA regarding the levels of individual impurities or reporting limits required in therapeutic oligonucleotides. The AstraZeneca method for quantitation of impurities has set a reporting limit (LOQ) of 0.2% of the sum of all RICC peak areas based on the

method validation package. In this research, the sensitivity afforded by the Waters SynaptG2 Si yields a signal to noise ratio of the smallest peaks of greater than 10, therefore percentages below 0.2% are able to be reported.

5.2 Source type

The levels of fragmentation occurring in the ion source of the mass spectrometer vary depending on the design of the source[94]. The data presented in this chapter were acquired using two source designs, the Waters Z-spray source used in the Waters Synapt and Waters ZQ mass spectrometers and the orthogonal ESI sources used in the Agilent 6130 and the Bruker MicrOTOF, which are very similar in design to one another. The Waters Synapt has been used to generate the Waters source design data for this chapter as the Waters ZQ is insufficiently sensitive for consistent quantitation of the impurities of interest.

The analytical method used by AstraZeneca for the quantitation of oligonucleotides and their impurities has been validated for the Agilent source design. The method developers stated that a Waters source type was not suitable for use with this method as a result of increased in-source fragmentation. To investigate whether this assertion is true when low in-source collision induced dissociation (in-source CID) voltages are used with the Waters Synapt, samples were analysed using the Waters Synapt with an in-source CID voltage of 20 V, compared to the Agilent 6130 with an in-source CID voltage of 100 V as specified in the AstraZeneca analytical method and the Bruker MicrOTOF with an in-source CID voltage of 90 V as used in the Southampton in-house oligonucleotide method for this instrument. These voltages are not directly comparable owing to differences in instrument construction, but are a measure of how much energy is supplied for in-source CID.

RICCs were generated for the ions shown in Table 5.2 and the peak area of each impurity calculated as a percentage of the peak area of the target oligonucleotide. These ions are based on the most prominent ion of the FLN peak for the charge state indicated. The expected difference between the mass of the impurity and the FLN oligonucleotide is used to calculate the *m/z* of the ions selected. Impurity 1 is a control impurity, while impurities 2 to 4 are abasic impurities caused by the loss

of guanine; the loss of adenine and/or the loss of guanine and the addition of water; and the loss of adenine and the addition of water, respectively.

The ions corresponding with impurities 2 to 4 can be formed during the synthesis of the oligonucleotide or by fragmentation of the sample in the ion source region of the mass spectrometer. Identical ions are produced by both methods of formation, so they cannot be distinguished in mass spectra.

Table 5.2 - *m/z* used for RICC peak areas for each impurity investigated

Impurity ID number	**Sample**	***m/z* used for RICC peak area**	
		SCM (-3 charge state)	**ACM (-4 charge state)**
Target Oligonucleotide (FLN)	SP_Oligo_01	1831.5	1373.4
	SP_Oligo_02	1806.2	1354.3
1	SP_Oligo_01	1826.2	1369.4
	SP_Oligo_02	1800.9	1350.3
2	SP_Oligo_01	1781.1	1335.6
	SP_Oligo_02	1755.8	1316.5
3	SP_Oligo_01	1786.8	1339.9
	SP_Oligo_02	1760.5	1320.8
4	SP_Oligo_01	1792.4	1344.1
	SP_Oligo_02	1767.1	1325.0

Table 5.3 shows the mean of the impurity ion RICC peak areas as a percentage of the FLN RICC peak area for SP_Oligo_01 and SP_Oligo_02. Sample SP_Oligo_01 was analysed using the Waters Synapt and both the ACM and SCM; the Bruker MicrOTOF and the SCM only; and the Agilent 6130 with the ACM only. SP_Oligo_02 was analysed using the Waters Synapt and both the ACM and SCM and the Bruker MicrOTOF and the SCM only. The data from the table are presented graphically in Figure 5.3 and Figure 5.4.

Table 5.3 - Mean RICC peak area as a percentage of FLN RICC peak area for each impurity investigated

Sample	Instrument	Chromatographic method	Impurity (% of FLN RICC peak area)			
			1	2	3	4
SP_Oligo_01	Waters Synapt	Southampton	5.1 ± 0.7	1.4 ± 0.2	3.7 ± 0.4	0.7 ± 0.1
		AZ	5.7 ± 0.9	1.9 ± 0.2	2.3 ± 0.3	1.1 ± 0.1
	Bruker MicrOTOF	Southampton	4.6 ± 0.4	0.4 ± 0.03	1.1 ± 0.1	0.9 ± 0.1
	Agilent 6130	AZ	6.2 ± 1.1	0.3 ± 0.04	1.8 ± 0.3	1.5 ± 0.3
SP_Oligo_02	Waters Synapt	Southampton	2.6 ± 0.2	0.4 ± 0.01	0.2 ± 0.01	0.7 ± 0.01
		AZ	2.1 ± 0.1	0.8 ± 0.03	0.5 ± 0.1	0.8 ± 0.03
	Bruker MicrOTOF	Southampton	3.4 ± 0.1	0.7 ± 0.03	0.7 ± 0.04	1.1 ± 0.04

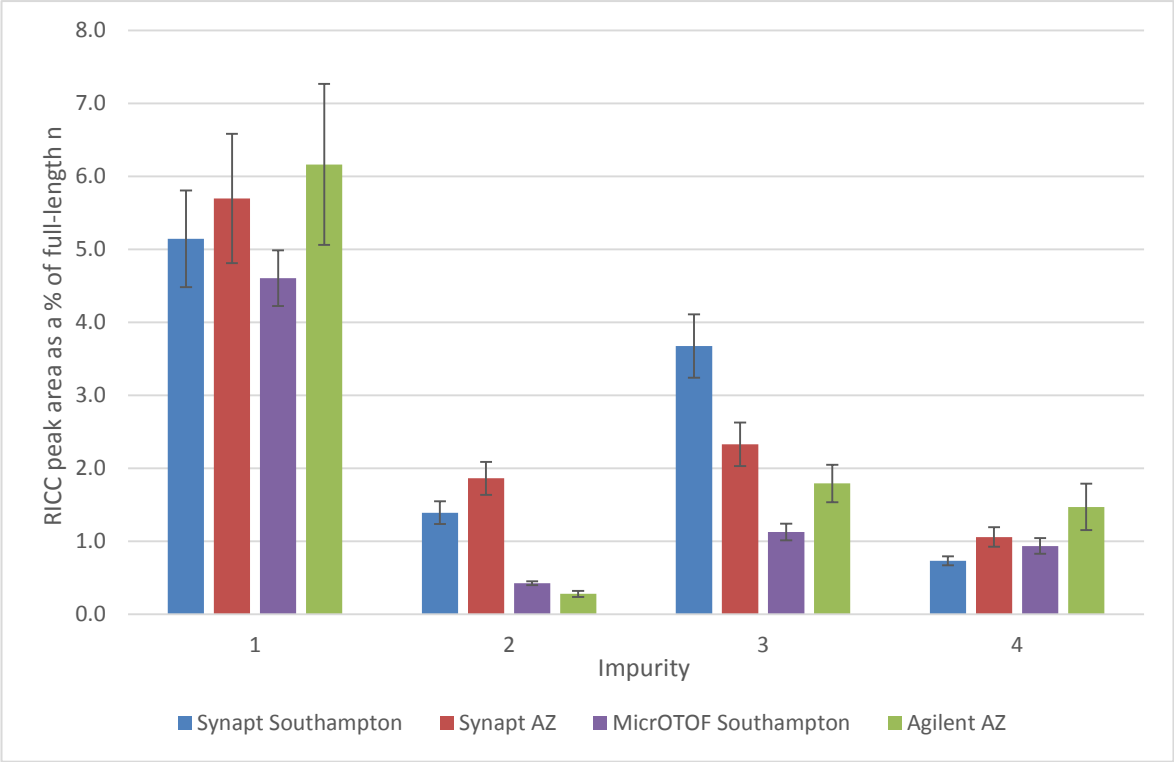

Figure 5.3 - Levels of impurity as a percentage of target oligonucleotide for SP_Oligo_01 across chromatographic methods and instruments

Figure 5.3 shows that differences in the calculated impurity 1 RICC peak area as a percentage of the FLN oligonucleotide for SP_Oligo_01 across chromatographic methods and instruments do not correlate strongly with source design, this is expected as the phosphodiester impurity results from the synthesis of the sample and is not created in the mass spectrometer. Differences are more strongly correlated with the chromatographic method used than the source design.

Comparing the column height in Figure 5.3 and the values in Table 5.3, and taking into account the variation between replicates, the ions corresponding to the impurities involving the loss of guanine (impurities 2 and 3) show the most obvious differences between instruments. The RICC peak area of the ion corresponding with impurity 2 is almost five-times higher as a percentage of the FLN RICC when analysed using the Waters Synapt with either chromatographic method than using the Agilent 6130 or the Bruker MicrOTOF. As the replicates analysed are all from the same sample batch, the level of the impurity generated by the synthesis of the original sample cannot be greater than the values recorded in the analysis using the Agilent and Bruker ion sources. The higher percentages observed in the replicates analysed using the Waters ion source must, therefore, indicate an enhancement of this ion by in-source fragmentation. The absolute level of

synthetic impurity could only be determined by a non-mass spectrometric method, such as capillary gel electrophoresis, as any MS method runs the risk of enhancement of the ions of interest as a result of in-source fragmentation.

Impurity 4, the loss of adenine plus the addition of water, does not appear to be affected by the source design, with Figure 5.3 and Table 5.3 showing that the two lowest recorded RICC peak areas as a percentage of the FLN RICC are found when using the SCM, with replicates analysed using the Waters Synapt and the Bruker MicrOTOF yielding the same percentage when inter-replicate variation is taken into account. There may be in-source fragmentation causing a loss of adenine, but if there is it occurs as readily in the Agilent and Bruker sources as in the Waters source. The consistency of observed percentages of impurity 4 across the ion source designs suggests that differences in the percentages observed for impurity 3 between the Waters source design and the Agilent and Bruker designs are the result of the loss of guanine plus the addition of water in the ion source, as the component of this ion corresponding to the loss of adenine is unlikely to change. Increases in the observed percentage of impurity 3 when using the Waters source design can be attributed to an increased level of in-source fragmentation removing guanine from the oligonucleotide.

These results suggest that the source design of the mass spectrometer influences the levels of in-source fragmentation of guanine residues in SP_Oligo_01.

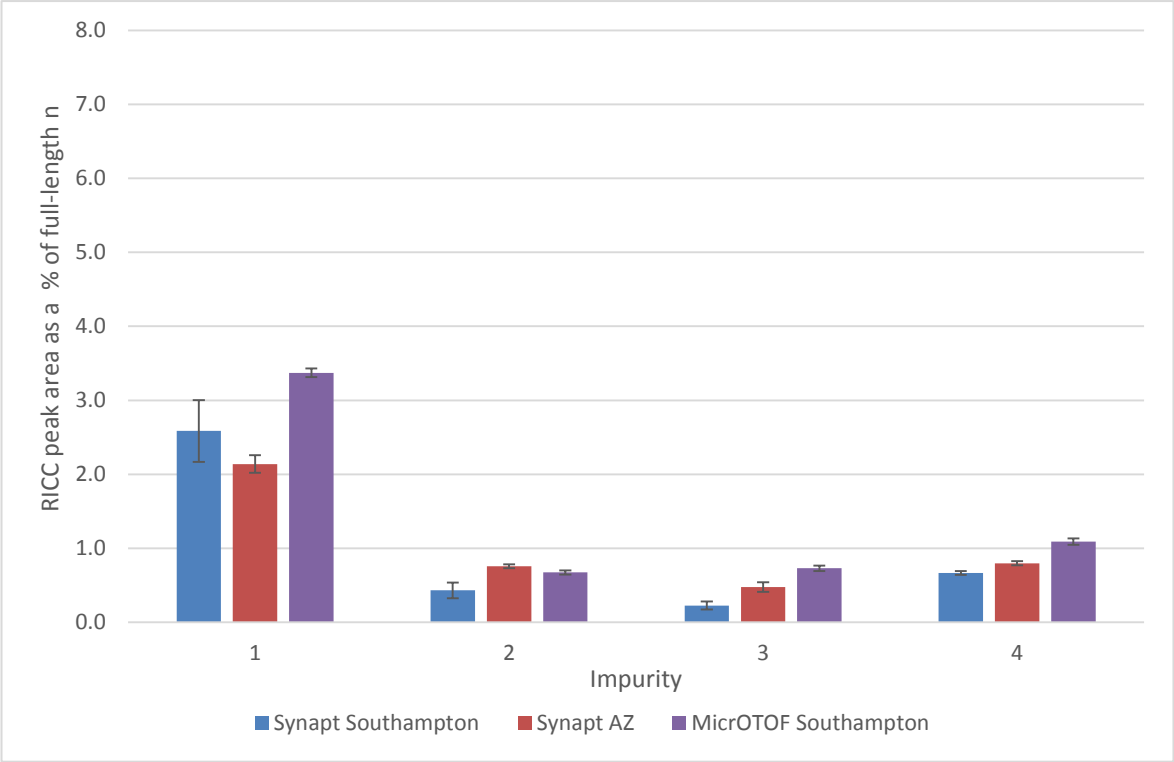

Figure 5.4 - Levels of impurity as a percentage of target oligonucleotide for SP_Oligo_02 across chromatographic methods and instruments

As illustrated in Figure 5.4 and Table 5.3, SP_Oligo_02 shows greater observed levels of impurity 1 in the replicates analysed using the SCM compared to the ACM and using the Bruker MicrOTOF compared to the Waters Synapt. This impurity cannot be generated in the mass spectrometer, so differences observed must be related to the sensitivity of the chromatographic method and instrument. The pattern observed in impurity 1 indicates that higher observed percentages of impurities in replicates analysed using the Bruker MicrOTOF and the SCM may be related to the chromatographic method and the sensitivity of the instrument rather than to the source design.

When impurity 2 is considered, Figure 5.4 and Table 5.3 show that the observed RICC peak area as a percentage of the FLP RICC peak area is similar across the SCM and ACM and the Waters Synapt and Bruker MicrOTOF, when inter-replicate variation is considered. When the mean of all replicates across the three experiments is generated, the result is 0.7% ± 0.03% with a variation of 19%, which suggests that there is no significant variation between the methods and instruments.

In contrast to SP_Oligo_01, the columns in Figure 5.4 and the values in Table 5.3 show that for SP_Oligo_02, impurity 4 constitutes a higher percentage of the FLP than impurity 3. Impurity 4 corresponds to the loss of adenine and the addition of water and impurity 3 to the loss of adenine and/or the loss of guanine and the addition of water. The levels of the ion corresponding to the loss of guanine are closer to the levels of impurity 4, suggesting that in SP_Oligo_02 the loss of guanine tends not to be accompanied by the addition of water but the loss of adenine is more likely to occur with an addition of water than the loss alone.

For the impurities involving the loss of guanine, the columns in Figure 5.4 and the values in Table 5.3 illustrate that the enhanced levels of in-source fragmentation observed in replicates of SP_Oligo_01 acquired using the Waters Synapt are not duplicated in SP_Oligo_02.

When comparing samples SP_Oligo_01 and SP_Oligo_02 in Table 5.3, the level of impurity 4 recorded across all chromatographic method and instrument combinations used is similar, indicating that there is a relatively consistent level of loss of adenine and addition of water across both samples. The ion corresponding to impurity 3, the loss of adenine and/or the loss of guanine with the addition of water, is observed at higher peak areas as a percentage of the FLP peak areas in SP_Oligo_01 than SP_Oligo_02 regardless of source design. This suggests that, the ion corresponding to impurity 3 is related more strongly to the loss of guanine and the addition of water in SP_Oligo_01 than in SP_Oligo_02.

The different patterns of fragmentation observed between the two samples analysed indicates that, although the Waters source causes increased levels of fragmentation of guanine compared to Agilent and Bruker sources for SP_Oligo_01, the relationship between source-type and fragmentation of oligonucleotides is not simple. SP_Oligo_01 and SP_Oligo_02 are both 16 bases in length but have different sequences. The guanines in SP_Oligo_01 are located in the middle of the sequence, whereas those in SP_Oligo_02 are closer to the ends of the oligonucleotide. It appears that the position of guanines affects the level of in-source depurination, so four new specially commissioned 12-mer sequences comprising of the same ratios of bases but different sequences have been analysed to test this theory.

5.3 In-source collision induced dissociation voltage

In-source collision induced dissociation (In-source CID) can be affected by changing the in-source fragmentation voltage – known by different terms depending on the instrument manufacturer, such as cone voltage (Waters systems) or fragmentor voltage (Agilent systems). In-source fragmentation occurs as a result of ions being accelerated by the electric field generated in the sampling orifice region of the ion source and colliding with gas molecules present causing bonds to break in the ions affected[98-99]. All data presented in this chapter were acquired using the Waters Synapt, so the term cone voltage will be used in the discussion of these specific results. The higher this voltage is set, the more fragmentation occurs. Traditionally, high in-source fragmentor voltages have been used to reduce adducts in oligonucleotide analysis, mirroring those used in protein analysis[95, 100]. The data presented in Section 5.2 indicate that, depending on the source type used, lower cone voltages may be appropriate for accurate quantitation of abasic oligonucleotide impurities.

To investigate the effect of cone voltage on the fragmentation of oligonucleotides to produce abasic impurities, samples SP_Oligo_01 and 02 were analysed using the Waters Synapt and the SCM and the ACM at a range of cone voltages. The two chromatographic methods were used to determine whether changing the cone voltage has more of an effect on the in-source fragmentation using one set of mobile phase additives or the other, given the differences noted in the observed level of depurination involving the loss of guanine in SP_Oligo_01 between the SCM and ACM.

Figure 5.5 and Figure 5.6 show the negative ionisation mass spectra for each sample analysed at cone voltages of 10 V, 20 V, 50 V, 80 V and 100 V using the SCM. All spectra in each figure are normalised to the ion intensity of the most abundant impurity (impurity 3 for SP_Oligo_01 and impurity 2 for SP_Oligo_02) in the 100 V spectrum to allow the differences between cone voltages to be clearly seen.

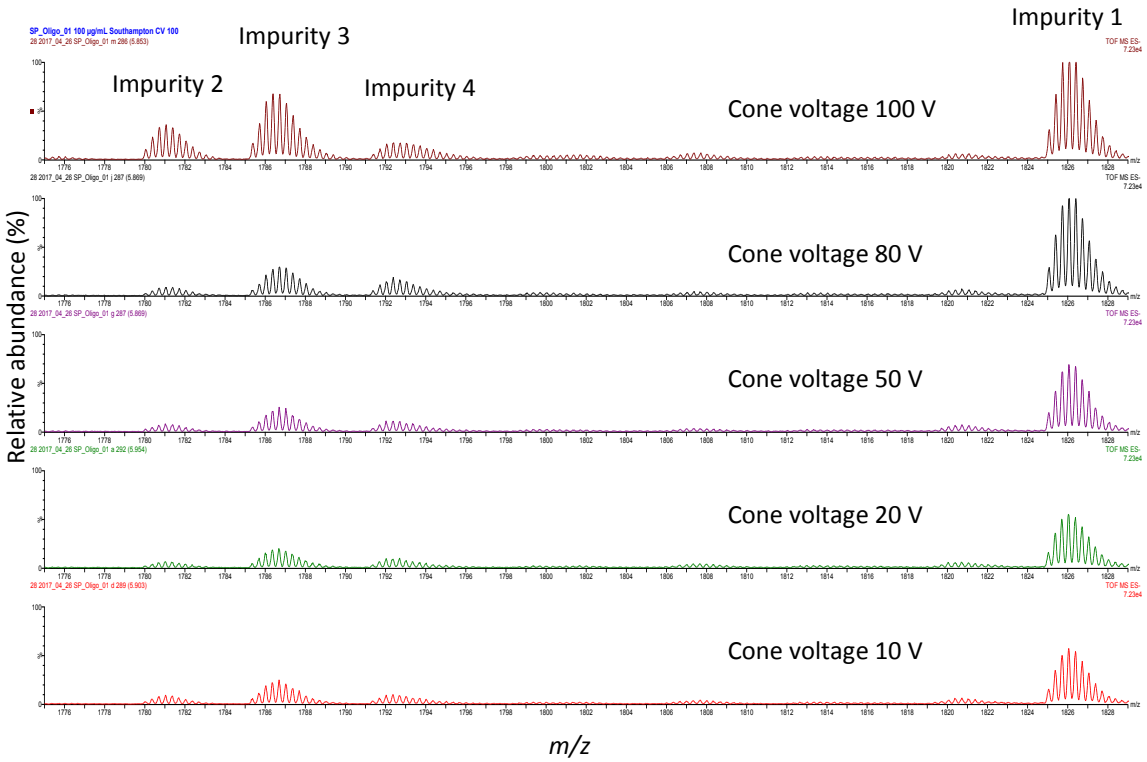

Figure 5.5 - Negative ionisation ESI mass spectra of SP_Oligo_01 analysed using the SCM at a range of cone voltages showing *m/z* 1775 - 1830. Normalised to ion intensity of impurity 1 at 100 V

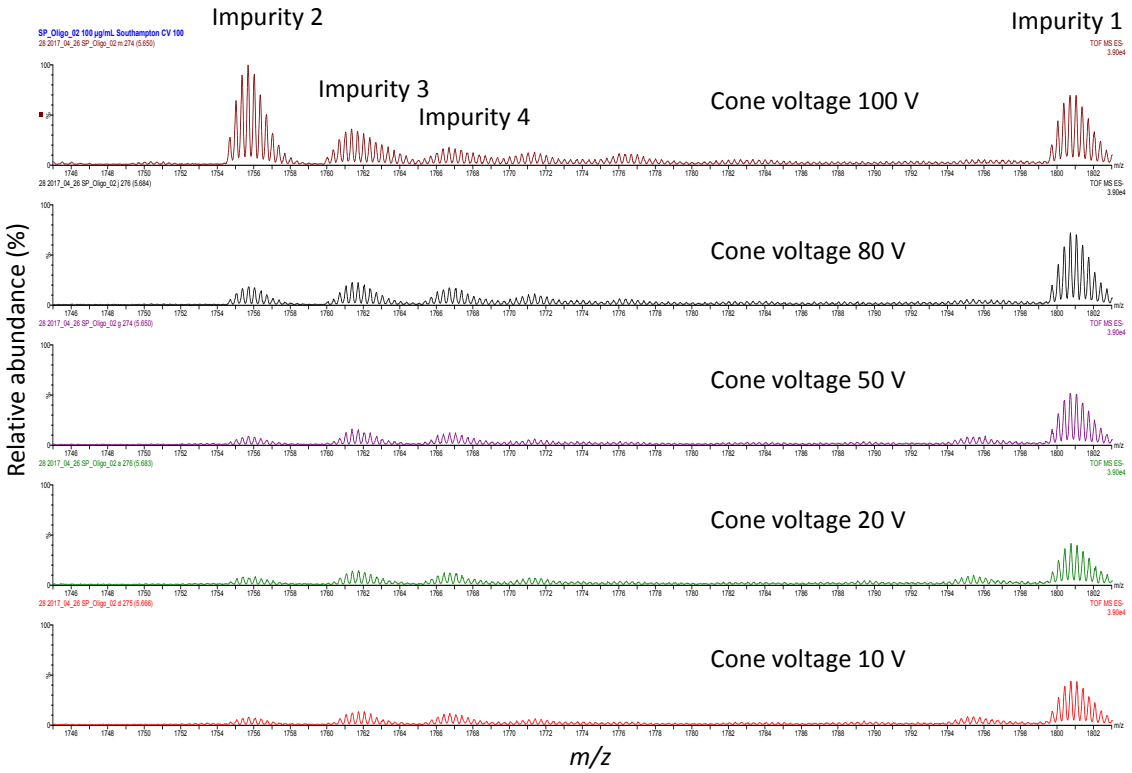

Figure 5.6 - Negative ionisation ESI mass spectra of SP_Oligo_02 analysed using the SCM at a range of cone voltages showing *m/z* 1745 - 1805. Normalised to ion intensity of impurity 2 at 100 V

The levels of the ions associated with depurination impurities and their corresponding fragments (impurities 2 and 3) shown in Figure 5.5 and Figure 5.6 are visibly greater in the replicates analysed using a cone voltage of 100 V for SP_Oligo_01 and SP_Oligo_02. The ion intensities observed in the mass spectra increase as the cone voltage applied reaches 80 V and is greatest at a cone voltage of 100 V. Table 5.4 shows the mean percentage of FLN of each impurity by sample, calculated using Equation 5.1.

Table 5.4 - Mean RICC peak area as a percentage of FLN RICC peak area for each impurity investigated by sequence analysed, chromatographic method used and cone voltage used. Values reported are a mean of three replicates.

Sample	Chromatographic method	Cone voltage (V)	Impurity (% of FLN RICC peak area)			
			1	2	3	4
SP_Oligo_01	Southampton	10	7.0 ± 0.1	0.9 ± 0.1	2.6 ± 0.1	1.2 ± 0.02
		20	7.1 ± 0.2	1.0 ± 0.2	2.9 ± 0.3	1.2 ± 0.01
		50	7.2 ± 0.3	0.6 ± 0.1	2.3 ± 0.2	1.2 ± 0.04
		80	7.3 ± 0.1	0.6 ± 0.04	2.1 ± 0.1	1.2 ± 0.03
		100	7.0 ± 0.2	2.5 ± 0.04	4.6 ± 0.1	1.2 ± 0.03
	AZ	10	9.0 ± 0.1	1.5 ± 0.1	3.8 ± 0.1	1.2 ± 0.01
		20	8.5 ± 0.5	1.5 ± 0.02	3.9 ± 0.1	1.3 ± 0.02
		80	9.3 ± 0.3	3.5 ± 0.04	6.2 ± 0.1	1.3 ± 0.01
		100	9.0 ± 0.1	14.3 ± 0.03	16.3 ± 0.3	1.8 ± 0.03
SP_Oligo_02	Southampton	10	2.6 ± 0.1	0.4 ± 0.01	0.2 ± 0.01	0.7 ± 0.01
		20	2.6 ± 0.2	0.4 ± 0.01	0.2 ± 0.01	0.7 ± 0.01
		50	2.7 ± 0.04	0.4 ± 0.01	0.2 ± 0.001	0.6 ± 0.01
		80	2.4 ± 0.1	0.6 ± 0.01	0.3 ± 0.01	0.6 ± 0.02
SP_Oligo_02	Southampton	100	2.5 ± 0.1	3.3 ± 0.1	0.7 ± 0.02	0.5 ± 0.01
	AZ	10	3.0 ± 0.1	1.3 ± 0.05	0.9 ± 0.02	0.6 ± 0.02
		20	2.9 ± 0.03	1.4 ± 0.03	1.0 ± 0.03	0.6 ± 0.02
		80	3.0 ± 0.02	4.5 ± 0.04	1.6 ± 0.02	0.6 ± 0.004
		100	2.9 ± 0.01	24.8 ± 0.3	4.9 ± 0.05	0.8 ± 0.003

The values presented in Table 5.4 show that replicates of SP_Oligo_01 and SP_Oligo_02 analysed using a cone voltage of 100 V and both the ACM and SCM show a marked increase in the observed percentage of the ions associated with impurities 2 and 3. As the amount of the impurity generated in the synthesis of the oligonucleotide cannot increase between replicates, these higher percentages must be caused by in-source fragmentation. As expected, the observed level of the ion associated with impurity 1 is not affected by the cone voltage as this impurity cannot be created in-source. Impurity 4, the loss of adenine and addtion of water, is unaffected by changing cone voltage, suggesting that the adenine is unlikely to be removed by ion-source fragmentation in the oligonucleotide sequences used in SP_Oligo_01 and SP_Oligo_02.
The SCM data for impurities 2 to 4 from Table 5.4 are presented graphically in Figure 5.7 and Figure 5.8 and the ACM data in Figure 5.9 and Figure 5.10.

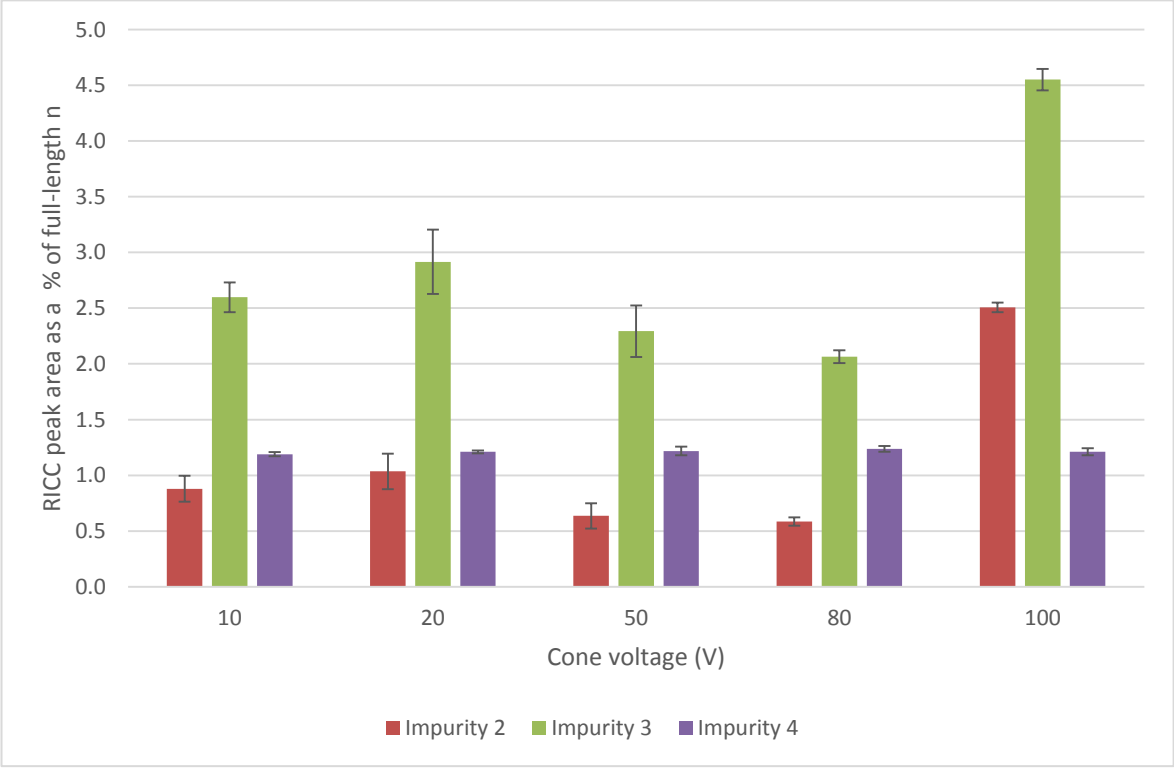

Figure 5.7 - Levels of observed ions associated with impurities 2 - 4 by cone voltage for SP_Oligo_01 analysed using the Southampton chromatographic method and the Waters Synapt. n = 3

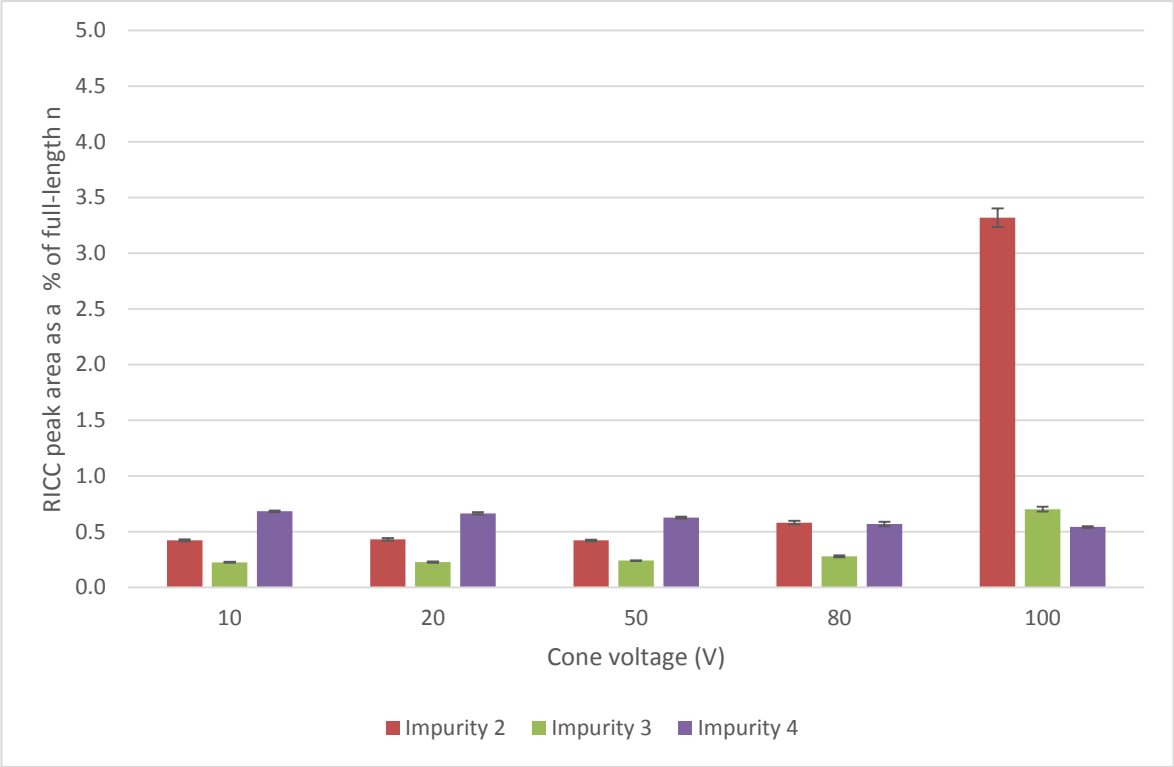

Figure 5.8 - Levels of observed ions associated with impurities 2 - 4 by cone voltage for SP_Oligo_02 analysed using the Southampton chromatographic method and the Waters Synapt. n = 3

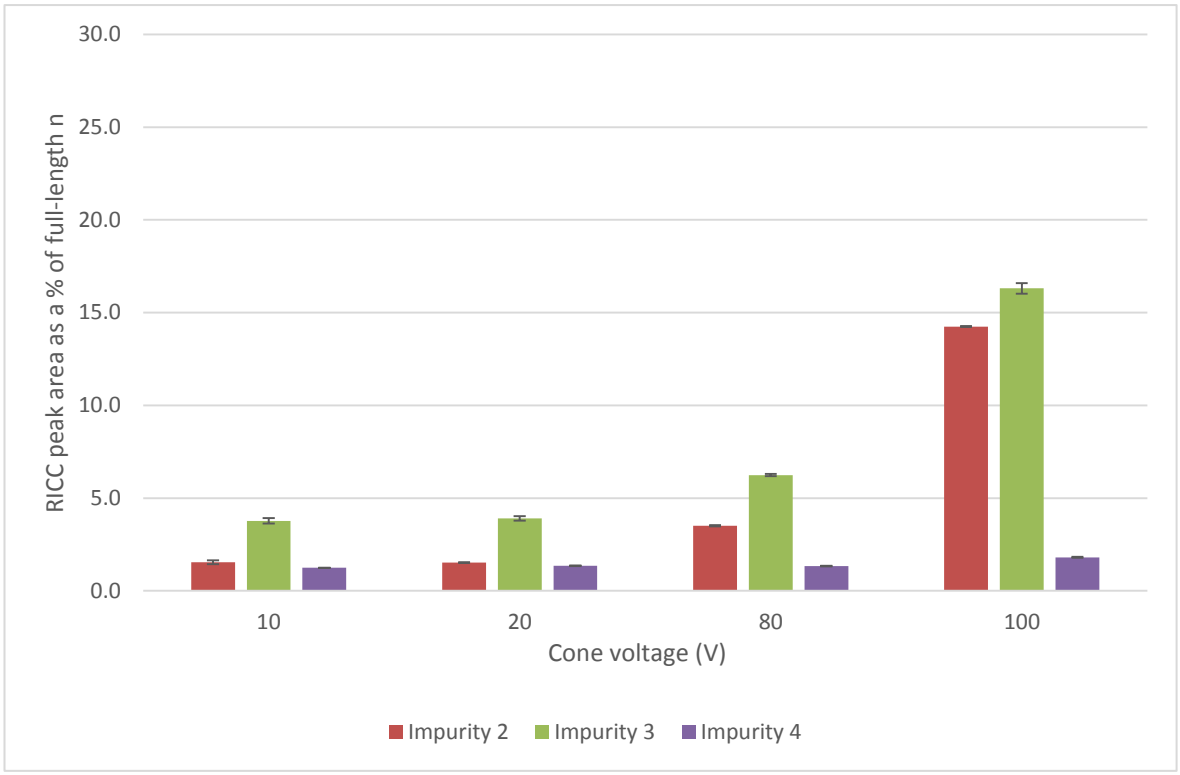

Figure 5.9 - Levels of observed ions associated with impurities 2 - 4 by cone voltage for SP_Oligo_01 analysed using the AZ chromatographic method and the Waters Synapt. n = 3

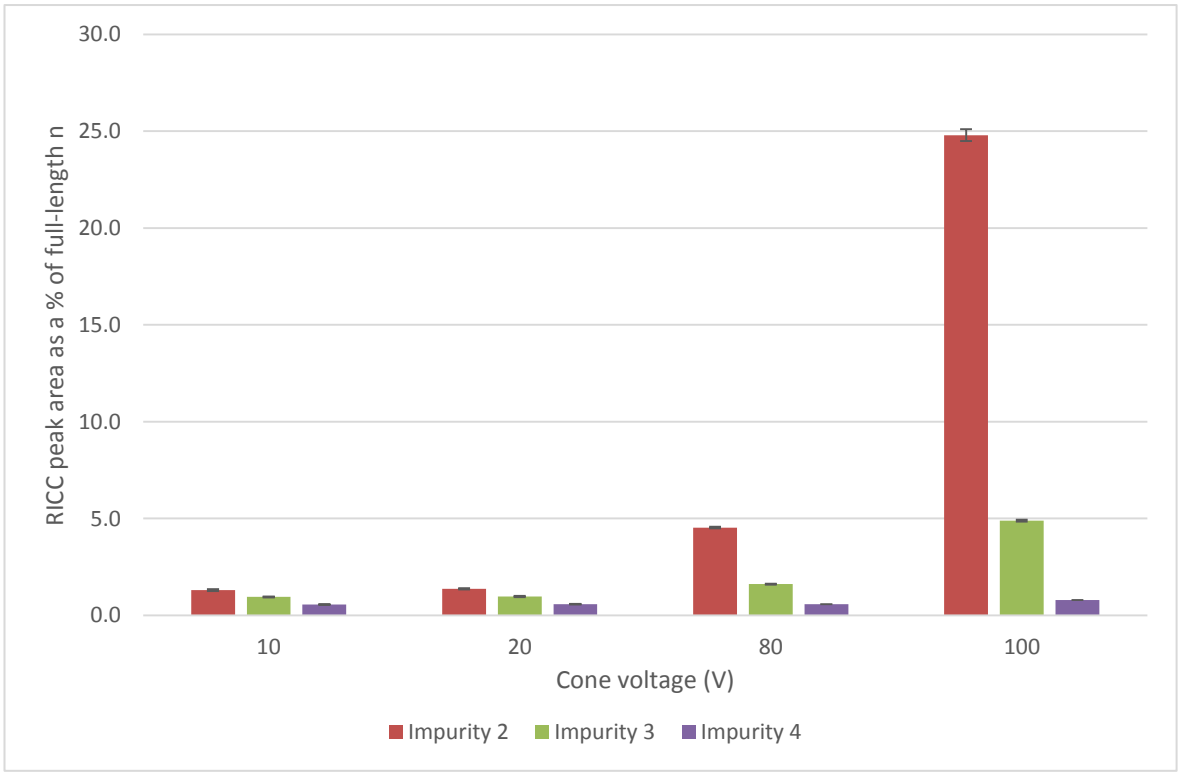

Figure 5.10 - Levels of observed ions associated with impurities 2 - 4 by cone voltage for SP_Oligo_02 analysed using the AZ chromatographic method and the Waters Synapt. n = 3

In all samples, a cone voltage of 100 V causes fragmentation leading to the loss of guanine and adenine & guanine (impurities 2 and 3).

Comparison of the levels of ions observed when samples are analysed using the SCM (Figure 5.7 andFigure 5.8) and the ACM (Figure 5.9 and Figure 5.10) shows that, at cone voltages of 80 and 100 V, the ACM appears to cause enhanced fragmentation resulting in the loss of guanine relative to the SCM. The possible causes of this difference are the higher column temperature in the ACM increasing the effect of the higher cone voltages or, perhaps more importantly for the quantitation of impurities, a difference in the levels of deprotonation between the FLN and the impurities.

Quantitation of the samples analysed using the ACM is undertaken using the -4 charge state, compared to the -3 charge state for the SCM. If more impurity molecules are in the -4 charge state and more FLN molecules are in the -3 charge state, this could create the differences observed. The ions associated with the loss of adenine do not show the same pattern, being consistent between the two analytical methods. This suggests that, if column temperature influences the level of in-source fragmentation, guanine is more prone to fragmentation under higher temperatures combined with high cone voltages than adenine. It has previously been observed that fragmentation occurs differently in ions of different charge states[85, 101]. The data presented here tend to support this observation when high cone voltages are used. Increased deprotonation may destabilise bonds to guanine residues and make them more likely to be lost in the ion source.

Higher cone voltages are often applied to reduce the formation of adducts in the ion source[95], which lead to a reduction in ion intensity of the target ions. Figure 5.11 shows the RICC peak area of the FLN oligonucleotide ion for each sample analysed using the SCM and the Waters Synapt across the range of cone voltages investigated.

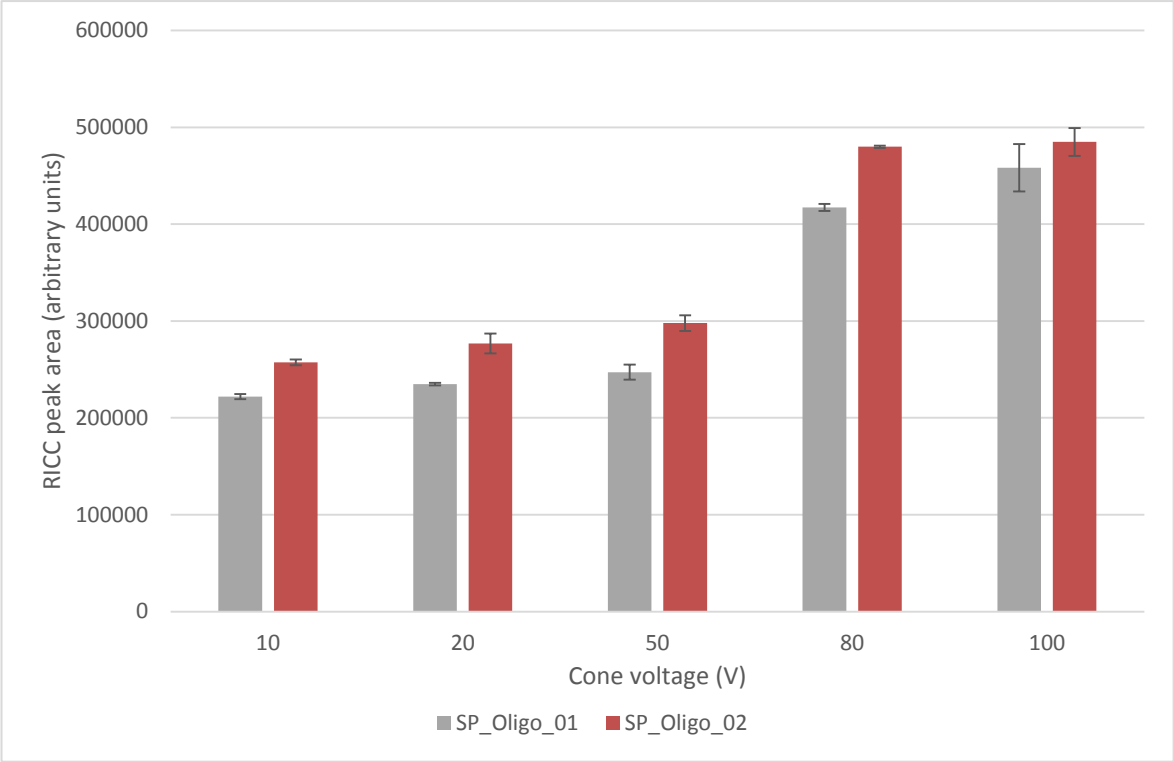

Figure 5.11 - RICC peak areas of FLN for all samples analysed using the Southampton chromatographic method and the Waters Synapt by cone voltage applied. n = 3

Samples SP_Oligo_01 and 02, show higher peak areas at cone voltages 80 V and 100 V, increasing from a minimum of 221989 arbitrary units to 458103 arbitrary units and from 257200 arbitrary units to 484816 arbitrary units, respectively. The increases in peak area indicate a possible reduction in adducts and a narrower distribution of ions as described by Guo *et al.*[95]. The increase in peak area and, therefore sensitivity, must be weighed against the increased in-source fragmentation occurring at higher cone voltages in order to determine an optimal cone voltage for accurate quantitation of therapeutic oligonucleotide impurities.

5.4 Sequence effect

The sequences used to investigate the effect of guanine positioning and grouping on in-source fragmentation are shown in Table 5.5 along with the ions used for generating RICC peak areas for each sequence. The ions used for SP_Oligo_04 are the deprotonated -3 charge state ions ($[M - 3H]^{3-}$) but in the samples provided for SP_Oligo_06, 07 and 08, the potassium adduct dominates, so these ions are the $[M + K - 4H]^{3-}$ ions of the given sequence. The ions used for the FLN (target

oligonucleotide) are *m/z* 1315.2 for SP_Oligo_04 and *m/z* 1329.1 for SP_Oligo_06, 07 and 08.

Table 5.5 - Oligonucleotide sequences and ions used for RICC peak areas

Sample	Sequence	*m/z* used for RICC peak area			
		1	2	3	4
SP_Oligo_04	G-G-G-A-A-A-C-C-C-T-T-T-T	1309.9	1264.8	1270.5	1726.1
SP_Oligo_06	A-A-A-G-G-C-C-C-G-T-T-T-T	1323.8	1278.7	1284.4	1290.0
SP_Oligo_07	G-A-A-A-G-C-C-C-G-T-T-T-T				
SP_Oligo_08	C-C-C-A-A-A-G-G-G-T-T-T-T				

The RICC peaks generated were used to calculate the impurity peak area as a percentage of the FLN peak area, as in described in Section 5.1. Table 5.6 shows the mean percentage of each impurity by sequence for samples analysed using the SCM and the Waters Synapt mass spectrometer at 20 V in-source CID voltage.

Table 5.6 - Mean RICC peak area as a percentage of FLN RICC peak area for each impurity investigated by sequence analysed at 20 V in-source CID voltage. n = 3

Sample	Impurity (% of FLN RICC peak area)			
	1	2	3	4
SP_Oligo_04	0.04 ± 0.004	0.05 ± 0.001	0.04 ± 0.003	0.01 ± 0.001
SP_Oligo_06	0.05 ± 0.004	0.06 ± 0.005	0.07 ± 0.003	0.01 ± 0.002
SP_Oligo_07	0.02 ± 0.001	0.04 ± 0.005	0.03 ± 0.004	0.01 ± 0.002
SP_Oligo_08	0.05 ± 0.002	0.11 ± 0.01	0.12 ± 0.01	0.02 ± 0.01

All impurities are at very low levels and are at similar levels across samples SP_Oligo_04, 06 and 07. The observed levels of the ions associated with depurination-related impurities (impurities 2 and 3) are much higher in SP_Oligo_08 than in the other samples. SP_Oligo_08 contains all three of its guanine residues consecutively in the sequence and close to the middle of the sequence. SP_Oligo_04 has its three guanines consecutively placed, but they are at one end of the oligonucleotide chain.

The second highest levels of impurities 2 and 3 are observed in SP_Oligo_06, which contains two consecutive guanines close to the centre of the sequence. SP_Oligo_07, where all guanines are separate from each other, shows the lowest levels of the guanine-loss impurities, despite two of the guanines being close to the centre of the oligonucleotide. Figure 5.12 presents the data from Table 5.6 graphically and, here, the difference between SP_Oligo_08 and the other samples with regard to the observed levels of the ions associated with guanine loss is readily apparent.

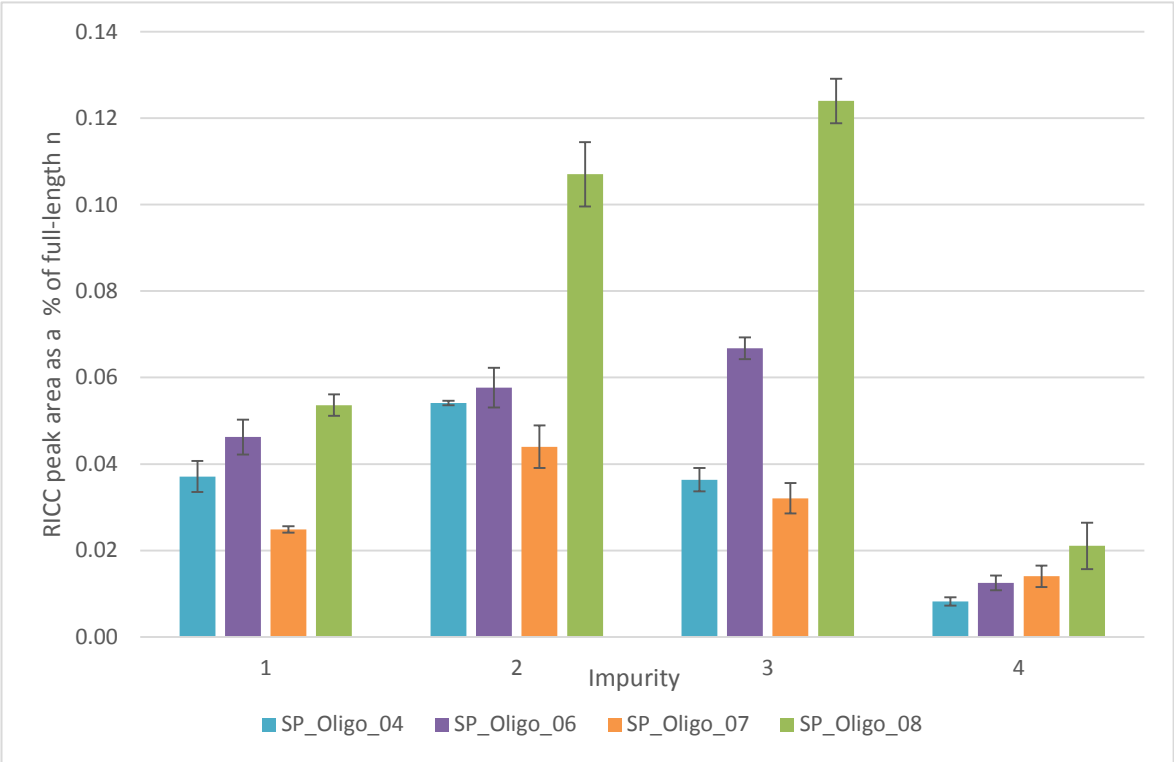

Figure 5.12 – Observed levels of ions associated with impurities by sequence for replicates analysed using the Southampton chromatographic method and the Waters Synapt at 20 V in-source CID voltage. n = 3

The level of impurity 1 is lower in SP_Oligo_07 than in the other samples analysed, but this impurity cannot be created by in-source fragmentation, so this is most likely to be a result of the synthesis of the samples.

To investigate whether the differences observed at 20 V in-source CID voltage were a result of in-source fragmentation or a true representation of the levels of synthetic depurination in the samples provided, the samples were also analysed at 100 V in-source CID voltage. Figure 5.13 shows the observed levels of the ions associated with the selected impurities, as a percentage of the FLN peak area and

Table 5.7 shows the difference between the calculated percentage at 20 V and 100 V in-source CID voltage.

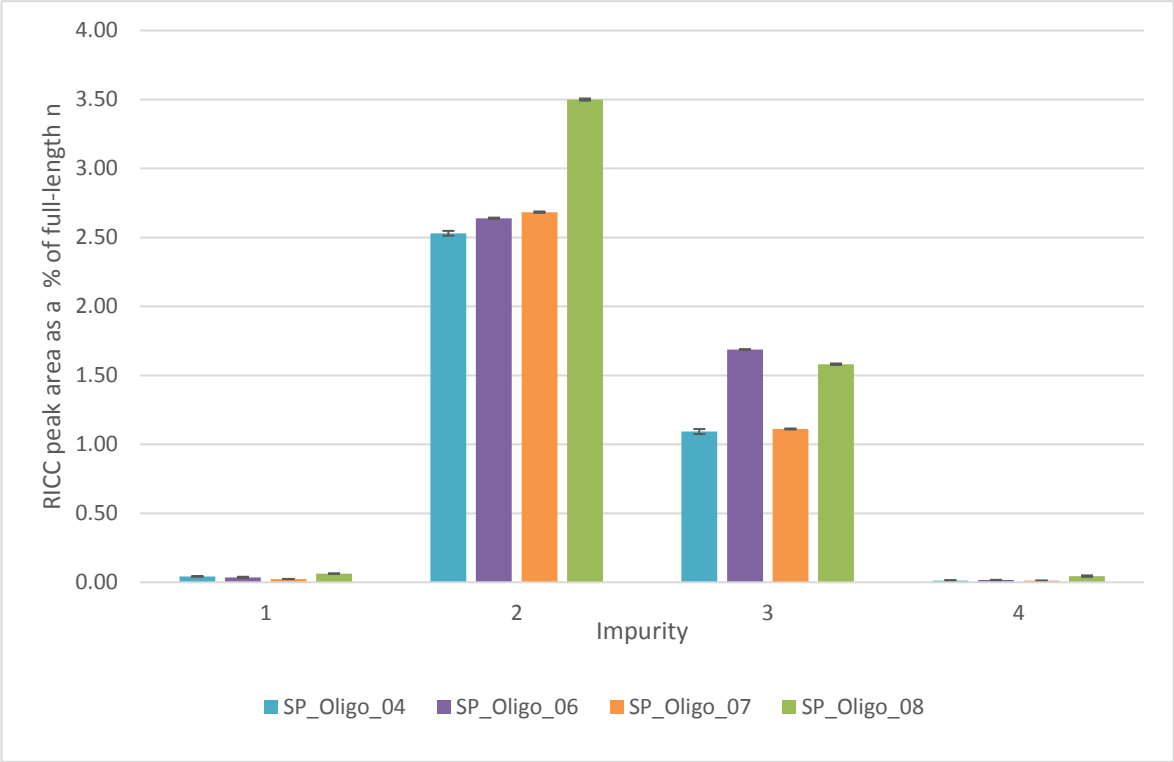

Figure 5.13 – Observed levels of ions associated with impurities by sequence for replicates analysed using the Southampton chromatographic method and the Waters Synapt at 100 V in-source CID voltage.

Table 5.7 - Mean difference in RICC peak area as a percentage of FLN RICC peak area for each impurity investigated between analysis at 20 V and 100 V in-source CID voltage. n = 3

Sample	Difference in impurity (% of FLN RICC peak area)			
	1	2	3	4
SP_Oligo_04	0.01 ± 0.005	2.48 ± 0.02	1.06 ± 0.02	0.00
SP_Oligo_06	-0.01 ± 0.004	2.58 ± 0.04	1.62 ± 0.04	0.00
SP_Oligo_07	0.00	2.64 ± 0.03	1.08 ± 0.07	0.00
SP_Oligo_08	0.01 ± 0.002	3.39 ± 0.01	1.46 ± 0.02	0.02 ± 0.003

The increase in observed level of the ions associated with impurity 2 is greatest in SP_Oligo_08 suggesting that, even if the differences noted in the samples at 20 V in-source CID voltage are related to synthesis, more depurination occurs in this

sample than in the other samples. For the ions associated with impurity 3, the increase in observed levels is greatest in SP_Oligo_06 and SP_Oligo_08, supporting the general trend seen in the replicates analysed using 20 V in-source CID voltage of these two sequences having more depurination than SP_Oligo_04 and SP_Oligo_07. SP_Oligo_06 has a greater increase than SP_Oligo_08, suggesting that the level of synthetic impurity 3 may be higher in SP_Oligo_08. The results presented in Figure 5.13 and Table 5.7 do not conclusively prove that the differences observed in apparent levels of depurination are sequence-driven in-source fragmentation related rather than differences in synthetic impurity levels in the samples, as this distinction is not possible. These results do, however, indicate that the effect of sequence cannot be ruled out.

The results presented in this section indicate that the position and grouping of guanines in an oligonucleotide sequence are important for the amount of in-source depurination occurring within a sample. The positioning of guanines close to the centre of the sequence increases the likelihood of one of them being lost during the ionisation process and the more guanines situated consecutively within the sequence the greater the chance of one being lost. SP_Oligo_04, with all of its guanines positioned consecutively at one end of the sequence loses more guanine than SP_Oligo_07, which has two guanines located close to the centre of the oligonucleotide but separate from each other, suggesting that the proximity of other guanines is as important as their location. Three guanines positioned at the centre of the sequence next to one another are the most likely to be lost. These results contradict those published by Suzuki *et al.*[96] and Nyakas *et al.*[97] who both reported that terminal guanines were more likely to be lost than internal bases but Pan *et al.*[102] noted that the location and tendency for bases to be lost varies according to the level of charges on the oligonucleotide, so the low levels of charge observed in these samples may have an effect. Research published by Marzilli *et al.*[103] suggests that the loss of a guanine from an oligonucleotide sequence favours cleavage at this site; this may contribute to the potential increased depurination observed when guanines are clustered together.

An ion mobility study of these sequences to investigate the shape of the oligonucleotides may help to explain these data; it is possible that samples with high levels of consecutive guanines close to the centre of the sequence take on a different shape in the ion source to those with guanines situated at the end of the

sequence or dispersed throughout the oligonucleotide. A difference in shape, such as a sphere rather than a linear shape may allow guanines to be removed more easily.

The differences in in-source fragmentation observed between different sequences has implications for the development and validation of a generic oligonucleotide impurity quantitation method. In-source loss of bases cannot be differentiated from synthetic abasic impurities, so any method developed must aim for as low as possible in-source fragmentation but these data show that the sequence of the oligonucleotide chosen for method validation is critical to ensure the mass spectrometer-related losses are minimised.

5.5 Column temperature

In sections 5.2 and 5.3, it was noted that levels of in-source fragmentation appeared to be higher when samples were analysed using the ACM compared to the SCM. Other than the mobile phase additives, the SCM and ACM differ in the LC column temperature employed. To investigate whether the column temperature has any effect on the level of in-source fragmentation observed as a result of increased sample degradation on-column, samples SP_Oligo_01 and 02 were analysed using the Waters Synapt and the SCM, the SCM mobile phase additives and gradient with a column temperature of 50 °C, the ACM and the ACM mobile phase additives and gradient with a column temperature of 40 °C. All replicates were analysed at a cone voltage of 20 V.

Table 5.8 shows the mean RICC peak area for SP_Oligo_01 and SP_Oligo_02 using each combination of chromatographic method and column temperature. The data from the table are presented graphically in Figure 5.14 and Figure 5.15.

Table 5.8 - Mean RICC peak area as a percentage of FLN RICC peak area for SP_Oligo_01 and SP_Oligo_02 by chromatographic method and column temperature used. n = 3

Sample	Chromatographic method	Impurity (% of FLN RICC peak area)			
		1	2	3	4
SP_Oligo_01	Southampton	8.7 ± 0.9	1.6 ± 0.02	2.8 ± 0.1	0.8 ± 0.02
	Southampton 50 °C	11.5 ± 0.2	1.6 ± 0.03	2.8 ± 0.02	0.8 ± 0.01
	AZ	9.0 ± 0.04	1.5 ± 0.1	2.8 ± 0.1	1.1 ± 0.03
	AZ 40 °C	8.9 ± 0.1	1.2 ± 0.04	2.3 ± 0.1	1.1 ± 0.03
SP_Oligo_02	Southampton	4.6 ± 0.1	1.8 ± 0.01	0.5 ± 0.01	0.8 ± 0.005
	Southampton 50 °C	5.1 ± 0.1	1.8 ± 0.02	0.5 ± 0.003	0.8 ± 0.002
	AZ	2.2 ± 0.03	1.2 ± 0.05	0.5 ± 0.02	0.8 ± 0.02
	AZ 40 °C	2.1 ± 0.03	0.9 ± 0.05	0.4 ± 0.01	0.9 ± 0.03

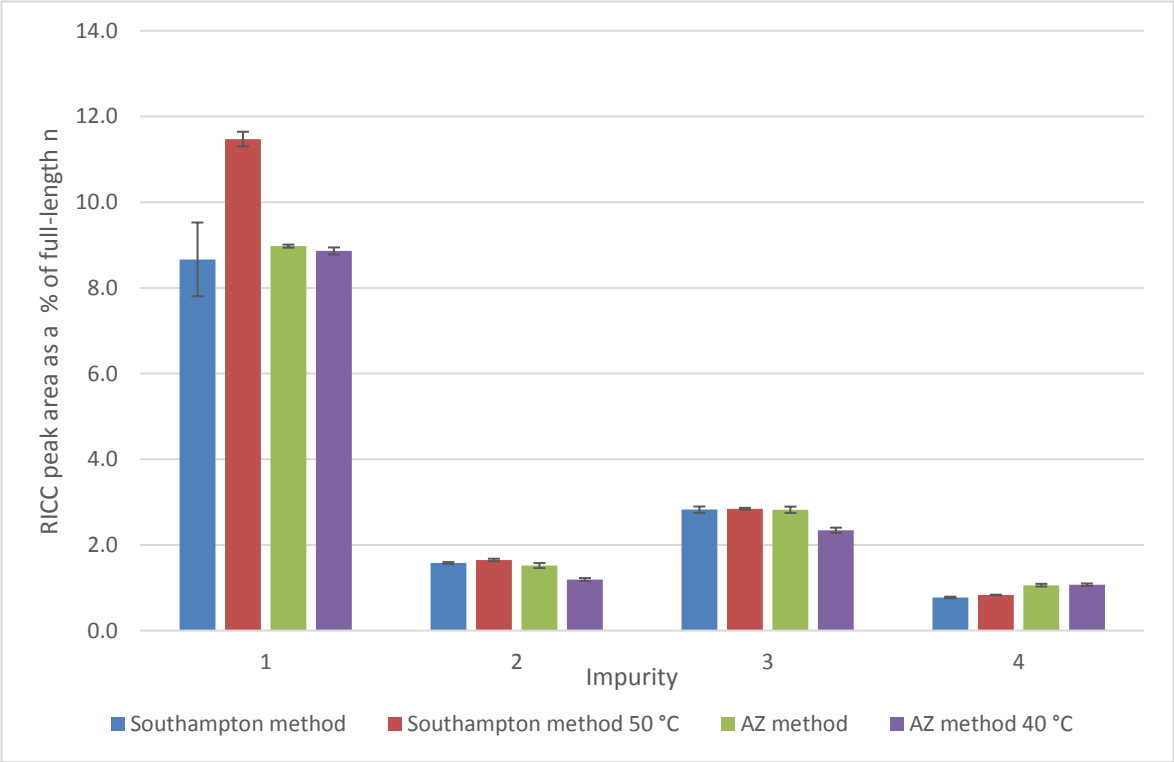

Figure 5.14 – Observed levels of ions associated with impurities by column temperature and chromatographic method for SP_Oligo_01 analysed using the Waters Synapt. n = 3

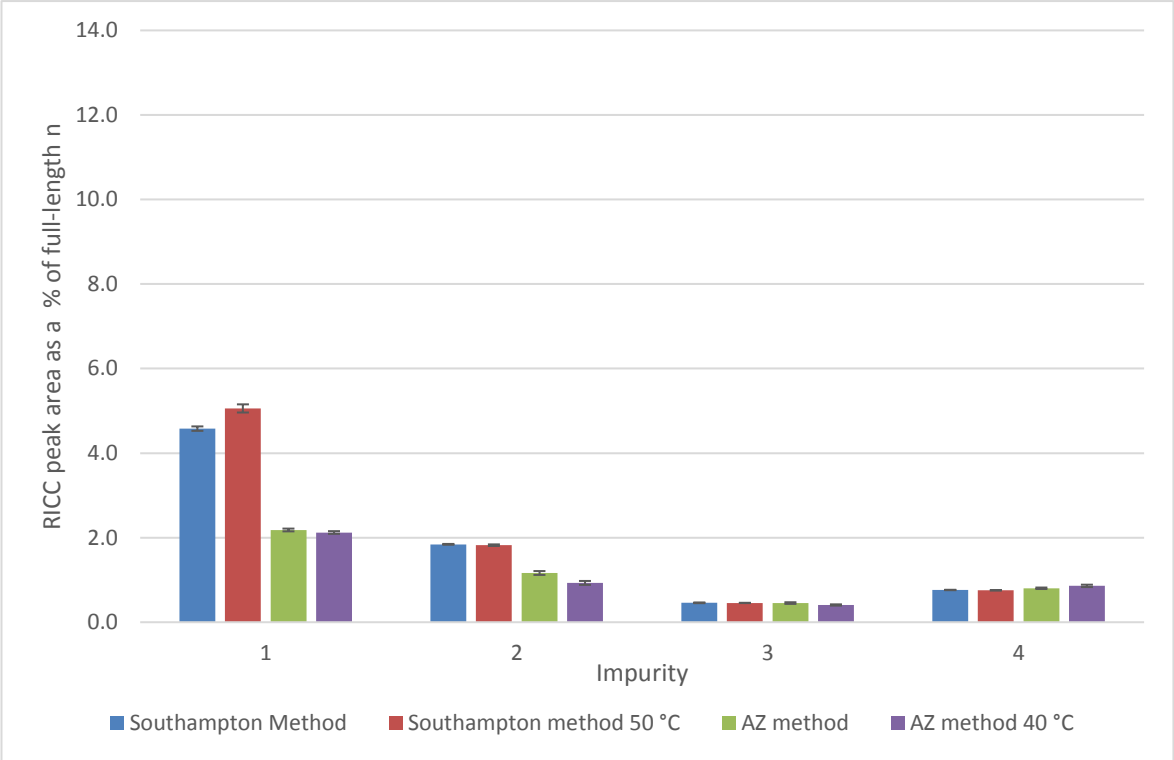

Figure 5.15 - Observed levels of ions associated with impurities by column temperature and chromatographic method for SP_Oligo_02 analysed using the Waters Synapt. n = 3

When using the SCM mobile phase additives and gradient, Figure 5.14 and Figure 5.15 show that column temperature does not affect the levels of impurities 2-4, indicating that column temperature is not an important factor in the in-source fragmentation of oligonucleotides. When the ACM mobile phase additives and gradient are used, the level of the ions associated with impurities 2 and 3 is slightly lower at a column temperature of 40 °C than at 50 °C but the levels observed are low, so variation is to be expected.

The data presented here indicate that column temperature is, for the two samples analysed, not a significant factor influencing the level of in-source fragmentation of oligonucleotides with any enhancement of sample degradation occurring at the higher temperature not leading to increased in-source depurination.

5.6 Fragmentation conclusions

The apparent levels of abasic impurities, particularly those involving the loss of guanine, present in oligonucleotide samples can be artificially enhanced by in-source fragmentation of the sample to produce identical ions. ESI source type, the oligonucleotide sequence and the in-source CID voltage (cone voltage) are all

important factors determining the apparent level of depurination impurities observed in a sample.

The Waters source design is more prone to in-source fragmentation than the Agilent and Bruker designs. This need not preclude the use of Waters instrumentation provided the method is properly optimised to minimise the amount of fragmentation occurring during analysis and that the instrument manufacturer is clearly stated when quantitated results are reported.

The in-source CID voltage used for analysis must be carefully considered. The results presented in this chapter show that the observed level of depurination impurities (the level of fragmentation occurring) rises dramatically at voltages of 80 V and above, but that RICC peak areas are greatest at voltages of 80 V and 100 V. In order to reduce the risk of reporting inaccurately high levels of impurities, it is reasonable to sacrifice some sensitivity to ensure that excessive fragmentation does not occur. There is little difference in RICC peak area between replicate analysed using cone voltages of 10 V to 50 V so a cone voltage, when using the Waters Synapt, of 10 V would allow for the lowest level of fragmentation without a dramatic loss of sensitivity. Fountain *et al.*[21] have found that the desolvation temperature also affects levels of in-source depurination, so this is a factor which may benefit from future investigation.

The difference in observed levels of ions associated with synthetic abasic impurities and their in-source fragmentation derived equivalents between charge states used for quantitation at high in-source CID voltages further lends weight to the recommendation for the use of a low voltage when Waters source designs are employed.

The factor which has the greatest influence when considering the development of a generic oligonucleotide impurity quantitation method is the sequence of the oligonucleotide to be analysed. The position and grouping of guanines within the sequence has a large effect on the level of in-source fragmentation occurring. The risk created by this phenomenon is that if a method is developed and validated using a sequence with low in-source fragmentation, it may appear that use of a higher cone voltage to maximise sensitivity is appropriate for analysis than is actually the case for other samples tested. To avoid the requirement for optimising and re-validating the method for each sample, a sequence with three or more

guanines situated in the centre of the oligonucleotide should be used to determine the cone voltage that produces the lowest level of in-source fragmentation with acceptable sensitivity.

Any generic method for the quantitation of oligonucleotide impurities must be developed and validated using more than one source type. Additionally, a “worst-case scenario” sequence should be used to optimise the cone voltage for each source type and allow settings for the lowest possible level of in-source fragmentation to be prescribed for any instrument used.

Chapter 6: Quantitation

All methods of quantitating impurities in oligonucleotide samples, with their multiple charge states, have some inherent risks for their accuracy and precision[81, 104]. The differences in charge state distribution observed between mass analyser types and mobile phase additives means that any approach must minimise these differences to allow consistent quantitation across laboratories and analytical methods.

In order to determine a robust method of quantitation that can be used for multiple mass analysers and chromatographic methods, the level of ion suppression occurring and the consistency of charge state distribution must be investigated. Different approaches to the quantitation, using a single charge state and single ion, using a range of ions and using deconvoluted data are compared to determine which is most robust and minimises the effects of different charge state distributions.

Published studies on quantitation specifically of oligonucleotides and their impurities focussing on the data processing are uncommon; papers by Smith & Beck[105], Ledman & Fox[106] and Gilar *et al.*[107] have been consulted in the process of this research along with Lavagnini *et al.*[108] on the general process of quantitation.

6.1 Current quantitation method

The method of impurity quantitation currently used by AstraZeneca selects the most dominant ion of the most dominant charge state of the full-length n (FLN) peak and takes the RICC peak area of this ion. When using the AZ chromatographic method and the Agilent 6130 mass spectrometer, the dominant charge state in the samples investigated here (SP_Oligo_01 and SP_Oligo_02) is the -4 charge state. The *m/z* of the ions used for each impurity are calculated by subtracting or adding the *m/z* of the change related to the impurity (*e.g.* loss of guanine) from the *m/z* of the dominant ion of the FLN peak. The RICC peak areas of these ions are then compared to the peak area of the FLN oligonucleotide. This approach is used for impurities located under the main peak in the UV chromatogram, impurities eluting before or after the main peak are grouped as shown in Figure 6.1. Early and late eluting impurities are reported as a percentage

of the UV peak area and typically not further identified. The use of UV peak area alone for the quantitation of these groups leads to the potential of over-reporting, if non-oligonucleotide related compounds co-elute in these regions, and also reduces the overall understanding of the impurities present in the sample. Reporting of impurities under the main peak using MS data and early and late eluting impurities using UV data also provides an inconsistent approach to the treatment of different impurities.

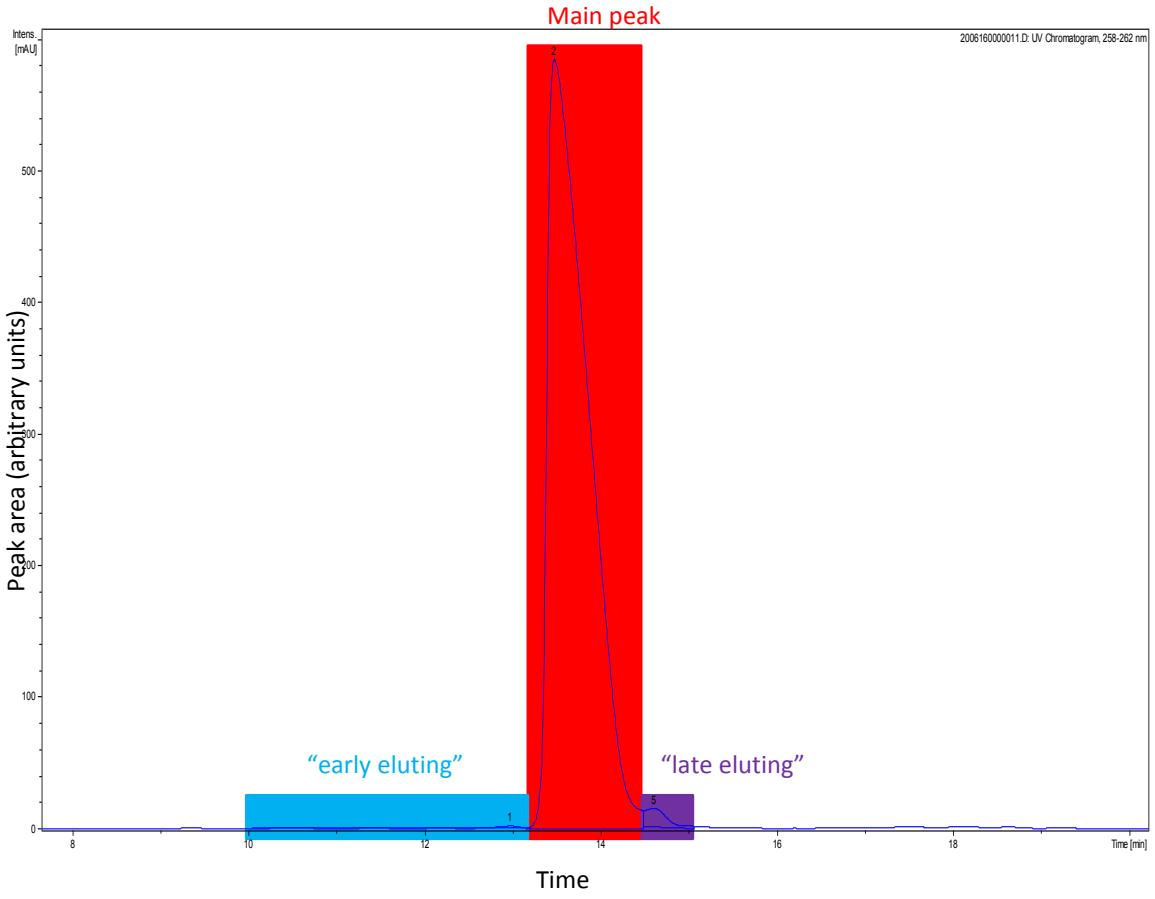

Figure 6.1 - Example of a UV chromatogram at 260 nm for SP_Oligo_01 analysed using the AZ chromatographic method and the Agilent 6130 LC-MS

The quantitation of the impurities under the main peak is based on a calibration curve generated by injecting different volumes of a given concentration (*e.g.* 100 µg/mL) solution of a standard oligonucleotide sample. The slope and intercept of the calibration curve are used to calculate the effective amount of each compound on the column and the amount of each compound is calculated as a percentage of the total amount (the sum of all compounds) with the final value taking into account the UV purity of the sample as calculated from a UV calibration curve of the standard injections.

The processing of data using this method is time consuming, containing many manual steps, increasing the potential for operator error and inconsistencies between analysts.

6.2 Alternative methods of quantitation

6.2.1 Use of selected ion monitoring (SIM)

The use of selected ion monitoring (SIM) with a quadrupole mass analyser allows an increase in sensitivity to be achieved when compared to scanning across a mass range. Allowing the mass filter of the quadrupole to switch between a limited number of DC voltages means that more time can be spent collecting ions of a given *m/z*, leading to more of the desired ions being detected compared to the background. Improved sensitivity would allow detection of lower level impurities with modern mass spectrometers and may permit the use of some legacy instruments.

Alongside the benefit of increased sensitivity, there are potential negative effects of using SIM to quantitate therapeutic oligonucleotides and their impurities. If SIM is used to collect ions of expected impurities, a scan of the *m/z* range of interest will also need to be part of the analytical procedure to ensure that any unexpected impurities can be observed and recorded. Any new impurities would then need to be re-analysed using SIM to allow consistent quantitation, adding complexity and time to the data analysis.

Another risk to the accurate quantitation of impurities with the use of SIM analysis is the potential for ion suppression and different ionisation efficiencies occurring between the FLN ion and the impurity ions. If either of these factors occur, the percentage abundance of the impurity reported may be artificially enhanced or depressed.

A final factor against the use of SIM for analysis of therapeutic oligonucleotides and their impurities is that TOF mass analysers cannot analyse in SIM mode, preventing a truly generic method from being developed if this technique is utilised.

6.2.2 Internal standard

The use of an internal standard in the form of a known oligonucleotide that elutes away from the sample FLN and is added at a set concentration to all standards and samples has several potential benefits for improved consistency in the quantitation of therapeutic oligonucleotides and their impurities[108].

The use of a specified concentration of internal standard in samples and calibration standards would allow the calculation of the concentration (*e.g.* µg/mL) of impurities as an addition or alternative to percentages, which could offer greater flexibility of reporting.

As the concentration of internal standard is kept constant, the peak area and shape can be monitored across the analytical run; this may help with troubleshooting in the case of any anomalies in data and could be used as a system suitability check.

The data presented in Section 4.2 indicate that the charge envelope does not change depending on where in the chromatographic gradient the sample elutes for the samples investigated, suggesting that the use of an internal standard eluting away from the sample should be suitable for use in quantitation. Full validation of any selected oligonucleotide sequence would be required to ensure that its use did not affect the ionisation of the sample by ion suppression or enhancement. To ensure that overlap of ions between the impurities of the sample oligonucleotide and the internal standard does not occur, a sequence different in length would be advisable.

6.2.3 Group of ions

When oligonucleotides are analysed using a TOF mass analyser, it is possible to detect the ^{12}C and ^{13}C ions, which may not be achievable when using a quadrupole mass analyser. The use of a group of ions to quantitate impurities may allow differences in mass resolution between TOF and quadrupole instruments to be minimised. To investigate this quantitation method, the RICC of five ions, the ^{12}C ion and the next four ions to include the most abundant ion, is generated for each analyte and the peak areas used for the impurity percentage calculations.

Figure 6.2 shows an example of the five ions selected for SP_Oligo_01 at the -3 charge state.

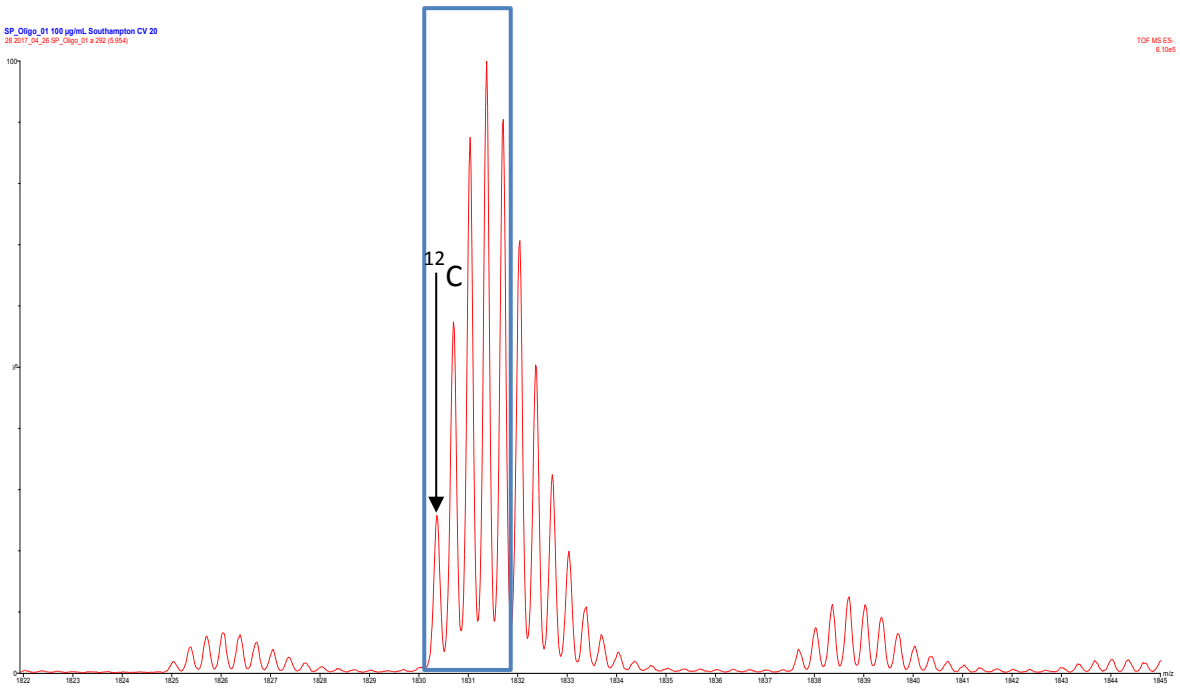

Figure 6.2 - Example of the selection of ions for the generation of an RICC

6.2.4 Deconvolution

Deconvolution of a mass spectrum is a process which allows the molecular mass spectrum of a multiply-charged analyte to be generated. The method of deconvolution used for this chapter is maximum entropy (MaxEnt). MaxEnt works by predicting a molecular mass spectrum based on a given mass range and its "damage model", a pre-programmed set of instructions on chemistry and the physics of mass spectrometers. A mass spectrum known as "mock data" is created and compared to the experimentally generated mass spectrum, with the software accepting the molecular mass spectrum with the least difference between its mock data and the actual mass spectrum. Figures 6.3 and 6.4 show an example of the mock data and molecular mass spectrum generated in MassLynx when using MaxEnt deconvolution alongside the experimental mass spectrum.

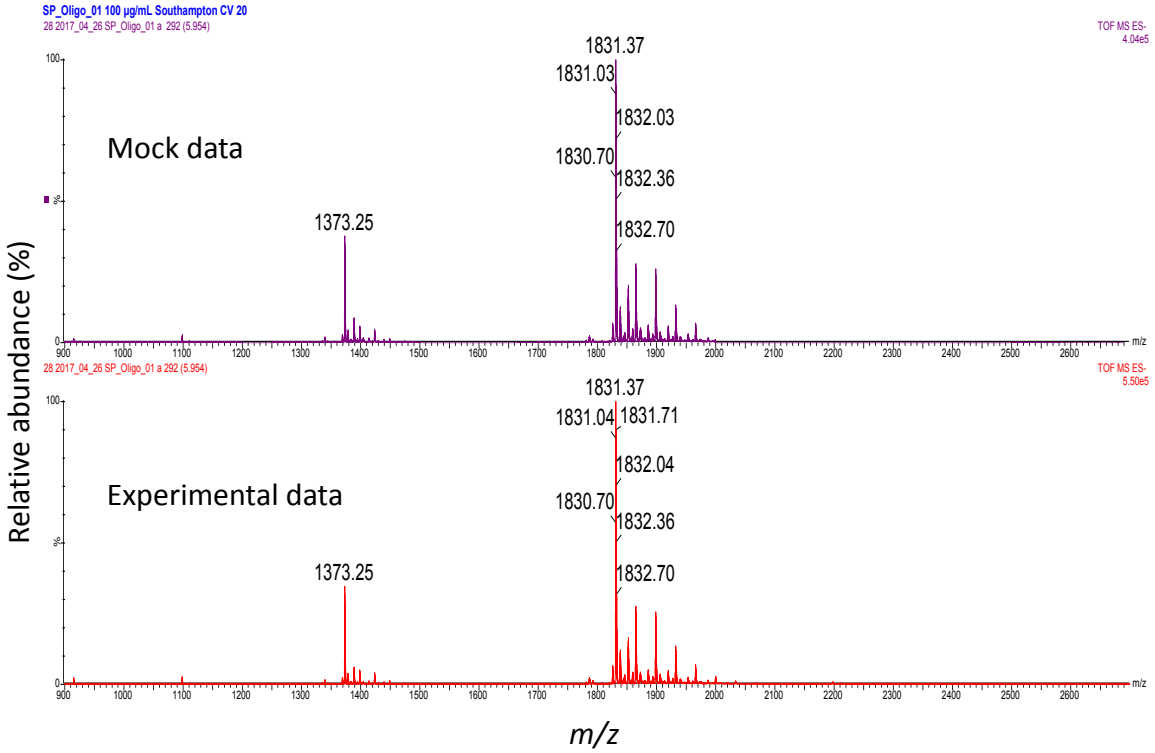

Figure 6.3 - Example of experimental and mock data negative ion ESI mass spectra for SP_Oligo_01

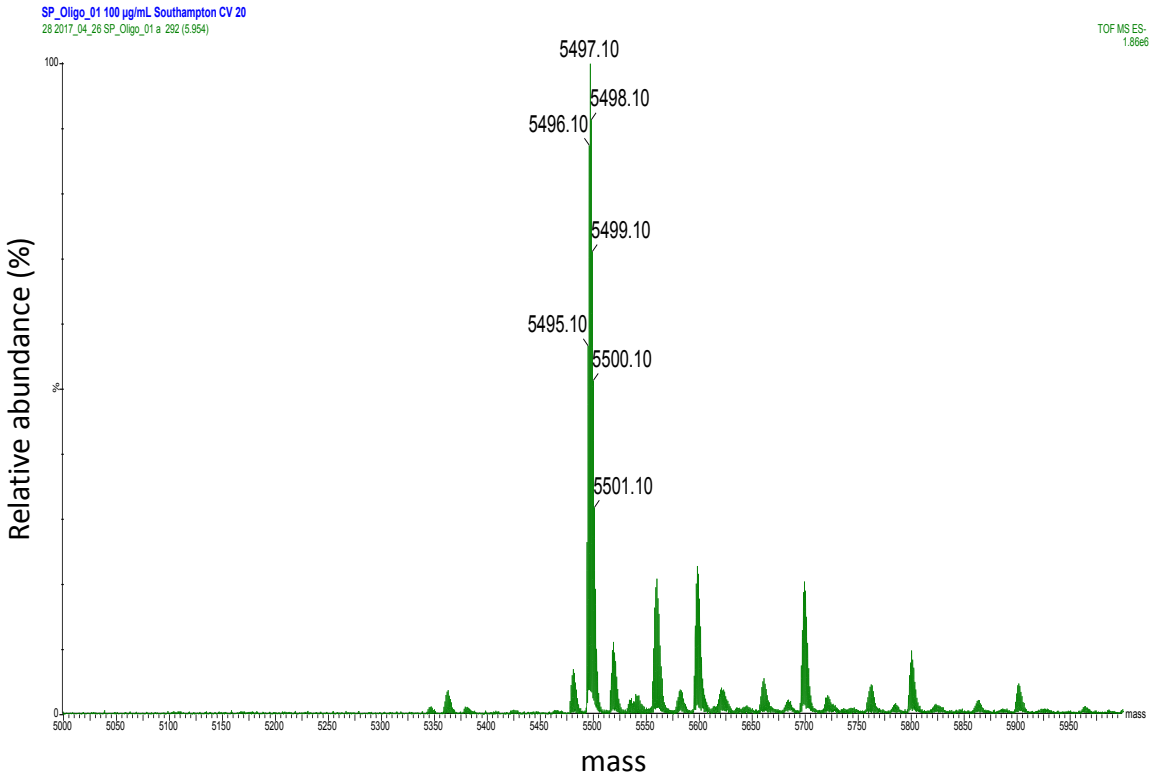

Figure 6.4 - Example of MaxEnt deconvoluted molecular mass spectrum for SP_Oligo_01

The main potential benefit of the use of deconvoluted data for the quantitation of therapeutic oligonucleotides and their impurities is that all ions in the mass spectrum are taken into account when generating the molecular mass spectrum, removing the need to select a charge state. The use of the whole mass spectrum may reduce the risk of operator error and compensate for differences in charge distribution between analytical runs and instruments[107].

6.3 Risks for accurate quantitation

There are challenges inherent in each quantitation method that pose risks for the accurate, consistent quantitation of therapeutic oligonucleotides and their impurities. Three factors will be considered in detail here: the differences in observed levels of ions associated with impurities between chromatographic methods as a result of different dominant charge states; the consistency of the charge distribution within and between chromatographic methods and instruments; and the level of ion suppression observed when analysing a known content of full-length n (FLN) and n-1 oligonucleotides.

6.3.1 Differences between charge states

As observed in Section 5.3, the level of the ions associated with the loss of guanine either synthetically or by in-source fragmentation are different depending on the chromatographic method employed, particularly when high in-source CID voltages are used. The main difference in the mass spectra of replicates analysed using the two chromatographic methods investigated is that with the Southampton chromatographic method (SCM), the -3 charge state is dominant; with the AZ chromatographic method (ACM) -4 is the dominant charge state (as discussed in Section 4.1). When using the method of quantitation described in 6.1, therefore, the -3 charge state ions are used for replicates analysed using the SCM and -4 charge state ions for the replicates analysed using the ACM. The different relative levels of the ions in question are shown in Figure 6.5 for the ACM and Figure 6.6 for the SCM, both using an in-source CID voltage of 100 V.

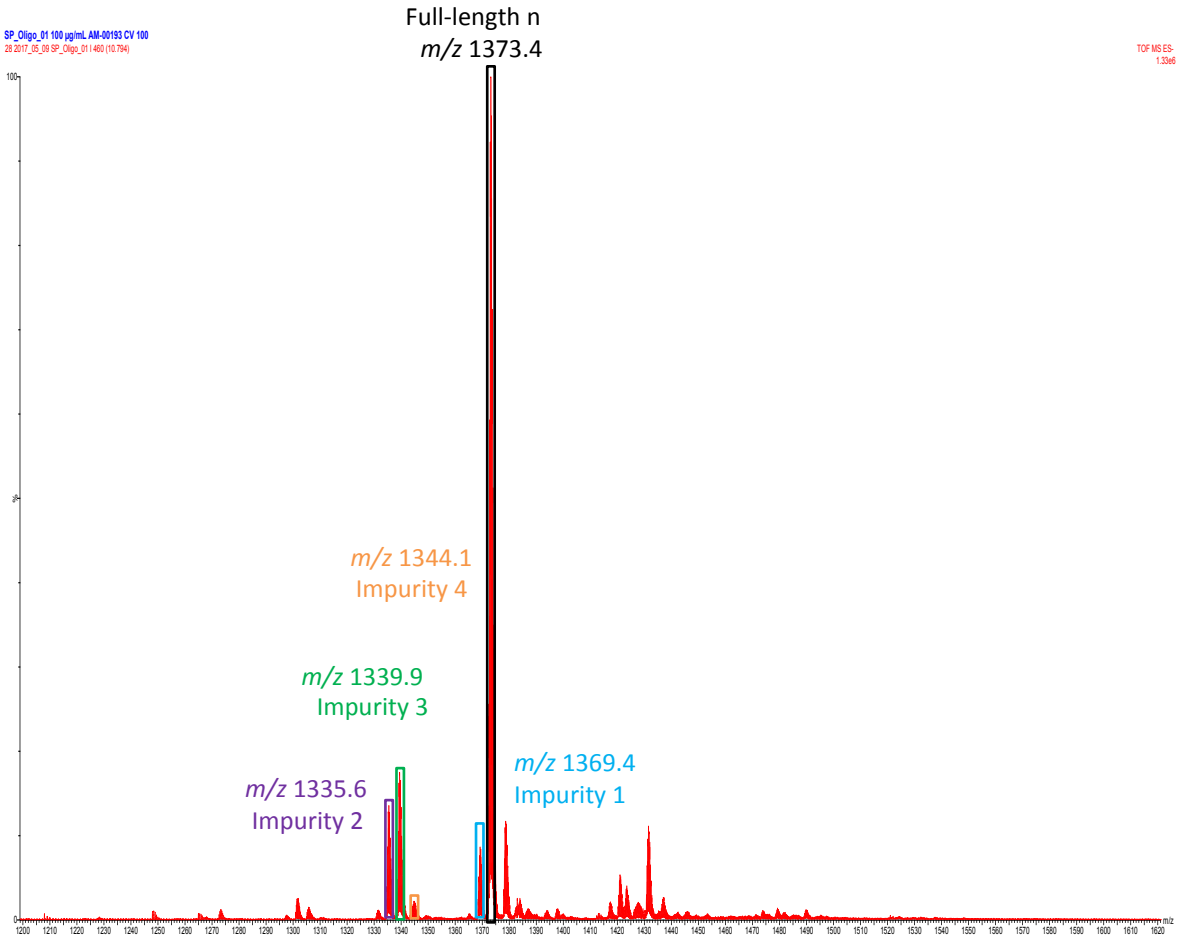

Figure 6.5 - Negative ion ESI mass spectrum of SP_Oligo_01 analysed using the Waters Synapt and the ACM showing *m/z* 1200 - 1620

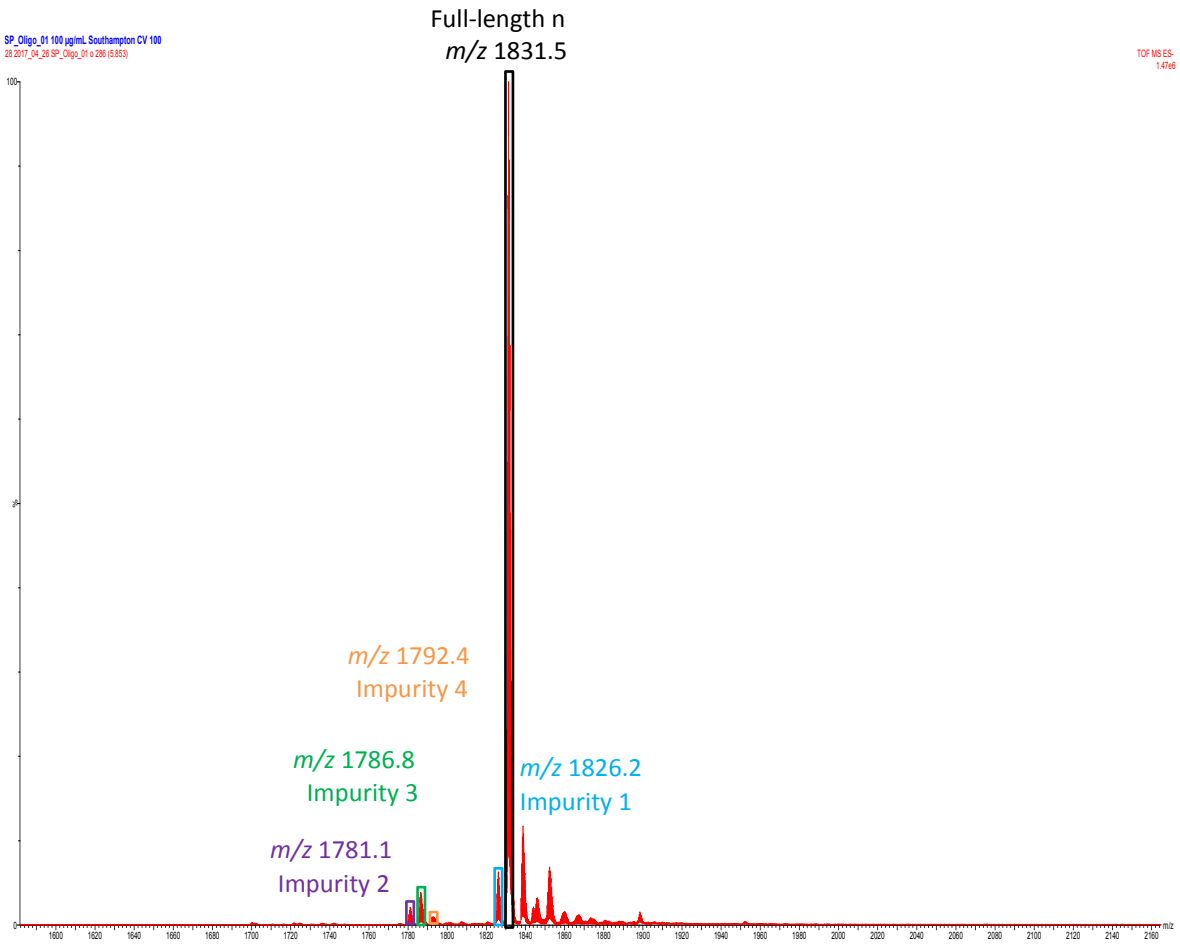

Figure 6.6 - Negative ion ESI mass spectrum of SP_Oligo_01 analysed using the Waters Synapt and the SCM showing *m/z* 1580 - 2160

In order to investigate the differences in levels of impurities/in-source fragmentation, three replicates each of samples SP_Oligo_01 and SP_Oligo_02 analysed using the SCM and ACM at in-source CID voltages of 20 V and 100 V using the Waters Synapt were processed using the ions for the -3 and -4 charge states and also by deconvoluting the mass spectra and recording the intensity of the neutral molecules calculated. Figure 6.7 and Figure 6.8 show the calculated levels of the ions that correspond with impurities 1 to 4 in SP_Oligo_01 analysed using the SCM (blue columns) and the ACM (red columns) when using the -3 and -4 charge states and the intensity of the neutral molecule for each replicate.

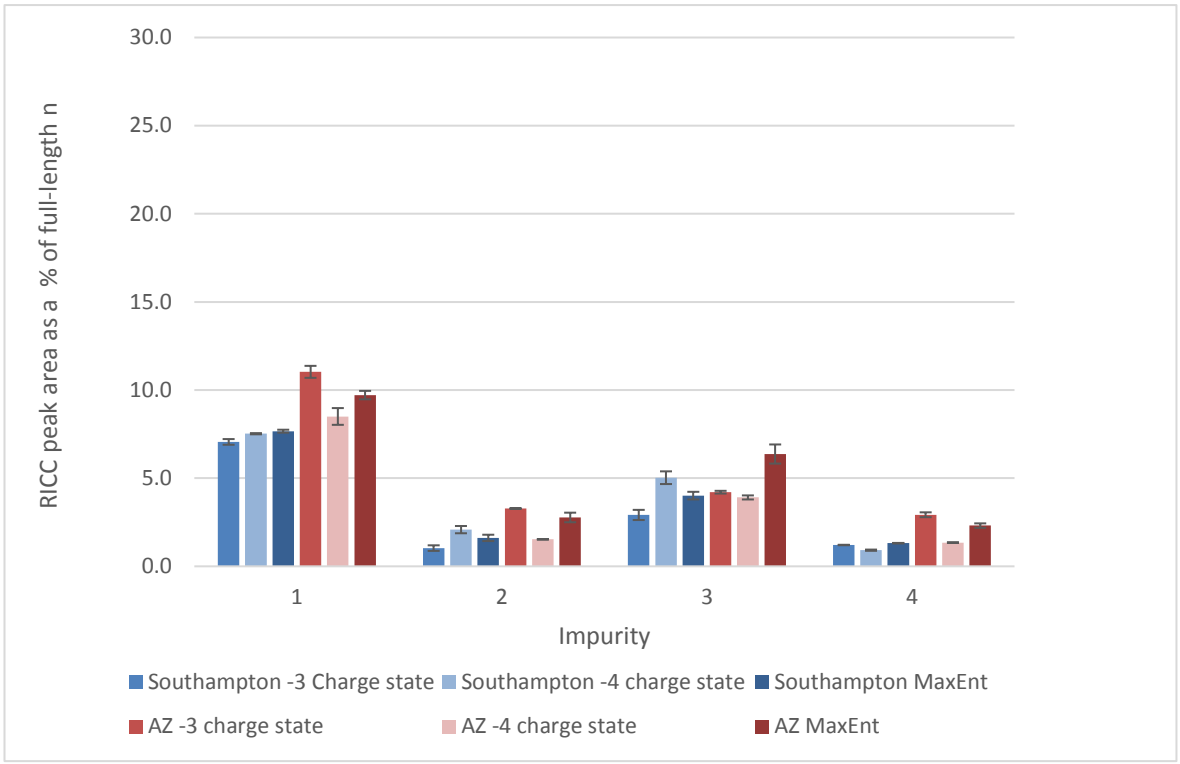

Figure 6.7 - Observed levels of ions associated with impurities as a percentage of FLN peak area by method of quantitation for SP_Oligo_01 analysed using the Waters Synapt at 20 V in-source CID voltage. n = 3

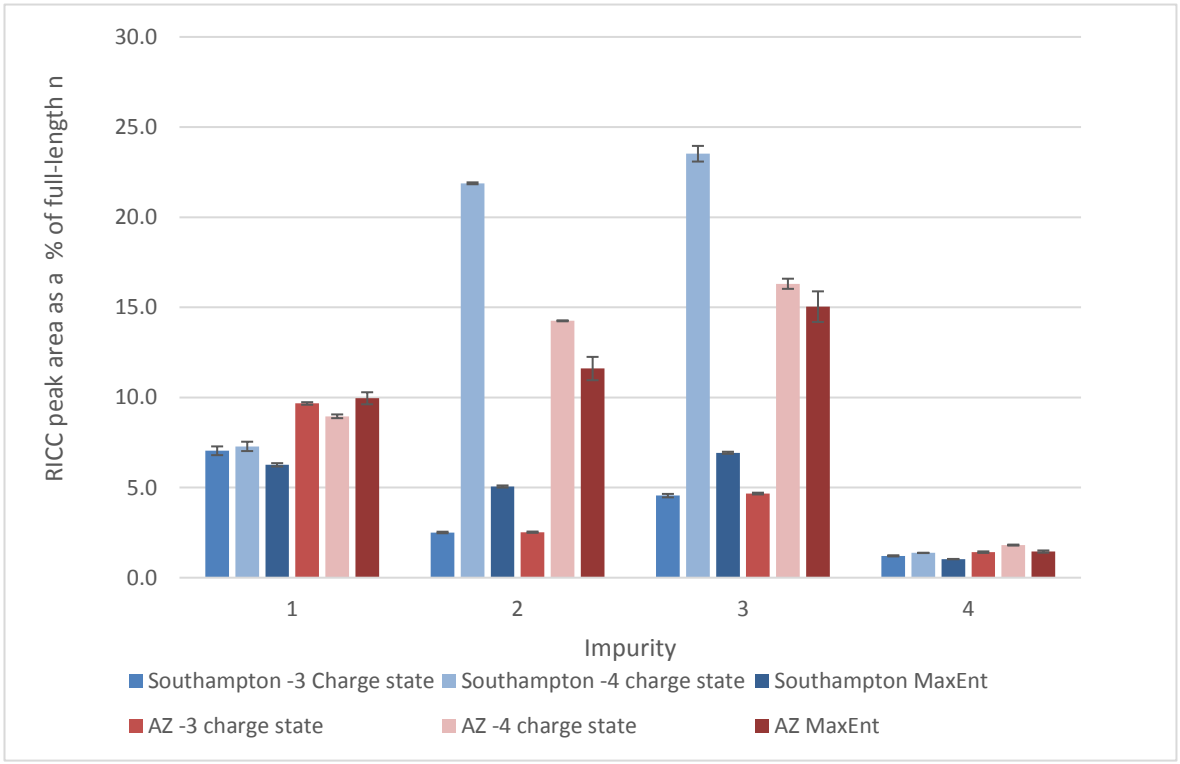

Figure 6.8 - Observed levels of ions associated with impurities as a percentage of FLN peak area by method of quantitation for SP_Oligo_01 analysed using the Waters Synapt at 100 V in-source CID voltage. n = 3

Figure 6.7 shows that, at 20 V in-source CID voltage using the SCM, there is little difference between the calculated percentages of the ions associated with impurities whether they are calculated using the -3 charge state, the -4 charge state or MaxEnt deconvoluted data. For the ACM at 20 V in-source CID voltage, use of the -3 charge state or MaxEnt data leads to slightly higher calculated percentages than if the -4 charge state is used. In the case of the MaxEnt data, the distribution of ions into higher charge states when the ACM is used may have an impact on the calculated percentages when compared to the -4 charge state.

When 100 V in-source CID voltage is used, Figure 6.8 shows that the calculated levels of the ions associated with impurities 1 and 4 are similar within the chromatographic methods whether they are determined using one of the charge states or the deconvoluted data, although there are differences between the chromatographic methods. There are, however, significant differences when considering impurities 2 and 3.

As discussed in Chapter 5, the ions associated with impurities 1 and 4 are not generated in the ion source, so the phenomenon observed here relating to impurities 2 and 3 must be related to in-source fragmentation. Figure 6.9 shows the RICC peak of the ion corresponding to impurity 2 relative to the FLN RICC peak for the -3 charge state (left) and -4 charge state (right) of SP_Oligo_01 analysed using the Waters Synapt with an in-source CID voltage of 100 V and using the SCM. The RICC peak of the -4 charge state of the ion associated with impurity 2 is around 10 % of the abundance of the FLN peak, whereas the -3 charge state peak is less than 5 % of the abundance of its corresponding FLN peak.

Regardless of the dominant charge state in the mass spectrum, when working with the -4 charge state, the calculated percentage of ions associated with impurities 2 and 3 is much higher than when using the -3 charge state. When MaxEnt deconvoluted data are compared, the calculated percentages tend to agree with those calculated using the dominant charge state for the method (-3 for the SCM and -4 for the ACM), which would be expected as the MaxEnt algorithm will attempt to match the ion distribution it is presented with.

Previously published research by Jockusch *et al.*[109] and Nyakas *et al.*[97] has indicated that differences occur in the fragmentation of oligonucleotides depending

on the charge state of the ion. In 2018, Ickert *et al.*[110] found that higher charge state ions requires a lower energy to fragment. The results of these studies are supported by, and go some way to explain, the results presented in this chapter. When the -4 charge state is considered, realtively more fragmentationis observed than for the -3 charge state.

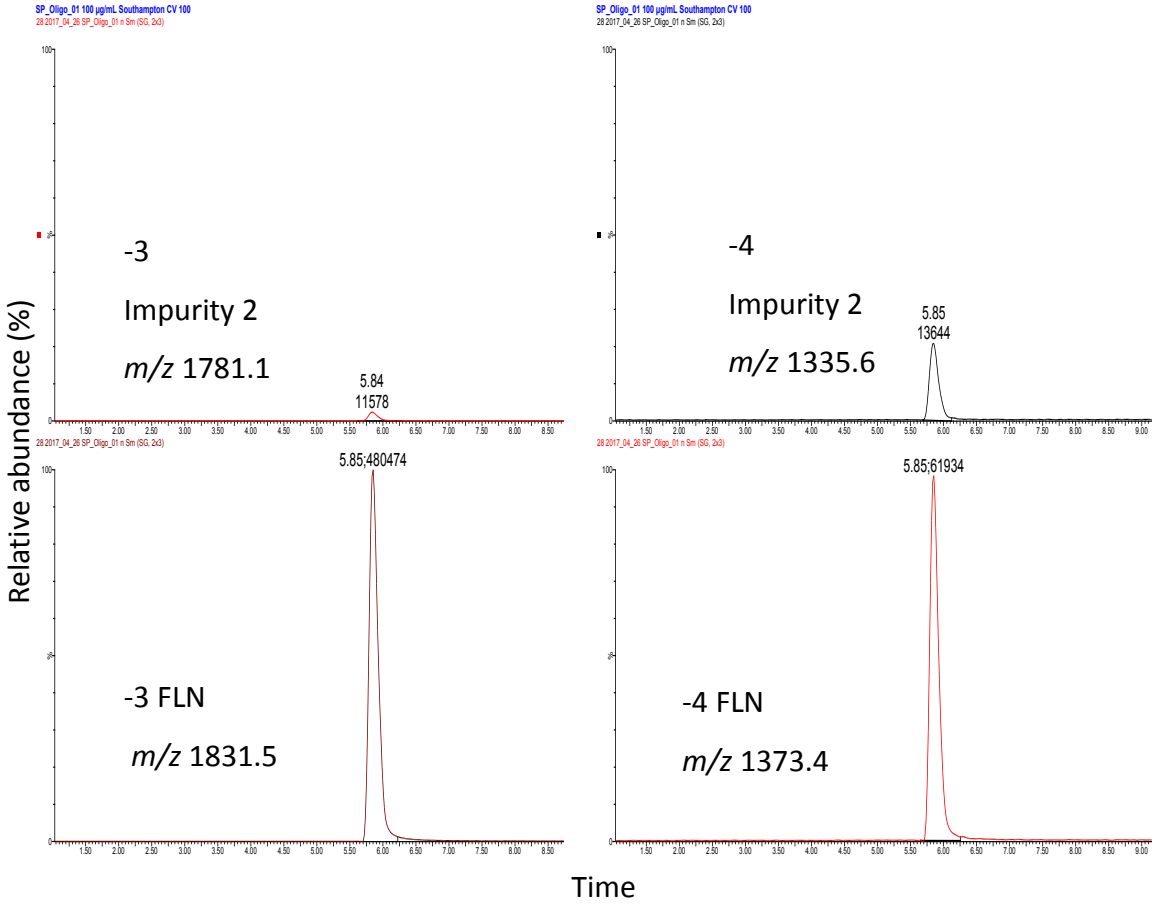

Figure 6.9 - SP_Oligo_01 RICC for the FLN and impurity 2 for the -3 and -4 charge states normalised to the FLN peak areas. Sample analysed using the SCM at an in-source CID voltage of 100 V

The use of a high in-source CID voltage is usually recommended to improve the transmission of large bio-molecule ions and reduce the levels of adducts detected in the mass spectrum[95, 100]. The data presented here indicate that if high in-source CID voltages are employed, increased in-source fragmentation of the oligonucleotide is observed and the accuracy of quantitation of impurity levels could, therefore, be compromised by the use of a single charge state. Use of a low in-source CID voltage when analysing therapeutic oligonucleotides and their impurities using a Waters instrument is essential and consistent mobile phase reagent use across laboratories is highly desirable to ensure uniformity.

6.3.2 Ion suppression

The levels of ion suppression occurring in the negative ionisation ESI of oligonucleotides and their impurities need to be understood to allow an assessment of the validity of using single ion monitoring/recording (SIM/SIR) as a method of quantitating oligonucleotide impurities. As discussed in Section 6.2, the use of SIM analysis increases the sensitivity of the target ions but assumes that the FLN oligonucleotide and its impurities have the same ionisation efficiency and that none of the compounds suppress ionisation of others in the sample.

To investigate the ion suppression occurring during the ionisation of oligonucleotides, a 13-mer sample (SP_Oligo_04) was mixed with a 12-mer sample (SP_Oligo_05) which has the same sequence minus one guanine and its associated sugar and phosphodiester. SP_Oligo_05 was added to SP_Oligo_04 at concentrations of 10%, 1%, 0.2% and 0.1%. The mixtures were then analysed using the SCM and ACM and the Waters Synapt and RICCs generated for the most abundant ion of the most abundant charge state of the FLN oligonucleotide for both samples. The RICC peak areas were compared to assess the difference between the percentage of SP_Oligo_05 observed to the percentage added.

Figure 6.10 and Figure 6.11 show the observed percentages of SP_Oligo_05 by the percentage added based on a mean of three replicates for the SCM and ACM, respectively. Figure 6.12 shows an example of a mass spectrum for the mixture of n (SP_Oligo_04) and n-1 (SP_Oligo_05) at the 1% addition of n-1 level.

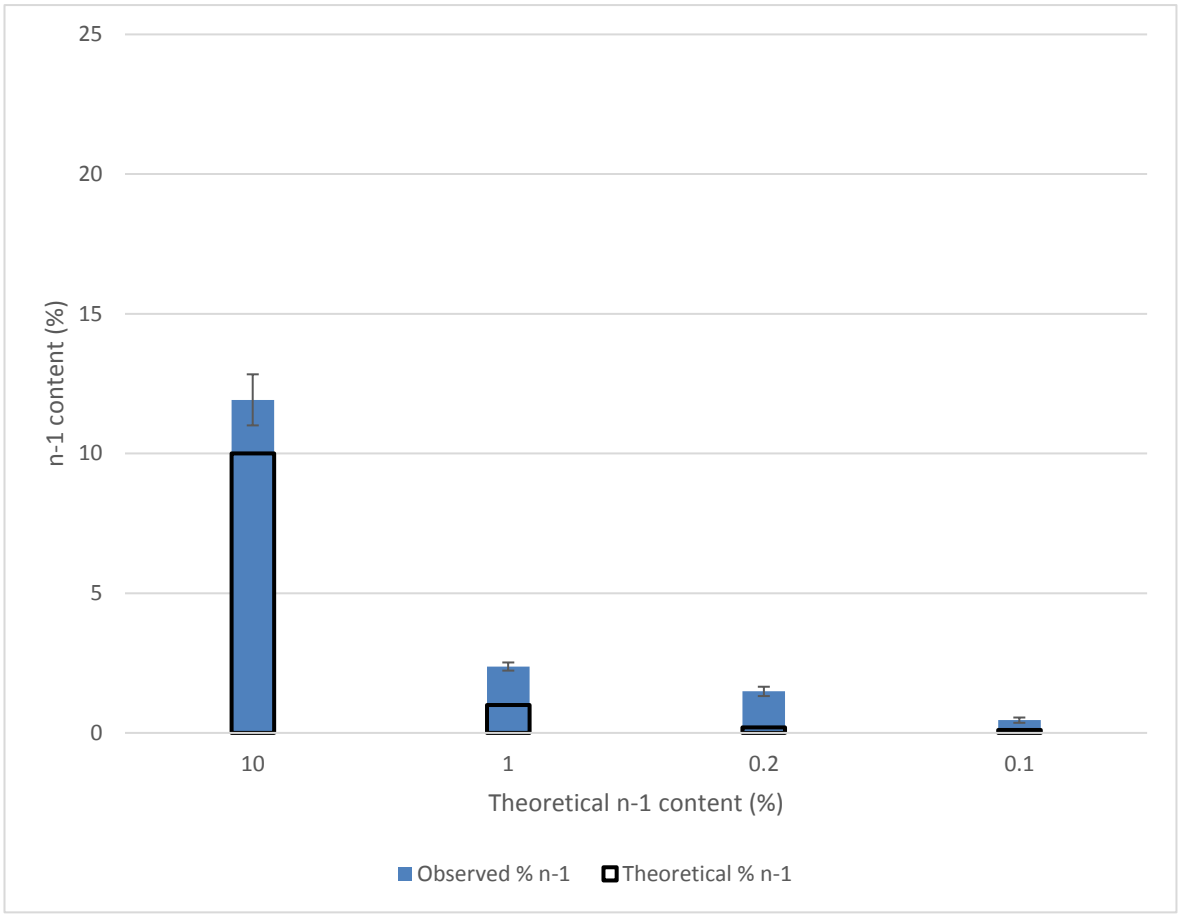

Figure 6.10 - Theoretical and observed levels of SP_Oligo_05 (n-1) as a percentage of SP_Oligo_04 analysed using the Waters Synapt and the SCM

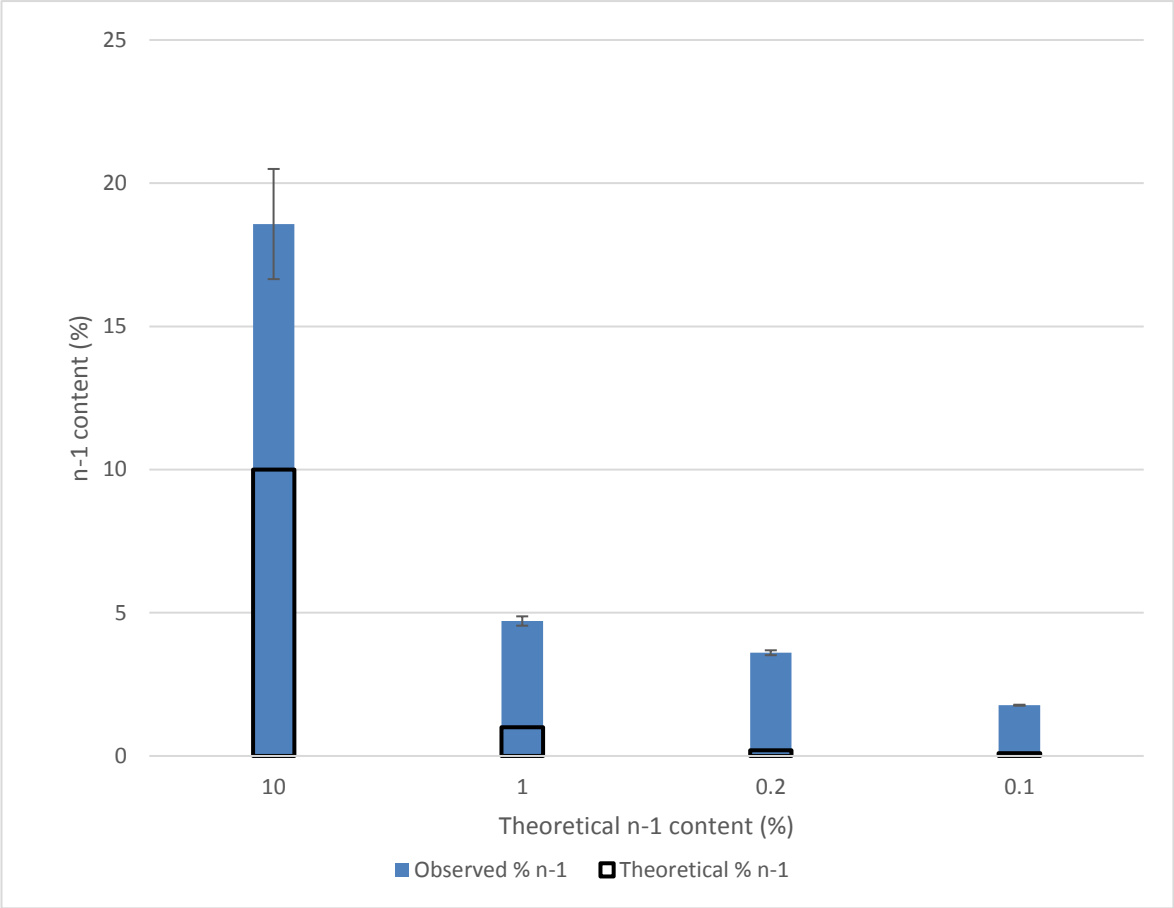

Figure 6.11 - Theoretical and observed levels of SP_Oligo_05 (n-1) as a percentage of SP_Oligo_04 analysed using the Waters Synapt and the ACM

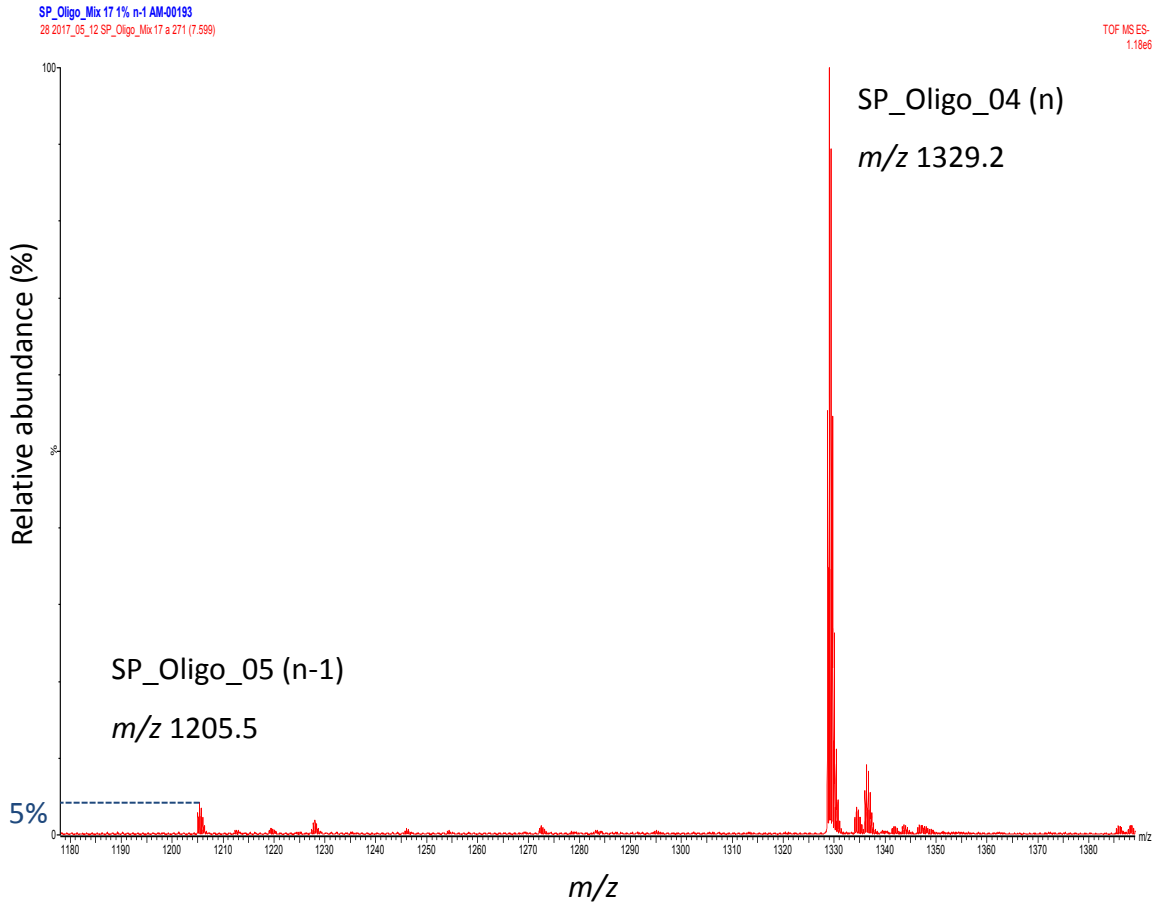

Figure 6.12 - Negative ion ESI mass spectrum of SP_Oligo_05 and SP_Oligo_04 analysed using the ACM and the Waters Synapt showing *m/z* 1180 - 1380. Added content of SP_Oligo_05 = 1%

At all added percentages of SP_Oligo_05, the RICC peak area of the ion associated with the FLN of SP_Oligo_05 is recorded as greater than would be expected given the amount added. For both the SCM and the ACM, the difference between the expected level of SP_Oligo_05 and the observed level is greater at the lower concentrations of the n-1 sequence. Table 6.1 shows the observed level of SP_Oligo_05 in the analysed replicates, indicating that any ion suppression or enhancement is more pronounced when using the ACM than the SCM.

Table 6.1 - Observed levels of SP_Oligo_05 (n-1) as a percentage of SP_Oligo_04 by chromatographic method. n = 3

Level of SP_Oligo_05 added (%)	Level of SP_Oligo_05 observed (%)	
	SCM	ACM
10	12 ± 0.9	19 ± 1.9
1	2 ± 0.1	5 ± 0.2
0.2	1 ± 0.2	4 ± 0.1
0.1	0.5 ± 0.1	2 ± 0.02

The higher than expected observed percentages of SP_Oligo_05 suggest that either the n-1 sequence is suppressing the FLN ion of SP_Oligo_04 or that SP_Oligo_04 is enhancing the FLN ion of SP_Oligo_05. Figure 6.13 and Figure 6.14 show the RICC peak areas of the FLN ion of SP_Oligo_04 at each level of n-1 addition for the SCM and ACM, respectively.

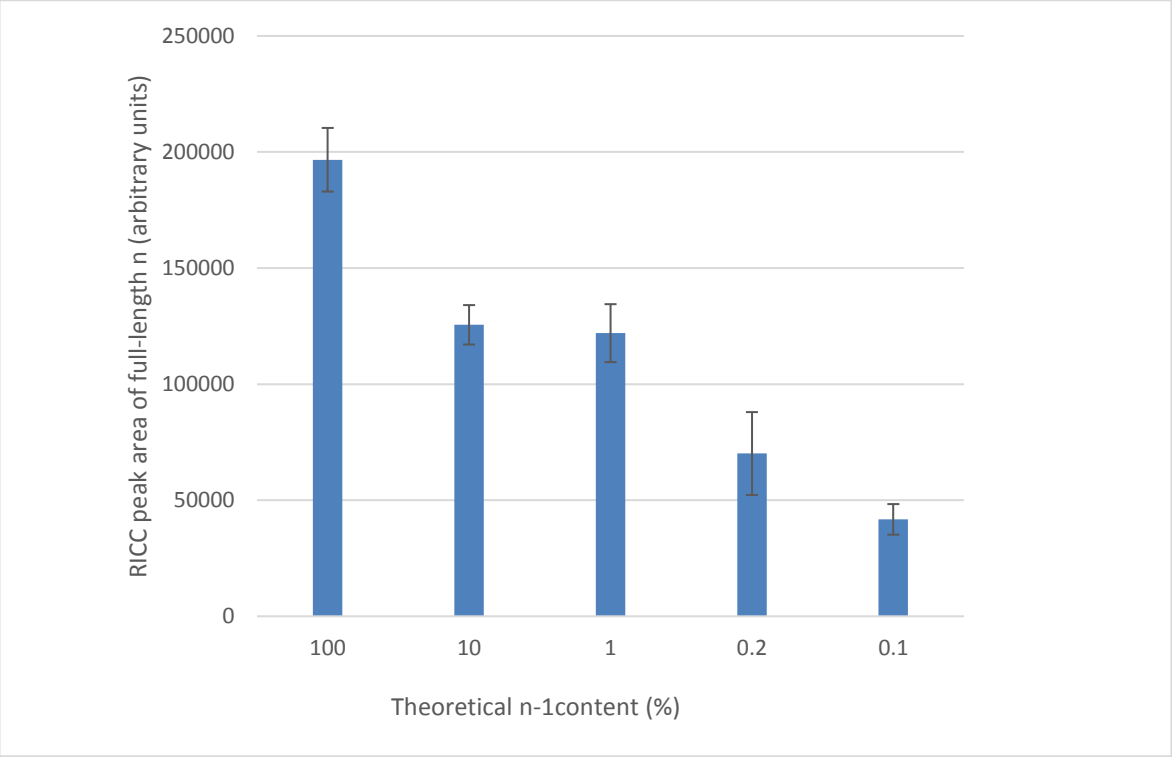

Figure 6.13 - RICC peak areas for FLN ion of SP_Oligo_04 by percentage of SP_Oligo_05 added for samples analysed using the Waters Synapt and the SCM. n = 3

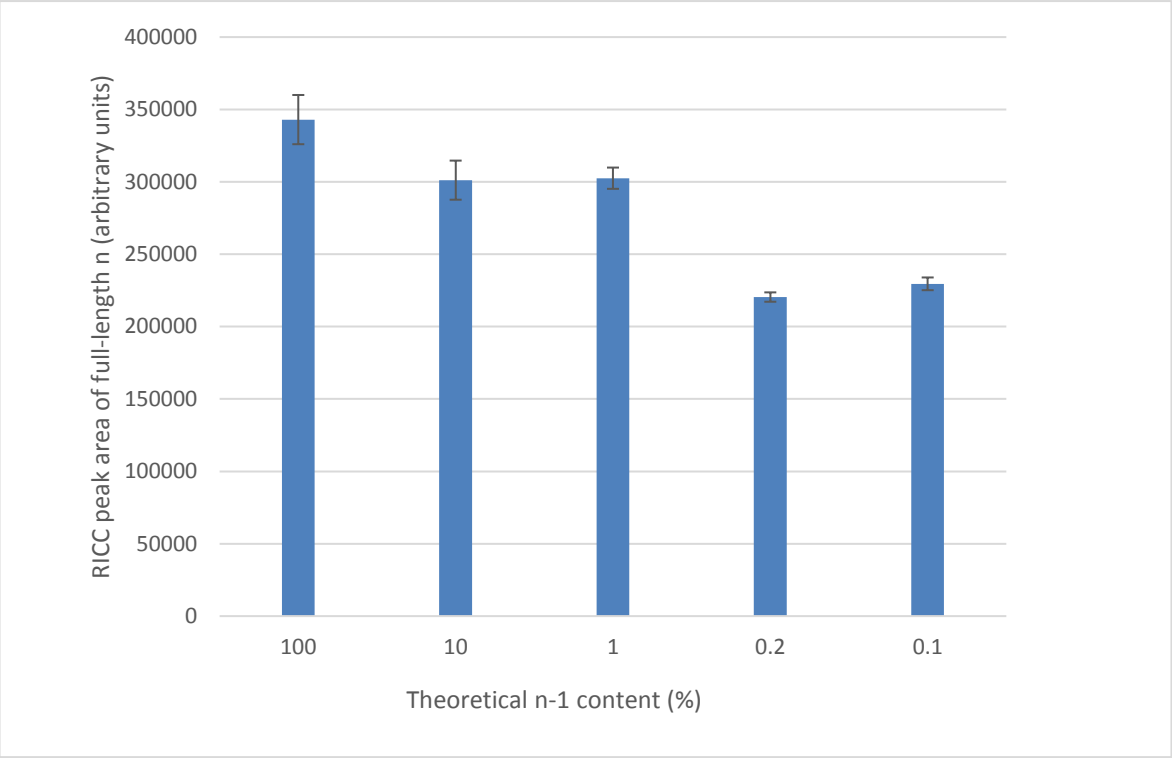

Figure 6.14- RICC peak areas for FLN ion of SP_Oligo_04 by percentage of SP_Oligo_05 added for samples analysed using the Waters Synapt and the ACM. n = 3

The decrease in RICC peak area observed between no SP_Oligo_05 added and the various percentages of SP_Oligo_05 indicates that the presence of the n-1 sequence causes some ion suppression of the target oligonucleotide. The RICC peak area, as demonstrated in Figure 6.13 and Figure 6.14, decreases as the level of SP_Oligo_05 added decreases, suggesting that ion suppression is enhanced by lower levels of the n-1 impurity. This phenomenon is observed in both the SCM and the ACM; these replicates were analysed separately, 10 days apart, which implies that this effect is related to the presence of the n-1 sequence rather than the chromatographic method or an instrument error. To further investigate, the samples containing the n-1 sequence were analysed using the Bruker MicrOTOF and the SCM. Figure 6.15 shows that the same pattern occurs when the Bruker MicrOTOF is used for analysis, confirming that the observation is not an instrument-specific occurrence.

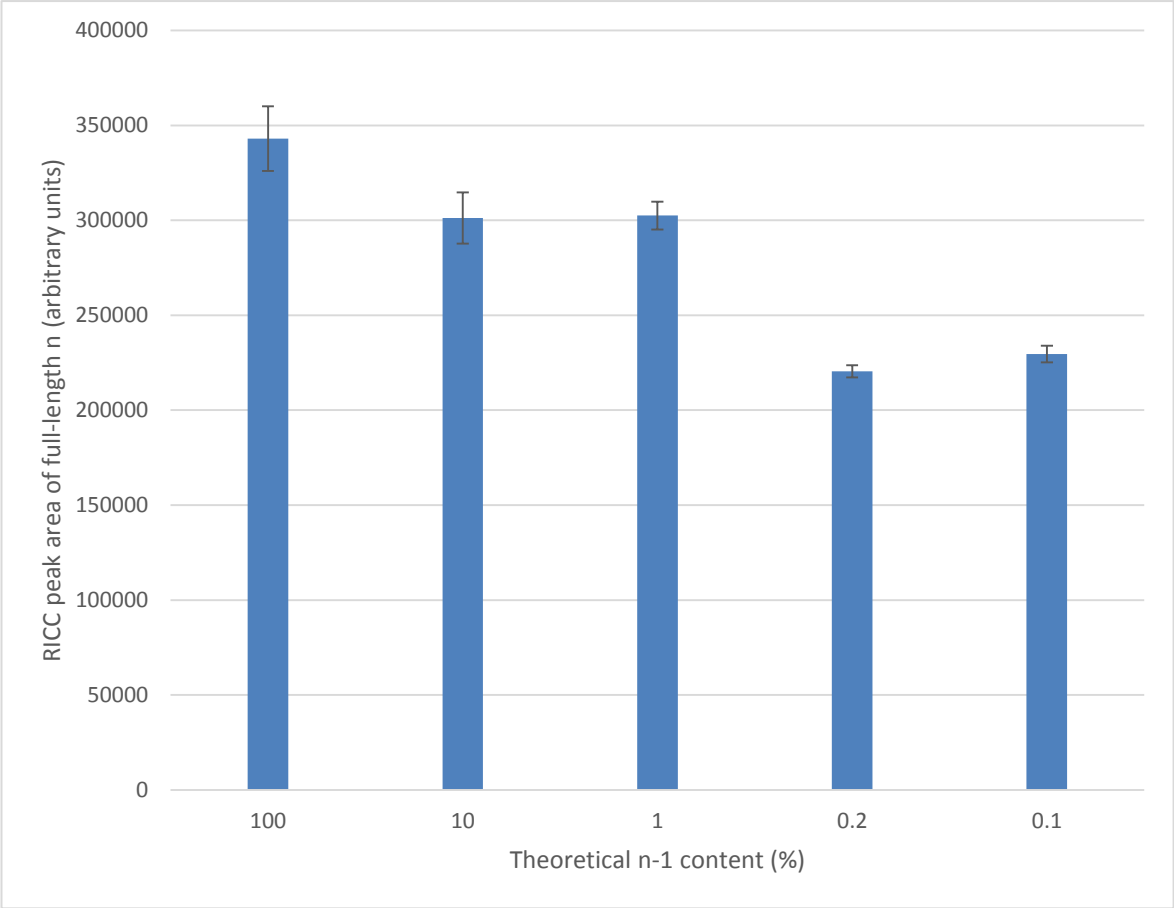

Figure 6.15 - RICC peak areas for FLN ion of SP_Oligo_04 by percentage of SP_Oligo_05 added for samples analysed using the Bruker MicrOTOF and the SCM. n = 3

To confirm that the additional SP_Oligo_04 ion recorded in the samples containing more SP_Oligo_05 is not coming from the latter sample, SP_Oligo_05 was analysed using the SCM and the ACM with the Waters Synapt and the SCM with the Bruker MicrOTOF. In all replicates, an RICC of the ion corresponding to the SP_Oligo_04 FLN gave an area of around 0.5 % of the RICC peak are of the ion corresponding with the SP_Oligo_05 FLN, suggesting their contribution to the peak areas observed in Figure 6.13,Figure 6.14 Figure 6.15 is minimal. Figure 6.16 shows an example of the relative abundance of the ions corresponding to the FLN of SP_Oligo_04 and SP_Oligo_05 in a replicate of SP_Oligo_05 analysed using the Waters Synapt and the ACM.

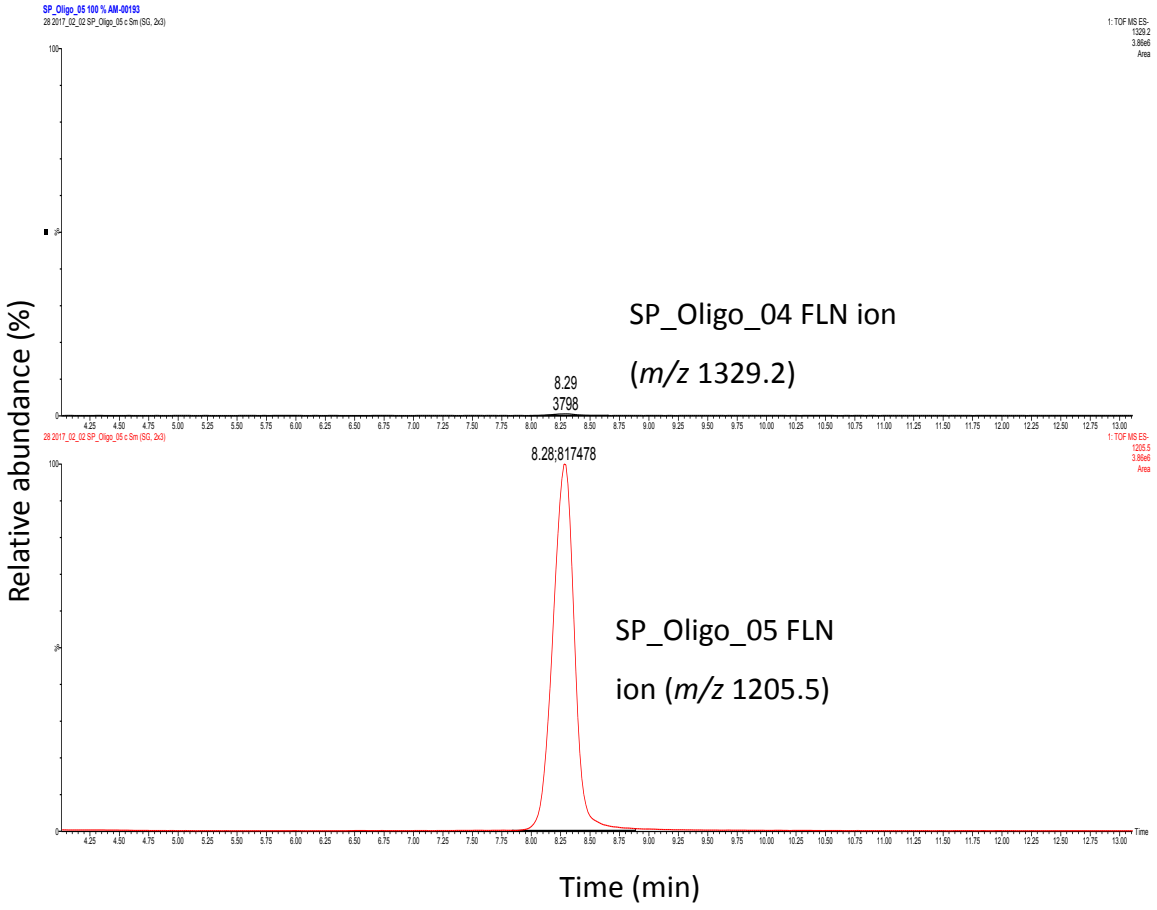

Figure 6.16 - RICC of an injection of SP_Oligo_05 analysed using the Waters Synapt and the ACM showing the relative abundance of the FLN ions

The data presented in this section suggest that impurities and the FLN of therapeutic oligonucleotides affect the ionisation of each other, meaning that the levels of ion suppression or enhancement occurring would need to be thoroughly investigated and understood before the use of SIM as a quantitation method could be recommended.

6.3.3 Charge state consistency

For methods of quantitation involving the use of a single charge state, it is important to understand the level of variation in the distribution of ions between charge states for a given chromatographic method and instrument. Using the RICC of the most abundant ion of the -3 and -4 charge state of the FLN peak, the peak areas of the two ions were compared to provide a ratio of -4/-3 for SP_Oligo_01 and SP_Oligo_02 analysed at a range of concentrations using: the

Waters Synapt with the SCM and ACM; the Bruker MicrOTOF with the SCM; and, for SP_Oligo_01 only, the Agilent 6130 with the ACM. Figure 6.17 and Figure 6.18 demonstrate the differences in charge distribution across the chromatographic methods and instruments used for SP_Oligo_01.

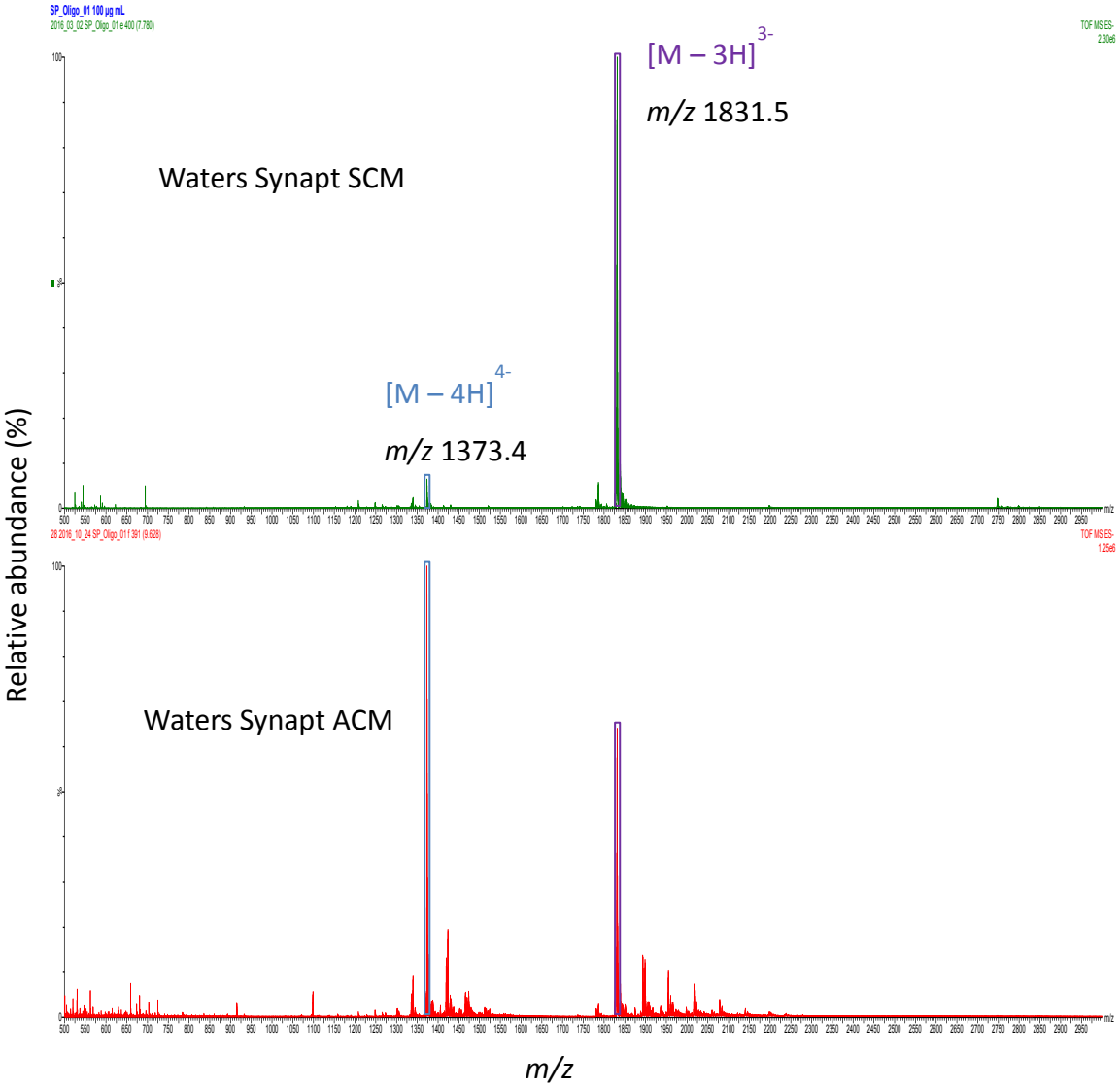

Figure 6.17 - Negative ion ESI mass spectra of SP_Oligo_01 analysed using the Waters Synapt showing the relative abundance of the -3 and -4 charge states for the SCM (top) and ACM (bottom)

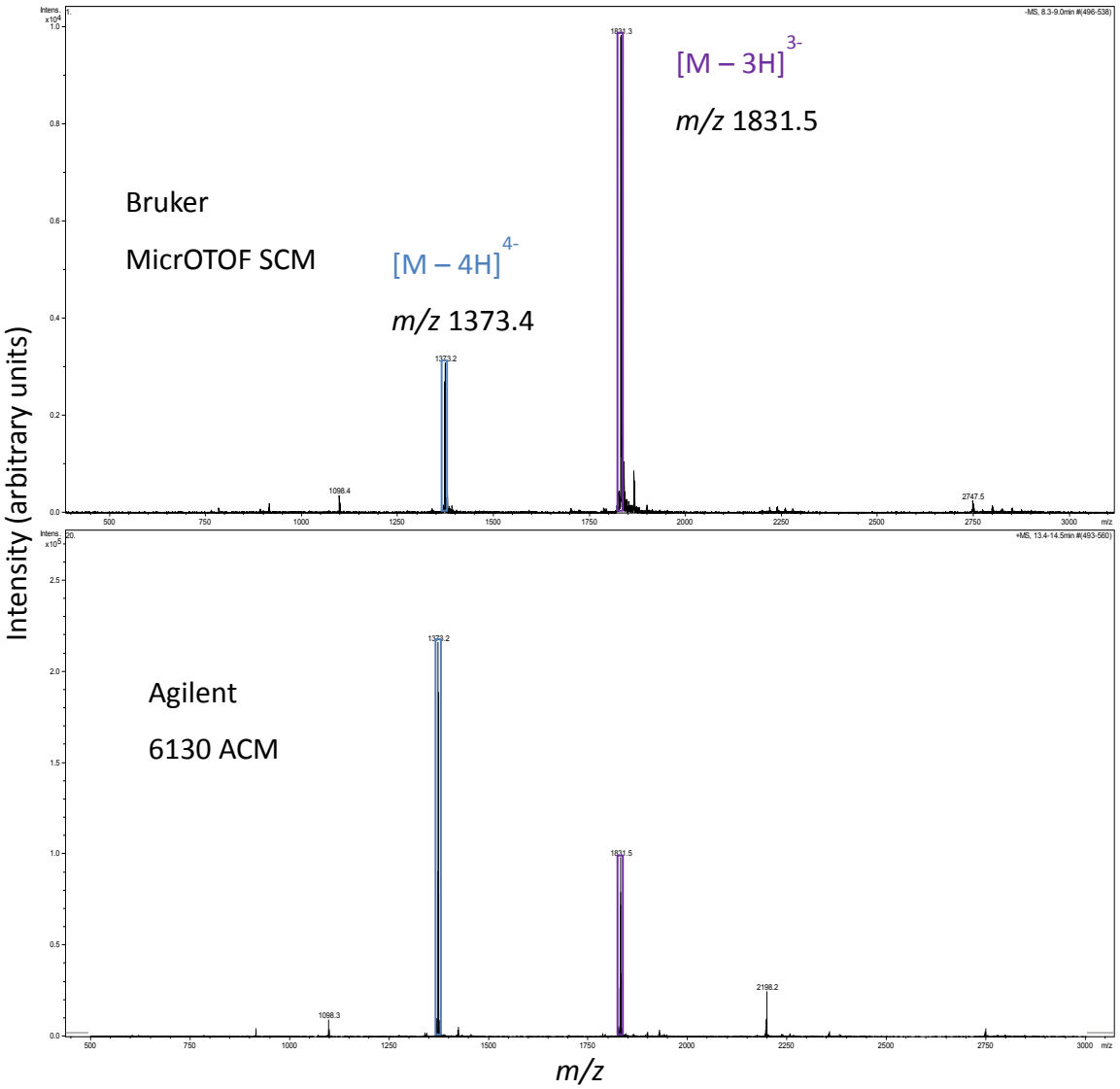

Figure 6.18 - Negative ion ESI mass spectra of SP_Oligo_01 analysed using the Bruker MicrOTOF (top) and Agilent 6130 (bottom) showing the relative abundance of the -3 and -4 charge states for the SCM and ACM, respectively

Figure 6.19 shows the charge state ratios calculated for each chromatographic method and instrument for SP_Oligo_01.

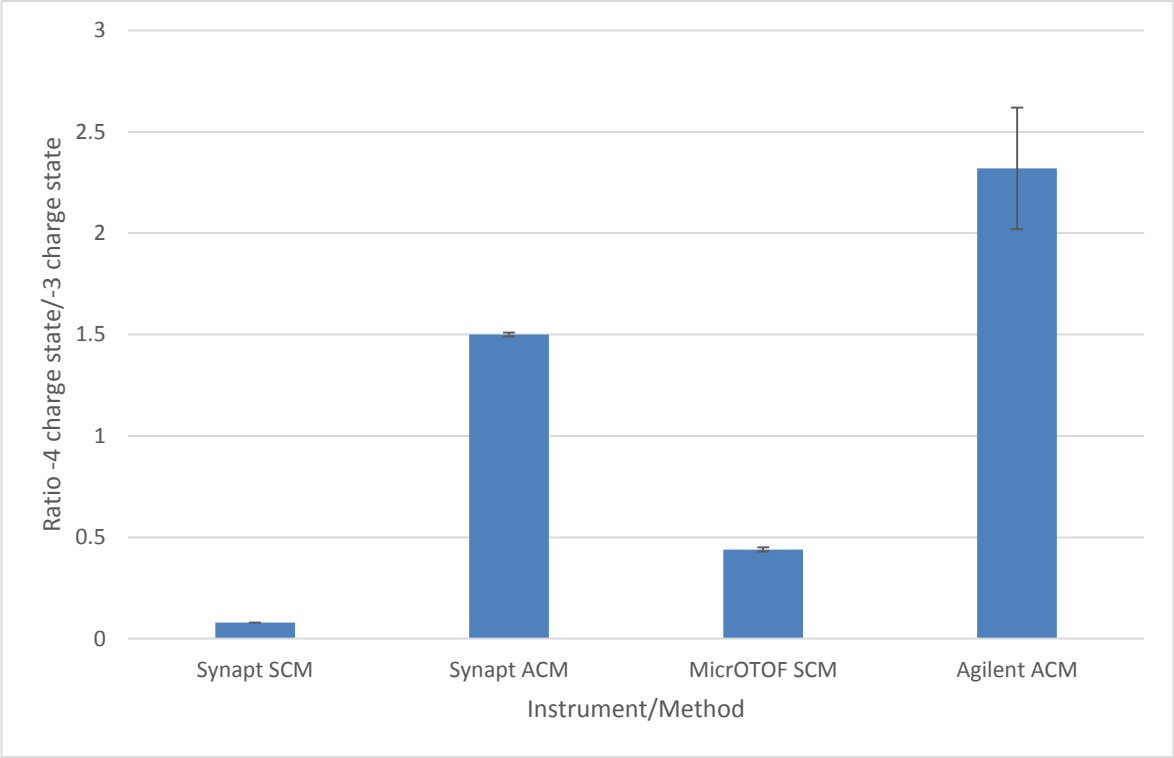

Figure 6.19 - Charge state ratios for SP_Oligo_01 by chromatographic method and instrument used (see Table 6.2 for numbers of replicates)

Table 6.2 shows the charge state ratios for SP_Oligo_01 and 02 when analysed using each method and instrument investigated, along with the concentrations of the oligonucleotides analysed.

Table 6.2 - Charge state ratios of SP_Oligo_01 and SP_Oligo_02 by instrument and chromatographic method

Instrument	**Chromatographic method**	**Concentrations analysed (µg/mL)**		**Ratio -4 charge state/ -3 charge state**	
		SP_Oligo_01	**SP_Oligo_02**	**SP_Oligo_01**	**SP_Oligo_02**
Waters Synapt	SCM (n = 23)	200, 100, 20, 10	200, 100, 20, 10	0.08 ± 0.003	0.15 ± 0.01
	ACM (n = 10)	200, 100	200, 100	1.5 ± 0.01	2.0 ± 0.01
Bruker MicrOTOF	SCM (n = 10)	200	200	0.44 ± 0.01	0.45 ± 0.01
Agilent 6130	ACM (n = 4)	100	-	2.3 ± 0.3	-

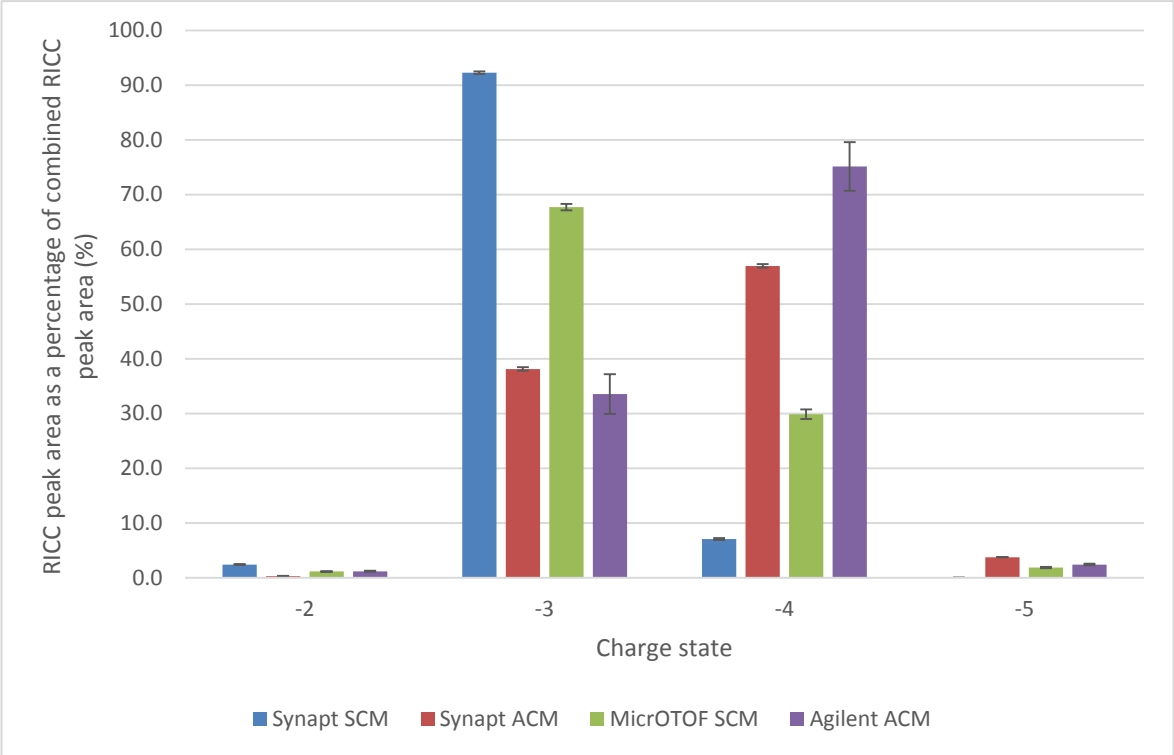

Figure 6.20 - Comparison of charge state intensities by chromatographic method and instrument for SP_Oligo_01

The RICC peak area of the most abundant FLN ion for charge states -2 to -5 was recorded and the percentage contribution of each charge state to a combined RICC of all four ions calculated. Figure 6.20 shows the calculated percentages for each chromatographic method and instrument combination investigated. Replicates analysed using the Waters Synapt and the SCM have the majority of ions recorded in a single state, with the -3 charge state contributing 92% to the total RICC peak area. When the Bruker MicrOTOF and the SCM or the Agilent 6130 and the ACM are used, the dominant charge state contributes more than twice the percentage of the combined RICC peak area as the next most dominant charge state. Ions in replicates analysed using the Waters Synapt and the ACM are more evenly distributed, with the -4 charge state only contributing around half as much again as the -3 charge state.

The data presented in Table 6.2 and Figure 6.19 and Figure 6.20 show that there are significant differences in the observed charge state ratios for each of the samples analysed depending on the chromatographic method and instrument used. As discussed in Section 4.1, the replicates analysed using the SCM have ratios below 1 as the -3 charge state is dominant. The replicates analysed using the ACM have ratios greater than 1 as the -4 charge state dominates with these

reagents. The replicates analysed using the Waters Synapt have lower ratios of -4/-3 than for those analysed using the Bruker MicrOTOF and the Agilent 6130 when comparing the same chromatographic methods. Use of the Waters Synapt appears to cause a greater abundance of ions to be detected in the 3 charge state than with the other two instruments. It is possible that the increased energy in the Waters source, causing the in-source fragmentation noted in Section 5.2, also encourages the formation of triply charged ions when compared to the Agilent and Bruker source designs.

The ratios of charge states are consistent within each method and instrument pairing. This means that using a selected charge state can lead to precise quantitation of therapeutic oligonucleotides and their impurities provided one chromatographic method and instrument type is used. If different methods or instruments are employed, there are risks for the consistency of the data as a result of the differences in charge distribution reported here.

6.4 Quantitation method comparison

The three methods of quantitation discussed here are: the AstraZeneca, single ion of the dominant charge state method; quantitation using a group of ions; and MaxEnt deconvolution of mass spectra.

The precision and accuracy of the quantitation generated using each method will be assessed by means of the linearity of a calibration curve and the calculation of the levels of the four selected impurities from Chapter 5: using Equation 5.1. Analysis of the linearity of the calibration curves will ensure that the methods of quantitation perform equally at high and low concentration and comparison of the calculated levels of impurities and the variation within methods will indicate whether the methods are robust and their relative accuracy.

6.4.1 Linearity

To compare the effectiveness of the different strategies for quantitation, linearity has been determined by generating a calibration curve of concentration *vs* peak area or ion intensity. The linear regression of each calibration curve is calculated and compared. The concentrations used to create the curves are 2, 10, 20, 100

and 200 µg/mL of SP_Oligo_01 and the same replicates, analysed using the Waters Synapt and the SCM have been used for each quantitation method.

Figure 6.21,Figure 6.22Figure 6.23 show the calibration curves for SP_Oligo_01 using the single ion of the dominant charge state, the group of ions and the MaxEnt deconvolution methods of quantitation, respectively.

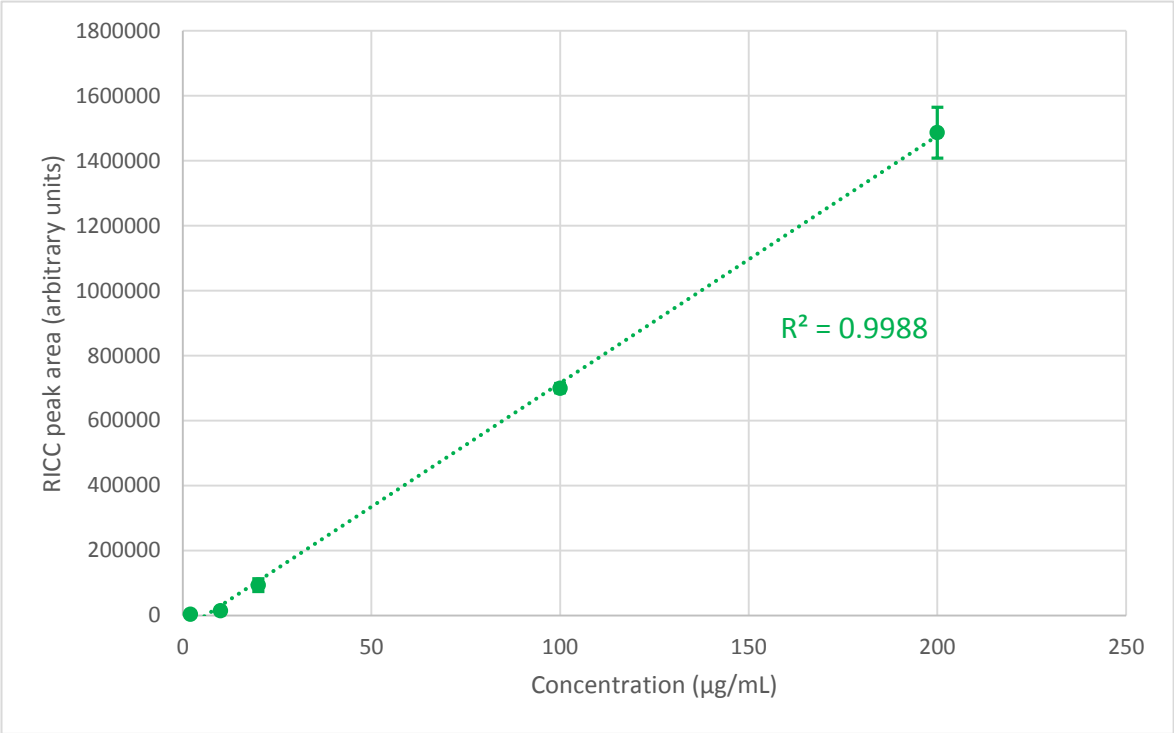

Figure 6.21 - Calibration curve for SP_Oligo_01 2 - 200 µg/mL analysed using the Waters Synapt and the SCM. Calculated using the single ion of the -3 charge state quantitation method

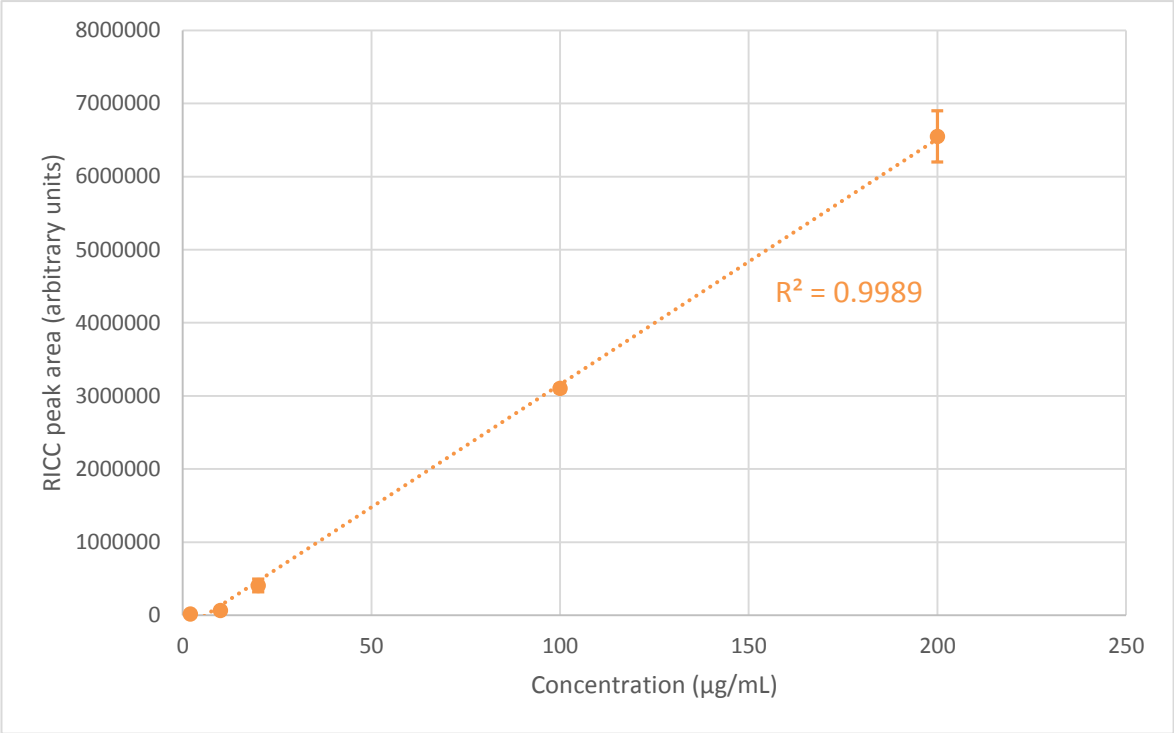

Figure 6.22 - Calibration curve for SP_Oligo_01 2 - 200 µg/mL analysed using the Waters Synapt and the SCM. Calculated using the group of ions quantitation method

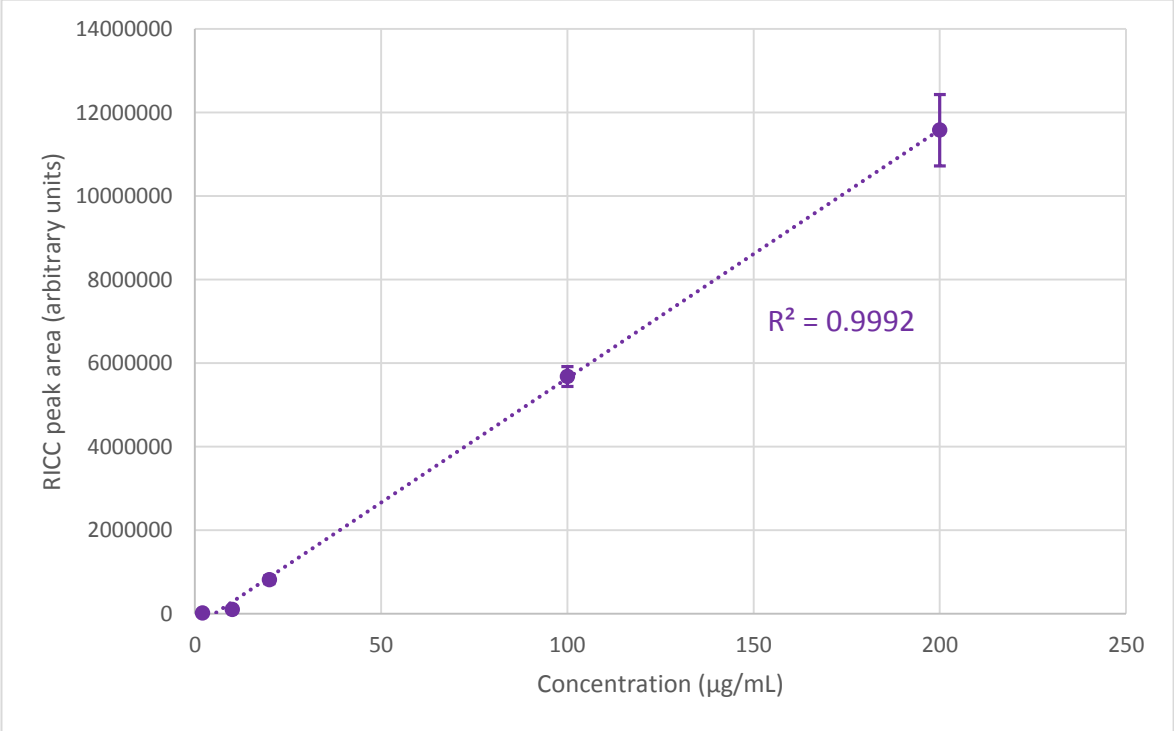

Figure 6.23 - Calibration curve for SP_Oligo_01 2 - 200 µg/mL analysed using the Waters Synapt and the SCM. Calculated using the MaxEnt deconvolution quantitation method

All of the calibration curves presented in Figure 6.21, Figure 6.22Figure 6.23 give a linear regression R^2 value of greater than 0.99, indicating that all three methods of quantitation provide linear data and behave in the same way at the upper and lower ends of the concentration range assessed. The curve created using MaxEnt deconvoluted data has the highest R^2 value at 0.992, suggesting that this method is the most consistent across the range of concentrations.

The data presented show that all three methods are suitable for the quantitation of therapeutic oligonucleotides and their impurities and suggest the deconvolution method to be the most robust and consistent.

6.4.2 Impurity calculations

Using Equation 5.1, the level of the ions associated with impurities 1 to 4 were calculated for three replicates each of SP_Oligo_01 and SP_Oligo_02. All replicates were analysed using the Waters Synapt and three replicates of each sample were analysed with the SCM and three with the ACM.

Figure 6.24Figure 6.25 show the calculated percentages of each impurity for SP_Oligo_01 and SP_Oligo_02, respectively. The blue bars represent replicates analysed using the SCM and red bars for replicates analysed with the ACM.

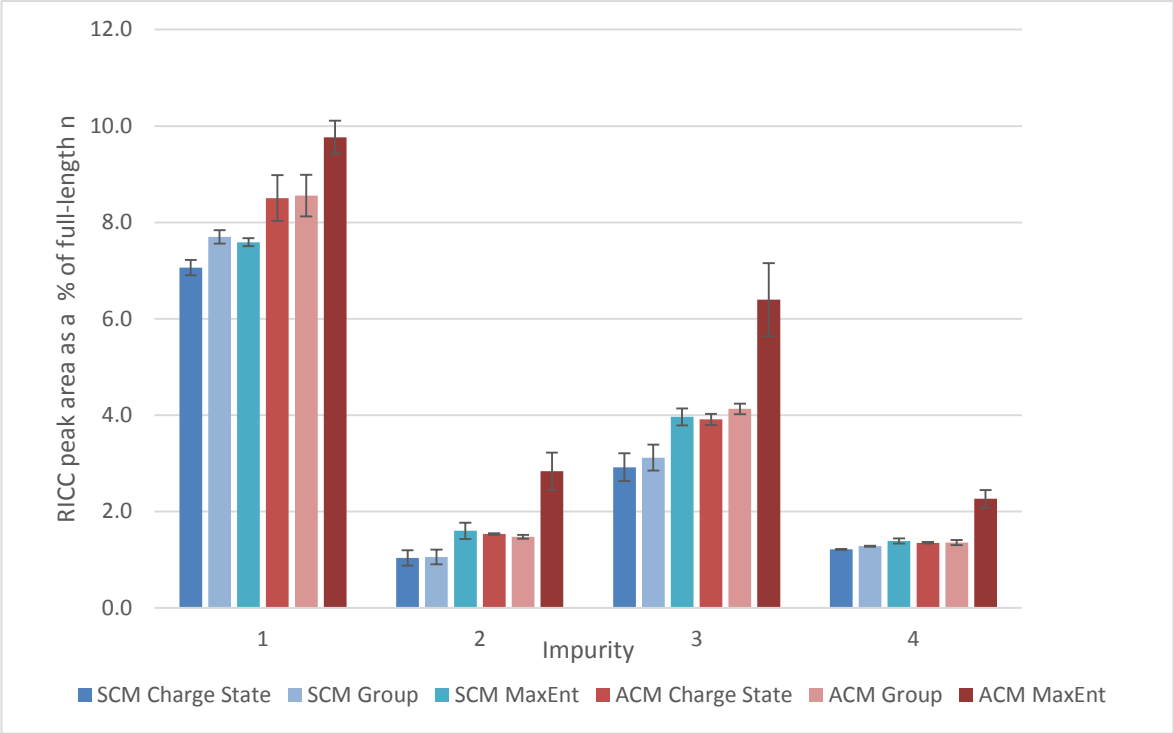

Figure 6.24 - Calculated percentages of ions associated with impurities 1-4 for SP_Oligo_01 analysed using the Waters Synapt by quantitation method

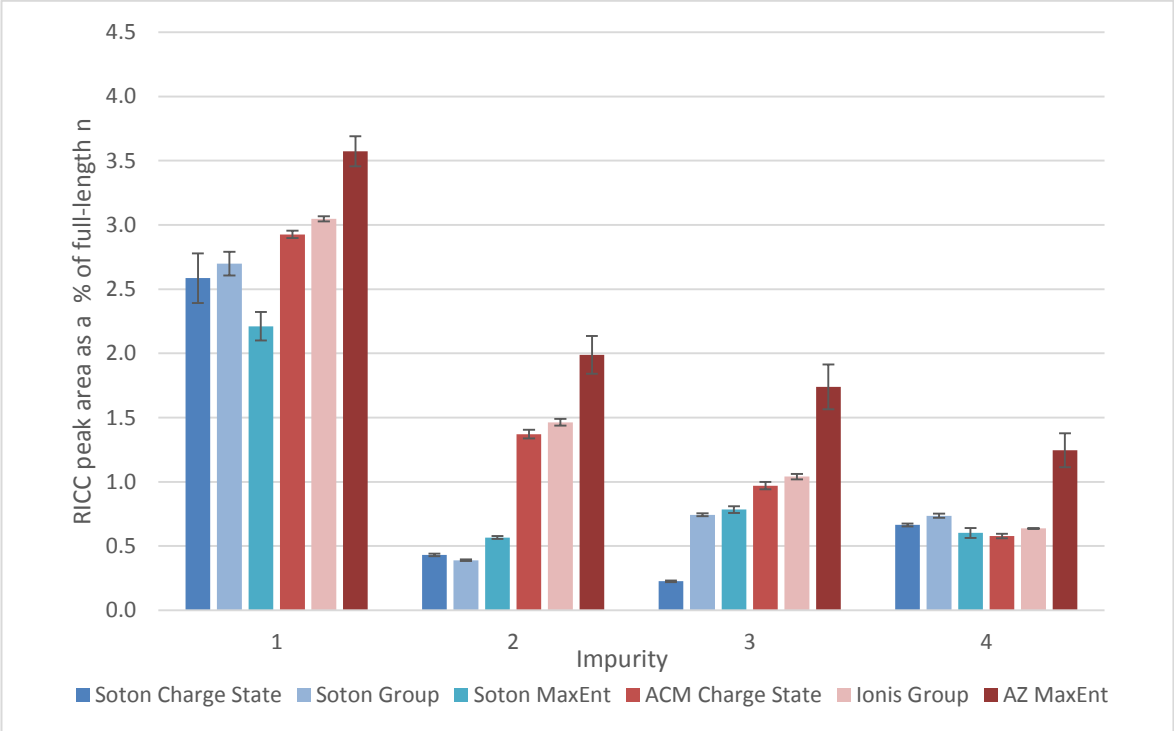

Figure 6.25 - Calculated percentages of ions associated with impurities 1-4 for SP_Oligo_02 analysed using the Waters Synapt by quantitation method

For replicates analysed using the SCM, Figure 6.24 shows that for SP_Oligo_01, all methods of quantitation result in similar calculated levels of impurities 1 to 4 as a percentage of FLN peak area. The ions associated with impurities 2 and 3, which involve the loss of guanine and can be artificially enhanced by in-source fragmentation, are calculated to be at slightly higher levels when the mass spectra are deconvoluted than when peak areas are used, ranging from means of 1 % to 1.6% and 2.9 % to 4 %, respectively. This increase is likely to be a result of the higher levels of in-source fragmentation noted in the -4 charge state (see Section 6.3.1) being taken into account when the mass spectra are deconvoluted; the differences between the charge states are small at the in-source CID voltage of 20 V used here, so the impact on the quantitation is similarly small.

Replicates of SP_Oligo_01 analysed using the ACM can be seen in Figure 6.24 to have consistent calculated levels of impurities 1 to 4 when the single ion of the dominant charge state or a group of ions of the dominant charge state are used. When the mass spectra are deconvoluted, the reported levels are higher for all impurities. These differences, along with the deconvoluted results for replicates analysed using the ACM being consistently higher than those quantitated in the same manner for replicates analysed with the SCM, lend further weight to the argument that results obtained from the two chromatographic methods cannot be readily compared.

Figure 6.25 shows that, for replicates of SP_Oligo_02 analysed using the SCM (blue bars) the ions associated with impurities 2 and 4 are calculated to be at a consistent percentage regardless of the method of quantitation used. The level of the ion associated with impurity 1 shows some variation but the difference in the mean percentages is 0.5%, so this may be attributable to inter-replicate variation in this small data set. In the case of the ion associated with impurity 3, the calculated percentage obtained using the single ion of the dominant charge state is lower than those obtained with the groups of ions and deconvoluted mass spectra. Analysis of more replicates of SP_Oligo_02 using the SCM may determine whether this is related to the sample size or if it is a wider trend.

When replicates of SP_Oligo_02 analysed using the ACM are considered, Figure 6.25 shows that the calculated level of the ions associated with all four impurities is consistent when the single ion of the dominant charge state and group of ions methods are employed. When the mass spectra are deconvoluted, the

percentages of the ions corresponding to the impurities are higher than for the other two methods. As for SP_Oligo_01, all methods of quantitation yield higher levels of impurity when the replicates are analysed using the ACM when compared to the SCM. It appears that, to be able to compare levels of impurities between batches and samples, it is essential that only one chromatographic method is utilised.

6.5 Quantitation conclusions

The current method of data analysis and quantitation of therapeutic oligonucleotides and their impurities employed by AstraZeneca is complex and time consuming. It also has the potential for operator error and subjectivity. The differences in calculated impurity levels between the charge states used also poses a risk to the consistency of data generated in different laboratories.

The data presented in this chapter on the differences between the calculated impurity levels when different charge states are used for quantitation, especially at high in-source CID voltages, support the assertion in Chapter 5 that a low in-source CID voltage should be used for analysis of oligonucleotide impurities to ensure accurate data reporting and avoid in-source fragmentation of the parent molecule.

The higher than expected levels of the n-1 sequence recorded mean that SIM analysis cannot be recommended without extensive further analysis to gain a deeper understanding of this phenomenon. The use of an internal standard may partially mitigate the effects of ion suppression but this would need to be fully validated. The use of SIM data recording also either reduces the flexibility of the analysis, preventing the observation and reporting of unexpected impurities, or increases the number of replicates that must be analysed if the sample is also scanned to look for unusual data.

The distribution of ions between charge states differs between chromatographic methods and instruments used for analysis. The distribution within each method/instrument combination is, however, consistent meaning that results reported with a chosen method will be precise.

The linearity shown by each method of quantitation investigated is good, with an R^2 value of greater than 0.99. When the SCM is used, levels of impurities calculated are consistent across the methods, with a slight enhancement when the mass spectra are deconvoluted. The use of deconvoluted data with the ACM shows an enhancement in calculated levels of impurities. The slight increase noted in replicates analysed using the SCM may be attributed to the inclusion of all charge states and, therefore, may be a more accurate representation of the impurity or in-source fragmentation levels in the sample.

Further validation is required to ensure a thorough understanding of how an internal standard could be used in the analytical method. The use of an internal standard and deconvoluted mass spectra is likely to produce the most robust, precise and accurate quantitation of therapeutic oligonucleotides and their impurities. Use of an internal standard will help to reduce inter-replicate variation and allow for an extra system suitability check, while quantitation based on deconvoluted mass spectra uses all charge states, reducing the complexity of the data and removing some analyst subjectivity. It is recommended that, regardless of quantitation method used, only data generated using the same chromatographic method be compared for inter-batch and sample variation as all strategies show differences between the SCM and the ACM.

Chapter 7: Concluding remarks and further work

7.1 Concluding remarks

As demand for therapeutic oligonucleotide drugs to treat a wider range of conditions increases, the requirement for a robust method for the quantitation of the impurities within a drug product becomes more pressing. The development of a method that can be employed across all laboratories, regardless of the specific LC-MS instrumentation used, is highly desirable to ensure consistency of testing and to confirm inter-batch variation.

The research presented in this thesis demonstrates that there are fundamental differences in the mass spectra of therapeutic oligonucleotide samples when they are analysed using different mobile phase reagents, types of mass analyser and ionisation source design. These differences must be understood and the most appropriate combination of variables selected for an effective method to be developed.

The requirement for quantitation of impurities at low levels means that the mass spectrometer used must be sufficiently sensitive that impurities can be detected without overloading the system. To be able to accurately and precisely quantitate low levels of impurity and to be prepared for any future decrease in reporting limit required, older “legacy” instruments, such as the single quadrupole Waters ZQ, are not appropriate for this analysis. Ideally a highly sensitive instrument, such as the Waters Synapt G2Si Q-TOF, would be used but with proper validation of limits of detection and quantitation newer quadrupole systems such as the Agilent 6130 may be suitable.

An understanding of the effects of mobile phase reagents and mass analyser type on the charge state distribution of ions is essential. Differences in distribution between chromatographic methods and instruments lead to inconsistency in the quantitation of therapeutic oligonucleotides and their impurities, and the data presented in this thesis highlight the need for a unified approach.

When a Q-TOF or TOF mass analyser is used, the ions are distributed between fewer charge states than when a quadrupole is employed; this provides improved sensitivity for these charge states which will enhance confidence in quantitation

based on these ions. The mass spectra are also less complex when Q-TOF and TOF mass analysers are used, which makes data analysis more straight-forward and helps to improve precision.

Use of HFIP and TEAA as mobile phase additives results in the -3 charge state being most dominant in the mass spectrum with relatively low levels of ions being observed in other charge states. When TBuAA and EDTA are the reagents added, the -4 charge state ions dominate, but relatively more ions are distributed into other charge states than for HFIP and TEAA. As for the mass analyser type, the distribution of ions into fewer charge states and a greater number of ions found in one charge state is desirable to enhance sensitivity of that ion.

To produce a charge state distribution that will lead to the least complexity of the mass spectrum and the greatest sensitivity for one charge state, it is recommended that the mobile phase reagents employed are TEAA and HFIP and a TOF or Q-TOF mass analyser is used.

When considering the quantitation of abasic impurities, the level of in-source CID creates complexity; synthetic impurities and in-source fragmentation base-loss are isobaric and cannot, therefore, be separated, making the minimisation of in-source fragmentation essential. The ion source design, in-source CID voltage and oligonucleotide sequence all affect the level of in-source fragmentation observed. Agilent and Bruker ion sources cause relatively low levels of depurination, when compared to the Waters source design. Waters instruments are suitable for use in the quantitation of therapeutic oligonucleotides and their impurities as long as the in-source CID voltage is kept to 20 V or lower; this low voltage causes a reduction in sensitivity of the FLN ion but the reduction is small compared to the enhanced accuracy of abasic impurity quantitation.

The position and grouping of guanine nucleobases with the oligonucleotide sequence affects the amount of guanine loss observed in-source. When guanines are located towards the centre of the sequence and grouped together they are more likely to be lost in the source than if they are at the ends of the sequence or situated separately. This effect means that, for a generic method to be developed, the balance of sensitivity and fragmentation should be validated using a worst-case scenario sequence to avoid setting the in-source CID voltage too high.

Ion suppression and the addition of extra analyses mean that the use of SIM data collection for the quantitation of therapeutic oligonucleotides and their impurities is not recommended. The use of a single ion of the dominant charge state, a group of ions or the MaxEnt deconvoluted mass spectrum all yield linear regressions of greater than 0.99 for the concentration range 2 µg/mL to 200 µg/mL. The use of deconvoluted data allows all ions in the mass spectrum to be taken into consideration, reducing analyst interpretation and the influence of small differences in charge distribution.

The development of a method using an internal standard oligonucleotide sequence of known concentration, eluting away from the target oligonucleotide will allow greater flexibility of reporting, with the potential for concentration rather than percentage to be calculated. It may also improve the robustness of the analytical method by creating an extra system suitability check.

When all of these factors are taken into account, the use of a Q-TOF or TOF mass analyser, a low in-source CID voltage if Waters instruments are utilised, a chromatographic method employing TEAA and HFIP and quantitation of the data using MaxEnt deconvoluted mass spectra and an internal standard would create a basis to develop a robust, consistent method.

7.2 Future work

To further improve understanding of the factors influencing the quantitation of therapeutic oligonucleotides and their impurities, several areas of investigation are recommended.

The use of an internal standard requires validation to select a sequence that will not be or produce impurities that are isobaric with impurities of target oligonucleotides. The behaviour of the chosen sequence must be understood to ensure that it can be reliably quantitated; its ionisation efficiency across the chromatographic gradient and level of in-source fragmentation are two aspects to be investigated.

The differences observed in the levels of in-source fragmentation depending on the position of guanine in the oligonucleotide sequence could be probed by the use of ion mobility mass spectrometry. Different sequences may have different

collisional cross-sections, resulting in different drift times. A greater understanding of the respective shapes of the ions will aid the creation of a hypothesis around the effect of guanine position on in-source fragmentation. Differences between the drift times of charge states may also help to explain why more in-source fragmentation is observed in the -4 charge state than the -3 charge state. The use of an orthogonal technique, such as capillary gel electrophoresis, may assist with understanding how much depurination is a true impurity coming from the synthesis of the oligonucleotide and how much occurs in the mass spectrometer.

If MaxEnt deconvoluted mass spectra are to be used for the quantitation of therapeutic oligonucleotides and their impurities, the parameters used must be optimised and the process validated to ensure consistency and robustness.

Appendix A Conferences and seminars attended

British Mass Spectrometry Society (BMSS) 36th Annual Meeting, Birmingham, UK, 15-17 September 2015

The ABCs of BioPharma: Accelerating Biologics Characterisation Seminar Day, Agilent & Crawford Scientific, London, UK, 06 October 2015

What Can Ion Mobility Do For Me? Seminar Day, Royal Society of Chemistry (RSC), London, UK, 26 November 2015

Oligonucleotide LC/MS training seminar, AstraZeneca, Macclesfield, UK, 27 – 30 June 2016

37th Annual BMSS Meeting, Eastbourne, UK, 14 September 2016. Poster presentation – Systematic cross-platform MS & chromatographic evaluation for the analysis of therapeutic oligonucleotides

Chemistry and Industry Evening – Pharmaceuticals, RSC, Southampton, UK, 10 November 2016

AstraZeneca Global MS Users Meeting, Macclesfield, UK, 21-22 Nov 2016

London Biological MS Discussion Group 10th Anniversary Meeting, London, UK, 15 December 2016

Aspects of Quality Throughout the Development of Oligonucleotides, AstraZeneca, Macclesfield, UK, 14 March 2017. Poster presentation - The effect of mobile phase additives, ion source design and mass analyser on the quantitation of therapeutic oligonucleotides using RP-HPLC and ESI MS

AstraZeneca PhD Review Event & Careers Event, Macclesfield, UK, 21-22 March 2017. Poster presentation - The effect of mobile phase additives, ion source design and mass analyser on the quantitation of therapeutic oligonucleotides using RP-HPLC and ESI MS

Emerging Separation Technologies 2017, RSC, London, UK, 30 March 2017

The Role of MS in Impurity Profiling, Joint Pharmaceutical Analysis Group, London, UK, 11 May 2017

List of References

1. Ponzoni, E.; Morello, L.; Giani, S.; Breviario, D., Traceback identification of plant components in commercial compound feed through an oligonucleotide microarray based on tubulin intron polymorphism. *Food Chem.* **2014,** *162*, 72-80.

2. Watts, J. K.; Corey, D. R., Silencing disease genes in the laboratory and the clinic. *The Journal of Pathology* **2012,** *226* (2), 365-379.

3. Capaldi, D.; Ackley, K.; Brooks, D.; Carmody, J.; Draper, K.; Kambhampati, R.; Kretschmer, M.; Levin, D.; McArdle, J.; Noll, B.; Raghavachari, R.; Roymoulik, I.; Sharma, B. P.; Thuermer, R.; Wincott, F., Quality Aspects of Oligonucleotide Drug Development: Specifications for Active Pharmaceutical Ingredients. *Drug Inf. J.* **2012,** *46* (5), 611-626.

4. Goodchild, J., Therapeutic Oligonucleotides. In *Therapeutic Oligonucleotides: Methods and Protocols*, Goodchild, J., Ed. Humana Press Inc: Totowa, **2011**; Vol. 764, pp 1-15.

5. Donovan, M. J.; Meng, L.; Chen, T.; Zhang, Y. F.; Sefah, K.; Tan, W. H., Aptamer-Drug Conjugation for Targeted Timor Cell Therapy. In *Therapeutic Oligonucleotides: Methods and Protocols*, Goodchild, J., Ed. Humana Press Inc: Totowa, **2011**; Vol. 764, pp 141-152.

6. Kauffmann, A. D.; Campagna, R. J.; Bartels, C. B.; Childs-Disney, J. L., Improvement of RNA secondary structure prediction using RNase H cleavage and randomized oligonucleotides. *Nucleic Acids Res.* **2009,** *37* (18), e121-e121.

7. Sontheimer, E. J.; Carthew, R. W., Silence from within: Endogenous siRNAs and miRNAs. *Cell* **2005,** *122* (1), 9-12.

8. Beaucage, S. L.; Caruthers, M. H., Deoxynucleoside phosphoramidites—A new class of key intermediates for deoxypolynucleotide synthesis. *Tetrahedron Lett.* **1981,** *22* (20), 1859-1862.

9. Blackburn, G. M. G., Michael J.; Loakes, David; Williams, David M.; Editors, Chapter 4 Synthesis of Oligonucleotides. In *Nucleic Acids in Chemistry and Biology (3)*, The Royal Society of Chemistry: **2006**; pp 143-166.

10. Iyer, R. P.; Egan, W.; Regan, J. B.; Beaucage, S. L., 3H-1,2-Benzodithiole-3-one 1,1-dioxide as an improved sulfurizing reagent in the solid-phase synthesis of oligodeoxyribonucleoside phosphorothioates. *J. Am. Chem. Soc.* **1990,** *112* (3), 1253-1254.

11. Liu, C.-H.; Lu, D.-D.; Deng, X.-X.; Wang, Y.; Zhang, J.-Y.; Zhang, Y.-L.; Wang, S.-Q., The analysis of major impurities of lipophilic-conjugated phosphorothioate oligonucleotides by ion-pair reversed-phase HPLC combined with MALDI-TOF-MS. *Anal. Bioanal. Chem.* **2012,** *403* (5), 1333-1342.

12. Sinha, N. D.; Kuchimanchi, S. N.; Miranda, G.; Shaikh, S., Manufacture of therapeutic oligonucleotides: development of new reagents and processes. *Indian J. Chem., Sect. B: Org. Chem. Incl. Med. Chem.* **2006,** *45B* (10), 2297-2304.

13. Tamm, I.; Dörken, B.; Hartmann, G., Antisense therapy in oncology: new hope for an old idea? *The Lancet* **2001,** *358* (9280), 489-497.

14. Seth, P. P.; Vasquez, G.; Allerson, C. A.; Berdeja, A.; Gaus, H.; Kinberger, G. A.; Prakash, T. P.; Migawa, M. T.; Bhat, B.; Swayze, E. E., Synthesis and Biophysical Evaluation of 2',4'-Constrained 2'O-Methoxyethyl and 2',4'-Constrained 2'O-Ethyl Nucleic Acid Analogues. *The Journal of Organic Chemistry* **2010,** *75* (5), 1569-1581.

15. Srivatsa, G. S., Regulatory considerations for the development of oligonucleotide therapeutics. In *Handbook of Analysis of Oligonucleotides and Related Products*, Bonilla, J. V.; Srivatsa, G. S., Eds. CRC Press: **2011**; pp 465-486.

16. ICH, Q3A (R2): Impurities in new drug substances **2006**.

17. ICH, Q3B (R2): Impurities in new drug products. **2006**.

18. Lee, S.-L.; Brown, P.; Wang, J.; Dorsam, R. T., Nonclinical Safety Assessments and Clinical Pharmacokinetics for Oligonucleotide Therapeutics: A Regulatory Perspective. In *Advanced Delivery and Therapeutic Applications of RNAi*, John Wiley and Sons, Ltd: **2013**; pp 63-81.

19. Okafo, G.; Levin, D. S.; Elder, D., Oligonucleotide Biopolymers–Future Challenges for Chromatography. *Chromatography Today* **2011,** *4* (1), 4-8.

20. Rodriguez, A. A.; Cedillo, I.; Mowery, B. P.; Gaus, H. J.; Krishnamoorthy, S. S.; McPherson, A. K., Formation of the N-2-acetyl-2,6-diaminopurine oligonucleotide impurity caused by acetyl capping. *Bioorg. Med. Chem. Lett.* **2014,** *24* (15), 3243-3246.

21. Fountain, K. J.; Gilar, M.; Gebler, J. C., Analysis of native and chemically modified oligonucleotides by tandem ion-pair reversed-phase high-performance liquid chromatography/electrospray ionization mass spectrometry. *Rapid Commun. Mass Spectrom.* **2003,** *17* (7), 646-653.

22. Cramer, H.; Finn, K. J.; Herzberg, E., Purity analysis and impurities determination by reversed-phase high-performance liquid chromatography. In *Handbook of Analysis of Oligonucleotides and Related Products*, Bonilla, J. V.; Srivatsa, G. S., Eds. CRC Press: **2011**; pp 1-46.

23. Biba, M.; Welch, C. J.; Foley, J. P.; Mao, B.; Vazquez, E.; Arvary, R. A., Evaluation of core-shell particle columns for ion-pair reversed-phase liquid chromatography analysis of oligonucleotides. *J. Pharm. Biomed. Anal.* **2013,** *72*, 25-32.

24. Biba, M.; Welch, C. J.; Foley, J. P., Investigation of a new core-shell particle column for ion-pair reversed-phase liquid chromatography analysis of oligonucleotides. *J. Pharm. Biomed. Anal.* **2014,** *96*, 54-57.

25. Pourshahian, S.; McCarthy, S. M., Analysis of oligonucleotides by liquid chromatography and mass spectrometry. In *Handbook of Analysis of Oligonucleotides and Related Products*, Bonilla, J. V.; Srivatsa, G. S., Eds. CRC Press: **2011**; pp 137-166.

26. Srivatsa, G. S., Considerations for defining and establishing the quality of oligonucleotides. In *Aspects of Quality Throughout the Development of Oligonucleotides*, AstraZeneca, Macclesfield, UK, **2017**.

27. Fanali, S.; Haddad, P. R.; Poole, C. F.; Schoenmakers, P.; Lloyd, D.; Editors, *Liquid Chromatography: Fundamentals And Instrumentation*. Elsevier Inc.: **2013**; p 504 pp.

28. Kealey, D.; Haines, P. J., *Instant Notes: Analytical Chemistry*. BIOS Scientific Publishers Ltd: UK, **2002**; p 342

29. Lundanes, E.; Reubsaet, L.; Greibrokk, T.; Editors, *Chromatography: Basic Principles, Sample Preparations and Related Methods*. Wiley: **2013**; p 224 pp.

30. van Deemter, J. J.; Zuiderweg, F. J.; Klinkenberg, A., Longitudinal diffusion and resistance to mass transfer as causes of nonideality in chromatography. *Chem. Eng. Sci.* **1956,** *5* (6), 271-289.

31. Wyndham, K.; Walter, T.; Iraneta, P.; Alden, B.; Bouvier, E.; Hudalla, C.; Lawrence, N.; Walsh, D., Synthesis and applications of BEH particles in liquid chromatography. *LCGC Europe* **2012,** (Suppl.), 15-20.

32. Wyndham, K. D.; O'Gara, J. E.; Walter, T. H.; Glose, K. H.; Lawrence, N. L.; Alden, B. A.; Izzo, G. S.; Hudalla, C. J.; Iraneta, P. C., Characterization and evaluation of C18 HPLC stationary phases based on ethyl-bridged hybrid organic/inorganic particles. *Anal. Chem.* **2003,** *75* (24), 6781-6788.

33. Horvath, C.; Melander, W.; Molnar, I.; Molnar, P., Enhancement of retention by ion-pair formation in liquid chromatography with nonpolar stationary phases. *Anal. Chem.* **1977,** *49* (14), 2295-2305.

34. Scott, R. P. W.; Kucera, P., Some aspects of ion-exchange chromatography employing adsobed ion exchangers on reversed-phase columns. *J. Chromatogr. A* **1979,** *175* (1), 51-63.

35. Cai, B.; Li, J., Evaluation of trifluoroacetic acid as an ion-pair reagent in the separation of small ionizable molecules by reversed-phase liquid chromatography. *Anal. Chim. Acta* **1999,** *399* (3), 249-258.

36. Shibue, M.; Mant, C. T.; Hodges, R. S., Effect of anionic ion-pairing reagent hydrophobicity on selectivity of peptide separations by reversed-phase liquid chromatography. *J. Chromatogr. A* **2005,** *1080* (1), 68-75.

37. Biba, M.; Mao, B.; Welch, C. J.; Foley, J. P., Liquid Chromatography methods for the separation of short RNA oligonucleotides. *LCGC Europe* **2014,** *27* (12), 632-639.

38. Zimmermann, A.; Greco, R.; Walker, I.; Horak, J.; Cavazzini, A.; Laemmerhofer, M., Synthetic oligonucleotide separations by mixed-mode reversed-phase/weak anion-exchange liquid chromatography. *J. Chromatogr. A* **2014,** *1354*, 43-55.

39. Sharma, V. K.; Glick, J.; Vouros, P., Reversed-phase ion-pair liquid chromatography electrospray ionization tandem mass spectrometry for separation, sequencing and mapping of sites of base modification of isomeric oligonucleotide adducts using monolithic column. *J. Chromatogr. A* **2012,** *1245*, 65-74.

40. Kebarle, P., A brief overview of the present status of the mechanisms involved in electrospray mass spectrometry. *J. Mass Spectrom.* **2000,** *35* (7), 804-817.

41. Dole, M.; Mack, L. L.; Hines, R. L.; Mobley, R. C.; Ferguson, L. D.; Alice, M. B., Molecular beams of macroions. *J. Chem. Phys.* **1968,** *49* (5), 2240-9.

42. Iribarne, J. V.; Thomson, B. A., On the evaporation of small ions from charged droplets. *J. Chem. Phys.* **1976,** *64* (6), 2287-94.

43. Crotti, S.; Seraglia, R.; Traldi, P., Some thoughts on electrospray ionization mechanisms. *Eur. J. Mass Spectrom.* **2011,** *17* (2), 85-100.

44. Kebarle, P.; Verkerk, U. H., Electrospray: from ions in solution to ions in the gas phase, what we know now. *Mass Spectrom. Rev.* **2009,** *28* (6), 898-917.

45. Hogan, C. J.; Carroll, J. A.; Rohrs, H. W.; Biswas, P.; Gross, M. L., Charge carrier field emission determines the number of charges on native state proteins in electrospray ionization. *J. Am. Chem. Soc.* **2008,** *130* (22), 6926-6927.

46. Langley, G. J.; Herniman, J. M.; Davies, N. L.; Brown, T., Simplified sample preparation for the analysis of oligonucleotides by matrix-assisted laser desorption/ionisation time-of-flight mass spectrometry. *Rapid Commun. Mass Spectrom.* **1999,** *13* (17), 1717-1723.

47. de Hoffmann, E.; Stroobant, V.; Editors, *Mass Spectrometry: Principles and Applications, Third Edition*. John Wiley & Sons, Ltd.: **2007**; p 489 pp.34

48. Zenobi, R.; Knochenmuss, R., Ion formation in MALDI mass spectrometry. *Mass Spectrom. Rev.* **1998,** *17* (5), 337-366.

49. Bökelmann, V.; Spengler, B.; Kaufmann, R., Dynamical Parameters of Ion Ejection and Ion Formation in Matrix-Assisted Laser Desorption/Ionization. *Eur. Mass Spectrom.* **1995,** *1* (1), 81-93.

50. Ehring, H.; Karas, M.; Hillenkamp, F., Role of photoionization and photochemistry in ionization processes of organic molecules and relevance for matrix-assisted laser desorption Ionization mass spectrometry. *Org. Mass Spectrom.* **1992,** *27* (4), 472-480.

51. Miller, P. E.; Denton, M. B., The quadrupole mass filter: Basic operating concepts. *J. Chem. Educ.* **1986,** *63* (7), 617.

52. de Hoffmann, E.; Stroobant, V.; Editors, *Mass Spectrometry: Principles and Applications, Third Edition*. John Wiley & Sons, Ltd.: **2007**; p 489 pp.131

53. Whittal, R. M.; Li, L., High-Resolution Matrix-Assisted Laser Desorption/Ionization in a Linear Time-of-Flight Mass Spectrometer. *Anal. Chem.* **1995,** *67* (13), 1950-1954.

54. Sin, C. H.; Lee, E. D.; Lee, M. L., Atmospheric pressure ionization time-of-flight mass spectrometry with a supersonic ion beam. *Anal. Chem.* **1991,** *63* (24), 2897-2900.

55. Smith, R. M., Instrumentation. In *Understanding Mass Spectra: A Basic Approach*, John Wiley & Sons, Inc.: **2005**; pp 1-55.

56. Ivleva, V. B.; Yu, Y. Q.; Gilar, M., Ultra-performance liquid chromatography/tandem mass spectrometry (UPLC/MS/MS) and UPLC/MSE analysis of RNA oligonucleotides. *Rapid Commun. Mass Spectrom.* **2010,** *24* (17), 2631-2640.

57. Banoub, J. H.; Newton, R. P.; Esmans, E.; Ewing, D. F.; Mackenzie, G., Recent Developments in Mass Spectrometry for the Characterization of Nucleosides, Nucleotides, Oligonucleotides, and Nucleic Acids. *Chem. Rev. (Washington, DC, U. S.)* **2005,** *105* (5), 1869-1915.

58. Hill, H. H.; Siems, W. F.; Louis, R. H. S.; McMinn, D. G., Ion Mobility Spectrometry. *Anal. Chem.* **1990,** *62* (23), 1201A-1209A.

59. Kanu, A. B.; Dwivedi, P.; Tam, M.; Matz, L.; Hill, H. H., Ion mobility–mass spectrometry. *J. Mass Spectrom.* **2008,** *43* (1), 1-22.

60. Fisher, H. C.; Smith, M.; Ashcroft, A. E., De novo sequencing of short interfering ribonucleic acids facilitated by use of tandem mass spectrometry with ion mobility spectrometry. *Rapid Commun. Mass Spectrom.* **2013,** *27* (20), 2247-2254.

61. Cumeras, R.; Figueras, E.; Davis, C. E.; Baumbach, J. I.; Gracia, I., Review on ion mobility spectrometry. Part 1: current instrumentation. *Analyst (Cambridge UK)* **2015,** *140* (5), 1376-1390.

62. Giles, K.; Williams, J. P.; Campuzano, I., Enhancements in travelling wave ion mobility resolution. *Rapid Commun. Mass Spectrom.* **2011,** *25* (11), 1559-1566.

63. Fritz, H. J.; Belagaje, R.; Brown, E. L.; Fritz, R. H.; Jones, R. A.; Lees, R. G.; Khorana, H. G., Studies on polynucleotides. 146. High-pressure liquid chromatography in polynucleotide synthesis. *Biochemistry* **1978,** *17* (7), 1257-1267.

64. Glover, R. P.; Sweetman, G. M. A.; Farmer, P. B.; Roberts, G. C. K., Sequencing of oligonucleotides using high-performance liquid-chromatography and electrospray mass-spectrometry. *Rapid Commun. Mass Spectrom.* **1995,** *9* (10), 897-901.

65. Huber, C. G.; Oberacher, H., Analysis of nucleic acids by on-line liquid chromatography-mass spectrometry. *Mass Spectrom. Rev.* **2002,** *20* (5), 310-343.

66. Rudge, J.; Scott, G.; Hail, M.; McGinley, M., Preparation and LC/MS Analysis of Oligonucleotide Therapeutics from Biological Matrices. *Chromatography Today* **2011,** *4* (1), 16-20.

67. van Dongen, W. D.; Niessen, W. M. A., Bioanalytical LC-MS of therapeutic oligonucleotides. *Bioanalysis* **2011,** *3* (5), 541-564.

68. Eeltink, S.; Wouters, S.; Dores-Sousa, J. L.; Svec, F., Advances in organic polymer-based monolithic column technology for high-resolution liquid chromatography-mass spectrometry profiling of antibodies, intact proteins, oligonucleotides, and peptides. *J. Chromatogr. A* **2017,** *1498*, 8-21.

69. Leblanc, Y.; Ramon, C.; Bihoreau, N.; Chevreux, G., Charge variants characterization of a monoclonal antibody by ion exchange chromatography coupled on-line to native mass spectrometry: Case study after a long-term storage at +5°C. *J. Chromatogr. B* **2017,** *1048*, 130-139.

70. Muneeruddin, K.; Bobst, C. E.; Frenkel, R.; Houde, D.; Turyan, I.; Sosic, Z.; Kaltashov, I. A., Characterization of a PEGylated protein therapeutic by ion exchange chromatography with on-line detection by native ESI MS and MS/MS. *Analyst (Cambridge, U. K.)* **2017,** *142* (2), 336-344.

71. Greig, M.; Griffey, R. H., Utility of organic-bases for improved electrospray mass-spectrometry of oligonucleotides. *Rapid Commun. Mass Spectrom.* **1995,** *9* (1), 97-102.

72. Apffel, A.; Chakel, J. A.; Fischer, S.; Lichtenwalter, K.; Hancock, W. S., Analysis of Oligonucleotides by HPLC-Electrospray Ionization Mass Spectrometry. *Anal. Chem.* **1997,** *69* (7), 1320-5.

73. Apffel, A.; Chakel, J. A.; Fischer, S.; Lichtenwalter, K.; Hancock, W. S., New procedure for the use of high-performance liquid chromatography-electrospray ionization mass spectrometry for the analysis of nucleotides and oligonucleotides. *J. Chromatogr. A* **1997,** *777* (1), 3-21.

74. Li, Z.; Schariter, J. A.; Zhang, J.; Davis, J. C.; Leone, A. M., Application of ultra-high performance liquid chromatography for chemical characterization of liposome-based therapeutic small-interfering RNA. *American Pharmaceutical Review* **2010,** *13* (6), 102-110.

75. Gilar, M. *Oligonucleotide separation technology: Synthesis challenges and HPLC isolation options*; 720002386EN; Waters: **2007**.

76. Chen, B.; Bartlett, M. G., Evaluation of mobile phase composition for enhancing sensitivity of targeted quantification of oligonucleotides using ultra-high performance liquid chromatography and mass spectrometry: Application to phosphorothioate deoxyribonucleic acid. *J. Chromatogr. A* **2013,** *1288*, 73-81.

77. Deng, P.; Chen, X.; Zhang, G.; Zhong, D., Bioanalysis of an oligonucleotide and its metabolites by liquid chromatography–tandem mass spectrometry. *J. Pharm. Biomed. Anal.* **2010,** *52* (4), 571-579.

78. Gong, L.; McCullagh, J. S. O., Comparing ion-pairing reagents and sample dissolution solvents for ion-pairing reversed-phase liquid chromatography/electrospray ionization mass spectrometry analysis of oligonucleotides. *Rapid Commun. Mass Spectrom.* **2014,** *28* (4), 339-350.

79. Williams, J. P.; Lough, J. A.; Campuzano, I.; Richardson, K.; Sadler, P. J., Use of ion mobility mass spectrometry and a collision cross-section algorithm to study an organometallic ruthenium anticancer complex and its adducts with a DNA oligonucleotide. *Rapid Commun. Mass Spectrom.* **2009,** *23* (22), 3563-3569.

80. Harper, B.; Neumann, E. K.; Solouki, T., DNA Oligonucleotide Fragment Ion Rearrangements Upon Collision-Induced Dissociation. *J. Am. Soc. Mass. Spectrom.* **2015,** *26* (8), 1404-1413.

81. Kurata, C.; Capaldi, D.; Wang, Z.; Luu, N.; Gaus, H.-J. Methods for detection, identification and quantification of impurities in oligonucleotide drug products using ion pair HPLC and mass spectrometry. WO2006107775A1, **2006**.

82. Lin, Z. J.; Li, W.; Dai, G., Application of LC–MS for quantitative analysis and metabolite identification of therapeutic oligonucleotides. *J. Pharm. Biomed. Anal.* **2007,** *44* (2), 330-341.

83. Cheng, X.; Gale, D. C.; Udseth, H. R.; Smith, R. D., Charge State Reduction of Oligonucleotide Negative Ions from Electrospray Ionization. *Anal. Chem.* **1995,** *67* (3), 586-593.

84. Muddiman, D. C.; Cheng, X.; Udseth, H. R.; Smith, R. D., Charge-state reduction with improved signal intensity of oligonucleotides in electrospray ionization mass spectrometry. *J. Am. Soc. Mass Spectrom.* **1996,** *7* (8), 697-706.

85. Premstaller, A.; Huber, C. G., Factors determining the performance of triple quadrupole, quadrupole ion trap and sector field mass spectrometer in electrospray ionization mass spectrometry. 2. Suitability for de novo sequencing. *Rapid Commun. Mass Spectrom.* **2001,** *15* (13), 1053-1060.

86. Erb, R.; Oberacher, H., Comparison of mobile-phase systems commonly applied in liquid chromatography-mass spectrometry of nucleic acids. *Electrophoresis* **2014,** *35* (9), 1226-1235.

87. Basiri, B.; Murph, M. M.; Bartlett, M. G., Assessing the Interplay between the Physicochemical Parameters of Ion-Pairing Reagents and the Analyte Sequence on the Electrospray Desorption Process for Oligonucleotides. *J. Am. Soc. Mass. Spectrom.* **2017,** *28* (8), 1647-1656.

88. Premstaller, A.; Ongania, K.-H.; Huber, C. G., Factors determining the performance of triple quadrupole, quadrupole ion trap and sector field mass spectrometers in electrospray ionization tandem mass spectrometry of oligonucleotides. 1. Comparison of performance characteristics. *Rapid Commun. Mass Spectrom.* **2001,** *15* (13), 1045-1052.

89. Cech, N. B.; Enke, C. G., Practical implications of some recent studies in electrospray ionization fundamentals. *Mass Spectrom. Rev.* **2001,** *20* (6), 362-387.

90. Basiri, B.; van Hattum, H.; van Dongen, W. D.; Murph, M. M.; Bartlett, M. G., The Role of Fluorinated Alcohols as Mobile Phase Modifiers for LC-MS Analysis of Oligonucleotides. *J. Am. Soc. Mass. Spectrom.* **2017,** *28* (1), 190-199.

91. Kida, T.; Sato, S.-i.; Yoshida, H.; Teragaki, A.; Akashi, M., 1,1,1,3,3,3-Hexafluoro-2-propanol (HFIP) as a novel and effective solvent to facilely prepare cyclodextrin-assembled materials. *Chem. Commun.* **2014,** *50* (91), 14245-14248.

92. Dawson, R. M. C., *Data for Biochemical Research. 3rd Ed*. Clarendon: 1986; p 580 pp.

93. Bleicher, K.; Bayer, E., Various factors influencing the signal intensity of oligonucleotides in electrospray mass spectrometry. *Biol. Mass Spectrom.* **1994,** *23* (6), 320-2.

94. Bristow, A. W. T.; Nichols, W. F.; Webb, K. S.; Conway, B., Evaluation of protocols for reproducible electrospray in-source collisionally induced dissociation on various liquid chromatography/mass spectrometry instruments and the development of spectral libraries. *Rapid Commun. Mass Spectrom.* **2002,** *16* (24), 2374-2386.

95. Guo, X.; Bruist, M. F.; Davis, D. L.; Bentzley, C. M., Secondary structural characterization of oligonucleotide strands using electrospray ionization mass spectrometry. *Nucleic Acids Res.* **2005,** *33* (11), 3659-3666.

96. Suzuki, T.; Ohsumi, S.; Makino, K., Mechanistic studies on depurination and apurinic site chain breakage in oligodeoxyribonucleotides. *Nucleic Acids Res.* **1994,** *22* (23), 4997-5003.

97. Nyakas, A.; Eberle, R. P.; Stucki, S. R.; Schurch, S., More Than Charged Base Loss - Revisiting the Fragmentation of Highly Charged Oligonucleotides. *J. Am. Soc. Mass Spectrom.* **2014,** *25* (7), 1155-1166.

98. Hunter, C. L.; Mauk, A. G.; Douglas, D. J., Dissociation of Heme from Myoglobin and Cytochrome b5: Comparison of Behavior in Solution and the Gas Phase. *Biochemistry* **1997,** *36* (5), 1018-1025.

99. Bruins, A. P., Mass spectrometry with ion sources operating at atmospheric pressure. *Mass Spectrom. Rev.* **1991,** *10* (1), 53-77.

100. Thomson, B. A., Declustering and fragmentation of protein ions from an electrospray ion source. *J. Am. Soc. Mass. Spectrom.* **1997,** *8* (10), 1053-1058.

101. Luo, H.; Lipton, M. S.; Smith, R. D., Charge effects for differentiation of oligodeoxynucleotide isomers containing 8-oxo-dG residues. *J. Am. Soc. Mass. Spectrom.* **2002,** *13* (3), 195-199.

102. Pan, S.; Verhoeven, K.; Lee, J. K., Investigation of the initial fragmentation of oligodeoxynucleotides in a quadrupole ion trap: Charge level-related base loss. *J. Am. Soc. Mass. Spectrom.* **2005,** *16* (11), 1853-1865.

103. Marzilli, L. A.; Barry, J. P.; Sells, T.; Law, S.-J.; Vouros, P.; Harsch, A., Oligonucleotide sequencing using guanine-specific methylation and electrospray ionization ion trap mass spectrometry. *J. Mass Spectrom.* **1999,** *34* (4), 276-280.

104. Zhang, G.; Lin, J.; Srinivasan, K.; Kavetskaia, O.; Duncan, J. N., Strategies for Bioanalysis of an Oligonucleotide Class Macromolecule from Rat Plasma Using Liquid Chromatography−Tandem Mass Spectrometry. *Anal. Chem.* **2007,** *79* (9), 3416-3424.

105. Smith, M.; Beck, T., Quantitation of a low level coeluting impurity present in a modified oligonucleotide by both LC-MS and NMR. *J. Pharm. Biomed. Anal.* **2016,** *118*, 34-40.

106. Ledman, D. W.; Fox, R. O., Water cluster calibration reduces mass error in electrospray ionization mass spectrometry of proteins. *J. Am. Soc. Mass. Spectrom.* **1997,** *8* (11), 1158-1164.

107. Gilar, M.; Fountain, K. J.; Budman, Y.; Holyoke, J. L.; Davoudi, H.; Gebler, J. C., Characterization of Therapeutic Oligonucleotides Using Liquid Chromatography with On-line Mass Spectrometry Detection. *Oligonucleotides* **2003,** *13* (4), 229-243.

108. Lavagnini, I.; Magno, F.; Seraglia, R.; Traldi, P., How to Design a Quantitative Analysis. In *Quantitative Applications of Mass Spectrometry*, John Wiley & Sons, Ltd: **2006**; pp 37-53.

109. Jockusch, R. A.; Schnier, P. D.; Price, W. D.; Strittmatter, E. F.; Demirev, P. A.; Williams, E. R., Effects of Charge State on Fragmentation Pathways, Dynamics, and Activation Energies of

Ubiquitin Ions Measured by Blackbody Infrared Radiative Dissociation. *Anal. Chem.* **1997,** *69* (6), 1119-1126.

110. Ickert, S.; Hofmann, J.; Riedel, J.; Beck, S.; Pagel, K.; Linscheid, M. W., Charge-induced geometrical reorganization of DNA oligonucleotides studied by tandem mass spectrometry and ion mobility. *Eur. J. Mass Spectrom.* **2018,** *24* (2), 225-230.